# INSIGHTS IN GYNECOLOGICAL ONCOLOGY: 2021

EDITED BY: Sarah M. Temkin and Sophia George
PUBLISHED IN: Frontiers in Oncology

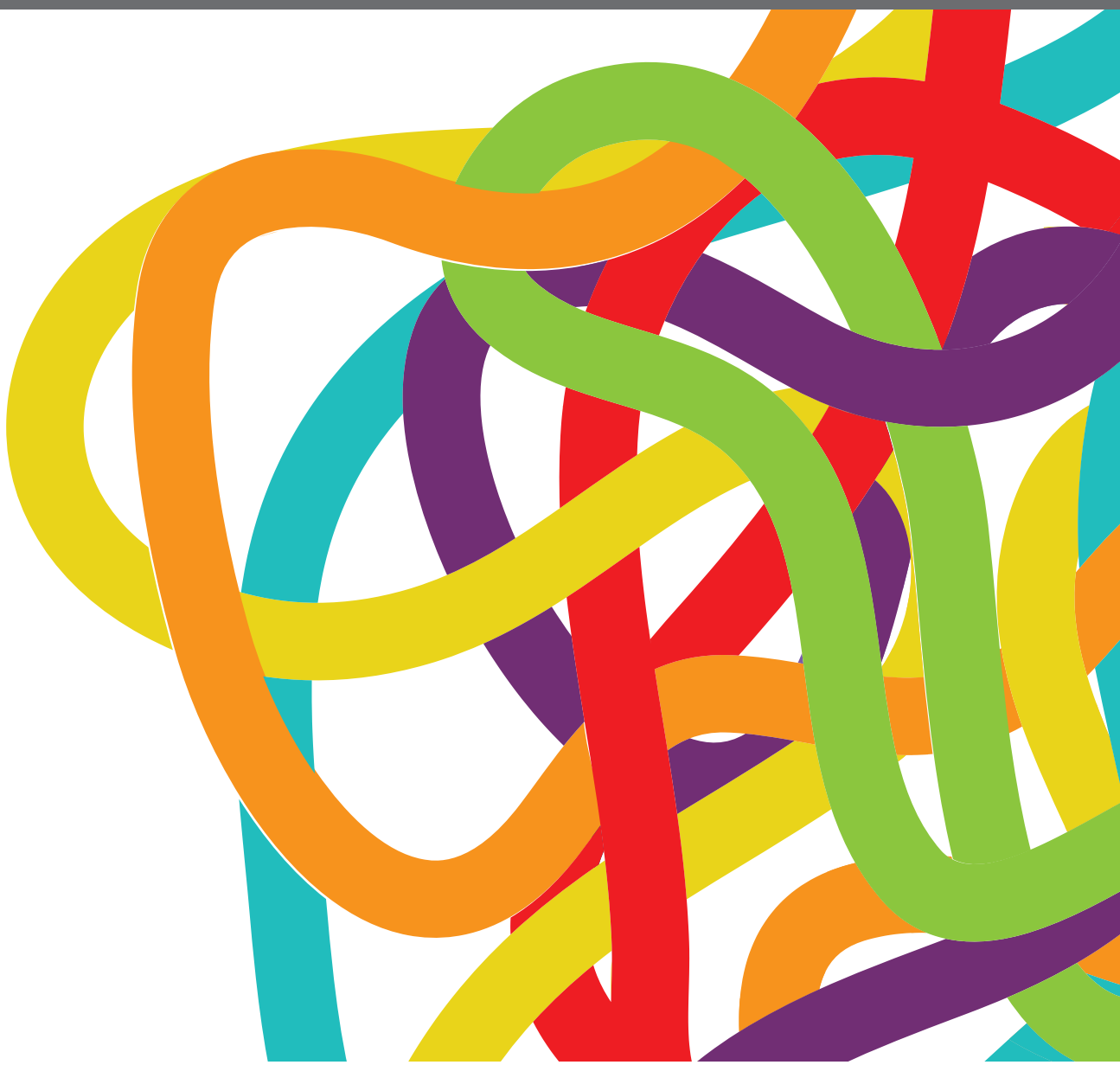

frontiers Research Topics

frontiers



ISSN 1664-8714
ISBN 978-2-83250-601-1
DOI 10.3389/978-2-83250-601-1

## About Frontiers

Frontiers is more than just an open-access publisher of scholarly articles: it is a pioneering approach to the world of academia, radically improving the way scholarly research is managed. The grand vision of Frontiers is a world where all people have an equal opportunity to seek, share and generate knowledge. Frontiers provides immediate and permanent online open access to all its publications, but this alone is not enough to realize our grand goals.

## Frontiers Journal Series

The Frontiers Journal Series is a multi-tier and interdisciplinary set of open-access, online journals, promising a paradigm shift from the current review, selection and dissemination processes in academic publishing. All Frontiers journals are driven by researchers for researchers; therefore, they constitute a service to the scholarly community. At the same time, the Frontiers Journal Series operates on a revolutionary invention, the tiered publishing system, initially addressing specific communities of scholars, and gradually climbing up to broader public understanding, thus serving the interests of the lay society, too.

## Dedication to Quality

Each Frontiers article is a landmark of the highest quality, thanks to genuinely collaborative interactions between authors and review editors, who include some of the world's best academicians. Research must be certified by peers before entering a stream of knowledge that may eventually reach the public - and shape society; therefore, Frontiers only applies the most rigorous and unbiased reviews.
Frontiers revolutionizes research publishing by freely delivering the most outstanding research, evaluated with no bias from both the academic and social point of view. By applying the most advanced information technologies, Frontiers is catapulting scholarly publishing into a new generation.

## What are Frontiers Research Topics?

Frontiers Research Topics are very popular trademarks of the Frontiers Journals Series: they are collections of at least ten articles, all centered on a particular subject. With their unique mix of varied contributions from Original Research to Review Articles, Frontiers Research Topics unify the most influential researchers, the latest key findings and historical advances in a hot research area! Find out more on how to host your own Frontiers Research Topic or contribute to one as an author by contacting the Frontiers Editorial Office: frontiersin.org/about/contact

# INSIGHTS IN GYNECOLOGICAL ONCOLOGY: 2021

Topic Editors:
**Sarah M. Temkin,** National Institutes of Health (NIH), United States
**Sophia George,** University of Miami, United States

**Citation:** Temkin, S. M., George, S., eds. (2022). Insights in Gynecological Oncology: 2021. Lausanne: Frontiers Media SA.
doi: 10.3389/978-2-83250-601-1

# Table of Contents

frontiers in Oncology

ORIGINAL RESEARCH
published: 07 July 2021
doi: 10.3389/fonc.2021.695404

# Identification of Predictive Biomarkers for Lymph Node Involvement in Obese Women With Endometrial Cancer

*Vanessa M. López-Ozuna[1,2], Liron Kogan[1,3], Mahmood Y. Hachim[4], Emad Matanes[1,2], Ibrahim Y. Hachim[5], Cristina Mitric[1,2], Lauren Liu Chen Kiow[1,2], Susie Lau[1,2], Shannon Salvador[1,2], Amber Yasmeen[1,2] and Walter H. Gotlieb[1,2]**

[1] Division of Gynecologic Oncology, Jewish General Hospital, McGill University, Montreal, QC, Canada, [2] Segal Cancer Center, Lady Davis Institute of Medical Research, McGill University, Montreal, QC, Canada, [3] Department of Gynecologic Oncology, Hadassah Medical Center, affiliated with Hebrew University Hadassah Medical School, Jerusalem, Israel, [4] College of Medicine, Mohammed Bin Rashid University of Medicine and Health Sciences, Dubai, United Arab Emirates, [5] College of Medicine, Sharjah Institute for Medical Research, University of Sharjah, Sharjah, United Arab Emirates

OPEN ACCESS

**Edited by:**
Fabio Martinelli,
Istituto Nazionale dei Tumori (IRCCS), Italy

**Reviewed by:**
Stephanie M. McGregor,
University of Wisconsin-Madison, United States
Antonio Raffone,
Federico II University Hospital, Italy

***Correspondence:**
Walter H. Gotlieb
walter.gotlieb@mcgill.ca

**Specialty section:**
This article was submitted to Gynecological Oncology, a section of the journal Frontiers in Oncology

**Received:** 14 April 2021
**Accepted:** 23 June 2021
**Published:** 07 July 2021

**Citation:**
López-Ozuna VM, Kogan L, Hachim MY, Matanes E, Hachim IY, Mitric C, Kiow LLC, Lau S, Salvador S, Yasmeen A and Gotlieb WH (2021) Identification of Predictive Biomarkers for Lymph Node Involvement in Obese Women With Endometrial Cancer. Front. Oncol. 11:695404. doi: 10.3389/fonc.2021.695404

Obesity, an established risk factor for endometrial cancer (EC), is also associated to increased risks of intraoperative and postoperative complications. A reliable tool to identify patients at low risk for lymph node (LN) metastasis may allow minimizing the surgical staging and omit lymphadenectomy in obese patients. To identify molecular biomarkers that could predict LN involvement in obese patients with EC we performed gene expression analysis in 549 EC patients using publicly available transcriptomic datasets. Patients were filtrated according to cancer subtype, weight (>30 kg/m$^2$) and LN status. While in the LN+ group, NEB, ANK1, AMIGO2, LZTS1, FKBP5, CHGA, USP32P1, CLIC6, CEMIP, HMCN1 and TNFRSF10C genes were highly expressed; in the LN- group CXCL14, FCN1, EPHX3, DDX11L2, TMEM254, RNF207, LTK, RPL36A, HGAL, B4GALNT4, KLRG1 genes were up-regulated. As a second step, we investigated these genes in our patient cohort of 35 patients (15 LN+ and 20 LN-) and found the same correlation with the in-silico analysis. In addition, immunohistochemical expression was confirmed in the tumor tissue. Altogether, our findings propose a novel panel of genes able to predict LN involvement in obese patients with endometrial cancer.

**Keywords: lymph node, molecular markers, endometrial cancer, obesity, tumor biomarkers, body mass index (BMI)**

## INTRODUCTION

Endometrial cancer (EC) is considered as the fourth most common malignancy among women and the second leading cause of death from gynecological cancers (1, 2). The standard surgical treatment of EC includes hysterectomy, bilateral salpingo-oophorectomy, and lymph node evaluation, either by sentinel lymph node mapping or by lymphadenectomy (3–6).

Obesity is defined by body mass index >30 kg/m$^2$ (7) and is believed to be in part responsible for the increasing incidence of EC in the last 30 years (8, 9). In the United States, around 57% of the EC cases were linked to overweight and obesity (10), and this is associated with the increase of estrogen production in the adipose tissue (11, 12).

Patients suffering from obesity represent a considerable challenge during the intra- and post-operative periods that has been associated with short and long term adverse clinical outcomes (13–17). In a previous report, our team assessed several clinical factors associated with LN involvement in obese patients with EC and found that sentinel node detection (SLN) and lymph node (LN) dissection decreased with increasing BMI, and lymph node involvement was inversely correlated with BMI (18). In view of the lower detection rate of SLN, the decreased risk of LN involvement, and the increased operative risk of LN dissection in this patient population, it is questionable whether LN dissection should be performed if SLN mapping failed in obese patients with EC.

New improvements have been made in genetic and molecular profiling that have facilitated the identification of gene signatures as diagnostic tools for clinical decision making, or as creators of targets that could have an impact in therapeutic approaches (19, 20). Here, we aimed to identify molecular markers, as predictors of LN involvement in obese women with EC.

# MATERIAL AND METHODS

## Study Design

This study was conducted in the division of Gynecologic Oncology at the Segal Cancer Center of the Jewish General Hospital. Between December 2007 and August 2017, 722 patients with uterine cancer underwent surgical staging in our institution. In this study we included patients with histologic diagnosis of endometrioid endometrial carcinoma, BMI above 30kg/m$^2$, known LN status after surgery, and material in our biobank for RNA extraction and processing. Patient's exclusion criteria were: patients with sarcomas, patients who received neoadjuvant therapy, patients whose body mass index was below 30kg/m$^2$. All patients underwent robotically assisted surgical staging which included total hysterectomy, bilateral salpingo-oophorectomy and LN assessment by either LN dissection or SLN mapping. Tumor samples were stored in the gynecologic oncology tumor bank for further processing.

## Ethics and Clinical Samples

The study was approved by the Institutional Review Ethics Board (protocol #2019-1547), with annual reviews. Prior to surgery, informed consent was obtained from all participants. Tissue samples were collected at the time of surgery, preserved in RNAlater (Qiagen) and stored at −80°C in the gynecologic oncology tumor bank (protocol #03-041). All samples were selected after histologic confirmation, and high tumor content (>70% tumor content) was confirmed by a gynecologic pathologist. Clinical data for each patient was available.

## Clinical Data Collection

All clinical data was entered in a prospective fashion into a clinical data base. We retrospectively analyzed the perioperative data for all cases. The operative, clinical, pathological and survival data were retrieved from electronic medical records.

## Antibodies

The following antibodies were used to perform the immunohistochemistry: CEMIP (ABclonal #A8587) 1:200 dilution, RPL36A (Novus biologicals #NBP2-38036) 1:25 dilution, CXCL14 (Thermofisher #10468-1-AP) 1:100 dilution, EPHX3 (Thermofisher #PA5-52992) 1:10 dilution, TMEM254 (Novus Biologicals, NBP2-68939) 1:50 dilution, LZTS1 (Novus Biologicals, NBP2-17195) 1:50 dilution, CLIC6 (Novus Biologicals, NBP2-38062) 1:10 dilution, HMNC1 (Thermofisher #PA5-62458) 1:50 dilution.

## RNA Extraction and Reverse Transcriptase Real-Time PCR

Total RNA was extracted from Formalin-Fixed, Paraffin-Embedded tissue (FFPE) using PureLink RNA Mini Kit (Thermo Fisher). First strand cDNA was synthesized using 5X All-In-On MasterMix (MasterMix-LR, Diamed) per manufacturer's protocol. Reverse transcriptase real-time PCR (RT-PCR) was carried out on 96-well plates using iTaq Universal SYBR Green Supermix (BioRad). Concentrations for each sample were measured using the NanoDrop ND-100 spectrophotometer 119 (NanoDrop Technologies, Wilmington, DE, USA) and Qubit (Thermo Fischer Scientific, 120 Waltham, MA, USA). The primer sequences were designed using Primer Express™ Software v3.0.1 (ThermoFisher Scientific, USA) (Supplemental material).

## *In Silico* Analysis

For biomarker discovery, we used the RNA-seq data of 549 uterine cancer patients extracted from TCGA, PanCancer Atlas using the publicly available cBioPortal online database https://www.cbioportal.org (21). The TCGA data contains 115 serous and 410 endometrioid endometrial cancers. Using the same program, the clinical and genomic profiles that include the gene expression levels, mutation profile, copy-number variance (CNV) as well as protein expression were assessed. In addition, the Kaplan–Meier survival analysis for different subgroups of endometrial cancer patients was also assessed according to cBioPortal instructions.

To investigate the association between different subgroups including obese and non-obese as well as LN negative and LN positive, the raw data files were extracted from the cBioPortal database and filtered for further analysis using our in-house pipeline for normalization and variant filtration. Height and weight were available for each patient and BMI was calculated using the following formula, BMI= weight (kg)/(height (m))$^2$. The shortlisted DEGs were obtained thought selection of genes that showed 2-fold change between the different groups and adjusted p value <0.05 as cut-offs. According to those conditions, the endometrioid subgroup were subdivided according to their BMI into obese (BMI>30) and non-obese (BMI<30). Each group was further divided into those with no pelvic LN involvement

(LN-) and those with any number of positive pelvic LN (LN+). The four groups were compared in terms of clinical, pathological, genomic and transcriptomic profiles. Differentially expressed genes between the different groups were shortlisted.

## Network and Pathway Interaction

Metscape online tool (http://metascape.org/) was used to investigate the network and interaction between the differential expressed genes and their biological function. This is a biological database and web resource of known and predicted protein–protein interactions. We used this tool to highlight the significance of the potential connectivity network of our genes that need to be considered for the full understanding of the biological process.

## Tissue Microarray

The tissue microarray (TMA) consists of 35 cases of endometrioid endometrial cancer (15 obese LN+, 20 obese LN-), and 10 normal adjacent tissue. Construction was performed as previously described by our group (22). Briefly, tissue cylinders with a diameter of 0.6 mm were punched from representative tumor areas of the tissue block selected for high tumor content, using a semiautomatic robotic precision instrument. Two sections of the TMA blocks were transferred to an adhesive coated slide system (Instrumedics Inc., Hackensack, New Jersey). Slides of the finished blocks were used for immunohistochemistry analysis.

## Immunohistochemistry (IHC) Analysis

IHC was performed at the Segal Cancer Centre Research Pathology Facility (JGH) using standard IHC protocols. Every tissue had a section stained with hematoxylin and eosin (H&E) and tumor content was assessed. Antibody immunostaining was performed using the Discovery XT Autostainer (Ventana Medical System) and a standardized diagnostic applications protocol. Two reference tissue samples were included on each slide as a positive and negative control. Sections were analyzed by conventional light microscopy.

CEMIP, RPL36A, CXCL14, EPHX3, TMEM254, CLIC6 and HMNC1 showed mainly cytoplasmic expression in the tumor epithelial cells. The immunoreactivity of all antibodies was classified according to the intensity into four categories. Cases with no evidence of cytoplasmic immunoreactivity considered as 0 score. Cases with weak immunoreactivity considered as +1 score. Cases with moderate immunostaining were given +2 score, +3 score were given to cases that showed strong immunoreactivity. For statistical analysis, cases considered positive if they are scored with +2, +3 category and negative if they fall into 0, + 1 categories. All the cases were reviewed by 2 pathologists that blindly and independently evaluated the slides.

## Statistical Analysis

The shortlisted DEGs were obtained thought selection of genes that showed 2-fold change between the different groups and adjusted p value <0.05 as cut-offs. All results are presented as the mean ± SEM for at least three independent experiments. The difference between groups was analyzed using Student's *t*-test, and $P < 0.05$ was considered statistically significant.

# RESULTS

## Categorization of Endometrioid Endometrial Cancer According to BMI to Investigate Top Differentially Expressed Genes (DEGs) That Can Differentiate Obese From Non-Obese Patients

For biomarker discovery, we used the RNA-seq data of uterine cancer patients extracted from TCGA PanCancer Atlas using the publicly available cBioPortal online database. The RNA-seq data was extracted from 549 uterine cancer patients and filtrated to classify them according to cancer subtypes. Using the same program, the clinical and genomic profile that includes the gene expression levels, mutation profile, copy-number variance (CNV) was assessed. In addition, the Kaplan–Meier survival analysis for different subgroups of endometrial cancer patients was also assessed according to cBioPortal instructions. The patients were filtrated according to cancer subtypes, 115 serous, 410 endometrioid and 24 other carcinomas were obtained. The second filtration was performed in the cohort of endometrioid EC (410 patients) where the raw data files were extracted from the cBioPortal database and filtered accordingly for further analysis using our in-house pipeline for normalization and variant filtration. The DEGs were obtained through selection of genes that showed 2-fold change or high between the different groups and adjusted p-value<0.05 as cut-offs. Next, using the associated clinical information provided by the databases, we classified endometrioid EC patients in obese (BMI>30) (249 patients) and non-obese (BMI<30) (161 patients) according to their BMI, that was obtained from the patient's height and weight, using the following formula, BMI = kg/m2. The obese group was further divided into those with no pelvic LN (LN-) (213 patients) and those with any number of pelvic LN (LN+) (36 patients) (**Figure 1A**).

## Identification of Top Differential Genes Between LN Negative and Positive Cases in Obese Endometrioid Cancer Patients

For better understanding of the association between obesity and LN involvement in endometrioid cancer subtype, we stratified patients with BMI >30 according to their LN status. The top DEGs between LN- and LN+ subgroups were identified. Eleven genes (CXCL14, FCN1, EPHX3, DDXIIL2, TMEM254, RNF207, LTK, HAGHL, RPL36A, BHGALNT4 and KLRC1) were up regulated in LN+ cases compared to LN- (**Figure 1B**). In contrast, a different set of eleven DEGs (NEB, ANK1, AMIGO2, LZTS1, FKBP5, CHGA, USP32PI, CLIC6, CEMIP and HMCN1) were found to be up regulated in LN- samples compared to LN+ (**Figure 1C**).

In order to investigate the network and interaction between the differentially expressed genes and their biological function, we used metscape online tool. Interestingly, we found that the panel of genes are directly involved in muscle contraction (CHGA, NEB

**A**

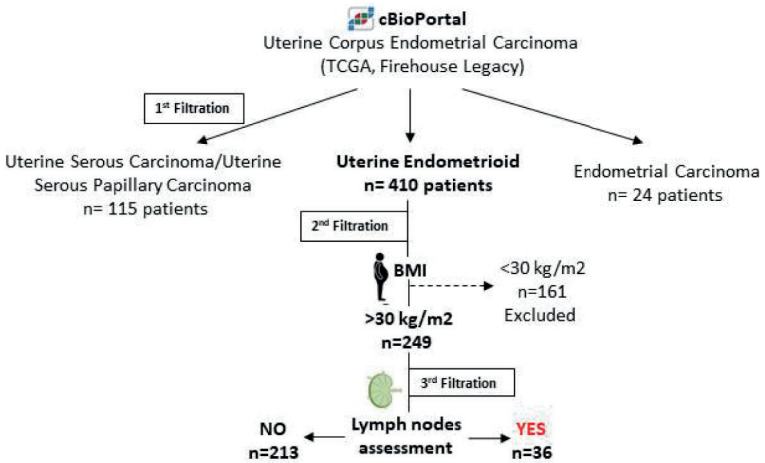


**B**

**Mean log2 expression of top DEGs in obese patients with LN+**

| Gene | Cytoband | LN(-) | LN(+) | Log Ratio | p-Value |
|---|---|---|---|---|---|
| DDX11L2 | 2q14.1 | 0.96±0.13 | 3.94±1.86 | -2.98 | 1.64E-09 |
| HAGHL | 16p13.3 | 5.01±0.11 | 7.73±1.92 | -2.72 | 1.29E-08 |
| RNF207 | 1p36.31 | 5.38±0.05 | 7.46±1.51 | -2.08 | 1.57E-08 |
| TMEM254-AS1 | 10q22.3 | 3.35±0.15 | 5.66±1.2 | -2.32 | 1.87E-08 |
| EPHX3 | 19p13.12 | 1.12±0.1 | 3.29±1.57 | -2.18 | 2.01E-08 |
| RPL36A | Xq22.1 | 4.34±0.16 | 7.09±1.11 | -2.75 | 3.59E-08 |
| LTK | 15q15.1 | 0.96±0.13 | 4.08±2.43 | -3.12 | 7.7E-08 |
| FCN1 | 9q34.3 | 2.09±0.08 | 4.49±1.9 | -2.4 | 9.01E-08 |
| KLRG1 | 12p13.31 | 2.24±0.12 | 4.29±0.79 | -2.05 | 1E-07 |
| B4GALNT4 | 11p15.5 | 7.11±0.16 | 9.41±1.66 | -2.3 | 1.84E-07 |
| CXCL14 | 5q31.1 | 6.34±0.2 | 10.24±3.49 | -3.9 | 1.09E-06 |

**C**

**Mean log2 expression of top DEGs in obese patients with LN-**

| Gene | Cytoband | LN(-) | LN(+) | Log Ratio | p-Value |
|---|---|---|---|---|---|
| NEB | 2q23.3 | 7.8±0.07 | 4.01±1.38 | 3.8 | 9.18E-16 |
| LZTS1 | 8p21.3 | 9.16±0.05 | 6.69±0.95 | 2.48 | 4.17E-15 |
| ANK1 | 8p11.21 | 9.53±0.08 | 4.82±1.93 | 4.71 | 2.01E-14 |
| FKBP5 | 6p21.31 | 10.08±0 | 8.07±1.38 | 2.01 | 4.53E-09 |
| CHGA | 14q32.12 | 12.74±0 | 7.63±3.77 | 5.1 | 2.14E-08 |
| USP32P1 | 17p11.2 | 8.53±0.02 | 6.32±1.91 | 2.21 | 4.19E-07 |
| CLIC6 | 21q22.12 | 10.41±0.16 | 6.62±3.26 | 3.79 | 4.51E-07 |
| CEMIP | 15q25.1 | 10.61±0.26 | 7.38±2.26 | 3.23 | 6.99E-07 |
| HMCN1 | 1q25.3-q31.1 | 9.43±0.25 | 6.65±2.07 | 2.78 | 3.08E-06 |
| AMIGO2 | 12q13.11 | 9.88±0.07 | 7.75±2.12 | 2.14 | 4.25E-06 |

**D**

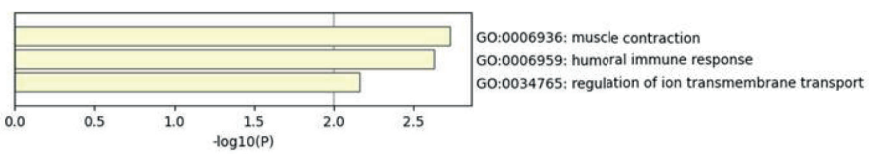


| Category | Term | Description | LogP | Symbols |
|---|---|---|---|---|
| GO Biological Processes | GO:0006936 | muscle contraction | -2.724735932 | CHGA,NEB,RNF207 |
| GO Biological Processes | GO:0006959 | humoral immune response | -2.623776331 | CHGA,FCN1,CXCL14 |
| GO Biological Processes | GO:0034765 | regulation of ion transmembrane transport | -2.159272598 | CLIC6,CEMIP,RNF207 |

**FIGURE 1** | **(A)** Schematic workflow describing biomarker discovery, **(B)** Log2 expression levels of the differential expressed genes discovered in LN+ patients **(C)** Log2 expression levels of the differential expressed genes discovered in LN- patients, **(D)** Pathway analysis of differentially expressed genes using metscape tool for the retrieval of interacting genes. Enriched biological process and molecular functions of those proteins are included.

and RNF207), humoral immune response (CHGA, FCN1 and CXCL14) and regulation of ion transmembrane transport (CLIC6, CEMIP and RNF207) as shown in **Figure 1D**.

## Validation of the LN Involvement Top DEGs in a Patients' Cohort From Our Tissue Bank

Thirty-five samples of endometroid EC patients were retrieved from our biobank and were used for validation. This panel includes LN+ (n=15) and LN- (n=20) patients. Overall median age was 69 years old, median BMI was 39.3kg and the majority of patients had a preoperative ASA score of 1 or 2 with no significant difference between the two groups. While all patients underwent LN dissection, 82% had SLN mapping performed (p=0.003). In the LN+ group deep myometrial invasion (>50%) was observed in all patients compared with LN- group (p=0.002) (**Figure 2**).

Following the identification of the candidate genes, we next validated the in-silico approach using qPCR analysis in this patient cohort. Samples of 15 obese EC patients with LN involvement and 20 obese EC patients with negative nodes were assessed. As shown in **Figure 3A**, a panel of eleven genes were identified to be upregulated in the LN+ group (CXCL14, FCN1, EPHX3, DDXIIL2, TMEM254, RNF207, LTK, HAGHL,

| | TOTAL (n-35) | Lymph node negative (n-20) | Lymph node positive (n-15) | P-VALUE |
|---|---|---|---|---|
| AGE, mean (SD) | 69.0 (9.9) | 71.1 (10.5) | 66.2 (8.5) | 0.14 |
| BMI, mean (SD) | 39.3 (5.7) | 40.7 (4.4) | 40.7 (4.4) | 0.18 |
| Gravidity, median (range) | 2 (0-7) | 2 (0-6) | 3 (0-7) | 0.50 |
| Parity, median (range) | 2 (0-6) | 2 (0-3) | 2 (0-6) | 0.54 |
| Figo 2009 stage | | | | <0.001 |
| I | 20 (57.1%) | 19 (95.0%) | 1 (6.7%) | |
| II | 1 (2.9%) | 1 (5.0%) | 0 (0) | |
| III | 13 (37.1%) | 0 (0) | 13 (86.7%) | |
| IV | 1 (2.9%) | 0 (0) | 1 (6.7%) | |
| Pre-op grade | | | | 0.048 |
| 1 | 18 (52.9%) | 13 (68.4%) | 5 (33.3%) | |
| 2 | 9 (26.5%) | 2 (10.5%) | 7 (46.7%) | |
| 3 | 7 (20.6%) | 4 (21.1) | 3 (20.0%) | |
| Surgical grade: | | | | 0.49 |
| 1 | 8 (22.9%) | 6 (30.0%) | 2 (13.3%) | |
| 2 | 18 (51.4%) | 9 (45.0%) | 9 (60.0%) | |
| 3 | 9 (25.7%) | 5 (25.0%) | 4 (26.7%) | |
| Histologic type | | | | |
| Endometroid | 35 (100%) | 20 (100%) | 15 (100%) | |
| Serous | 0 (0) | 0 (0) | 0 (0) | |
| Clear cell | 0 (0) | 0 (0) | 0 (0) | |
| Myometrial invasion | | | | 0.002 |
| <50% | | 10 (50.0%) | 0 (0) | |
| >50% | | 10 (50.0%) | 15 (100%) | |
| LVSI | | | | 0.04 |
| Present | 12 (34.3%) | 4 (20.0%) | 8 (53.3%) | |
| Absent | 23 (65.7%) | 16 (80.0%) | 7 (46.7%) | |
| Sentinel lymph node preformed | 29 (82.9%) | 20 (100.0%) | 9 (60.0%) | 0.003 |
| Pelvic LND performed | 35 (100%) | 20 (100%) | 15 (100%) | |
| Para aortic LND performed | 9 (25.7%) | 4 (20.0%) | 5 (33.3%) | 0.30 |
| ICG used | 20 (57.1%) | 14 (70.0%) | 6 (40.0%) | 0.07 |
| Lower uterine segment involvement | 5 (14.3%) | 2 (10%) | 3 (20%) | 0.36 |
| Number of dissected nodes, median (range) | 7 (2-33) | 4 (2-25) | 12 (3-33) | 0.008 |
| Adjuvant treatment | | | | |
| Brachytherapy | 14 (43.8%) | 11 (55.0%) | 3 (20.0%) | 0.09 |
| Pelvic radiation | 9 (28.1%) | 0 (0) | 9 (60.0%) | <0.001 |
| Chemotherapy | 16 (48.5%) | 4 (21.1%) | 12 (80.0%) | <0.001 |

**FIGURE 2** | Basic characteristics of the validation cohort.

RPL36A, BHGALNT4 and KLRC1). Ten genes were found upregulated in ≥70% of the patients and TMEM254 gene was highly expressed in 53% of the patients. (**Figure 3C**). Moreover, in the LN- group out of ten identified genes that were upregulated, only 8 genes (NEB, ANK1, AMIGO2, LZTS1, FKBP5, CHGA and USP32P) were able to be validated in the majority of the patients (≥70% of expression), while CLIC6 and HMCN1 were found expressed in only 50% of the patients (**Figures 3B, D**). Most importantly, 10 out 11 genes in LN+ group are potential precise predictors of LN involvement (>80% expression) in obese woman with EC. Furthermore, hierarchical clustering of patients according to the expression of the genes

**A** **Mean expression of top DEGs in obese patients with LN+ by RT-qPCR analysis**

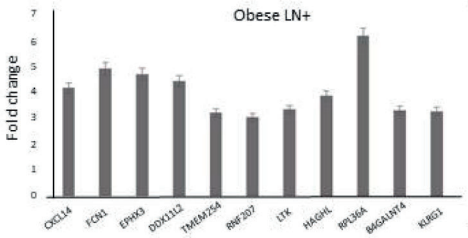


| GENE | AVERAGE |
|---|---|
| CXCL14 | 4.1464016 |
| FCN1 | 4.89140593 |
| EPHX3 | 4.68247868 |
| DDX11L2 | 4.41788338 |
| TMEM 254 | 3.1914345 |
| RNF207 | 3.03065979 |
| LTK | 3.32247843 |
| HAGHL | 3.84514399 |
| RPL36A | 6.14260085 |
| B4GALNT4 | 3.29660226 |
| KLRG1 | 3.25416692 |

**B** **Mean expression of top DEGs in obese patients with LN- by RT-qPCR analysis**

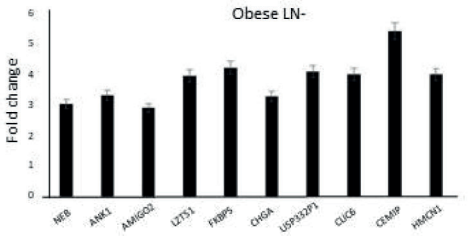


| | |
|---|---|
| NEB | 3.0672593 |
| ANK1 | 3.35595872 |
| AMIGO2 | 2.93704131 |
| LZTS1 | 3.99606759 |
| FKBP5 | 4.26629251 |
| CHGA | 3.31553696 |
| USP32P1 | 4.13812616 |
| CLIC6 | 4.05523045 |
| CEMIP | 5.47565542 |
| HMCN1 | 4.04237017 |

**C** **% of expression of each DEGs in obese patients with LN+**

| Gene in LN+ group | Total patients/UP regulated gene | % |
|---|---|---|
| **CXCL14** | 15/12 | 80 |
| **FCN1** | 15/15 | 100 |
| **EPHX3** | 15/15 | 100 |
| **DDX11L2** | 15/14 | 93 |
| **TMEM 254** | 15/8 | 53 |
| **RNF207** | 15/15 | 100 |
| **HAGHL** | 15/12 | 80 |
| **RPL36A** | 15/15 | 100 |
| **B4GALNT4** | 15/15 | 100 |
| **KLRG1** | 15/15 | 100 |
| **LTK** | 15/13 | 86 |

**D** **% of expression of each DEGs in obese patients with LN-**

| Gene in LN- group | Total patients/UP regulated gene | % |
|---|---|---|
| **NEB** | 20/14 | 70 |
| **ANK1** | 20/17 | 85 |
| **AMIGO2** | 20/14 | 70 |
| **LZTS1** | 20/16 | 80 |
| **FKBP5** | 20/15 | 75 |
| **CHGA** | 20/16 | 80 |
| **USP32P1** | 20/17 | 85 |
| **CEMIP** | 20/16 | 80 |
| **CLIC6** | 20/11 | 55 |
| **HMCN1** | 20/10 | 50 |

**FIGURE 3** | mRNA expression levels (fold change) of the differential expressed genes in **(A)** obese patients with LN+ and **(B)** LN- patients, using RT-qPCR analysis. **(C)** Percentage of expression of the differential expressed genes in patients with LN+ and **(D)** LN- patients.

showed that LN- patients were clustered together, while those in the LN+ group were clustered separately (**Figure 4**).

## CXCL14, EPHX3, TMEM 254, RPL36A, LZTS1, CLIC6, CEMIP and HMCN1 Protein Expression Levels Were Identified in the Validation Cohort Tissue Microarrays (TMA)

Using the portal of the publicly available Human Protein Atlas of the TCGA, we were able to find the protein expression status of our identified genes in EC tissue. We found that eight genes from our panel were expressed at the protein level: CXCL14, EPHX3, TMEM254, RPL36A (LN+), LZTS1, CLIC6, CEMIP and HMCN1 (LN-). Next, using immunohistochemistry we examined the protein expression levels using TMAs containing the tissue samples of our validation cohort. Our analysis revealed that the protein expressions of all of the 8 genes were confirmed to be upregulated in the EC samples compared to the normal tissue (**Figure 5**).

Furthermore, LN+ genes where highly expressed at the protein level with statistical significance (CXCL14 (P=0.045), EPHX3 (P=0.023), TMEM254 (P=0.024) and RPL36A (P=0.050)). In contrast, the same trend was also observed in LN- patients but we did not observe any statistically significant difference (LZTS1 (P= 0.18), CLIC6 (P=0.81), CEMIP (P=0.35) and HMCN1 (P=0.14)) (**Table 1**).

## DISCUSSION

The association between EC and obesity has been extensively investigated and prior reports highlighted the critical role of obesity in the development of EC, impact on patient's outcome and determination of therapeutical options (23). Indeed, surgical staging including LN assessment represents a cornerstone in the standard of care for EC (24, 25) however, in obese women, surgical intervention comprises significant challenges due to the patient's comorbidities (cardiovascular, respiratory and metabolic diseases) and the peri- and post-operative risks (vascular injury and lymphedema) (12). Furthermore, our research group showed previously a positive correlation between morbid obesity and lower detection rate of SLNs (12, 18). This highlights the value of discovering novel markers that can predict LN involvement in the preoperative period. The implementation of such biomarkers that indicate the probability for LN involvement will be valuable not only to improve patient's stratification before surgery, but also to predict patient's prognosis.

The current study approach was based on using large publicly available databases to shortlist potential genes that can predict LN involvement. This was followed by two levels of validation through RT-qPCR and immunohistochemistry using in-house patient's samples. Interestingly, we found a panel of eleven genes (CXCL14, FCN1, EPHX3, DDXIIL2, TMEM254, RNF207, LTK, HAGHL, RPL36A, BHGALNT4 and KLRC1) that were upregulated in patients with LN involvement. Among these genes, CXCL14, EPHX3, TMEM254, and RPL36A were able to detect LN involvement in obese women with EC at the mRNA and protein levels. Moreover, NEB, ANK1, AMIGO2, LZTS1, FKBP5, CHGA, USP32PI, CLIC6, CEMIP and HMCN1 genes were found to be down regulated.

In support of these findings, recently Chemokine (C-X-C Motif) Ligand 14 (CXCL14) was recently proposed through CXCL14-CXCR4 and CXCL12-CXCR4 axes to be essential for

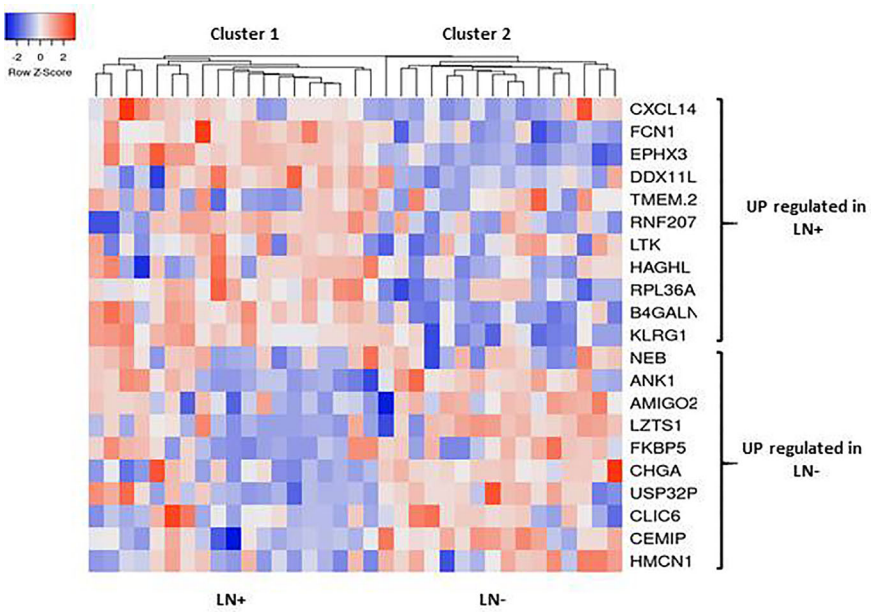


**FIGURE 4** | Hierarchical clustering heat map of differential expressed genes (rows) between LN+ and LN- tumors. Red indicates high expression and blue low expression.

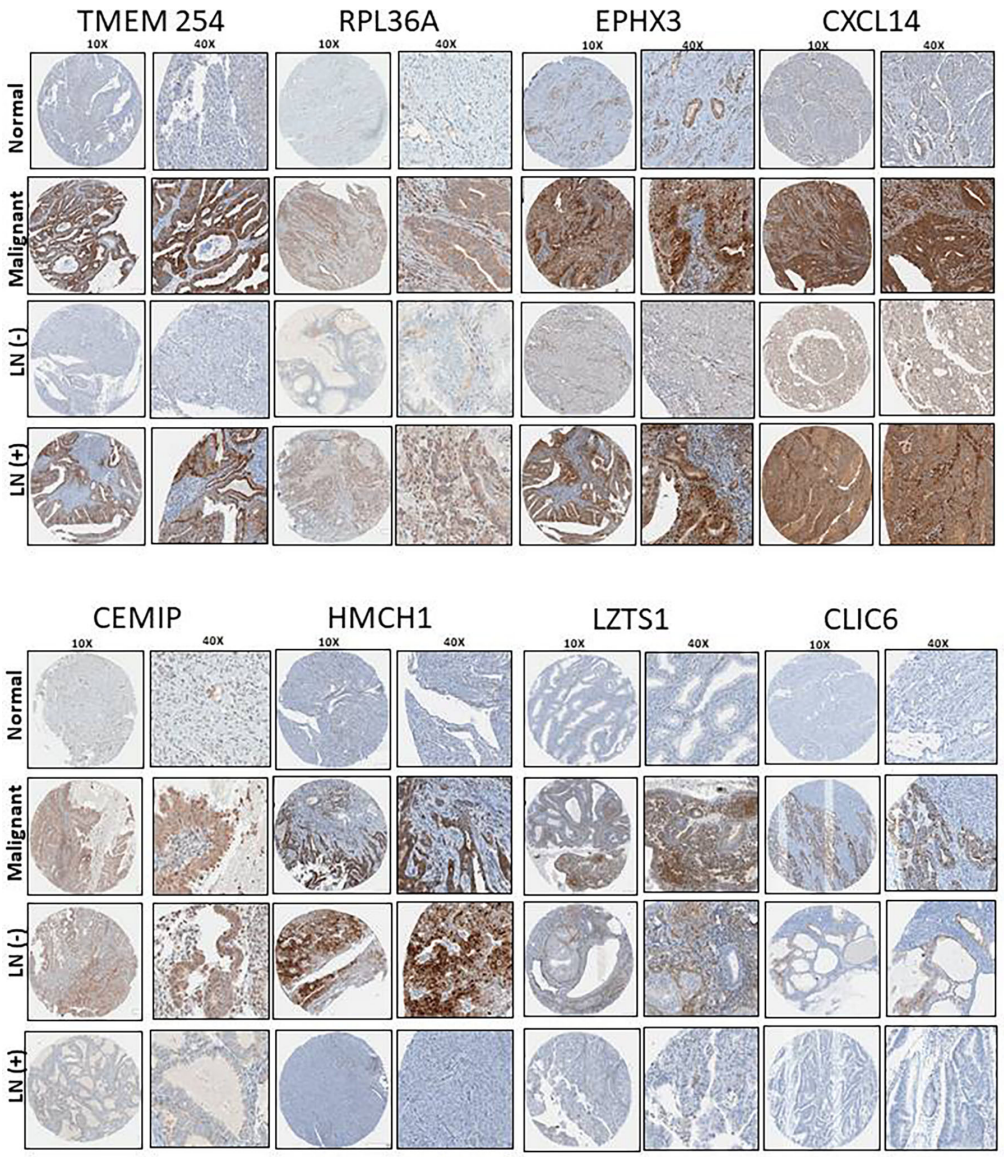


**FIGURE 5** | TMA representative images (10X and 40X) of the protein expression levels of the shortlisted genes and its association with LN status in our patient cohort consisting on 35 obese patients with EC.

the EC invasion process as well as myometrial invasion (26). Similarly, the ribosomal protein L36A (RPL36A) was also shown to play a role in the proliferation of malignant cells and was proposed as a new target for anticancer therapies. Moreover, it was overexpressed and associated with cellular proliferation in metastatic hepatocellular carcinoma (27). In addition, RPL36A was found to be one of 11 alternative splicing genes signature that can predict the prognosis of EC and was proposed as a potential target for new therapies (28). The function of the Epoxide Hydrolase 3 (EPHX3, and also known as ABDH9) is not fully understood. However, its expression, in addition to other alpha-beta hydrolase, was found to be increased in some cancers like bladder, lung carcinoids and acute myeloid leukemia (29–31).

In contrast, Leucine zipper putative tumor suppressor 1 (LZTS1), that was found to be down regulated in obese EC patients with LN involvement, is known to be a tumor suppressor gene and its expression was confirmed to be reduced in a number of malignancies including breast, esophageal and prostate cancers. Similarly, Hemicentin 1 (HMCN1, also known as fibulin 6 (FBLN6)), is an extra cellular matrix (ECM) protein, that is believed to be essential for stable cell-to-cell interactions as well as stabilization to ECM structure (32). For that reason, it was proposed to function as a

**TABLE 1** | The expression levels of the 8 shortlisted genes and its association with LN status in our patient cohort consist of 35 obese patients diagnosed with endometrioid endometrial cancer

| Protein | IHC | NAT | Malignant | P-value | LN negative | LN positive | Total | P-value |
|---|---|---|---|---|---|---|---|---|
| **HMCN1** | Positive | 3 (30%) | 19 (54.28%) | 0.31 | 13 (65%) | 6 (40%) | 19 | 0.14 |
| | Negative | 7 (70%) | 16 (45.71%) | | 7 (35%) | 9 (60%) | 18 | |
| **CLIC6** | Positive | 0 (0%) | 4 (11.42%) | 0.62 | 3 (15%) | 1 (7.1%) | 4 | 0.81 |
| | Negative | 10 (100%) | 31 (88.57%) | | 17 (85%) | 14 (93.33%) | 31 | |
| **CEMIP** | Positive | 5 (50%) | 25 (71.42%) | 0.37 | 16 (80%) | 9 (60%) | 25 | 0.35 |
| | Negative | 5 (50%) | 10 (28.57%) | | 4 (20%) | 6 (40%) | 10 | |
| **LZTS1** | Positive | 4 (40%) | 23 (65.71%) | 0.27 | 15 (75%) | 8 (53.33%) | 23 | 0.18 |
| | Negative | 6 (60%) | 12 (34.28%) | | 5 (25%) | 7 (46.67%) | 12 | |
| **CXCL14** | Positive | 1 (10%) | 24 (70.5%) | 0.001 | 11 (55%) | 13 (86.67%) | 24 | 0.045 |
| | Negative | 9 (90%) | 11 (29.5%) | | 9 (40%) | 2 (13.33%) | 11 | |
| **EPHX3** | Positive | 4 (40%) | 23 (65.71%) | 0.14 | 10 (50%) | 13 (86.67%) | 23 | 0.023 |
| | Negative | 6 (60%) | 12 (34.28%) | | 10 (50%) | 2 (13.33%) | 12 | |
| **RPL36** | Positive | 1 (10%) | 19 (54.28%) | 0.03 | 8 (40%) | 11 (73.33%) | 19 | 0.050 |
| | Negative | 9 (90%) | 16 (45.71%) | | 12 (60%) | 4 (26.67%) | 16 | |
| **TMEM254** | Positive | 3 (30%) | 18 (52.43%) | 0.23 | 7 (35%) | 11 (73.33%) | 17 | 0.024 |
| | Negative | 7 (70%) | 17 (48.57%) | | 13 (65%) | 4 (26.67%) | 18 | |

*IHC, Immunohistochemistry; NAT, normal adjacent tissue; LN, lymph node.*

metastatic suppressor in gallbladder cancer, head and neck and breast cancers (33–35). Moreover, CLIC6, is a member of the Chloride Intracellular Channel (CLIC) family, was found to be modulated in many cancers and its expression was found to be correlated with favorable outcome and better survival (36).

One of the limitations of this study is the sample number of the validation cohort, for that reason we divided the cases into only LN positive and LN negative groups. Further studies are needed to investigate not only the presence or absence of LNs, also the size and number of the LN involved that can improve our understanding of the predictive value of these markers.

In future studies, the incorporation of these predictive markers with other novel molecular groups and clinicopathological prognostic factors, might be essential to improve patient's stratification and risk assessment (37–42), that will tailor the management of endometrial cancer patients to avoid unnecessary surgical approaches. Moreover, while our results were focused on patients with endometrioid endometrial cancer further studies are needed to investigate these new biomarkers in other histological and molecular subgroups (43, 44). Notably, we can highlight that the validation of our genes using immunohistochemical analysis provide a reliable, cheaper, and widely available tool (45–47). For that reason, the accuracy of our panel at the immunohistochemistry level highlighted its feasibility and cost-effective alternative in the clinical setting.

To conclude, using publicly available microarray datasets in this study, we were able to discover a set of genes that was associated with LN status. Furthermore, the candidate genes were validated in an independent cohort from our biobank, using RT-qPCR and immunohistochemistry. Our results suggest that this novel panel might enable to predict LN involvement in obese EC patients preoperatively and may help to individualize the therapeutic approach and to reduce surgical morbidities in this high-risk population. Future studies are needed to evaluate the clinical application of these results and to investigate whether LN assessment, on the basis of this genetic panel, could be safely omitted in obese patients with EC.

## DATA AVAILABILITY STATEMENT

Publicly available datasets were analyzed in this study. This data can be found here: https://www.cbioportal.org.

## AUTHOR CONTRIBUTIONS

LL and VL-O performed RNA extractions, qPCRs and analyzed the results. MH carried out all the in-silica analysis. IH performed the histopathological evaluation. CM and EM helped in the analysis of the clinical information. VL-O conceptualization, research design and wrote the manuscript. LK, SL, and SS revised and edited the manuscript. AY and WG research design, supervised the study and drafting the manuscript. All authors made substantial contributions to the conception, design, acquisition of data, analysis and interpretation of data, all authors have been involved in revising and critically evaluating the manuscript for important intellectual content. In addition, each author has agreed to be accountable for the accuracy and integrity of this research work. All authors contributed to the article and approved the submitted version.

## FUNDING

This work was supported by grants from the Israel Cancer Research Fund (ICRF), the Gloria's Girls Fund, and the Susan and Jonathan Wener Fund.

## SUPPLEMENTARY MATERIAL

The Supplementary Material for this article can be found online at: https://www.frontiersin.org/articles/10.3389/fonc.2021.695404/full#supplementary-material

**Supplementary Figure 1** | Fold change expression of differential expressed genes in each obese patient with **(A)** LN+ and **(B)** LN-.

## REFERENCES


1. Arem H, Irwin ML. Obesity and Endometrial Cancer Survival: A Systematic Review. *Int J Obes (Lond)* (2013) 37(5):634–9. doi: 10.1038/ijo.2012.94
2. Creasman WT, Odicino F, Maisonneuve P, Quinn MA, Beller U, Benedet JL, et al. Carcinoma of the Corpus Uteri. FIGO 26th Annual Report on the Results of Treatment in Gynecological Cancer. *Int J Gynaecol Obstet* (2006) 95 (Suppl 1):S105–43. doi: 10.1016/S0020-7292(06)60031-3
3. AlHilli MM, Mariani A. The Role of Para-Aortic Lymphadenectomy in Endometrial Cancer. *Int J Clin Oncol* (2013) 18(2):193–9. doi: 10.1007/s10147-013-0528-7
4. group As, Kitchener H, Swart AM, Qian Q, Amos C, Parmar MK. Efficacy of Systematic Pelvic Lymphadenectomy in Endometrial Cancer (MRC ASTEC Trial): A Randomised Study. *Lancet* (2009) 373(9658):125–36. doi: 10.1016/S0140-6736(08)61766-3
5. Benedetti Panici P, Basile S, Maneschi F, Alberto Lissoni A, Signorelli M, Scambia G, et al. Systematic Pelvic Lymphadenectomy vs. No Lymphadenectomy in Early-Stage Endometrial Carcinoma: Randomized Clinical Trial. *J Natl Cancer Inst* (2008) 100(23):1707–16. doi: 10.1093/jnci/djn397
6. Niikura H, Kaiho-Sakuma M, Tokunaga H, Toyoshima M, Utsunomiya H, Nagase S, et al. Tracer Injection Sites and Combinations for Sentinel Lymph Node Detection in Patients With Endometrial Cancer. *Gynecol Oncol* (2013) 131(2):299–303. doi: 10.1016/j.ygyno.2013.08.018
7. Pi-Sunyer FX, Becker DM, Bouchard C, Carleton RA, Colditz GA, Dietz DH, et al. Clinical Guidelines on the Identification, Evaluation, and Treatment of Overweight and Obesity in Adults–The Evidence Report. National Institutes of Health. *Obes Res* (1998) 6 Suppl 2:51S–209S. doi: 10.1002/j.1550-8528.1998.tb00690.x
8. Calle EE, Kaaks R. Overweight, Obesity and Cancer: Epidemiological Evidence and Proposed Mechanisms. *Nat Rev Cancer* (2004) 4(8):579–91. doi: 10.1038/nrc1408
9. Renehan AG, Tyson M, Egger M, Heller RF, Zwahlen M. Body-Mass Index and Incidence of Cancer: A Systematic Review and Meta-Analysis of Prospective Observational Studies. *Lancet* (2008) 371(9612):569–78. doi: 10.1016/S0140-6736(08)60269-X
10. Daley-Brown D, Oprea-Ilies GM, Lee R, Pattillo R, Gonzalez-Perez RR. Molecular Cues on Obesity Signals, Tumor Markers and Endometrial Cancer. *Horm Mol Biol Clin Investig* (2015) 21(1):89–106. doi: 10.1515/hmbci-2014-0049
11. Kaaks R, Lukanova A, Kurzer MS. Obesity, Endogenous Hormones, and Endometrial Cancer Risk: A Synthetic Review. *Cancer Epidemiol Biomarkers Prev* (2002) 11(12):1531–43.
12. Onstad MA, Schmandt RE, Lu KH. Addressing the Role of Obesity in Endometrial Cancer Risk, Prevention, and Treatment. *J Clin Oncol* (2016) 34(35):4225–30. doi: 10.1200/JCO.2016.69.4638
13. Akbayir O, Corbacioglu Esmer A, Numanoglu C, Cilesiz Goksedef BP, Akca A, Bakir LV, et al. Influence of Body Mass Index on Clinicopathologic Features, Surgical Morbidity and Outcome in Patients With Endometrial Cancer. *Arch Gynecol Obstet* (2012) 286(5):1269–76. doi: 10.1007/s00404-012-2431-2
14. Everett E, Tamimi H, Greer B, Swisher E, Paley P, Mandel L, et al. The Effect of Body Mass Index on Clinical/Pathologic Features, Surgical Morbidity, and Outcome in Patients With Endometrial Cancer. *Gynecol Oncol* (2003) 90 (1):150–7. doi: 10.1016/S0090-8258(03)00232-4
15. Modesitt SC, van Nagell JRJr. The Impact of Obesity on the Incidence and Treatment of Gynecologic Cancers: A Review. *Obstet Gynecol Surv* (2005) 60 (10):683–92. doi: 10.1097/01.ogx.0000180866.62409.01
16. Kamal M, Burmeister C, Zhang Z, Munkarah A, Elshaikh MA. Obesity and Lymphovascular Invasion in Women With Uterine Endometrioid Carcinoma. *Anticancer Res* (2015) 35(7):4053–7.
17. von Gruenigen VE, Tian C, Frasure H, Waggoner S, Keys H, Barakat RR. Treatment Effects, Disease Recurrence, and Survival in Obese Women With Early Endometrial Carcinoma: A Gynecologic Oncology Group Study. *Cancer* (2006) 107(12):2786–91. doi: 10.1002/cncr.22351
18. Wissing M, Mitric C, Amajoud Z, Abitbol J, Yasmeen A, Lopez-Ozuna V, et al. Risk Factors for Lymph Nodes Involvement in Obese Women With Endometrial Carcinomas. *Gynecol Oncol* (2019) 155(1):27–33. doi: 10.1016/j.ygyno.2019.07.016
19. Malone ER, Oliva M, Sabatini PJB, Stockley TL, Siu LL. Molecular Profiling for Precision Cancer Therapies. *Genome Med* (2020) 12(1):8. doi: 10.1186/s13073-019-0703-1
20. Huang CY, Liao KW, Chou CH, Shrestha S, Yang CD, Chiew MY, et al. Pilot Study to Establish a Novel Five-Gene Biomarker Panel for Predicting Lymph Node Metastasis in Patients With Early Stage Endometrial Cancer. *Front Oncol* (2019) 9:1508. doi: 10.3389/fonc.2019.01508
21. Cerami E, Gao J, Dogrusoz U, Gross BE, Sumer SO, Aksoy BA, et al. The Cbio Cancer Genomics Portal: An Open Platform for Exploring Multidimensional Cancer Genomics Data. *Cancer Discovery* (2012) 2(5):401–4. doi: 10.1158/2159-8290.CD-12-0095
22. Octeau D, Kessous R, Klein K, Kogan L, Pelmus M, Ferenczy A, et al. Outcome-Related Differences in Gene Expression Profiles of High-Grade Serous Ovarian Cancers Following Neoadjuvant Chemotherapy. *Mol Cancer Res* (2019) 17(12):2422–31. doi: 10.1158/1541-7786.MCR-19-0398
23. Orekoya O, Samson ME, Trivedi T, Vyas S, Steck SE. The Impact of Obesity on Surgical Outcome in Endometrial Cancer Patients: A Systematic Review. *J Gynecol Surg* (2016) 32(3):149–57. doi: 10.1089/gyn.2015.0114
24. Amant F, Moerman P, Neven P, Timmerman D, Van Limbergen E, Vergote I. Treatment Modalities in Endometrial Cancer. *Curr Opin Oncol* (2007) 19 (5):479–85. doi: 10.1097/CCO.0b013e32827853c0
25. Santi A, Kuhn A, Gyr T, Eberhard M, Johann S, Gunthert AR, et al. Laparoscopy or Laparotomy? A Comparison of 240 Patients With Early-Stage Endometrial Cancer. *Surg Endosc* (2010) 24(4):939–43. doi: 10.1007/s00464-009-0565-5
26. Kojiro-Sanada S, Yasuda K, Nishio S, Ogasawara S, Akiba J, Ushijima K, et al. CXCL14-CXCR4 and CXCL12-CXCR4 Axes May Play Important Roles in the Unique Invasion Process of Endometrioid Carcinoma With Melf-Pattern Myoinvasion. *Int J Gynecol Pathol* (2017) 36(6):530–9. doi: 10.1097/PGP.0000000000000362
27. Kim JH, You KR, Kim IH, Cho BH, Kim CY, Kim DG. Over-Expression of the Ribosomal Protein L36a Gene is Associated With Cellular Proliferation in Hepatocellular Carcinoma. *Hepatology* (2004) 39(1):129–38. doi: 10.1002/hep.20017
28. Wang Q, Xu T, Tong Y, Wu J, Zhu W, Lu Z, et al. Prognostic Potential of Alternative Splicing Markers in Endometrial Cancer. *Mol Ther Nucleic Acids* (2019) 18:1039–48. doi: 10.1016/j.omtn.2019.10.027
29. Dyrskjot L, Kruhoffer M, Thykjaer T, Marcussen N, Jensen JL, Moller K, et al. Gene Expression in the Urinary Bladder: A Common Carcinoma in Situ Gene Expression Signature Exists Disregarding Histopathological Classification. *Cancer Res* (2004) 64(11):4040–8. doi: 10.1158/0008-5472.CAN-03-3620
30. Bhattacharjee A, Richards WG, Staunton J, Li C, Monti S, Vasa P, et al. Classification of Human Lung Carcinomas by mRNA Expression Profiling Reveals Distinct Adenocarcinoma Subclasses. *Proc Natl Acad Sci USA* (2001) 98(24):13790–5. doi: 10.1073/pnas.191502998
31. Andersson A, Ritz C, Lindgren D, Eden P, Lassen C, Heldrup J, et al. Microarray-Based Classification of a Consecutive Series of 121 Childhood Acute Leukemias: Prediction of Leukemic and Genetic Subtype as Well as of Minimal Residual Disease Status. *Leukemia* (2007) 21(6):1198–203. doi: 10.1038/sj.leu.2404688
32. Sisto M, D'Amore M, Lofrumento DD, Scagliusi P, D'Amore S, Mitolo V, et al. Fibulin-6 Expression and Anoikis in Human Salivary Gland Epithelial Cells: Implications in Sjogren's Syndrome. *Int Immunol* (2009) 21(3):303–11. doi: 10.1093/intimm/dxp001
33. Li M, Liu F, Zhang Y, Wu X, Wu W, Wang XA, et al. Whole-Genome Sequencing Reveals the Mutational Landscape of Metastatic Small-Cell Gallbladder Neuroendocrine Carcinoma (GB-SCNEC). *Cancer Lett* (2017) 391:20–7. doi: 10.1016/j.canlet.2016.12.027
34. Ledgerwood LG, Kumar D, Eterovic AK, Wick J, Chen K, Zhao H, et al. The Degree of Intratumor Mutational Heterogeneity Varies by Primary Tumor Sub-Site. *Oncotarget* (2016) 7(19):27185–98. doi: 10.18632/oncotarget.8448
35. Kikutake C, Yoshihara M, Sato T, Saito D, Suyama M. Intratumor Heterogeneity of HMCN1 Mutant Alleles Associated With Poor Prognosis in Patients With Breast Cancer. *Oncotarget* (2018) 9(70):33337–47. doi: 10.18632/oncotarget.26071
36. Gururaja Rao S, Patel NJ, Singh H. Intracellular Chloride Channels: Novel Biomarkers in Diseases. *Front Physiol* (2020) 11:96. doi: 10.3389/fphys.2020.00096
37. Concin N, Creutzberg CL, Vergote I, Cibula D, Mirza MR, Marnitz S, et al. ESGO/ESTRO/ESP Guidelines for the Management of Patients With

Endometrial Carcinoma. *Virchows Arch* (2021) 478(2):153–90. doi: 10.1007/s00428-020-03007-z
38. Concin N, Matias-Guiu X, Vergote I, Cibula D, Mirza MR, Marnitz S, et al. ESGO/ESTRO/ESP Guidelines for the Management of Patients With Endometrial Carcinoma. *Int J Gynecol Cancer* (2021) 31(1):12–39. doi: 10.1136/ijgc-2020-002230
39. Concin N, Matias-Guiu X, Vergote I, Cibula D, Mirza MR, Marnitz S, et al. ESGO/ESTRO/ESP Guidelines for the Management of Patients With Endometrial Carcinoma. *Radiother Oncol* (2021) 154:327–53. doi: 10.1016/j.radonc.2020.11.018
40. Raffone A, Travaglino A, Raimondo D, Boccellino MP, Maletta M, Borghese G, et al. Tumor-Infiltrating Lymphocytes and POLE Mutation in Endometrial Carcinoma. *Gynecol Oncol* (2021) 161(2):621–8. doi: 10.1016/j.ygyno.2021.02.030
41. Travaglino A, Raffone A, Stradella C, Esposito R, Moretta P, Gallo C, et al. Impact of Endometrial Carcinoma Histotype on the Prognostic Value of the TCGA Molecular Subgroups. *Arch Gynecol Obstet* (2020) 301(6):1355–63. doi: 10.1007/s00404-020-05542-1
42. Travaglino A, Raffone A, Mollo A, Borrelli G, Alfano P, Zannoni GF, et al. TCGA Molecular Subgroups and FIGO Grade in Endometrial Endometrioid Carcinoma. *Arch Gynecol Obstet* (2020) 301(5):1117–25. doi: 10.1007/s00404-020-05531-4
43. Travaglino A, Raffone A, Gencarelli A, Saracinelli S, Riccardi C, Mollo A, et al. Clinico-Pathological Features Associated With Mismatch Repair Deficiency in Endometrial Undifferentiated/Dedifferentiated Carcinoma: A Systematic Review and Meta-Analysis. *Gynecol Oncol* (2021) 160(2):579–85. doi: 10.1016/j.ygyno.2020.11.015
44. Travaglino A, Raffone A, Gencarelli A, Mollo A, Guida M, Insabato L, et al. TCGA Classification of Endometrial Cancer: The Place of Carcinosarcoma. *Pathol Oncol Res* (2020) 26(4):2067–73. doi: 10.1007/s12253-020-00829-9
45. Raffone A, Travaglino A, Cerbone M, De Luca C, Russo D, Di Maio A, et al. Diagnostic Accuracy of P53 Immunohistochemistry as Surrogate of TP53 Sequencing in Endometrial Cancer. *Pathol Res Pract* (2020) 216(8):153025. doi: 10.1016/j.prp.2020.153025
46. Raffone A, Travaglino A, Cerbone M, Gencarelli A, Mollo A, Insabato L, et al. Diagnostic Accuracy of Immunohistochemistry for Mismatch Repair Proteins as Surrogate of Microsatellite Instability Molecular Testing in Endometrial Cancer. *Pathol Oncol Res* (2020) 26(3):1417–27. doi: 10.1007/s12253-020-00811-5
47. Travaglino A, Raffone A, Saccone G, De Luca C, Mollo A, Mascolo M, et al. Immunohistochemical Nuclear Expression of Beta-Catenin as a Surrogate of CTNNB1 Exon 3 Mutation in Endometrial Cancer. *Am J Clin Pathol* (2019) 151(5):529–38. doi: 10.1093/ajcp/aqy178

**Conflict of Interest:** The authors declare that the research was conducted in the absence of any commercial or financial relationships that could be construed as a potential conflict of interest.

frontiers in Oncology

REVIEW
published: 28 July 2021
doi: 10.3389/fonc.2021.722639

# Cervicovaginal Microbiome Factors in Clearance of Human Papillomavirus Infection

*Wenkui Dai*[1,2,3†], *Hui Du*[1,2,3†], *Shuaicheng Li*[4*] and *Ruifang Wu*[1,2,3*]

[1] Department of Obstetrics and Gynecology, Peking University Shenzhen Hospital, Shenzhen, China, [2] Institute of Obstetrics and Gynecology, Shenzhen Peking University-The Hong Kong University of Science and Technology (PKU-HKUST) Medical Center, Shenzhen, China, [3] Shenzhen Key Laboratory on Technology for Early Diagnosis of Major Gynecologic Diseases, Shenzhen, China, [4] Department of Biomedical Engineering, City University of Hong Kong, Hong Kong, China

OPEN ACCESS

**Edited by:**
*Andrea Tinelli, Moscow Institute of Physics and Technology, Russia*

**Reviewed by:**
*Davide Carati, Ekuberg Pharma, Italy*
*Enes Taylan, Mount Sinai Hospital, United States*

***Correspondence:**
*Shuaicheng Li*
*shuaicli@cityu.edu.hk*
*Ruifang Wu*
*wurfpush@126.com*

[†]*These authors have contributed equally to this work*

**Specialty section:**
*This article was submitted to Gynecological Oncology, a section of the journal Frontiers in Oncology*

**Received:** *09 June 2021*
**Accepted:** *13 July 2021*
**Published:** *28 July 2021*

**Citation:**
*Dai W, Du H, Li S and Wu R (2021) Cervicovaginal Microbiome Factors in Clearance of Human Papillomavirus Infection. Front. Oncol. 11:722639. doi: 10.3389/fonc.2021.722639*

Persistent high-risk human papillomavirus (hrHPV) infection is the highest risk to cervical cancer which is the fourth most common cancer in women worldwide. A growing body of literatures demonstrate the role of cervicovaginal microbiome (CVM) in hrHPV susceptibility and clearance, suggesting the promise of CVM-targeted interventions in protecting against or eliminating HPV infection. Nevertheless, the CVM-HPV-host interactions are largely unknown. In this review, we summarize imbalanced CVM in HPV-positive women, with or without cervical diseases, and the progress of exploring CVM resources in HPV clearance. In addition, microbe- and host-microbe interactions in HPV infection and elimination are reviewed to understand the role of CVM in remission of HPV infection. Lastly, the feasibility of CVM-modulated and -derived products in promoting HPV clearance is discussed. Information in this article will provide valuable reference for researchers interested in cervical cancer prevention and therapy.

**Keywords: cervical cancer, high-risk HPV, CVM-targeted intervention, CVM-derived product, HPV clearance**

## INTRODUCTION

Persistent high-risk human papillomavirus (hrHPV) infection is the highest risk to invasive cervical cancer (ICC), which has caused an estimated 570,000 new cases and 311,000 deaths in 2018 (1). Prophylactic vaccines are effective in preventing HPV infection, but providing limited protection against pre-existing HPV infection which impact large populations in developing countries for a long-lasting period (2, 3). It will be an imperative alternative to prevent HPV-infected cervical intraepithelial neoplasia (CIN) and ICC by eliminating HPV infection. An increasing number of literatures suggests the association of natural HPV clearance and CIN regression with cervicovaginal microbiome (CVM) (4–8), which modulate a finely-tuned immune responses balancing reproductive tolerance with protection against genital infections (9). Our and other studies demonstrated predominance of one or few *Lactobacillus* species in CVM of healthy lower reproductive tract (LRT), including *Lactobacillus crispatus* (community-state type I, CST I), *Lactobacillus gasseri* (CST II), *Lactobacillus iners* (CST III) and *Lactobacillus jensenii* (CST V) (10–14). These *Lactobacillus* species benefit reproductive health by inhibiting pathogens *via* produced bacteriocins, lactic acid and hydrogen peroxide (15).

Emerging reports demonstrate imbalanced CVM in women with HPV infection, including increased bacterial diversity, depletion of *Lactobacillus* as well as identified high rate of natural HPV clearance in women with predominant *L. crispatus* in CVM (4, 8, 16–21). To the best of our knowledge, there is no public report investigating the mechanism of interaction between HPV and microbiome, due to difficulties to cultivate HPV *in vitro* and limited mouse models for HPV-medicated cervical dysplasia or cancer. Nevertheless, a number of studies support the concept that CVM modulates immune microenvironment through microbe- or microbe-host interactions to impact the risk of viral infections and clearance (9, 22–25). For instance, *Lactobacillus* conferred colonization resistance to *Gardnerella vaginalis* which induced suppressive immune responses beneficial to persistent HPV infection (22). M N Anahtar et al. demonstrated that CVM was the main modulator of immune responses in lower reproductive tract (LRT) and affected the risk of human immunodeficiency virus (HIV) infection (23). Peptidoglycans (PGN) produced by isolated vaginal *L. crispatus* activate Langerhans cells (LCs), which is the most important antigen presenting cells (APCs) in cervical epithelium (25), and several follow-up investigations further suggest a strong *in vivo* relationship between LCs activities and HPV clearance (26–28).

In this review, we first summarize the association of CVM with HPV infection and clearance, then discuss mechanisms of microbiome, host responses and HPV interaction. Lastly, several potentials are explored about how to eliminate pre-existing HPV infection *via* microbiome-derived products or microbiome-targeted interventions.

## IMBALANCED CVM IN HPV INFECTION

Emerging evidence suggests association between CVM and HPV infection and persistence. Almost all cross-sectional studies consistently found higher diversity of CVM in HPV-positive women, with or without CIN, as compared to HPV-negative individuals (16–21, 29–32). In recent decade, a growing body of literature suggests that depletion of *Lactobacillus* and overgrowth of anaerobic bacteria is associated with increased CVM diversity (**Figure 1**) (16–21, 29, 30). For individuals infected with HPV but without CIN or ICC, initial cross-sectional studies involving Korean (n=68 selected from 912 women in Healthy Twin Study) and Chinese (n=70) women identified reduced levels of *Lactobacillus* as well as higher abundance of bacterial vaginitis (BV)-associated bacteria such as *Gardnerella*, *Sneathia* and *Megasphaera* (18, 30). This is consistent with increased susceptibility to HPV infection in women with BV revealed by meta-analysis (33). Besides to *Gardnerella*, *Sneathia* and *Megasphaera*, additional reports found greater relative abundance of *Atopobium*, *Bacteroides*, *Prevotella* and lower proportion of *Lactobacillus* in CVM of HPV-positive women (16, 17, 29). Studies involving women with CIN or ICC consistently found significant decrease of *Lactobacillus* and substantial increase in CVM diversity compared with HPV-negative individuals (18, 19, 31, 32).

At species level of *Lactobacillus*, a marked decrease of *L. crispatus* was found in CVM of women with HPV infection, CIN or ICC, while *L. iners*-dominant CVM had higher risk of CIN (8, 18, 31, 32, 34). Additionally, women with HPV infection had accumulation of *Bacteroides plebeius*, *Acinetobacter lwoffii*, *Prevotella buccae*, *Dialister invisus*, *G. vaginalis*, *Prevotella buccalis* and *Prevotella timonensis* in CVM (29, 31, 32, 34). For instance, a study involving 70 women with CIN and 50 HPV-negative women indicated that 6-fold risk of CIN associated with unique CVM, which is characterized by paucity of *L. crispatus*, enriched *A. vaginae*, *G. vaginalis* and *L. iners* (30). Two independent systematic reviews and meta-analysis also found that *L. crispatus* correlated with decreased risk of hrHPV infection and CIN (35, 36). Compared with *L. crispatus*-dominant CVM, women with non-*Lactobacillus*- or *L. iners*-dominant CVM had 2-3 times higher odds of hrHPV prevalence and CIN, as well as 3-5 times higher odds of any prevalent HPV (95% CI) (35).

Besides to microbial components, emerging literature explores functional difference of CVM between HPV-positive and HPV-negative women (37–39). Functional prediction of 16S rDNA amplicon sequencing data found accumulation of multiple pathways in HPV-infected and CIN women, including those of folate biosynthesis and oxidative phosphorylation (37). Metagenomic analysis of 17 CIN, 12 ICC cases and 18 healthy individuals found enriched genes related to peptidoglycan synthesis as well as depletion of dioxin degradation and 4-oxalocrotonate tautomerase in CVM of women with CIN or ICC (38). Biofilm formation assessment identified higher formation rate in HPV-positive women (45%) compared to HPV-negative women (21.9%) (39), which may be

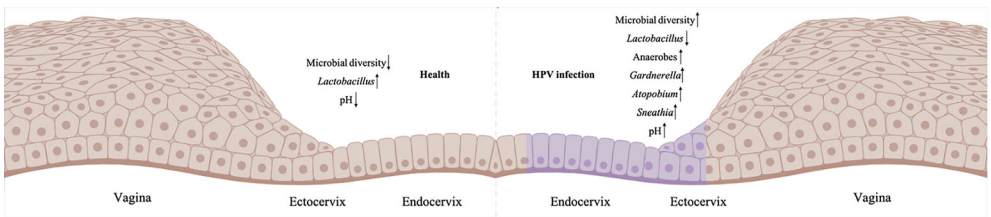


**FIGURE 1** | Imbalanced CVM in HPV-infected cervix. The left is the normal cervicovaginal microenvironment without HPV infection, and the right is HPV-positive microenvironment (HPV-infected cells are labelled purple). Created in BioRender.com.

attributed to increased levels of obligate anaerobic bacteria in CVM of HPV-infected women, such as *G. vaginalis* with sialidase-encoding gene involved in biofilm formation (8).

Above-mentioned observational studies are only possible to demonstrate association of CVM with HPV infection and CIN diseases rather than causality. Longitudinal data is increasingly applied to explore the causal link (7, 40, 41), which has profound clinical impact to provide effective alternatives for therapeutic strategies of HPV-infected CIN. Six-month follow-up of 211 Nigerian women showed the association of *Lactobacillus* paucity and high CVM diversity with persistent hrHPV infection (40). Analysis of serial cervicovaginal specimens obtained over 8-10 years unraveled that high relative abundance of *L. crispatus* in CVM had the lowest risk of HPV infection compared to other types of CVM, according to 16S V1-V2 rRNA gene amplicon sequencing and HPV DNA testing conducted annually (41). Brotman and colleagues collected self-sampled mid-vaginal swabs twice a week for 16 weeks from 32 reproductive-age women, and showed that depletion of *Lactobacillus* in CVM may increase the chance to acquire transient and persistent HPV infection (7). Consistently, meta-analysis involving 39 articles suggests the protection against HPV infection imposed by *Lactobacillus*-dominant CVM (42). Another systematic review and meta-analysis of longitudinal studies also support a causal relationship between non-*Lactobacillus*-dominant CVM and cervical carcinogenesis *via* the effect of CVM on HPV infection (RR 1.33, 95% CI) and persistence (RR 1.14) (43).

## CVM IS ASSOCIATED WITH NATURAL HPV CLEARANCE AND CIN REGRESSION

According to a follow-up analysis on 55 women with HPV infection and 17 age-matched healthy HPV-negative women, *L. crispatus* was the most abundant *Lactobacillus* species in individuals with natural HPV clearance (**Figure 2A**) (8). Conversely, high proportion of *Atopobium* in CVM had significantly slowed HPV remission rate in 16-week follow-up, compared to *L. crispatus*-dominant CVM[8]. Another longitudinal study involving 64 HPV16-positive women found more frequent transition between identified CSTs, including dominant *Lactobacillus* sp., *L. iners*, two mixed non-*Lactobacillus* of CVM, in women with persistent HPV16 infection (34% with averaged 155.5 days interval) when compared to women with natural clearance of HPV16 (19% with averaged 162 days interval) (**Figure 2A**) (6). Consistently, Anita Mitra and partners found more stable CVM in women with CIN2 regression, as compared to individuals with CIN persistence or progression[4]. In this study,

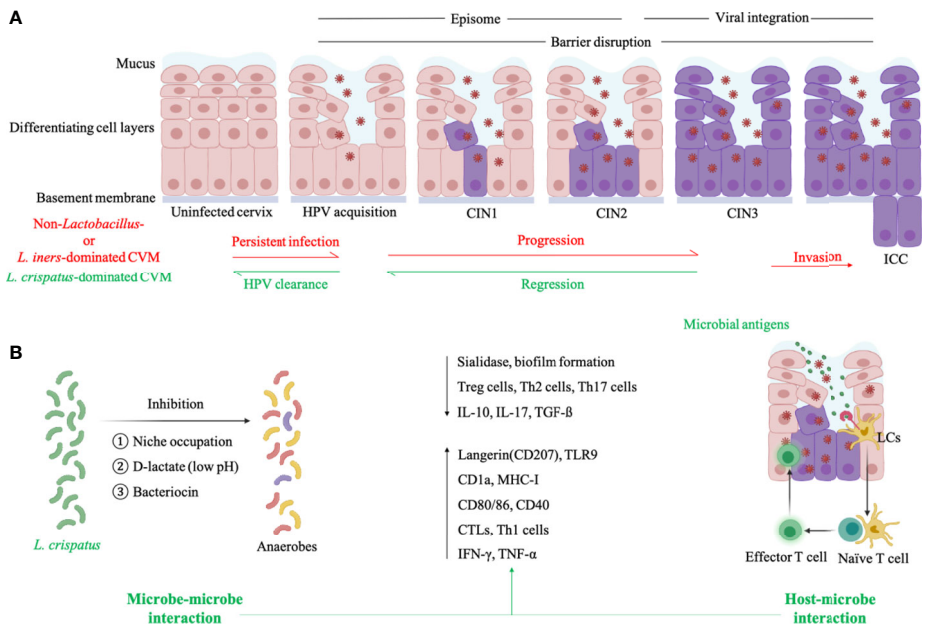


**FIGURE 2** | Cervicovaginal microenvironment in persistent HPV infection and natural HPV clearance. **(A)** *L. iners*- or non-*Lactobacillus*-dominated CVM is characterized by allowing the proliferation of anaerobes which produce sialidase to disrupt epithelial barrier and then facilitate the entry of HPV. HPV particles exist in infected keratinocytes as episomes before entry into the nucleus, and viral integration induces high expression of E6/E7 proteins to promote abnormal cell proliferation as well as carcinogenesis. *L. crispatus*-dominated CVM is associated with natural HPV clearance and CIN regression. **(B)** For HPV-positive women with *L. crispatus*-dominated CVM, *L. crispatus* can inhibit growth of anaerobes through several mechanisms (microbe-microbe interaction) and activate LCs which is the only APCs in cervical epithelium to present HPV antigens and induce HPV-specific CMI (host-microbe interaction). Both microbe- and host-microbe interaction decrease the level of factors correlated with barrier impairment (sialidase and biofilm of anaerobes) and suppressive immunity (Treg, Th2, Th17 cells, IL-10, IL-17, TGF-ß), and increase the expression of biomarkers in activated LCs (antigen-binding langerin and TLR9, antigen-presenting CD1a and MHC-I, co-stimulatory molecule CD80/86 and CD40) as well as CMI-associated molecules (cytotoxic T lymphocytes-CTLs, Th1 cells, IFN-γ, TNF-α). This figure applied icons in BioRender.com.

87 CIN2 patients aged 16-26 years old were included in two-year follow-up showing that women with *Lactobacillus*-dominant CVM at baseline are more likely to regress at 12 months while slower regression was associated with *Lactobacillus* depletion as well as increased abundance of *Megasphaera*, *Prevotella timonensis* and *G. vaginalis* (4). At species level, women with *L. crispatus*-dominant CVM had faster regression and higher rate of CIN remission at 12 and 24 months (4).

A total of four CSTs, dominated by *L. crispatus*, *L. iners*, *G. vaginalis* and mixed genus, was identified in another study involving 273 women aged 18-25 years old (5). At first visit, *Lactobacillus* and *Gardnerella* abundance was associated with CIN2 regression and progression respectively. Second visit was conducted at least 305 days after first visit, and CIN2 progression had strong correlation with increased bacterial diversity. Functional prediction of 16S rDNA amplicon sequencing data further showed the positive relationship between pathway of cell motility and CIN2 regression, while progression was in association with "Xenobiotics Biodegradation and Metabolism" pathway in CVM.

Fungal components in CVM were also associated with HPV-infected CIN regression (5). Mykhaylo Usyk and colleagues found the protective effect of fungal diversity against CIN progression (OR=0.90, 0.82-1.00) (5). Among fungus *Candida*, *Malassezia* and Sporidiobolaceae, the accumulation of *Candida* was identified in CVM of CIN1 which had the highest regression rate (5). Additionally, a retrospective investigation on 100,605 women who had 2 smears each over a period of 12 years, found that common fungus *Candida* in cervicovaginal microenvironment decreased the risk of squamous intraepithelial lesions (44).

## MICROBE- AND HOST-MICROBE INTERACTIONS IN HPV CLEARANCE

The complexity of cervicovaginal microenvironment of women with HPV infection is determined by HPV, CVM and the host. To explore the contribution of CVM to promote or protect against HPV infection, there is much work to be done in exploring microbe-microbe interactions in CVM, as well as the interactions between microbe and HPV/host (**Figure 2B**).

Sialidase are a group of mucin-degrading enzymes produced by BV-associated *G. vaginalis* and *Prevotella*, and disrupt the integrity of mucosa as well as epithelium to aid the entry of HPV to basal keratinocytes (**Figure 2A**) (45). Besides to compromised cervical epithelial barrier, BV-associated anaerobes also impact several cellular pathways to enable persistent viral infection and subsequent disease development (46–50). *Sneathia* spp., commonly accumulated in CVM of BV and HPV-infected patients, belongs to *Fusobacterium* genus which can activate proinflammatory pathways and inhibit immunocytotoxicity to promote carcinogenesis (51). This information may explain the high susceptibility to HPV infection in women with BV and accumulation of vaginal obligate anaerobic bacteria in women with persistent HPV infection or cervical dysplasia progression (16–18, 29, 30, 33).

Vaginal *Lactobacillus* spp. can produce a large amount of lactic acid through glycogen fermentation, maintaining acidic environment to inhibit the colonization of several pathogenic species such as *Chlamydia trachomatis*, *Neisseria gonorrhoeae* and BV-associated *G. vaginalis* (**Figure 2B**) (15, 52–55). Bacteriocins produced by vaginal *Lactobacillus* also exhibit inhibitory effects on common pathogenic bacteria and certain fungi, such as *G. vaginalis* and *Candida albicans* (**Figure 2B**) (15, 56, 57). In addition, *Lactobacillus* hold the potential to alter surface tension and thus bacterial adhesion which is pivotal in biofilm formation *via* excreted biosurfactants, therefore preventing overgrowth of pathogenic anaerobes, especially *G. vaginalis* (**Figure 2B**) (22, 58–60). Another defense factor derived from vaginal *Lactobacillus* is $H_2O_2$, which destroys vaginal bacterial components with limited expression of $H_2O_2$-degrading enzymes, including *Prevotella* and *Gardnerella* (60, 61). Besides direct inhibition on pathogens, *Lactobacillus* can occupy possible niches to indirectly protect against pathogen colonization (**Figure 2B**). For instance, epithelium adhesin facilitates the adhesion of *L. crispatus* to genital mucosa and then additionally inhibits pilus-mediated adhesion of *G. vaginalis* (22).

As discussed above, vaginal *Lactobacillus* play critical roles in cervicovaginal health, but not all *Lactobacillus*-dominant CVM benefit the host in the same manner. Lactic acid has D- and L-isomer while the former is mainly produced by *L. jensenii*, *L. crispatus*, *L. gasseri* and the latter is produced by *L. iners* and a variety of anaerobes (62). Women with *L. iners*- or non-*Lactobacillus*-dominant CVM therefore have a higher ratio of L- and D-lactate, increasing the expression of extracellular matrix metalloproteinase inducer and activating matrix metalloproteinase 8, which facilitate the entry of HPV to the basal keratinocytes by altering cervical integrity (**Figure 2A**) (62). Conversely, *L. crispatus*-dominant CVM can lead to increased cervicovaginal mucus viscosity and promote viral capture (63). Additionally, CVM predominated by *L. iners* is more instable than CVM with other dominant *Lactobacillus* species and therefore allows growth of strict anaerobes resulting in transition to non-*Lactobacillus*-dominant CVM (4, 64). This is consistent with findings that *L. iners*-dominant CVM tends to be identified in women with persistent HPV infection and progression of cervical diseases (**Figure 2A**) (8, 18, 31, 32, 34). On the contrary, *L. crispatus*-dominant CVM has the lowest possibility in transition to other CVM types (4, 13, 64), and is thus positively associated with cervicovaginal health (**Figure 2A**).

Though many clues exist in microbe-microbe interactions, there are no published reports exploring the mechanism of interaction between CVM and HPV, due to the difficulties of *in vitro* HPV cultivation. Nevertheless, a growing number of literatures demonstrate unique host immune responses (**Figure 2B**) (65), which mediate the CVM-HPV interactions in women with HPV infection. Oncoproteins of hrHPV can suppress presentation of hrHPV antigens and impair alarm functions of infected basal keratinocytes where HPV thrive. For example, hrHPV E7 protein can lead to repression of major histocompatibility complex I (MHC I), LMP2 as well as

TAP1 gene through interaction with MHC I promoter, and E5 protein blocks the transport of MHC I and CD1d to the cell surface, which is crucial for HPV antigen presentation (66–71). Infection of hrHPV also reduce the expression of infected keratinocyte-derived chemokine (C-C motif) ligand 20 (CCL20) (72, 73), attracting the migration of LCs which is the only APCs in vaginal epithelium where HPV infection occurs. In addition, hrHPV infection is associated with suppressed LCs activities, including decreased levels of E-cadherin remaining LCs in infected epidermis to capture HPV antigens, and antigen-binding langerin as well as TLR (74–78). Once internalizating HPV antigens, LCs become mature and migrate to lymph nodes *via* chemokine (C-C-motif) receptor 7 (CCR7) on cell surface. However, prior reports found reduced expression of CCR7 in ICC patients, and identified decreased levels of LCs-membrane antigen-presenting and co-stimulatory molecules in exposure to HPV virus-like particles (VLPs), including CD1a, MHC I, CD40 and CD80/86 (66, 67, 75, 76, 79–81).

To the best of our knowledge, no report established *in vivo* CVM-LCs relationship, which can partly improve the understanding of CVM-HPV interactions. Nevertheless, *in vitro* experiment found that a *L. crispatus* strain isolated from vagina activated LCs *via* cell wall-derived PGN, being assessed by elevated expression of TLR (**Figure 2B**) (25). This is consistent with prior findings that TLR agonists promote LCs activation and the induction of HPV-specific cell-mediated immunity (CMI) (77, 78, 82). Candin, produced by *Candida* which is inversely associated with HPV infection, can induce proliferation of T cells to enhance the effect of therapeutic vaccines against HPV (44, 83, 84). Herbst-Kralovetz MM and colleagues also found significant differences of CVM and cervical immune microenvironment between HPV-negative women (n=18), HPV-infected individuals without squamous intraepithelial lesion (n=11), HPV-positive women with low (n=12)/high (n=27) intraepithelial lesion, and ICC patients (n=10) (85–88). For instance, inhibitory immune checkpoint protein PD-L1 and LAG-3 were negatively correlated with *Lactobacillus* abundance in CVM, while TLR2 was in positive relationship with *Lactobacillus* abundance. Conversely, PD-L1 and LAG-3 positively correlated to dysbiosis-associated *Gardnerella*, *Sneathia*, *Atopobium* and *Prevotella*. At species level, *L. crispatus* and *L. jensenii* were in negative relationship with PD-L1, while *L. gasseri* was negatively associated with LAG-3. In addition, a 12-month observational study applied the combination of 16S rDNA amplicon sequencing, metagenome, transcriptional profiling and immunological profiling to demonstrate the critical role of cervicovaginal bacteria in modulating cervicovaginal immune responses and the host susceptibility to HIV (23).

## APPLICATION OF CVM IN PROMOTING HPV CLEARANCE

Given the critical roles of CVM in modulating cervical immune responses, it is promising to promote HPV clearance by re-constructing CVM (**Figure 3A**). Taken vaginal probiotics *L. crispatus* strain CTV-05 for example, a randomized placebo-controlled clinical trial showed that the vaginal colonization with CTV-05 following 28-day treatment inhibited BV-associated *Atopobium* growth (89, 90). Another trial involving 100 participants assessed the efficacy of CTV-05 on preventing urinary tract infection (UTI), indicating the reduction of recurrent UTI when compared to placebo treatment (91). Disrupting biofilm of anaerobes is also an alternative therapy against vaginal dysbiosis, and Marrozzo J. M. et al. found 50-59% clinical cure rate of BV in 106 participants 9-12 days after treatment (92).

In addition, several *in vitro* and *in vivo* studies suggest the promise of prebiotics, which are indigestible carbohydrates, in promoting the growth of probiotics or beneficial commensals in the vagina (**Figure 3A**) (93–95). For example, fructo-oligosaccharide (FOS) and gluco-oligosaccharide (GOS) benefited the growth of *L. crispatus*, *L. jensenii* and *L. vaginalis in vitro*, while pathogen *C. albicans*, *Escherichia coli* and *G. vaginalis* could not utilize FOS/GOS as energy sources for growth (93). Significant reduction of Nugent scores was also identified in BV patients receiving intravaginal GOS gel immediately following metronidazole treatment (94). Additionally, glucomannan hydrolysates (GMH) also held the potential to promote *Lactobacillus* spp. colonization, conferring health to the host in *C. albicans*-infected women (95). To re-establish the CVM completely, two studies in 2019 conducted vaginal microbiota transplantation (VMT) (**Figure 3A**) (96, 97). A total of 5 women with antibiotic-unresponsive and recurrent BV were included in one study, and 4 out of 5 participants had restoration of *Lactobacillus*-dominant CVM and long-term remission without any adverse effect at the follow-up of 5-21 months. The other study involving 20 women explained and implemented a screening approach for universal VMT donors.

Besides to CVM-targeted interventions, CVM-derived products hold the promise as immune modulators, such as adjuvants of therapeutic vaccines (**Figure 3B**). Jie Song and co-workers demonstrated that PGN produced by a vaginal *L. crispatus* strain enhanced the expression of cell-membrane TLR2 and TLR6 to activate LCs (25), which play a pivotal role in capturing and presenting HPV antigens. The products of specific bacterial components have the potential to be effective adjuvants as a series of clinical trials demonstrated enhanced efficacy of therapeutic vaccines adjuvanted with TLR agonists which could be served by bacterial products (98–101). Furthermore, bacterial vectors are increasingly explored as alternative live vectors due to their potential as "natural" adjuvants, which attributed to the wide range of pathogen-associated molecular pattern molecules and damage-associated molecular pattern molecules (102–106). Additionally, candin produced by common vaginal fungal pathobiont *Candida* could be utilized as adjuvant for therapeutic vaccine, which partly explain the protection of vaginal *Candida* against HPV infection (44, 83, 84).

## CONCLUSION

CVM appears to play a crucial role in HPV acquisition and persistence as well as subsequent development of squamous

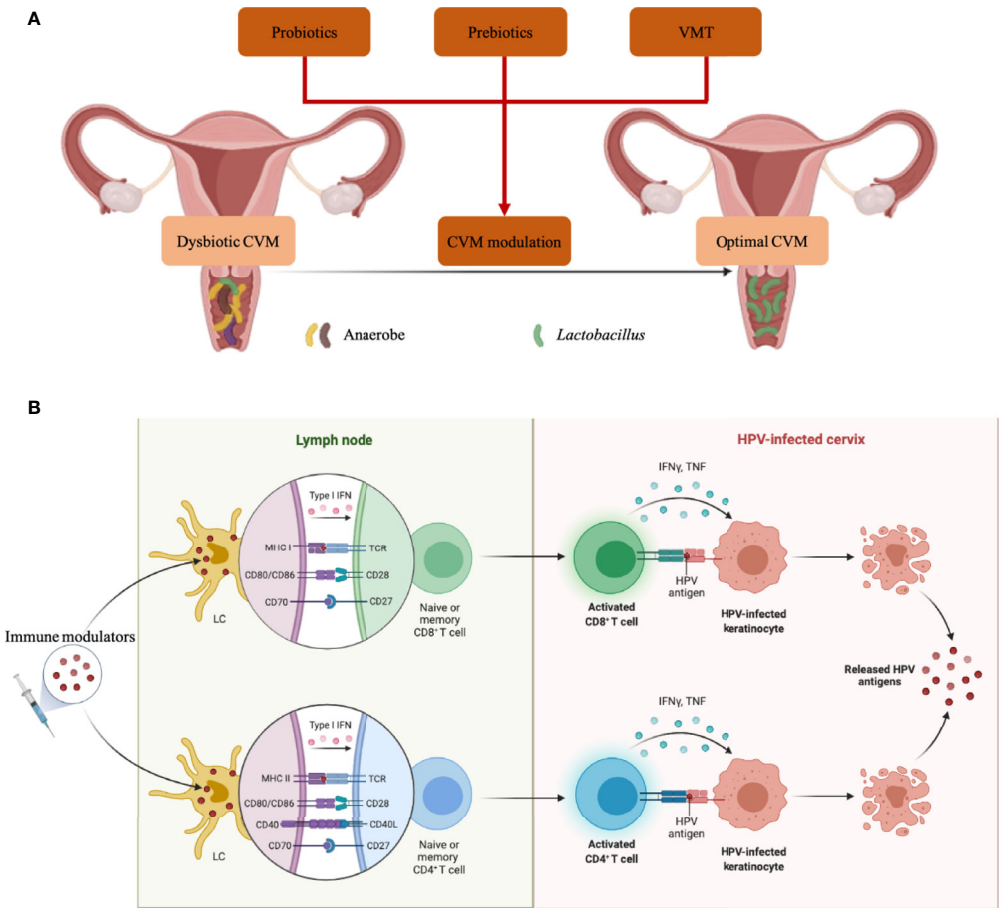


**FIGURE 3** | CVM-modulated and -derived products in eliminating HPV infection. **(A)** Strategies to modulate dysbiotic CVM were characterized by anaerobe overgrowth. **(B)** Molecules produced by specific microbial strains in CVM can activate LCs in the cervical epithelium, then promote T cell priming and eliminate HPV-infected cells. Icons in BioRender.com were utilized to prepare this figure.

intraepithelial lesion. Cross-sectional nature of most studies makes it difficult to derive a causal link between CVM and HPV infection or clearance. In addition, many prior reports described CVM in relatively small cohorts, which analysis results could be compounded by various factors, such as smoking and sex activities. Prospective cohort study will be needed in the future to prove that CVM could prevent HPV infection and promote HPV clearance. This information will determine the promise of CVM interventions as novel therapies, with the advantage of low-cost feasibility in developing countries. Nevertheless, it is imperative to find the most protective strains before developing CVM-targeted probiotics or prebiotics, for which the efficacy can be impacted by pre-existed CVM. For example, *L. crispatus*-dominated CVM confers high colonization resistance to other microbes and even probiotic *L. crispatus* strain, while pre-colonization of the vagina with endogenous *L. iners* allows growth of anaerobes. Therefore, CVM structure should be taken into consideration when it comes to assess the efficacy of specific probiotics and prebiotics. However, 16S rDNA amplicon sequencing that most studies applied has limitations in conducting strain-level analysis and microbe-microbe/host interactions of CVM, necessitating the utilization of multi-omics in analyzing "key microbial strains". Then mechanistic studies of these strains should be conducted to further the utilization of "key microbial strains" as immune modulators in prevention and clearance of HPV infection. Given the importance of cervical epithelial LCs in presenting HPV antigens to induce HPV-specific CMI, it will be an effective mediator of therapeutic vaccine immunity. As discussed above, specific microbial strains in CVM hold the potential to activate HPV-suppressed LCs, suggesting the promise of microbial products as robust activator of immunity against HPV or adjuvants in therapeutic vaccines. In the future, the combination of culture-independent and -dependent techniques should be applied to screen promising microbial strains and products which functions can be assessed in cell lines or animal models. Lastly, though VMT can modify the whole cervicovaginal microenvironment, randomized, placebo-controlled studies for large cohorts are required to determine the clinical efficacy as well as long-term benefits.

## AUTHOR CONTRIBUTIONS

WD and RW made substantial contributions to the design and writing of this manuscript. HD and SL contributed to the discussion and conception of the work. All authors contributed to the article and approved the submitted version.

## FUNDING

This work was supported by Shenzhen High-level Hospital Construction Fund (YBH2019-260), Shenzhen Key Medical Discipline Construction Fund (No. SZXK027) and Sanming Project of Medicine in Shenzhen (No. SZSM202011016).

## REFERENCES

1. Bray F, Ferlay J, Soerjomataram I, Siegel RL, Torre LA, Jemal A. Global Cancer Statistics 2018: GLOBOCAN Estimates of Incidence and Mortality Worldwide for 36 Cancers in 185 Countries. *CA Cancer J Clin* (2018) 68 (6):394–424. doi: 10.3322/caac.21492
2. Hildesheim A, Herrero R, Wacholder S, Rodriguez AC, Solomon D, Bratti MC, et al. Effect of Human Papillomavirus 16/18 L1 Viruslike Particle Vaccine Among Young Women With Preexisting Infection: A Randomized Trial. *JAMA* (2007) 298(7):743–53. doi: 10.1001/jama.298.7.743
3. Group FIS. Quadrivalent Vaccine Against Human Papillomavirus to Prevent High-Grade Cervical Lesions. *N Engl J Med* (2007) 356(19):1915–27. doi: 10.1056/NEJMoa061741
4. Mitra A, MacIntyre DA, Ntritsos G, Smith A, Tsilidis KK, Marchesi JR, et al. The Vaginal Microbiota Associates With the Regression of Untreated Cervical Intraepithelial Neoplasia 2 Lesions. *Nat Commun* (2020) 11 (1):1999. doi: 10.1038/s41467-020-15856-y
5. Usyk M, Zolnik CP, Castle PE, Porras C, Herrero R, Gradissimo A, et al. Cervicovaginal Microbiome and Natural History of HPV in a Longitudinal Study. *PloS Pathog* (2020) 16(3):e1008376. doi: 10.1371/journal.ppat.1008376
6. Berggrund M, Gustavsson I, Aarnio R, Lindberg JH, Sanner K, Wikstrom I, et al. Temporal Changes in the Vaginal Microbiota in Self-Samples and its Association With Persistent HPV16 Infection and CIN2. *Virol J* (2020) 17 (1):147. doi: 10.1186/s12985-020-01420-z
7. Brotman RM, Shardell MD, Gajer P, Tracy JK, Zenilman JM, Ravel J, et al. Interplay Between the Temporal Dynamics of the Vaginal Microbiota and Human Papillomavirus Detection. *J Infect Dis* (2014) 210(11):1723–33. doi: 10.1093/infdis/jiu330
8. Di Paola M, Sani C, Clemente AM, Iossa A, Perissi E, Castronovo G, et al. Characterization of Cervico-Vaginal Microbiota in Women Developing Persistent High-Risk Human Papillomavirus Infection. *Sci Rep* (2017) 7 (1):10200. doi: 10.1038/s41598-017-09842-6
9. Al-Nasiry S, Ambrosino E, Schlaepfer M, Morre SA, Wieten L, Voncken JW, et al. The Interplay Between Reproductive Tract Microbiota and Immunological System in Human Reproduction. *Front Immunol* (2020) 11:378. doi: 10.3389/fimmu.2020.00378
10. Chen C, Song X, Wei W, Zhong H, Dai J, Lan Z, et al. The Microbiota Continuum Along the Female Reproductive Tract and Its Relation to Uterine-Related Diseases. *Nat Commun* (2017) 8(1):875. doi: 10.1038/s41467-017-00901-0
11. Ma B, France MT, Crabtree J, Holm JB, Humphrys MS, Brotman RM, et al. A Comprehensive Non-Redundant Gene Catalog Reveals Extensive Within-Community Intraspecies Diversity in the Human Vagina. *Nat Commun* (2020) 11(1):940. doi: 10.1038/s41467-020-14677-3
12. Ravel J, Gajer P, Abdo Z, Schneider GM, Koenig SS, McCulle SL, et al. Vaginal Microbiome of Reproductive-Age Women. *Proc Natl Acad Sci U S A* (2011) 108(Suppl 1):4680–7. doi: 10.1073/pnas.1002611107
13. Gajer P, Brotman RM, Bai G, Sakamoto J, Schutte UM, Zhong X, et al. Temporal Dynamics of the Human Vaginal Microbiota. *Sci Transl Med* (2012) 4(132):132ra52. doi: 10.1126/scitranslmed.3003605
14. Chaban B, Links MG, Jayaprakash TP, Wagner EC, Bourque DK, Lohn Z, et al. Characterization of the Vaginal Microbiota of Healthy Canadian Women Through the Menstrual Cycle. *Microbiome* (2014) 2:23. doi: 10.1186/2049-2618-2-23
15. Kovachev S. Defence Factors of Vaginal Lactobacilli. *Crit Rev Microbiol* (2018) 44(1):31–9. doi: 10.1080/1040841X.2017.1306688
16. Cheng L, Norenhag J, Hu YOO, Brusselaers N, Fransson E, Ahrlund-Richter A, et al. Vaginal Microbiota and Human Papillomavirus Infection Among Young Swedish Women. *NPJ Biofilms Microbiomes* (2020) 6(1):39. doi: 10.1038/s41522-020-00146-8
17. Zhou Y, Wang L, Pei F, Ji M, Zhang F, Sun Y, et al. Patients With Lr-Hpv Infection Have a Distinct Vaginal Microbiota in Comparison With Healthy Controls. *Front Cell Infect Microbiol* (2019) 9:294. doi: 10.3389/fcimb.2019.00294
18. Oh HY, Kim BS, Seo SS, Kong JS, Lee JK, Park SY, et al. The Association of Uterine Cervical Microbiota With an Increased Risk for Cervical Intraepithelial Neoplasia in Korea. *Clin Microbiol Infect* (2015) 21(7):674 e1–9. doi: 10.1016/j.cmi.2015.02.026
19. Mitra A, MacIntyre DA, Lee YS, Smith A, Marchesi JR, Lehne B, et al. Cervical Intraepithelial Neoplasia Disease Progression Is Associated With Increased Vaginal Microbiome Diversity. *Sci Rep* (2015) 5:16865. doi: 10.1038/srep16865
20. Borgogna JC, Shardell MD, Santori EK, Nelson TM, Rath JM, Glover ED, et al. The Vaginal Metabolome and Microbiota of Cervical HPV-Positive and HPV-Negative Women: A Cross-Sectional Analysis. *BJOG* (2020) 127 (2):182–92. doi: 10.1111/1471-0528.15981
21. Lee JE, Lee S, Lee H, Song YM, Lee K, Han MJ, et al. Association of the Vaginal Microbiota With Human Papillomavirus Infection in a Korean Twin Cohort. *PloS One* (2013) 8(5):e63514. doi: 10.1371/journal.pone.0063514
22. Ojala T, Kankainen M, Castro J, Cerca N, Edelman S, Westerlund-Wikstrom B, et al. Comparative Genomics of Lactobacillus Crispatus Suggests Novel Mechanisms for the Competitive Exclusion of Gardnerella Vaginalis. *BMC Genomics* (2014) 15:1070. doi: 10.1186/1471-2164-15-1070
23. Anahtar MN, Byrne EH, Doherty KE, Bowman BA, Yamamoto HS, Soumillon M, et al. Cervicovaginal Bacteria Are a Major Modulator of Host Inflammatory Responses in the Female Genital Tract. *Immunity* (2015) 42(5):965–76. doi: 10.1016/j.immuni.2015.04.019
24. Doerflinger SY, Throop AL, Herbst-Kralovetz MM. Bacteria in the Vaginal Microbiome Alter the Innate Immune Response and Barrier Properties of the Human Vaginal Epithelia in a Species-Specific Manner. *J Infect Dis* (2014) 209(12):1989–99. doi: 10.1093/infdis/jiu004
25. Song J, Lang F, Zhao N, Guo Y, Zhang H. Vaginal Lactobacilli Induce Differentiation of Monocytic Precursors Toward Langerhans-Like Cells: *In Vitro* Evidence. *Front Immunol* (2018) 9:2437. doi: 10.3389/fimmu.2018.02437
26. Shannon B, Yi TJ, Perusini S, Gajer P, Ma B, Humphrys MS, et al. Association of HPV Infection and Clearance With Cervicovaginal Immunology and the Vaginal Microbiota. *Mucosal Immunol* (2017) 10 (5):1310–9. doi: 10.1038/mi.2016.129
27. Kindt N, Descamps G, Seminerio I, Bellier J, Lechien JR, Pottier C, et al. Langerhans Cell Number Is a Strong and Independent Prognostic Factor for Head and Neck Squamous Cell Carcinomas. *Oral Oncol* (2016) 62:1–10. doi: 10.1016/j.oraloncology.2016.08.016
28. Miyagi J, Kinjo T, Tsuhako K, Higa M, Iwamasa T, Kamada Y, et al. Extremely High Langerhans Cell Infiltration Contributes to the Favourable Prognosis of HPV-Infected Squamous Cell Carcinoma and Adenocarcinoma of the Lung. *Histopathology* (2001) 38(4):355–67. doi: 10.1046/j.1365-2559.2001.01067.x
29. Chao XP, Sun TT, Wang S, Fan QB, Shi HH, Zhu L, et al. Correlation Between the Diversity of Vaginal Microbiota and the Risk of High-Risk Human Papillomavirus Infection. *Int J Gynecol Cancer* (2019) 29(1):28–34. doi: 10.1136/ijgc-2018-000032
30. Gao W, Weng J, Gao Y, Chen X. Comparison of the Vaginal Microbiota Diversity of Women With and Without Human Papillomavirus Infection: A Cross-Sectional Study. *BMC Infect Dis* (2013) 13:271. doi: 10.1186/1471-2334-13-271
31. So KA, Yang EJ, Kim NR, Hong SR, Lee JH, Hwang CS, et al. Changes of Vaginal Microbiota During Cervical Carcinogenesis in Women With

Human Papillomavirus Infection. *PloS One* (2020) 15(9):e0238705. doi: 10.1371/journal.pone.0238705
32. Zhang C, Liu Y, Gao W, Pan Y, Gao Y, Shen J, et al. The Direct and Indirect Association of Cervical Microbiota With the Risk of Cervical Intraepithelial Neoplasia. *Cancer Med* (2018) 7(5):2172–9. doi: 10.1002/cam4.1471
33. Liang Y, Chen M, Qin L, Wan B, Wang H. A Meta-Analysis of the Relationship Between Vaginal Microecology, Human Papillomavirus Infection and Cervical Intraepithelial Neoplasia. *Infect Agent Cancer* (2019) 14:29. doi: 10.1186/s13027-019-0243-8
34. Seo SS, Oh HY, Lee JK, Kong JS, Lee DO, Kim MK. Combined Effect of Diet and Cervical Microbiome on the Risk of Cervical Intraepithelial Neoplasia. *Clin Nutr* (2016) 35(6):1434–41. doi: 10.1016/j.clnu.2016.03.019
35. Norenhag J, Du J, Olovsson M, Verstraelen H, Engstrand L, Brusselaers N. The Vaginal Microbiota, Human Papillomavirus and Cervical Dysplasia: A Systematic Review and Network Meta-Analysis. *BJOG* (2020) 127(2):171–80. doi: 10.1111/1471-0528.15854
36. Wang H, Ma Y, Li R, Chen X, Wan L, Zhao W. Associations of Cervicovaginal Lactobacilli With High-Risk Human Papillomavirus Infection, Cervical Intraepithelial Neoplasia, and Cancer: A Systematic Review and Meta-Analysis. *J Infect Dis* (2019) 220(8):1243–54. doi: 10.1093/infdis/jiz325
37. Tango CN, Seo SS, Kwon M, Lee DO, Chang HK, Kim MK. Taxonomic and Functional Differences in Cervical Microbiome Associated With Cervical Cancer Development. *Sci Rep* (2020) 10(1):9720. doi: 10.1038/s41598-020-66607-4
38. Kwon M, Seo SS, Kim MK, Lee DO, Lim MC. Compositional and Functional Differences Between Microbiota and Cervical Carcinogenesis as Identified by Shotgun Metagenomic Sequencing. *Cancers (Basel)* (2019) 11(3):309. doi: 10.3390/cancers11030309
39. Donmez HG, Sahal G, Akgor U, Cagan M, Ozgul N, Beksac MS. The Relationship Between the Presence of HPV Infection and Biofilm Formation in Cervicovaginal Smears. *Infection* (2020) 48(5):735–40. doi: 10.1007/s15010-020-01478-5
40. Dareng EO, Ma B, Adebamowo SN, Famooto A, Ravel J, Pharoah PP, et al. Vaginal Microbiota Diversity and Paucity of Lactobacillus Species Are Associated With Persistent hrHPV Infection in HIV Negative But Not in HIV Positive Women. *Sci Rep* (2020) 10(1):19095. doi: 10.1038/s41598-020-76003-7
41. Reimers LL, Mehta SD, Massad LS, Burk RD, Xie X, Ravel J, et al. The Cervicovaginal Microbiota and Its Associations With Human Papillomavirus Detection in HIV-Infected and HIV-Uninfected Women. *J Infect Dis* (2016) 214 (9):1361–9. doi: 10.1093/infdis/jiw374
42. Tamarelle J, Thiebaut ACM, de Barbeyrac B, Bebear C, Ravel J, Delarocque-Astagneau E. The Vaginal Microbiota and its Association With Human Papillomavirus, Chlamydia Trachomatis, Neisseria Gonorrhoeae and Mycoplasma Genitalium Infections: A Systematic Review and Meta-Analysis. *Clin Microbiol Infect* (2019) 25(1):35–47. doi: 10.1016/j.cmi.2018.04.019
43. Brusselaers N, Shrestha S, van de Wijgert J, Verstraelen H. Vaginal Dysbiosis and the Risk of Human Papillomavirus and Cervical Cancer: Systematic Review and Meta-Analysis. *Am J Obstet Gynecol* (2019) 221(1):9–18.e8. doi: 10.1016/j.ajog.2018.12.011
44. Engberts MK, Verbruggen BS, Boon ME, van Haaften M, Heintz AP. Candida and Dysbacteriosis: A Cytologic, Population-Based Study of 100,605 Asymptomatic Women Concerning Cervical Carcinogenesis. *Cancer* (2007) 111(5):269–74. doi: 10.1002/cncr.22947
45. Briselden AM, Moncla BJ, Stevens CE, Hillier SL. Sialidases (Neuraminidases) in Bacterial Vaginosis and Bacterial Vaginosis-Associated Microflora. *J Clin Microbiol* (1992) 30(3):663–6. doi: 10.1128/JCM.30.3.663-666.1992
46. Holmes KK, Chen KC, Lipinski CM, Eschenbach DA. Vaginal Redox Potential in Bacterial Vaginosis (Nonspecific Vaginitis). *J Infect Dis* (1985) 152(2):379–82. doi: 10.1093/infdis/152.2.379
47. Anderson BL, Cu-Uvin S, Raker CA, Fitzsimmons C, Hillier SL. Subtle Perturbations of Genital Microflora Alter Mucosal Immunity Among Low-Risk Pregnant Women. *Acta Obstet Gynecol Scand* (2011) 90(5):510–5. doi: 10.1111/j.1600-0412.2011.01082.x
48. Hedges SR, Barrientes F, Desmond RA, Schwebke JR. Local and Systemic Cytokine Levels in Relation to Changes in Vaginal Flora. *J Infect Dis* (2006) 193(4):556–62. doi: 10.1086/499824
49. Uren A, Fallen S, Yuan H, Usubutun A, Kucukali T, Schlegel R, et al. Activation of the Canonical Wnt Pathway During Genital Keratinocyte Transformation: A Model for Cervical Cancer Progression. *Cancer Res* (2005) 65(14):6199–206. doi: 10.1158/0008-5472.CAN-05-0455
50. Cheriyan VT, Krishna SM, Kumar A, Jayaprakash PG, Balaram P. Signaling Defects and Functional Impairment in T-Cells From Cervical Cancer Patients. *Cancer Biother Radiopharm* (2009) 24(6):667–73. doi: 10.1089/cbr.2009.0660
51. Gur C, Ibrahim Y, Isaacson B, Yamin R, Abed J, Gamliel M, et al. Binding of the Fap2 Protein of Fusobacterium Nucleatum to Human Inhibitory Receptor TIGIT Protects Tumors From Immune Cell Attack. *Immunity* (2015) 42(2):344–55. doi: 10.1016/j.immuni.2015.01.010
52. Mastromarino P, Di Pietro M, Schiavoni G, Nardis C, Gentile M, Sessa R. Effects of Vaginal Lactobacilli in Chlamydia Trachomatis Infection. *Int J Med Microbiol* (2014) 304(5-6):654–61. doi: 10.1016/j.ijmm.2014.04.006
53. Breshears LM, Edwards VL, Ravel J, Peterson ML. Lactobacillus Crispatus Inhibits Growth of Gardnerella Vaginalis and Neisseria Gonorrhoeae on a Porcine Vaginal Mucosa Model. *BMC Microbiol* (2015) 15:276. doi: 10.1186/s12866-015-0608-0
54. Gong Z, Luna Y, Yu P, Fan H. Lactobacilli Inactivate Chlamydia Trachomatis Through Lactic Acid But Not H2O2. *PloS One* (2014) 9(9): e107758. doi: 10.1371/journal.pone.0107758
55. Graver MA, Wade JJ. The Role of Acidification in the Inhibition of Neisseria Gonorrhoeae by Vaginal Lactobacilli During Anaerobic Growth. *Ann Clin Microbiol Antimicrob* (2011) 10:8. doi: 10.1186/1476-0711-10-8
56. Stoyancheva G, Marzotto M, Dellaglio F, Torriani S. Bacteriocin Production and Gene Sequencing Analysis From Vaginal Lactobacillus Strains. *Arch Microbiol* (2014) 196(9):645–53. doi: 10.1007/s00203-014-1003-1
57. Dover SE, Aroutcheva AA, Faro S, Chikindas ML. Natural Antimicrobials and Their Role in Vaginal Health: A Short Review. *Int J Probiotics Prebiotics* (2008) 3(4):219–30.
58. Reid G, Heinemann C, Velraeds M, van der Mei HC, Busscher HJ. Biosurfactants Produced by Lactobacillus. *Methods Enzymol* (1999) 310:426–33. doi: 10.1016/s0076-6879(99)10033-8
59. Zarate G, Nader-Macias ME. Influence of Probiotic Vaginal Lactobacilli on *In Vitro* Adhesion of Urogenital Pathogens to Vaginal Epithelial Cells. *Lett Appl Microbiol* (2006) 43(2):174–80. doi: 10.1111/j.1472-765X.2006.01934.x
60. Strus M, Brzychczy-Wloch M, Gosiewski T, Kochan P, Heczko PB. The *In Vitro* Effect of Hydrogen Peroxide on Vaginal Microbial Communities. *FEMS Immunol Med Microbiol* (2006) 48(1):56–63. doi: 10.1111/j.1574-695X.2006.00120.x
61. Vallor AC, Antonio MA, Hawes SE, Hillier SL. Factors Associated With Acquisition of, or Persistent Colonization by, Vaginal Lactobacilli: Role of Hydrogen Peroxide Production. *J Infect Dis* (2001) 184(11):1431–6. doi: 10.1086/324445
62. Witkin SS, Mendes-Soares H, Linhares IM, Jayaram A, Ledger WJ, Forney LJ. Influence of Vaginal Bacteria and D- and L-Lactic Acid Isomers on Vaginal Extracellular Matrix Metalloproteinase Inducer: Implications for Protection Against Upper Genital Tract Infections. *mBio* (2013) 4(4): e00460–13. doi: 10.1128/mBio.00460-13
63. Nunn KL, Wang YY, Harit D, Humphrys MS, Ma B, Cone R, et al. Enhanced Trapping of HIV-1 by Human Cervicovaginal Mucus Is Associated With Lactobacillus crispatus-Dominant Microbiota. *mBio* (2015) 6(5):e01084–15. doi: 10.1128/mBio.01084-15
64. Romero R, Hassan SS, Gajer P, Tarca AL, Fadrosh DW, Nikita L, et al. The Composition and Stability of the Vaginal Microbiota of Normal Pregnant Women Is Different From That of non-Pregnant Women. *Microbiome* (2014) 2(1):4. doi: 10.1186/2049-2618-2-4
65. Zhou C, Tuong ZK, Frazer IH. Papillomavirus Immune Evasion Strategies Target the Infected Cell and the Local Immune System. *Front Oncol* (2019) 9:682. doi: 10.3389/fonc.2019.00682
66. Georgopoulos NT, Proffitt JL, Blair GE. Transcriptional Regulation of the Major Histocompatibility Complex (MHC) Class I Heavy Chain, TAP1 and LMP2 Genes by the Human Papillomavirus (HPV) Type 6b, 16 and 18 E7 Oncoproteins. *Oncogene* (2000) 19(42):4930–5. doi: 10.1038/sj.onc.1203860
67. Heller C, Weisser T, Mueller-Schickert A, Rufer E, Hoh A, Leonhardt RM, et al. Identification of Key Amino Acid Residues That Determine the Ability of High Risk HPV16-E7 to Dysregulate Major Histocompatibility Complex

Class I Expression. *J Biol Chem* (2011) 286(13):10983–97. doi: 10.1074/jbc.M110.199190
68. Zhou F, Leggatt GR, Frazer IH. Human Papillomavirus 16 E7 Protein Inhibits Interferon-Gamma-Mediated Enhancement of Keratinocyte Antigen Processing and T-Cell Lysis. *FEBS J* (2011) 278(6):955–63. doi: 10.1111/j.1742-4658.2011.08011.x
69. Cortese MS, Ashrafi GH, Campo MS. All 4 Di-Leucine Motifs in the First Hydrophobic Domain of the E5 Oncoprotein of Human Papillomavirus Type 16 Are Essential for Surface MHC Class I Downregulation Activity and E5 Endomembrane Localization. *Int J Cancer* (2010) 126(7):1675–82. doi: 10.1002/ijc.25004
70. Gruener M, Bravo IG, Momburg F, Alonso A, Tomakidi P. The E5 Protein of the Human Papillomavirus Type 16 Down-Regulates HLA-I Surface Expression in Calnexin-Expressing But Not in Calnexin-Deficient Cells. *Virol J* (2007) 4:116. doi: 10.1186/1743-422X-4-116
71. Miura S, Kawana K, Schust DJ, Fujii T, Yokoyama T, Iwasawa Y, et al. CD1d, a Sentinel Molecule Bridging Innate and Adaptive Immunity, Is Downregulated by the Human Papillomavirus (HPV) E5 Protein: A Possible Mechanism for Immune Evasion by HPV. *J Virol* (2010) 84 (22):11614–23. doi: 10.1128/JVI.01053-10
72. Sperling T, Oldak M, Walch-Ruckheim B, Wickenhauser C, Doorbar J, Pfister H, et al. Human Papillomavirus Type 8 Interferes With a Novel C/EBPbeta-Mediated Mechanism of Keratinocyte CCL20 Chemokine Expression and Langerhans Cell Migration. *PloS Pathog* (2012) 8(7): e1002833. doi: 10.1371/journal.ppat.1002833
73. Guess JC, McCance DJ. Decreased Migration of Langerhans Precursor-Like Cells in Response to Human Keratinocytes Expressing Human Papillomavirus Type 16 E6/E7 Is Related to Reduced Macrophage Inflammatory protein-3alpha Production. *J Virol* (2005) 79(23):14852–62. doi: 10.1128/JVI.79.23.14852-14862.2005
74. Laurson J, Khan S, Chung R, Cross K, Raj K. Epigenetic Repression of E-Cadherin by Human Papillomavirus 16 E7 Protein. *Carcinogenesis* (2010) 31 (5):918–26. doi: 10.1093/carcin/bgq027
75. Hubert P, Caberg JH, Gilles C, Bousarghin L, Franzen-Detrooz E, Boniver J, et al. E-Cadherin-Dependent Adhesion of Dendritic and Langerhans Cells to Keratinocytes Is Defective in Cervical Human Papillomavirus-Associated (Pre)Neoplastic Lesions. *J Pathol* (2005) 206(3):346–55. doi: 10.1002/path.1771
76. Connor JP, Ferrer K, Kane JP, Goldberg JM. Evaluation of Langerhans' Cells in the Cervical Epithelium of Women With Cervical Intraepithelial Neoplasia. *Gynecol Oncol* (1999) 75(1):130–5. doi: 10.1006/gyno.1999.5559
77. Fahey LM, Raff AB, Da Silva DM, Kast WM. Reversal of Human Papillomavirus-Specific T Cell Immune Suppression Through TLR Agonist Treatment of Langerhans Cells Exposed to Human Papillomavirus Type 16. *J Immunol* (2009) 182(5):2919–28. doi: 10.4049/jimmunol.0803645
78. Kumar MM, Adurthi S, Ramachandran S, Mukherjee G, Joy O, Krishnamurthy H, et al. Toll-Like Receptors 7, 8, and 9 Expression and Function in Primary Human Cervical Cancer Langerhans Cells: Evidence of Anergy. *Int J Gynecol Cancer* (2013) 23(1):184–92. doi: 10.1097/IGC.0b013e31827a2003
79. Pahne-Zeppenfeld J, Schroer N, Walch-Ruckheim B, Oldak M, Gorter A, Hegde S, et al. Cervical Cancer Cell-Derived Interleukin-6 Impairs CCR7-Dependent Migration of MMP-9-Expressing Dendritic Cells. *Int J Cancer* (2014) 134(9):2061–73. doi: 10.1002/ijc.28549
80. Da Silva DM, Movius CA, Raff AB, Brand HE, Skeate JG, Wong MK, et al. Suppression of Langerhans Cell Activation Is Conserved Amongst Human Papillomavirus Alpha and Beta Genotypes, But Not a Micro Genotype. *Virology* (2014) 452-453:279–86. doi: 10.1016/j.virol.2014.01.031
81. Fausch SC, Da Silva DM, Rudolf MP, Kast WM. Human Papillomavirus Virus-Like Particles do Not Activate Langerhans Cells: A Possible Immune Escape Mechanism Used by Human Papillomaviruses. *J Immunol* (2002) 169(6):3242–9. doi: 10.4049/jimmunol.169.6.3242
82. Da Silva DM, Woodham AW, Skeate JG, Rijkee LK, Taylor JR, Brand HE, et al. Langerhans Cells From Women With Cervical Precancerous Lesions Become Functionally Responsive Against Human Papillomavirus After Activation With Stabilized Poly-I:C. *Clin Immunol* (2015) 161(2):197–208. doi: 10.1016/j.clim.2015.09.003
83. Coleman HN, Greenfield WW, Stratton SL, Vaughn R, Kieber A, Moerman-Herzog AM, et al. Human Papillomavirus Type 16 Viral Load Is Decreased Following a Therapeutic Vaccination. *Cancer Immunol Immunother* (2016) 65(5):563–73. doi: 10.1007/s00262-016-1821-x
84. Kim KH, Horn TD, Pharis J, Kincannon J, Jones R, O'Bryan K, et al. Phase 1 Clinical Trial of Intralesional Injection of Candida Antigen for the Treatment of Warts. *Arch Dermatol* (2010) 146(12):1431–3. doi: 10.1001/archdermatol.2010.350
85. Laniewski P, Barnes D, Goulder A, Cui H, Roe DJ, Chase DM, et al. Linking Cervicovaginal Immune Signatures, HPV and Microbiota Composition in Cervical Carcinogenesis in Non-Hispanic and Hispanic Women. *Sci Rep* (2018) 8(1):7593. doi: 10.1038/s41598-018-25879-7
86. Ilhan ZE, Laniewski P, Thomas N, Roe DJ, Chase DM, Herbst-Kralovetz MM. Deciphering the Complex Interplay Between Microbiota, HPV, Inflammation and Cancer Through Cervicovaginal Metabolic Profiling. *EBioMedicine* (2019) 44:675–90. doi: 10.1016/j.ebiom.2019.04.028
87. Laniewski P, Cui H, Roe DJ, Barnes D, Goulder A, Monk BJ, et al. Features of the Cervicovaginal Microenvironment Drive Cancer Biomarker Signatures in Patients Across Cervical Carcinogenesis. *Sci Rep* (2019) 9(1):7333. doi: 10.1038/s41598-019-43849-5
88. Laniewski P, Cui H, Roe DJ, Chase DM, Herbst-Kralovetz MM. Vaginal Microbiota, Genital Inflammation, and Neoplasia Impact Immune Checkpoint Protein Profiles in the Cervicovaginal Microenvironment. *NPJ Precis Oncol* (2020) 4:22. doi: 10.1038/s41698-020-0126-x
89. Ngugi BM, Hemmerling A, Bukusi EA, Kikuvi G, Gikunju J, Shiboski S, et al. Effects of Bacterial Vaginosis-Associated Bacteria and Sexual Intercourse on Vaginal Colonization With the Probiotic Lactobacillus Crispatus CTV-05. *Sex Transm Dis* (2011) 38(11):1020–7. doi: 10.1097/OLQ.0b013e3182267ac4
90. Hemmerling A, Harrison W, Schroeder A, Park J, Korn A, Shiboski S, et al. Phase 2a Study Assessing Colonization Efficiency, Safety, and Acceptability of Lactobacillus Crispatus CTV-05 in Women With Bacterial Vaginosis. *Sex Transm Dis* (2010) 37(12):745–50. doi: 10.1097/OLQ.0b013e3181e50026
91. Stapleton AE, Au-Yeung M, Hooton TM, Fredricks DN, Roberts PL, Czaja CA, et al. Randomized, Placebo-Controlled Phase 2 Trial of a Lactobacillus Crispatus Probiotic Given Intravaginally for Prevention of Recurrent Urinary Tract Infection. *Clin Infect Dis* (2011) 52(10):1212–7. doi: 10.1093/cid/cir183
92. Marrazzo JM, Dombrowski JC, Wierzbicki MR, Perlowski C, Pontius A, Dithmer D, et al. Safety and Efficacy of a Novel Vaginal Anti-infective, TOL-463, in the Treatment of Bacterial Vaginosis and Vulvovaginal Candidiasis: A Randomized, Single-Blind, Phase 2, Controlled Trial. *Clin Infect Dis* (2019) 68(5):803–9. doi: 10.1093/cid/ciy554
93. Rousseau V, Lepargneur JP, Roques C, Remaud-Simeon M, Paul F. Prebiotic Effects of Oligosaccharides on Selected Vaginal Lactobacilli and Pathogenic Microorganisms. *Anaerobe* (2005) 11(3):145–53. doi: 10.1016/j.anaerobe.2004.12.002
94. Coste I, Judlin P, Lepargneur JP, Bou-Antoun S. Safety and Efficacy of an Intravaginal Prebiotic Gel in the Prevention of Recurrent Bacterial Vaginosis: A Randomized Double-Blind Study. *Obstet Gynecol Int* (2012) 2012:147867. doi: 10.1155/2012/147867
95. Tester R, Al-Ghazzewi F, Shen N, Chen Z, Chen F, Yang J, et al. The Use of Konjac Glucomannan Hydrolysates to Recover Healthy Microbiota in Infected Vaginas Treated With an Antifungal Agent. *Benef Microbes* (2012) 3(1):61–6. doi: 10.3920/BM2011.0021
96. Lev-Sagie A, Goldman-Wohl D, Cohen Y, Dori-Bachash M, Leshem A, Mor U, et al. Vaginal Microbiome Transplantation in Women With Intractable Bacterial Vaginosis. *Nat Med* (2019) 25(10):1500–4. doi: 10.1038/s41591-019-0600-6
97. DeLong K, Bensouda S, Zulfiqar F, Zierden HC, Hoang TM, Abraham AG, et al. Conceptual Design of a Universal Donor Screening Approach for Vaginal Microbiota Transplant. *Front Cell Infect Microbiol* (2019) 9:306. doi: 10.3389/fcimb.2019.00306
98. Da Silva DM, Skeate JG, Chavez-Juan E, Luhen KP, Wu JM, Wu CM, et al. Therapeutic Efficacy of a Human Papillomavirus Type 16 E7 Bacterial Exotoxin Fusion Protein Adjuvanted With CpG or GPI-0100 in a Preclinical Mouse Model for HPV-Associated Disease. *Vaccine* (2019) 37 (22):2915–24. doi: 10.1016/j.vaccine.2019.04.043
99. Maynard SK, Marshall JD, MacGill RS, Yu L, Cann JA, Cheng LI, et al. Vaccination With Synthetic Long Peptide Formulated With CpG in an Oil-

in-Water Emulsion Induces Robust E7-Specific CD8 T Cell Responses and TC-1 Tumor Eradication. *BMC Cancer* (2019) 19(1):540. doi: 10.1186/s12885-019-5725-y

100. Gandhapudi SK, Ward M, Bush JPC, Bedu-Addo F, Conn G, Woodward JG. Antigen Priming With Enantiospecific Cationic Lipid Nanoparticles Induces Potent Antitumor CTL Responses Through Novel Induction of a Type I IFN Response. *J Immunol* (2019) 202(12):3524–36. doi: 10.4049/jimmunol.1801634
101. Daayana S, Elkord E, Winters U, Pawlita M, Roden R, Stern PL, et al. Phase II Trial of Imiquimod and HPV Therapeutic Vaccination in Patients With Vulval Intraepithelial Neoplasia. *Br J Cancer* (2010) 102(7):1129–36. doi: 10.1038/sj.bjc.6605611
102. Ribelles P, Benbouziane B, Langella P, Suarez JE, Bermudez-Humaran LG. Protection Against Human Papillomavirus Type 16-Induced Tumors in Mice Using Non-Genetically Modified Lactic Acid Bacteria Displaying E7 Antigen at Its Surface. *Appl Microbiol Biotechnol* (2013) 97(3):1231–9. doi: 10.1007/s00253-012-4575-1
103. Lee TY, Kim YH, Lee KS, Kim JK, Lee IH, Yang JM, et al. Human Papillomavirus Type 16 E6-Specific Antitumor Immunity Is Induced by Oral Administration of HPV16 E6-Expressing Lactobacillus Casei in C57BL/6 Mice. *Cancer Immunol Immunother* (2010) 59(11):1727–37. doi: 10.1007/s00262-010-0903-4
104. Kawana K, Adachi K, Kojima S, Taguchi A, Tomio K, Yamashita A, et al. Oral Vaccination Against HPV E7 for Treatment of Cervical Intraepithelial Neoplasia Grade 3 (CIN3) Elicits E7-Specific Mucosal Immunity in the Cervix of CIN3 Patients. *Vaccine* (2014) 32(47):6233–9. doi: 10.1016/j.vaccine.2014.09.020
105. Adachi K, Kawana K, Yokoyama T, Fujii T, Tomio A, Miura S, et al. Oral Immunization With a Lactobacillus Casei Vaccine Expressing Human Papillomavirus (HPV) Type 16 E7 Is an Effective Strategy to Induce Mucosal Cytotoxic Lymphocytes Against HPV16 E7. *Vaccine* (2010) 28(16):2810–7. doi: 10.1016/j.vaccine.2010.02.005
106. Poo H, Pyo HM, Lee TY, Yoon SW, Lee JS, Kim CJ, et al. Oral Administration of Human Papillomavirus Type 16 E7 Displayed on Lactobacillus Casei Induces E7-Specific Antitumor Effects in C57/BL6 Mice. *Int J Cancer* (2006) 119(7):1702–9. doi: 10.1002/ijc.22035

**Conflict of Interest:** The authors declare that the research was conducted in the absence of any commercial or financial relationships that could be construed as a potential conflict of interest.

**Publisher's Note:** All claims expressed in this article are solely those of the authors and do not necessarily represent those of their affiliated organizations, or those of the publisher, the editors and the reviewers. Any product that may be evaluated in this article, or claim that may be made by its manufacturer, is not guaranteed or endorsed by the publisher.

frontiers in Oncology

ORIGINAL RESEARCH
published: 16 August 2021
doi: 10.3389/fonc.2021.706043

# Radiomic Score as a Potential Imaging Biomarker for Predicting Survival in Patients With Cervical Cancer

*Handong Li[1†], Miaochen Zhu[2†], Lian Jian[1†], Feng Bi[1], Xiaoye Zhang[2], Chao Fang[3], Ying Wang[2], Jing Wang[4*], Nayiyuan Wu[2*] and Xiaoping Yu[1*]*

[1] Department of Radiology, Hunan Cancer Hospital, The Affiliated Cancer Hospital of Xiangya School of Medicine, Central South University, Changsha, China, [2] Central Laboratory, Hunan Cancer Hospital, The Affiliated Cancer Hospital of Xiangya School of Medicine, Central South University, Changsha, China, [3] Department of Clinical Pharmaceutical Research Institution, Hunan Cancer Hospital, Affiliated Tumor Hospital of Xiangya Medical School of Central South University, Changsha, China, [4] Gynecological Oncology Clinical Research Center, Hunan Cancer Hospital, Affiliated Tumor Hospital of Xiangya Medical School of Central South University, Changsha, China

OPEN ACCESS

**Edited by:**
*Kathy Han,*
*University Health Network, Canada*

**Reviewed by:**
*Federica Perelli,*
*Santa Maria Annunziata Hospital, Italy*
*Fleur Huang,*
*University of Alberta, Canada*

***Correspondence:**
*Xiaoping Yu*
*yuxiaoping@hnca.org.cn*
*Nayiyuan Wu*
*wunayiyuan@163.com*
*Jing Wang*
*wangjing0081@hnszlyy.com*

[†]*These authors have contributed equally to this work*

**Specialty section:**
*This article was submitted to Gynecological Oncology, a section of the journal Frontiers in Oncology*

**Received:** *06 May 2021*
**Accepted:** *19 July 2021*
**Published:** *16 August 2021*

**Citation:**
*Li H, Zhu M, Jian L, Bi F, Zhang X, Fang C, Wang Y, Wang J, Wu N and Yu X (2021) Radiomic Score as a Potential Imaging Biomarker for Predicting Survival in Patients With Cervical Cancer. Front. Oncol. 11:706043. doi: 10.3389/fonc.2021.706043*

**Objectives:** Accurate prediction of prognosis will help adjust or optimize the treatment of cervical cancer and benefit the patients. We aimed to investigate the incremental value of radiomics when added to the FIGO stage in predicting overall survival (OS) in patients with cervical cancer.

**Methods:** This retrospective study included 106 patients with cervical cancer (FIGO stage IB1–IVa) between October 2017 and May 2019. Patients were randomly divided into a training cohort ($n$ = 74) and validation cohort ($n$ = 32). All patients underwent contrast-enhanced computed tomography (CT) prior to treatment. The ITK-SNAP software was used to delineate the region of interest on pre-treatment standard-of-care CT scans. We extracted 792 two-dimensional radiomic features by the Analysis Kit (AK) software. Pearson correlation coefficient analysis and Relief were used to detect the most discriminatory features. The radiomic signature (i.e., Radscore) was constructed *via* Adaboost with Leave-one-out cross-validation. Prognostic models were built by Cox regression model using Akaike information criterion (AIC) as the stopping rule. A nomogram was established to individually predict the OS of patients. Patients were then stratified into high- and low-risk groups according to the Youden index. Kaplan–Meier curves were used to compare the survival difference between the high- and low-risk groups.

**Results:** Six textural features were identified, including one gray-level co-occurrence matrix feature and five gray-level run-length matrix features. Only the FIGO stage and Radscore were independent risk factors associated with OS ($p < 0.05$). The C-index of the FIGO stage in the training and validation cohorts was 0.703 (95% CI: 0.572–0.834) and 0.700 (95% CI: 0.526–0.874), respectively. Correspondingly, the C-index of Radscore was 0.794 (95% CI: 0.707–0.880) and 0.754 (95% CI: 0.623–0.885). The incorporation of the FIGO stage and Radscore achieved better performance, with a C-index of 0.830 (95% CI: 0.738–0.922) and 0.772 (95% CI: 0.615–0.929), respectively. The nomogram based

on the FIGO stage and Radscore could individually predict the OS probability with good discrimination and calibration. The high-risk patients had shorter OS compared with the low-risk patients ($p < 0.05$).

**Conclusion:** Radiomics has the potential for noninvasive risk stratification and may improve the prediction of OS in patients with cervical cancer when added to the FIGO stage.

**Keywords: cervical cancer, computed tomography, radiomics, nomogram, overall survival**

## INTRODUCTION

Cervical cancer is one of the fourth most common female malignancies worldwide (1). More than 80% of patients are typically diagnosed at a locally advanced stage (2). Five-year overall survival (OS) can be significantly distinct, ranging from 80% (stage IB) to 15% (stage IVa-b) (3). Despite the fact that outcomes of cervical cancer had been improved with multimodality treatment, around 30%–40% of patients still suffer from recurrence (4). Thus, it is of great significance to identify high-risk patients who may benefit from aggressive treatment.

The International Federation of Gynecology and Obstetrics (FIGO) stage has been established as the most crucial prognostic factor for cervical cancer (5). The treatment modality choice is mainly based on the FIGO stage and N staging (6). However, clinical outcomes are markedly different among patients with similar stages (6). Imaging plays an essential role in the pre-treatment evaluation of cervical cancer. However, conventional medical images only provide structural information of cancer; it fails to detect the intratumoral heterogeneity associated with treatment response and prognosis (7). Thus, the search for new non-invasive biomarkers with the potential to offer more specific tumor characterization before therapy is urgently needed, which may inform clinicians to make a more individualized treatment plan.

Statistical models, medical images, and machine learning have been widely used for outcome prediction in cervical cancer. Machine learning has merits in dealing with the complexity of high-dimensional data and discovering prognostic factors. Radiomics refers to a variety of mathematical methods such as machine learning that converts digital medical images into a huge number of minable high-dimensional features for cancer diagnosis or prediction (8, 9). Radiomic signature can be used as a surrogate biomarker for biological tumor traits such as tumor morphology and intratumor heterogeneity (10, 11). Currently, radiomics has been used to predict tumor stage, histological type, lymph node metastasis, relapse, and survival in patients with cervical cancer (12). However, the additional value of radiomics to the FIGO stage in prognostication of cervical cancer remains unclear. Thus, this study aimed to develop and validate a radiomic model for predicting survival in patients with cervical cancer.

## MATERIALS AND METHODS

### Patient Cohort

This retrospective study included patients with a diagnosis of cervical cancer between October 2017 and May 2019 at our institution. Inclusion criteria were (1) patients with histologically confirmed cervical cancer, (2) patients with tumor staged IB1-IVa (FIGO 2009 definition), (3) patients who were not previously treated with any anti-cancer treatment, and (4) patients who underwent a pre-treatment contrast-enhanced computed tomography (CT) scan. Exclusion criteria were (1) patients with a history of previous chemotherapy or radiotherapy, (2) patients with a diagnosis of other cancers, or (3) patients with distant metastatic disease (para-aortic nodes involvement was not included). Institutional ethics review board approval was acquired for this study and written informed consent was waived. Finally, a total of 106 patients (mean age, 63.8 years) were included in this study. Eligible patients for the radiomic study were randomly divided into a training cohort ($n = 74$) and a validation cohort ($n = 32$). The clinical information of patients was collected from electronic medical records, including age, FIGO stage, histological type, differentiation, lymph node metastasis (LNM), and treatment regimens. Of note, a lymph node with a short-axis diameter larger than 10 mm was considered to be metastasis (13).

### Treatment Characteristics and Follow-Up

All patients were treated with image-guided external beam radiotherapy (EBRT) and brachytherapy (BT), to a total dose of 85–90 Gy (EQD2, equivalent dose in 2 Gy single dose fractions). EBRT was delivered in 1.8–2.0 Gy/fraction, to a range of 45–50 Gy, using a 3D conformal technique. BT boost was volumetrically planned and delivered as weekly high-dose-rate fractions of 8 Gy EQD2 each after 15 times of EBRT. The external irradiation was not performed on the day of intracavitary and interstitial after loading BT. The radiation volumes covered the pelvic cavity and, if clinically indicated, the para-aortic and/or inguinal nodal regions. CT-positive lymph nodes were simultaneously boosted to a total dose of 55–60 Gy. Concurrent weekly chemotherapy with cisplatin (40 mg/m$^2$) was delivered for 4–6 weeks or carboplatin (AUC = 2) when feasible. The endpoint OS was defined as the interval from the date of treatment to death from any cause. The patients were followed up until November 19, 2020.

### CT Image Acquisitions

CT scans were performed on a 64-row CT scanner (Somatom definition AS large-aperture, Siemens Healthcare) using the following parameters: 120-kVp tube voltage, 252-mAs tube current, a field of view (FOV) of 384 × 384 mm$^2$, a width of detector of 40 mm, a beam pitch of 0.6, a gantry rotation time of

0.5 s, and a slice thickness of 5 mm. Iohexol (350 mg I/ml) was administrated with a rate of 2.5–3.0 ml/s through the elbow vein by a high-pressure injector. Enhanced CT images were obtained at 30 s after injection.

## Radiomic Analysis

Our radiomic workflow is illustrated in **Figure 1**.

### Image Segmentation

We used an open-source ITK-SNAP software (version 3.6.0, www.itksnap.org) for manual segmentation on CT images (**Figure 2**). Tumor lesion segmentation was performed on the maximum level of tumor by a radiologist (with 6-year experience) and subsequently reviewed by a board-certified radiologist (>10 years experience).

### Feature Extraction

The radiomic features were automatically calculated by AK software (Artificial Intelligence Kit, GE Life Sciences, AA R&D team, Shanghai, China), which comply with the standards set by the Image Biomarker Standardization Initiative. In total, 792 radiomic features were extracted from pre-contrast and post-contrast CT images, including (1) histogram features, such as energy, entropy, uniformity, skewness, and kurtosis; (2) form factor features, such as sphericity, surface area, compactness, surface volume ratio, maximum 3D diameter, spherical disproportion, volume CC, and volume MM; and (3) texture features including gray-level co-occurrence matrix (GLCM), gray-level size zone matrix (GLZSM), gray-level run-length matrix (GLRLM), and Haralick parameters. The offsets of GLCM and GLRLM were 1, 4, and 7.

### Feature Pre-Processing and Selection

Feature pre-processing was done in two steps: step 1—outliers and null values were replaced by mean values, and step 2—values standardization was carried out to eliminate the influence of the dimension (14). Feature selection is a critically important step for better generalization of models because high-dimensional data usually comprise a large number of irrelevant, redundant, and noisy features, which may result in the curse of dimensionality and model overfitting (15). In terms of feature selection, Pearson correction coefficient (PCC) analysis was used to assess the correlation between feature pairs, and one feature was randomly excluded from each pair with a correlation

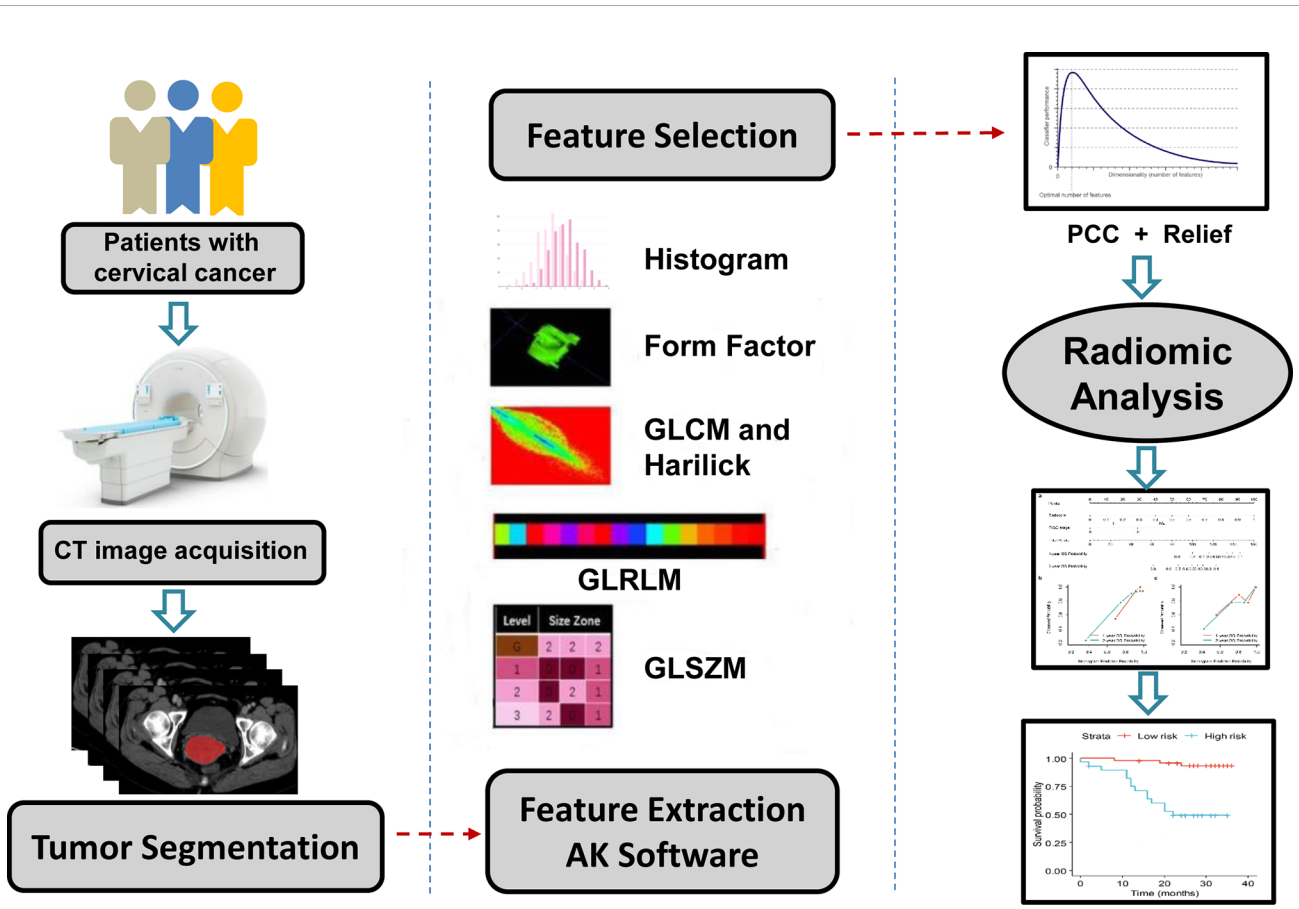


**FIGURE 1** | Schematic diagram exhibition of the radiomic workflow. A radiomic study design and workflow mainly include (I) Image segmentation, (II) Radiomic feature extraction, (III) Dimension reduction and feature selection, (IV) Statistics analysis and model building. CT, computed tomography; GLCM, gray-level co-occurrence matrix; GLZSM, gray-level size zone matrix; GLRLM, gray-level run-length matrix; PCC, Pearson correction coefficient.

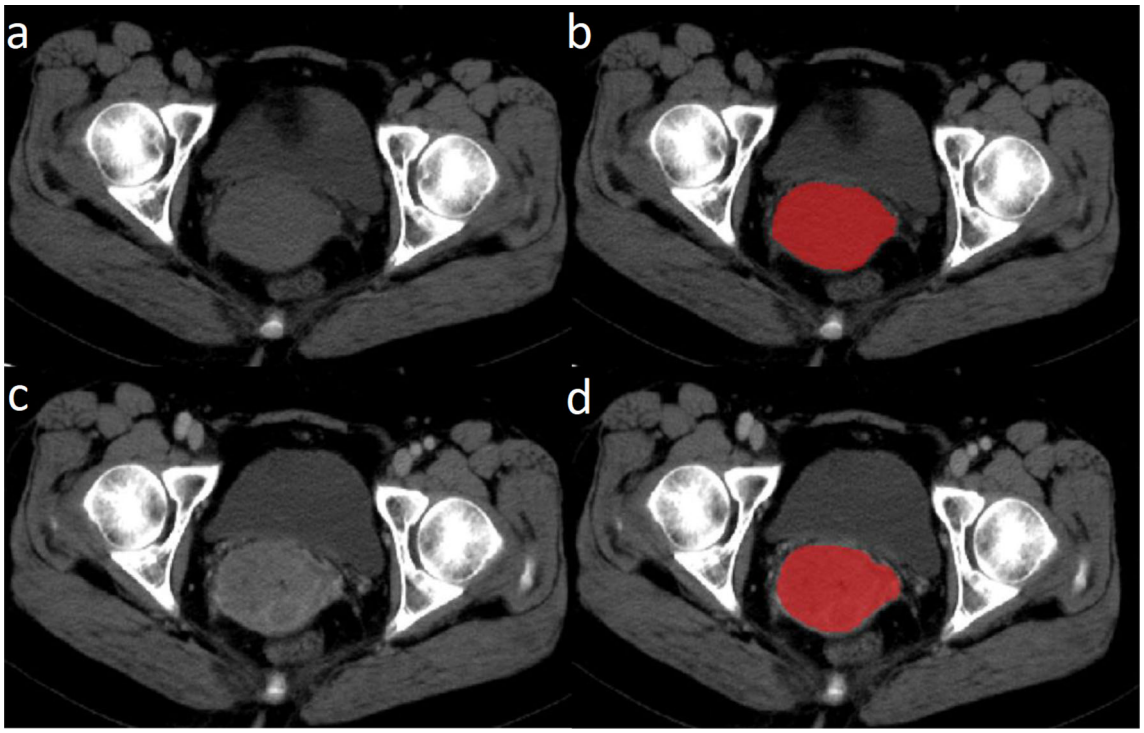


**FIGURE 2** | Illustration of tumor segmentation on the maximum level of tumor. **(A)** Raw pre-contrast image; **(B)** pre-contrast image after delineation; **(C)** raw post-contrast image; and **(D)** post-contrast image after delineation.

coefficient >0.9. After this process, the dimension of the variable space was reduced, and each variable was independent of each other. Then, we used Relief, a feature weighting algorithm, to detect the most discriminatory features. Finally, radiomic signature (i.e., Radscore) based on the selected features was constructed *via* Adaboost with Leave-one-out cross-validation.

## Prognostic Model Construction

Variables with missing data of more than 20% were excluded for analysis. The significant variables were identified by the univariate and multivariate Cox regression model. The variables with $p < 0.10$ in the univariate analysis were entered into multivariate analysis to obtain independent risk factors for OS ($p < 0.05$). The prognostic models were constructed by Cox proportional hazard model, using the Akaike information criterion (AIC) as the stopping rule. For convenient use by clinicians, we built a nomogram to individually predict the OS of patients based on the optimal prognostic model. The calibration curves reflecting the goodness of fit of the nomograms generated were assessed by plotting the predicted probabilities against the observed event proportions. The receiver operating characteristic (ROC) curve was used to determine cutoff values of models according to the Youden index to generate Kaplan–Meier curves for OS in the training and validation cohorts. The Log-rank test was used for comparisons in the Kaplan–Meier curves.

## Statistical Analysis

The clinicopathologic characteristics were assessed by applying two-sample *t*-test, chi-squared test, or Mann–Whitney *U*-test in the training and validation cohorts, where appropriate. The discrimination of each model was quantified by the C-index and 95% confidence interval (CI). The models were subjected to bootstrapping validation (1000 bootstrap resamples) to obtain a relatively corrected C-index. All statistical analyses were performed using 3.6.0 R software (http://www.Rproject.org). A two-tailed $p < 0.05$ was considered statistically significant.

# RESULTS

## The Patient Cohort of the Radiomic Study

There were no significant differences in the clinicopathologic characteristics between the training and validation cohorts (all *P* values >0.05) (**Table 1**).

## Feature Selection and Radscore Construction

A total of 428 radiomic features were retained after PCC analysis; only six texture features were then selected by Relief, including one GLCM feature (pre_*GLCMEntropy_AllDirection_offset7_SD*) and five GLRLM features (post_*LongRunEmphasis_angle135_offset1.1*, pre_*LongRunEmphasis_AllDirection_offset1_SD.1*, pre_*LongRunLow*

**TABLE 1** | Patients' characteristics.

| Characteristics | Training cohort ($n$ = 74) | Validation cohort ($n$ = 32) | $p$-value |
|---|---|---|---|
| **Age (years)** | 59.0 ± 8.3 | 60.3 ± 9.7 | 0.495 |
| **FIGO stage** | | | 0.427 |
| IB | 1 (1.4) | 2 (6.3) | |
| II | 41 (55.4) | 20 (62.5) | |
| III | 28 (37.8) | 9 (28.1) | |
| IVa | 4 (5.4) | 1 (3.1) | |
| **Histological type** | | | 0.866 |
| Squamous | 68 (91.9) | 30 (93.8) | |
| Adenocarcinoma | 4 (5.4) | 1 (3.1) | |
| Adenosquamous carcinoma | 2 (2.7) | 1 (3.1) | |
| **Lymph node involvement on CT** | | | 0.206 |
| Uninvolved | 29 (39.2) | 17 (53.1) | |
| Involved | 45 (60.8) | 15 (46.9) | |
| **Differentiation** | | | 0.999 |
| Poor | 3 (4.1) | 1 (3.1) | |
| Poor-moderate | 12 (16.2) | 5 (15.6) | |
| Moderate | 41 (55.4) | 18 (56.3) | |
| Well-moderate | 4 (5.4) | 2 (6.3) | |
| Unknown | 14 (18.9) | 6 (18.8) | |
| **Concurrent chemotherapy** | | | 0.602 |
| With | 60 (81.1) | 24 (75.0) | |
| Without | 14 (18.9) | 8 (25.0) | |
| Median OS (months) | 27.0 | 28.0 | 0.756 |

*Data were expressed as number (percentage) or mean (standard deviation). FIGO, International Federation of Gynecology and Obstetrics; OS, overall survival.*

*GreyLevelEmphasis_AllDirection_offset1*, post_*LongRun Emphasis_angle45_offset1*, and post_*LongRunHighGrey LevelEmphasis_AllDirection_offset4_SD.1*). Pre_ and post_ denote the pre-contrast and post-contrast features, respectively. The histogram and form factor features were omitted. The Radscore was built by the Adaboost classifier based on the six textural features.

## Independent Indicators of OS

Multivariate Cox regression analysis showed that among clinicopathologic characteristics, only the FIGO stage was an independent factor of OS ($p < 0.002$). The hazard ratio (HR) for the FIGO stage was 3.24 (95% CI: 1.55–6.76). When adding the Radscore to the aforementioned features, only Radscore was an independent indicator of OS ($p = 0.002$). The HRs for the FIGO stage and Radscore were 2.07 (95% CI: 0.89–4.83) and 153.0 (95% CI: 6.29–3721.16), respectively.

## Performance of Prognostic Models

The C-index of the FIGO stage in the training and validation cohorts was 0.703 (95% CI: 0.572–0.834) and 0.700 (95% CI: 0.526–0.874), respectively (**Table 2**). The C-index of Radscore was 0.794 (95% CI: 0.707–0.880) and 0.754 (95% CI: 0.623–0.885), respectively (**Table 2**). The incorporation of the FIGO stage and Radscore achieved better performance, with a C-index of 0.830 (95% CI: 0.738–0.922) and 0.772 (95% CI: 0.615–0.929), respectively (**Table 2**). The nomogram based on the FIGO stage and Radscore could individually predict the OS probability (**Figure 3**). Calibration curves demonstrated good agreement between the predicted probability and observed probability (**Figure 3**).

## Kaplan–Meier Survival Analysis

Kaplan–Meier curves demonstrate that by using a cutoff value of 0.59, Radscore alone could stratify patients into the low- and high-risk groups, with significant OS differences. The high-risk patients had significantly shorter OS than the low-risk patients (training cohort: $p < 0.0001$; validation cohort: $p = 0.03$). The combined FIGO stage and Radscore could achieve better risk stratification using a cutoff value of 0.57 (training cohort: $p < 0.0001$, validation cohort: $p = 0.02$) (**Figure 4**).

# DISCUSSION

In this radiomic study, we demonstrated that capturing intratumoral radiomics from pretherapy CT images could

**TABLE 2** | The performance of FIGO stage, Radscore, and the combined model for OS evaluation in patients with cervical cancer.

| Models | AIC | C-index (95% CI) | |
|---|---|---|---|
| | | Training cohort | Validation cohort |
| FIGO stage | 132.9 | 0.703 (0.572–0.834) | 0.700 (0.526–0.874) |
| Radscore | 121.4 | 0.794 (0.707–0.880) | 0.754 (0.623–0.885) |
| Combined model | 120.5 | 0.830 (0.738–0.922) | 0.772 (0.615–0.929) |

*FIGO, International Federation of Gynecology and Obstetrics; AIC, Akaike information criterion; CI, confidence interval; OS, overall survival.*

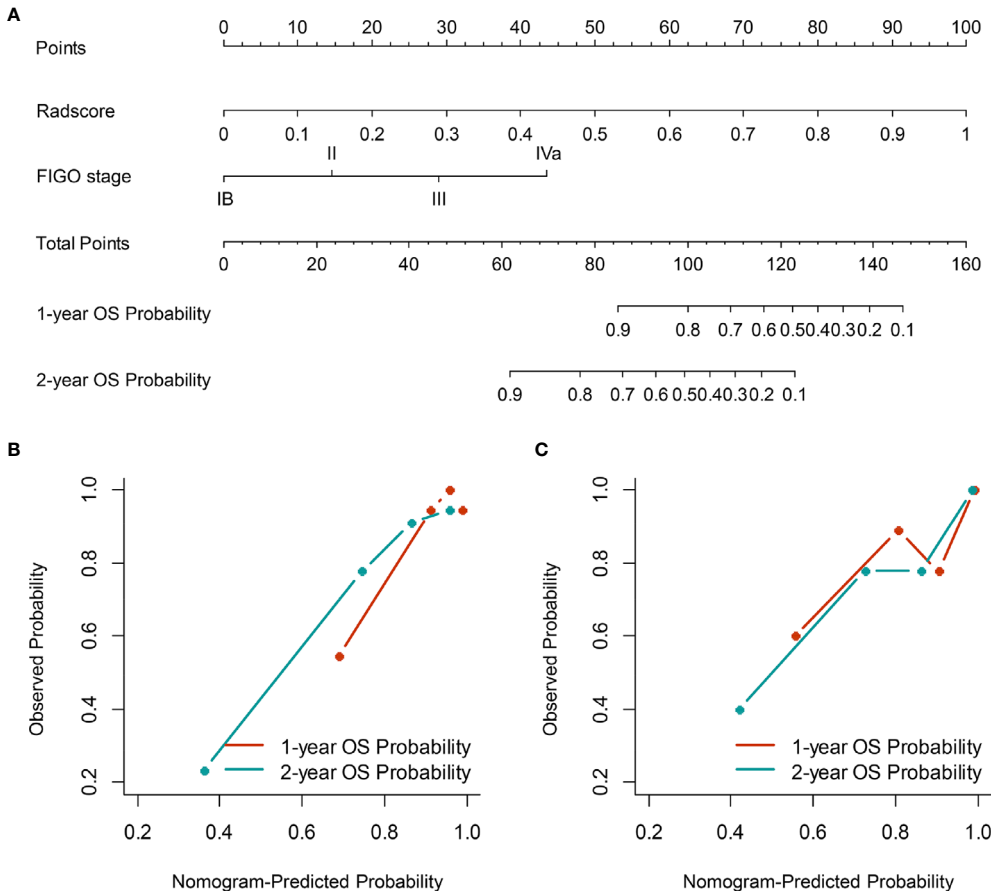


**FIGURE 3** | The nomogram **(A)** based on the FIGO stage and Radscore was used to estimate OS individually, along with the assessment of the model calibration. Calibration curves for the nomogram to the 1-year and 2-year OS rate in the training **(B)** and validation cohorts **(C)**. FIGO, International Federation of Gynecology and Obstetrics; OS, overall survival.

significantly improve the performance of the FIGO stage for OS evaluation. The combined model yielded the optimal performance for OS prediction in patients with cervical cancer. We established a radiomic nomogram derived from a combined model to individually estimate the OS of patients. The nomogram could successfully stratify these patients into high-risk and low-risk subgroups, and these two subgroups had different OS in both training and validation cohorts.

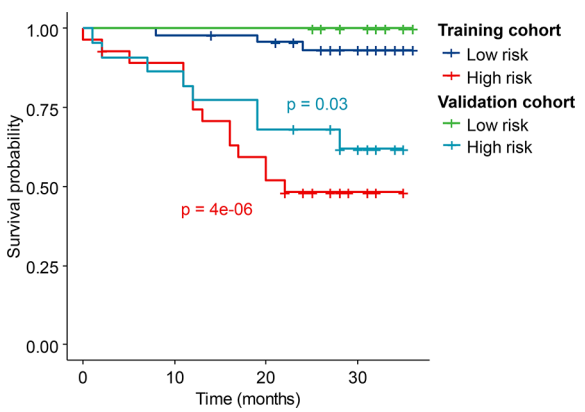


**FIGURE 4** | Kaplan–Meier curves of the high- and low-risk patients stratified by the combined model in the training cohort and validation cohort.

Prognosis evaluation in advance will greatly improve the treatment outcome in patients with cervical cancer. The most relevant tumor-related prognostic factors for locally advanced cervical cancer are tumor size at diagnosis, FIGO stage, and LNM (6, 16). However, our work showed that only the FIGO stage was an independent risk factor of OS in stage IB1–IVa cervical cancer. FIGO stage is the current standard staging system for cervical cancer based on findings from physical inspection and imaging examinations (17). The limitations of the FIGO stage are that it depends on many examinations and its classification is not objective enough (18). Therefore, an objective and efficient evaluation method that complements cervical cancer staging is of clinical significance.

The current radiomic workflow consists of adding quantitative data to visual analysis rather than replacing it entirely (19). In the

field of oncology, translational approaches are increasingly explored, for instance, Radiogenomics. Such studies usually need "big data" approaches and collaborative research (20). In this work, we proposed a new approach, translational but able to be quickly implemented for clinicians. To the best of our knowledge, this is the first study to integrate accessible FIGO stage and radiomic features extracted from pre-treatment CT images to predict the survival of cervical cancer. Radscore may be a more powerful predictor compared with the FIGO stage. With the help of Radscore, the prognostic value of the FIGO stage was significantly improved, leading to better risk stratification of patients. This score may be used for adaptive strategies to improve patient outcomes.

Radiomics has been involved in many aspects of cervical cancer, including prediction of tumor staging (21, 22), histological grading (23, 24), lymphovascular space invasion (LVI) (25), LNM (26–36), treatment response (37–42), and outcome (43–48) based on multimodal imaging tools (e.g., CT, MRI, and PET/CT). In clinical practice, the issues of most concern may be the evaluation of LNM, treatment response, and survival prediction. Hence, most radiomic studies focused on the evaluation of these in a non-invasive way. LNM is a key prognostic factor that affects the treatment decision and survival in cervical cancer. Song et al. combined the Radscore and morphological features of lymph nodes to assess the LNM in cervical cancer patients (26). Some studies developed radiomic models based on Radscore and clinical factors (e.g., MRI-reported lymph node status and FIGO stage) for predicting LNM in cervical cancer (27–36). Treatment response to neoadjuvant or concurrent chemotherapy may have a significant impact on patient management by identifying tailored approaches for patient subgroups to achieve a better clinical outcome. All relevant studies showed the additional value of radiomics to clinical factors and its potential to screen patients who are sensitive to chemotherapy (37–42). Survival evaluation is an eternal proposition for the field of oncology, which may benefit treatment strategies and follow-up plans. Ferreira et al. tested the feasibility of PET radiomic features combined with clinical information in predicting disease-free survival (DFS) in patients with cervical cancer (43). Fang et al. used MRI-based Radscore, LNM, and LVI to predict the DFS of early-stage cervical cancer (45). Lucia et al. found that the combination of PET/CT and MRI could result in more favorable survival prediction (47). Another study suggested that Radscore could enhance the prediction efficiency of conventional PET parameters in cervical cancer (48). In this current study, the results indicated that Radscore was an independent risk factor strongly associated with OS of cervical cancer and only texture features contributed to the survival prediction in cervical cancer. The HR of the Radscore was significantly higher than that of the FIGO stage, suggesting that the Radscore may provide more prognostic information than the FIGO stage in predicting the OS.

This study also had some limitations. First, selection bias was inevitable because of a retrospective study. Second, the sample size was small for a radiomic study. However, we performed a bootstrap to obtain corrected results. Third, the overall treatment times were not readily available, which is a well-recognized factor in cervical cancer outcomes. Fourth, this study had no local/regional failures, recognizing the short follow-up time. The additional evaluation of local control could be more clinically significant. Fifth, our radiomic features were extracted from CT images; those features from MRI or PET/CT images may provide different information about intratumoral heterogeneity. Sixth, the image analysis was based on the maximum level of the tumor instead of the whole tumor. However, some previous studies (45, 49) showed that the predictive performance of features extracted from the maximum level of the tumor was higher than that of those features extracted from the whole tumor. Two-dimensional features may increase the robustness of features compared with three-dimensional features. Seventh, the biological interpretation of radiomics remains an open question warranting further investigation (50). Finally, this is a single-institution study that needs external validation of the findings.

In conclusion, this present study provided a combined model, incorporating the FIGO stage and a Radscore derived from CT-based textural features, with favorable performance, and the study developed a noninvasive radiomic nomogram based on the results of the combined model for the pretherapy and personalized estimation of OS in patients with cervical cancer. In addition, the combined model serves as a collection of potential biomarkers and perfectly stratifies these patients into high-risk and low-risk subgroups. The identification of high-risk patients at diagnosis can allow tailored treatments involving higher doses of radiation boost, consolidation chemotherapy, and/or adjuvant hysterectomy, when indicated, and should be confirmed in external cohorts and prospective studies.

## DATA AVAILABILITY STATEMENT

The original contributions presented in the study are included in the article/supplementary material. Further inquiries can be directed to the corresponding authors.

## ETHICS STATEMENT

The studies involving human participants were reviewed and approved by Hunan Cancer Hospital, The Affiliated Cancer Hospital of Xiangya School of Medicine, Central South University. Written informed consent was waived.

## AUTHOR CONTRIBUTIONS

HL, MZ, and LJ designed the study. HL, MZ, and LJ contributed to the conception of the study and completed the manuscript together. JL, FB, and XZ contributed significantly to statistical analysis. YW and JW completed the following-up information. LJ, NW, and XY drafted the manuscript. All authors contributed to the article and approved the submitted version.

## REFERENCES


1. Sung H, Ferlay J, Siegel RL, Laversanne M, Soerjomataram I, Jemal A, et al. Global Cancer Statistics 2020: GLOBOCAN Estimates of Incidence and Mortality Worldwide for 36 Cancers in 185 Countries. *CA Cancer J Clin* (2021) 70(4):313. doi: 10.3322/caac.21660
2. Cohen PA, Jhingran A, Oaknin A, Denny L. Cervical Cancer. *Lancet* (2019) 393:169–82. doi: 10.1016/S0140-6736(18)32470-X
3. Edge SB, Compton CC. The American Joint Committee on Cancer: The 7th Edition of the AJCC Cancer Staging Manual and the Future of TNM. *Ann Surg Oncol* (2010) 17:1471–4. doi: 10.1245/s10434-010-0985-4
4. Herrera FG, Breuneval T, Prior JO, Bourhis J, Ozsahin M. [18f]FDG-PET/CT Metabolic Parameters as Useful Prognostic Factors in Cervical Cancer Patients Treated With Chemo-Radiotherapy. *Radiat Oncol* (2016) 11(1):43. doi: 10.1186/s13014-016-0614-x
5. Monk BJ, Tewari KS, Koh WJ. Multimodality Therapy for Locally Advanced Cervical Carcinoma: State of the Art and Future Directions. *J Clin Oncol* (2007) 25:2952–65. doi: 10.1200/JCO.2007.10.8324
6. Rose PG, Java J, Whitney CW, Stehman FB, Lanciano R, Thomas GM, et al. Nomograms Predicting Progression-Free Survival, Overall Survival, and Pelvic Recurrence in Locally Advanced Cervical Cancer Developed From an Analysis of Identifiable Prognostic Factors in Patients From NRG Oncology/Gynecologic Oncology Group Randomized Trials of Chemoradiotherapy. *J Clin Oncol* (2015) 33(19):2136. doi: 10.1200/JCO.2014.57.7122
7. Caudell JJ, Torres-Roca JF, Gillies RJ, Enderling H, Kim S, Rishi A, et al. The Future of Personalised Radiotherapy for Head and Neck Cancer. *Lancet Oncol* (2017) 18:e266–73. doi: 10.1016/S1470-2045(17)30252-8
8. Bi WL, Hosny A, Schabath MB, Giger ML, Birkbak NJ, Mehrtash A, et al. Artificial Intelligence in Cancer Imaging: Clinical Challenges and Applications. *CA Cancer J Clin* (2019) 69:127–57. doi: 10.3322/caac.21552
9. Lambin P, Leijenaar RTH, Deist TM, Peerlings J, de Jong EEC, van Timmeren J, et al. Radiomics: The Bridge Between Medical Imaging and Personalized Medicine. *Nat Rev Clin Oncol* (2017) 14:749–62. doi: 10.1038/nrclinonc.2017.141
10. Aerts HJ, Velazquez ER, Leijenaar RT, Parmar C, Grossmann P, Carvalho S, et al. Decoding Tumour Phenotype by Noninvasive Imaging Using a Quantitative Radiomics Approach. *Nat Commun* (2014) 5:4006. doi: 10.1038/ncomms5644
11. Lambin P, Rios-Velazquez E, Leijenaar R, Carvalho S, van Stiphout RG, Granton P, et al. Radiomics: Extracting More Information From Medical Images Using Advanced Feature Analysis. *Eur J Cancer* (2012) 48(4):441–6. doi: 10.1016/j.ejca.2011.11.036
12. Ai Y, Zhu H, Xie C, Jin X. Radiomics in Cervical Cancer: Current Applications and Future Potential. *Crit Rev Oncol Hematol* (2020) 152:102985. doi: 10.1016/j.critrevonc.2020.102985
13. McMahon CJ, Rofsky NM, Pedrosa I. Lymphatic Metastases From Pelvic Tumors: Anatomic Classification, Characterization, and Staging. *Radiology* (2010) 254:31–46. doi: 10.1148/radiol.2541090361
14. Zhang Y, Yu S, Zhang L, Kang L. Radiomics Based on CECT in Differentiating Kimura Disease From Lymph Node Metastases in Head and Neck: A Non-Invasive and Reliable Method. *Front Oncol* (2020) 10:1121. doi: 10.3389/fonc.2020.01121
15. Limkin EJ, Sun R, Dercle L, Zacharaki EI, Robert C, Reuzé S, et al. Promises and Challenges for the Implementation of Computational Medical Imaging (Radiomics) in Oncology. *Ann Oncol* (2017) 28:1191–206. doi: 10.1093/annonc/mdx034
16. Kristensen GB, Abeler VM, Risberg B, Tropé C, Bryne M. Tumor Size, Depth of Invasion, and Grading of the Invasive Tumor Front are the Main Prognostic Factors in Early Squamous Cell Cervical Carcinoma. *Gynecoloncol* (1999) 74(2):245–51. doi: 10.1006/gyno.1999.5420
17. Creasman WT. New Gynecologic Cancer Staging. *Obstetr Gynecol* (1990) 75 (2):287–8.
18. Nordström B, Strang P, Lindgren A, Bergström R, Tribukait B. Carcinoma of the Endometrium: Do the Nuclear Grade and DNA Ploidy Provide More Prognostic Information Than do the FIGO and WHO Classifications? *Int J Gynecol Pathol* (1996) 15(3):191–201. doi: 10.1097/00004347-199607000-00002
19. Aerts HJWL. The Potential of Radiomic-Based Phenotyping in Precision Medicine: A Review. *JAMA Oncol* (2016) 2(12):1636–42. doi: 10.1001/jamaoncol.2016.2631
20. Andreassen CN, Schack LMH, Laursen LV, Alsner J. Radiogenomics – Current Status, Challenges and Future Directions. *Cancer Lett* (2016) 382:127–36. doi: 10.1016/j.canlet.2016.01.035
21. Mu W, Chen Z, Liang Y, Shen W, Yang F, Dai R, et al. Staging of Cervical Cancer Based on Tumor Heterogeneity Characterized by Texture Features on 18F-FDG PET Images. *Phys Med Biol* (2015) 60(13):5123. doi: 10.1088/0031-9155/60/13/5123
22. Umutlu L, Nensa F, Demircioglu A, Antoch G, Herrmann K, Forsting M, et al. Radiomics Analysis of Multiparametric PET/MRI for N- and M-Staging in Patients With Primary Cervical Cancer. *Rofo* (2020) 192:754–63. doi: 10.1055/a-1100-0127
23. Liu Y, Zhang Y, Cheng R, Liu S, Qu F, Yin X, et al. Radiomics Analysis of Apparent Diffusion Coefficient in Cervical Cancer: A Preliminary Study on Histological Grade Evaluation. *J Magn Reson Imaging* (2019) 49:280–90. doi: 10.1002/jmri.26192
24. Shen WC, Chen SW, Liang JA, Hsieh TC, Yen KY, Kao CH. [18] Fluorodeoxyglucose Positron Emission Tomography for the Textural Features of Cervical Cancer Associated With Lymph Node Metastasis and Histological Type. *Eur J Nucl Med Mol I* (2017) 44(10):1721–31. doi: 10.1007/s00259-017-3697-1
25. Jiang X, Li J, Kan Y, Yu T, Chang S, Sha X, et al. MRI Based Radiomics Approach With Deep Learning for Prediction of Vessel Invasion in Early-Stage Cervical Cancer. *IEEE/ACM Trans Comput Biol Bioinform* (2020) 18 (3):995–1002. doi: 10.1109/TCBB.2019.2963867
26. Song J, Hu Q, Ma Z, Zhao M, Chen T, Shi H. Feasibility of TWI-MRI-Based Radiomics Nomogram for Predicting Normal-Sized Pelvic Lymph Node Metastasis in Cervical Cancer Patients. *Eur Radiol* (2021). doi: 10.1007/s00330-021-07735-x
27. Deng X, Liu M, Sun J, Li M, Liu D, Li L, et al. Feasibility of MRI-Based Radiomics Features for Predicting Lymph Node Metastases and VEGF Expression in Cervical Cancer. *Eur J Radiol* (2021) 134:109429. doi: 10.1016/j.ejrad.2020.109429
28. Chen X, Liu W, Thai TC, Castellano T, Gunderson CC, Moore K, et al. Developing a New Radiomics-Based CT Image Marker to Detect Lymph Node Metastasis Among Cervical Cancer Patients. *Comput Methods Progr BioMed* (2020) 197:105759. doi: 10.1016/j.cmpb.2020.105759
29. Hou L, Zhou W, Ren J, Du X, Xin L, Zhao X, et al. Radiomics Analysis of Multiparametric MRI for the Preoperative Prediction of Lymph Node Metastasis in Cervical Cancer. *Front Oncol* (2020) 10:1393. doi: 10.3389/fonc.2020.01393
30. Dong T, Yang C, Cui B, Zhang T, Sun X, Song K, et al. Development and Validation of a Deep Learning Radiomics Model Predicting Lymph Node Status in Operable Cervical Cancer. *Front Oncol* (2020) 10:464. doi: 10.3389/fonc.2020.00464
31. Xiao M, Ma F, Li Y, Li Y, Li M, Zhang G, et al. Multiparametric MRI-Based Radiomics Nomogram for Predicting Lymph Node Metastasis in Early-Stage Cervical Cancer. *J Magn Reson Imaging* (2020) 52:885–96. doi: 10.1002/jmri.27101
32. Jin X, Ai Y, Zhang J, Zhu H, Jin J, Teng Y, et al. Noninvasive Prediction of Lymph Node Status for Patients With Early-Stage Cervical Cancer Based on Radiomics Features From Ultrasound Images. *Eur Radiol* (2020) 30:4117–24. doi: 10.1007/s00330-020-06692-1
33. Wu Q, Wang S, Chen X, Wang Y, Dong L, Liu Z, et al. Radiomics Analysis of Magnetic Resonance Imaging Improves Diagnostic Performance of Lymph Node Metastasis in Patients With Cervical Cancer. *Radiother Oncol* (2019) 138:141–8. doi: 10.1016/j.radonc.2019.04.035
34. Wang T, Gao T, Yang J, Yan X, Wang Y, Zhou X, et al. Preoperative Prediction of Pelvic Lymph Nodes Metastasis in Early-Stage Cervical Cancer Using Radiomics Nomogram Developed Based on T2-Weighted MRI and Diffusion-Weighted Imaging. *Eur J Radiol* (2019) 114:128–35. doi: 10.1016/j.ejrad.2019.01.003
35. Li Z, Li H, Wang S, Dong D, Yin F, Chen A, et al. MR-Based Radiomics Nomogram of Cervical Cancer in Prediction of the Lymph-Vascular Space Invasion Preoperatively. *J Magn Reson Imaging* (2019) 49:1420–6. doi: 10.1002/jmri.26531
36. Kan Y, Dong D, Zhang Y, Jiang W, Zhao N, Han L, et al. Radiomic Signature as a Predictive Factor for Lymph Node Metastasis in Early-Stage Cervical Cancer. *J Magn Reson Imaging* (2019) 49:304–10. doi: 10.1002/jmri.26209

37. Gui B, Autorino R, Miccò M, Nardangeli A, Pesce A, Lenkowicz J, et al. Pretreatment MRI Radiomics Based Response Prediction Model in Locally Advanced Cervical Cancer. *Diagnost (Basel)* (2021) 11(4). doi: 10.3390/diagnostics11040631
38. Liu D, Zhang X, Zheng T, Shi Q, Cui Y, Wang Y, et al. Optimisation and Evaluation of the Random Forest Model in the Efficacy Prediction of Chemoradiotherapy for Advanced Cervical Cancer Based on Radiomics Signature From High-Resolution T2 Weighted Images. *Arch Gynecol Obstet* (2021) 303:811–20. doi: 10.1007/s00404-020-05908-5
39. Fang M, Kan Y, Dong D, Yu T, Zhao N, Jiang W, et al. Multi-Habitat Based Radiomics for the Prediction of Treatment Response to Concurrent Chemotherapy and Radiation Therapy in Locally Advanced Cervical Cancer. *Front Oncol* (2020) 10:563. doi: 10.3389/fonc.2020.00563
40. Tian X, Sun C, Liu Z, Li W, Duan H, Wang L, et al. Prediction of Response to Preoperative Neoadjuvant Chemotherapy in Locally Advanced Cervical Cancer Using Multicenter CT-Based Radiomic Analysis. *Front Oncol* (2020) 10:77. doi: 10.3389/fonc.2020.00077
41. Sun C, Tian X, Liu Z, Li W, Li P, Chen J, et al. Radiomic Analysis for Pretreatment Prediction of Response to Neoadjuvant Chemotherapy in Locally Advanced Cervical Cancer: A Multicentre Study. *EBioMedicine* (2019) 46:160–9. doi: 10.1016/j.ebiom.2019.07.049
42. Bowen SR, Yuh WTC, Hippe DS, Wu W, Partridge SC, Elias S, et al. Tumor Radiomic Heterogeneity: Multiparametric Functional Imaging to Characterize Variability and Predict Response Following Cervical Cancer Radiation Therapy. *J Magn Reson Imaging* (2018) 47:1388–96. doi: 10.1002/jmri.25874
43. Ferreira M, Lovinfosse P, Hermesse J, Decuypere M, Rousseau C, Lucia F, et al. [F]FDG PET Radiomics to Predict Disease-Free Survival in Cervical Cancer: A Multi-Scanner/Center Study With External Validation. *Eur J Nucl Med Mol Imaging* (2021). doi: 10.1007/s00259-021-05303-5
44. Park SH, Hahm MH, Bae BK, Chong GO, Jeong SY, Na S, et al. Magnetic Resonance Imaging Features of Tumor and Lymph Node to Predict Clinical Outcome in Node-Positive Cervical Cancer: A Retrospective Analysis. *Radiat Oncol* (2020) 15:86. doi: 10.1186/s13014-020-01502-w
45. Fang J, Zhang B, Wang S, Jin Y, Wang F, Ding Y, et al. Association of MRI-Derived Radiomic Biomarker With Disease-Free Survival in Patients With Early-Stage Cervical Cancer. *Theranostics* (2020) 10:2284–92. doi: 10.7150/thno.37429
46. Lucia F, Visvikis D, Vallières M, Desseroit MC, Miranda O, Robin P, et al. External Validation of a Combined PET and MRI Radiomics Model for Prediction of Recurrence in Cervical Cancer Patients Treated With Chemoradiotherapy. *Eur J Nucl Med Mol Imaging* (2019) 46:864–77. doi: 10.1007/s00259-018-4231-9
47. Lucia F, Visvikis D, Desseroit MC, Miranda O, Malhaire JP, Robin P, et al. Prediction of Outcome Using Pretreatment F-FDG PET/CT and MRI Radiomics in Locally Advanced Cervical Cancer Treated With Chemoradiotherapy. *Eur J Nucl Med Mol Imaging* (2018) 45:768–86. doi: 10.1007/s00259-017-3898-7
48. Schernberg A, Reuze S, Orlhac F, Buvat I, Dercle L, Sun R, et al. A Score Combining Baseline Neutrophilia and Primary Tumor SUV Measured From FDG PET is Associated With Outcome in Locally Advanced Cervical Cancer. *Eur J Nucl Med Mol Imaging* (2018) 45:187–95. doi: 10.1007/s00259-017-3824-z
49. Zhang L, Wu X, Liu J, Zhang B, Mo X, Chen Q, et al. MRI-Based Deep-Learning Model for Distant Metastasis-Free Survival in Locoregionally Advanced Nasopharyngeal Carcinoma. *J Magn Reson Imaging* (2021) 53:167–78. doi: 10.1002/jmri.27308
50. Fournier L, Costaridou L, Bidaut L, Michoux N, Lecouvet FE, de Geus-Oei LF, et al. Incorporating Radiomics Into Clinical Trials: Expert Consensus Endorsed by the European Society of Radiology on Considerations for Data-Driven Compared to Biologically Driven Quantitative Biomarkers. *Eur Radiol* (2021) 31:6001–12. doi: 10.1007/s00330-020-07598-8


**Conflict of Interest:** The authors declare that the research was conducted in the absence of any commercial or financial relationships that could be construed as a potential conflict of interest.

**Publisher's Note:** All claims expressed in this article are solely those of the authors and do not necessarily represent those of their affiliated organizations, or those of the publisher, the editors and the reviewers. Any product that may be evaluated in this article, or claim that may be made by its manufacturer, is not guaranteed or endorsed by the publisher.

frontiers in Oncology

ORIGINAL RESEARCH
published: 17 August 2021
doi: 10.3389/fonc.2021.729219

# A 4-Gene Signature Associated With Recurrence in Low- and Intermediate-Risk Endometrial Cancer

*Diocésio Alves Pinto de Andrade[1,2]*, Luciane Sussuchi da Silva[2], Ana Carolina Laus[2], Marcos Alves de Lima[3], Gustavo Nóriz Berardinelli[2], Vinicius Duval da Silva[4], Graziela de Macedo Matsushita[4], Murilo Bonatelli[2], Aline Larissa Virginio da Silva[2], Adriane Feijó Evangelista[2], Jesus Paula Carvalho[5], Rui Manuel Reis[2,6,7] and Ricardo dos Reis[8]*

*[1] InORP ONCOCLÍNICAS Group, Oncology Institute of Ribeirão Preto, Ribeirão Preto, Brazil, [2] Molecular Oncology Research Center, Barretos Cancer Hospital, Barretos, Brazil, [3] Epidemiology and Biostatistics Nucleus, Barretos Cancer Hospital, Barretos, Brazil, [4] Departament of Pathology, Barretos Cancer Hospital, Barretos, Brazil, [5] Discipline of Gynecology, Instituto do Cancer do Estado de São Paulo (ICESP), Faculdade de Medicina da Universidade de São Paulo, São Paulo, Brazil, [6] Life and Health Sciences Research Institute (ICVS), School of Medicine, University of Minho, Braga, Portugal, [7] ICVS/3B's - PT Government Associate Laboratory, Braga/Guimarães, Portugal, [8] Department of Gynecologic Oncology, Barretos Cancer Hospital, Barretos, Brazil*

OPEN ACCESS

**Edited by:**
*Jian-Jun Wei, Northwestern University, United States*

**Reviewed by:**
*Enes Taylan, Mount Sinai Hospital, United States*
*Julio de la Torre-Montero, Comillas Pontifical University, Spain*

***Correspondence:**
*Diocésio Alves Pinto de Andrade*
*diocesio@yahoo.com*

**Specialty section:**
*This article was submitted to Gynecological Oncology, a section of the journal Frontiers in Oncology*

**Received:** *22 June 2021*
**Accepted:** *30 July 2021*
**Published:** *17 August 2021*

**Citation:**
*de Andrade DAP, da Silva LS, Laus AC, de Lima MA, Berardinelli GN, da Silva VD, Matsushita GdM, Bonatelli M, da Silva ALV, Evangelista AF, Carvalho JP, Reis RM and dos Reis R (2021) A 4-Gene Signature Associated With Recurrence in Low- and Intermediate-Risk Endometrial Cancer. Front. Oncol. 11:729219. doi: 10.3389/fonc.2021.729219*

**Background:** The molecular profile of endometrial cancer has become an important tool in determining patient prognosis and their optimal adjuvant treatment. In addition to The Cancer Genome Atlas (TCGA), simpler tools have been developed, such as the Proactive Molecular Risk Classifier for Endometrial Cancer (ProMisE). We attempted to determine a genetic signature to build a recurrence risk score in patients diagnosed with low- and intermediate-risk endometrial cancer.

**Methods:** A case-control study was conducted. The eligible patients were women diagnosed with recurrence low- and intermediate-risk endometrial cancer between January 2009 and December 2014 at a single institution; the recurrence patients were matched to two nonrecurrence patients with the same diagnosis by age and surgical staging. Following RNA isolation of 51 cases, 17 recurrence and 34 nonrecurrence patients, the expression profile was determined using the *nCounter® PanCancer Pathways Panel*, which contains 770 genes.

**Results:** The expression profile was successfully characterized in 49/51 (96.1%) cases. We identified 12 genes differentially expressed between the recurrence and nonrecurrence groups. The ROC curve for each gene was generated, and all had AUCs higher than 0.7. After backward stepwise logistic regression, four genes were highlighted: *FN1, DUSP4, LEF1, and SMAD9*. The recurrence risk score was calculated, leading to a ROC curve of the 4-gene model with an AUC of 0.93, sensitivity of 100%, and specificity of 72.7%.

**Conclusion:** We identified a four-gene signature that may be associated with recurrence in patients with low- and intermediate-risk endometrial cancer. This finding suggests a new prognostic factor in this poorly explored group of patients with endometrial cancer.

**Keywords: low- and intermediate-risk endometrioid endometrial carcinoma, genetic signature, recurrence risk score, biomarkers, Brazil**

# INTRODUCTION

Endometrial cancer is the most prevalent gynecological tumor in developed countries, such as the USA and members of the European Union (1). The number of cases in the last decade have increased, possibly due to the increase in obesity in these countries (2). In Brazil, endometrial cancer is the eighth most commonly diagnosed cancer in women, with 6,540 new cases in 2020 (3). When diagnosed at an early stage, these patients have an excellent prognosis. Countless risk stratifications associate staging with other variables, such as tumor grade, lymphovascular space invasion (LVSI) and histology, to define sequential adjuvant treatments (4).

Traditionally, it has been considered two distinct diseases since Bokhman's publication in the early 1980s (low-grade endometrioid adenocarcinomas (type I, "well-differentiated") and nonendometrioid carcinomas (type II, "poorly differentiated") (5). Recently, The Cancer Genome Atlas (TCGA) project changed the understanding of the carcinogenesis of this tumor, leading to four molecular subgroups with different prognoses (DNA polymerase epsilon (*POLE*) ultramutated, microsatellite instability (MSI) hypermutated, copy number (CN) low, and CN high) (6). Due to the complexity (whole genome sequencing, exome sequencing, microsatellite assays, and CN aberration analysis), costs, and need for ideally frozen tissue for reproducibility of this classification in clinical practice, new methodologies have been developed. The two most currently used are the Proactive Molecular Risk Classifier for Endometrial Cancer (ProMisE) and Leiden/TransPORTEC classification, in which the four groups with different prognoses are also described (7, 8). Immunohistochemistry was used to detect the presence/absence of mismatch repair (MMR) proteins and to evaluate *TP53* mutations, and only one step used genetic sequencing (next-generation or Sanger sequencing) to identify *POLE* hotspot exonuclease domain mutations (7, 8).

Using the TCGA consortium database, some studies have built prognostic models of endometrial cancer recurrence according to genetic signatures or evaluated RNA expression (9, 10). Furthermore, other studies correlate potential genetic signatures with histopathological markers such as tumor-infiltrating immune cells (11, 12).

The aim of this study was to determine a genetic signature of recurrence risk in patients diagnosed with low- and intermediate-risk endometrial cancer in routine formalin-fixed paraffin-embedded (FFPE) tissue using a large panel of 770 genes covering 13 key cancer-related pathways by NanoString, a highly sensitive and robust methodology for RNA expression of FFPE samples.

# MATERIAL AND METHODS

## Patients and Specimens

From a retrospective cohort of 195 patients diagnosed with low- and intermediate-risk endometrial cancer between January 2009 and December 2014 at Barretos Cancer Hospital (BCH), two pathologists with oncogynecologic expertise reviewed the initial report of all patients to confirm their diagnosis. Clinical and pathological features were obtained from the medical records. Of the 22 patients who initially presented recurrence, the diagnosis remained low- and intermediate-risk endometrial cancer for 17 patients. We define low- and intermediate-risk endometrial cancer according to the European Society of Medical Oncology (ESMO)-modified criteria (4). Based on these results, a case-control study was carried out. Nonrecurrence patients with the same histopathological diagnosis were matched to recurrence cases in a 2:1 ratio by age and FIGO (International Federation of Gyneocologic and Obstetrics) staging (IA and IB). Overall, 51 patients (17 recurrence and 34 non-recurrence) were analyzed.

This study was conducted following the ethical principles of the Declaration of Helsinki, and the BCH Ethical Review Board approved it in March 2017 (Reference number 1.942.488).

## DNA and RNA Isolation

DNA and RNA were isolated from 10 μm-thick formalin-fixed paraffin-embedded (FFPE) tumor samples sectioned on slides, as previously reported (13). One slide was stained with hematoxylin and eosin (H&E) and evaluated by experienced pathologists for identification, sample adequacy assessment, and selection of the tumor tissue area (minimum of 60% tumor area). DNA and RNA were isolated using the QiaAmp DNA Micro kit (Qiagen, Hilden, Germany) and the RecoverAll™ Total Nucleic Acid Isolation kit (Ambion by Life Technologies, Austin, TX, USA), respectively. The quality and concentration of DNA and RNA were measured by both a NanoDrop ND-200 spectrophotometer (NanoDrop Products, Wilmington, DE, USA) and Qubit Fluorometric Quantitation (Thermo Fisher Scientific, USA). The samples were stored at -80°C until molecular analysis.

## ProMisE Evaluation

The ProMisE assessment was performed using molecular methodologies, namely, molecular evaluation of MSI, *TP53* mutation analyses by next-generation sequencing, and *POLE* hotspot mutations by Sanger sequencing.

To define MSI, we performed hexaplex PCR with six monomorphic mononucleotide markers (NR21, NR24, NR27, BAT25, BAT26, and HSP110), followed by fragment analysis in a 3500XL Genetic Analyzer sequencer (Applied Biosystems, Foster City, CA, USA), as previously described by our group (14). The presence of two or more markers with instability classified the cases as high microsatellite instability (MSI-H), the presence of one marker with instability was classified as low MSI (MSI-L), and the absence of any marker with instability as microsatellite stable (MSS). Presence of MSI was determined only for MSI-H cases.

To evaluate *POLE* mutations, we used direct Sanger sequencing, as described by Britton et al. PCR was performed using targeted primers for the exonuclease domain (exons 9-14) of *POLE* (15). The purified samples were subjected to capillary electrophoresis in a 3500XL Genetic Analyzer sequencer (Applied Biosystems, Foster City, CA, USA), and the results were analyzed with SegScape v2.7 software (Applied Biosystems, Foster City, CA, USA).

*TP53* mutations were detected with an NGS-based assay using the Illumina TruSight Tumor 15 (TST15) on the MiSeq instrument (Illumina, San Diego, CA, USA) according to the manufacturer's instructions, as previously reported (16). The TST15 panel assesses

all coding sequences of the *TP53* gene. Read alignment and variant calling were performed with BaseSpace BWA Enrichment version 2.1 (Illumina, San Diego, CA, USA) and Sophia DDM® software version 5.7.3 (Sophia Genetics SA, Switzerland). The identification of pathogenic variants occurred after the application of filters to remove low-quality variants. Variants with < 500X read depth, VAF <10%, and intronic, intergenic, 3' UTR, and synonymous variants were excluded. Thereafter, the variants that presented as polymorphisms, within a frequency >1% in the GnomAD database, were removed (those that had no population frequency information followed in the analyses). Finally, the pathogenicity of variants was checked in the databases ClinVar, IARC TP53, COSMIC, and CGI.

## NanoString nCounter Analysis

Samples were processed for analysis on the NanoString nCounter Flex system using the 770 gene nCounter® PanCancer Pathways Panel (NanoString Technologies, Inc., Seattle, WA, USA), as previously reported (17). This panel assesses 13 cancer-associated canonical pathways related to basic cancer biology (Notch, Wnt, Hedgehog, Chromatin modification, Transcriptional regulation, DNA damage control, TGF-β, MAPK, STAT, PI3K, RAS, Cell cycle, Apoptosis). Briefly, 100 ng of total RNA, quantified by a Qubit Fluorometric System (Thermo Fisher Scientific, USA), from each sample was hybridized for 21 hours at 65°C, followed by purification and RNA/probe complex immobilization in nCounter PrepStation (NanoString Technologies, Inc., Seattle, WA, USA) and cartridge scanning in a digital analyzer (NanoString Technologies, Inc., Seattle, WA, USA), according to the manufacturer's protocol. Reading with 280 field-of-views (FOVs) was used in the study samples.

## Bioinformatics and Statistical Analysis

We used nSolver™ Analysis Software, version 4.0 (NanoString Technologies, Inc., Seattle, WA, USA) to assess the quality control parameters of all samples. Further analyses were performed using the *R language* and environment for statistical computing (R-project (v3.6.3); The R Foundation, Vienna, Austria) (18). The quantro package (v1.18.0) was applied for cartridge evaluation and to assist in choosing the normalization method. The gene expression data were normalized by the quantile method implemented in the NanoStringNorm package and transformed into a *log2* scale. RNA differential expression was evaluated in the NanoStringNorm package considering two different groups (recurrent *vs*. nonrecurrent low- and intermediate-risk endometrial cancer) with a significance level of $p \leq 0.01$ and fold change of 2.0 (19). Heatmaps and hierarchical clustering of differentially expressed genes were built with the ComplexHeatmap package (v2.0.0) (20). The STRING database was applied to predict interaction networks from differentially expressed genes (21).

Through the ROC curves, we evaluated the sensitivity and specificity of differential RNA expression by comparing patients with recurrence with those who did not have recurrence using the pROC package (22). An area under the curve (AUC) above 0.7 was considered acceptable for further gene evaluation. We used the backward stepwise logistic regression technique within the MASS package (version 7.3.53) to build a recurrence risk model according to the RNA expression of the samples.

Data analysis was performed using IBM Statistical Package for the Social Sciences (SPSS) database version 27.0 (SPSS, Chicago, IL, USA). Descriptive statistical analysis for quantitative variables used mean, maximum, and minimum and for qualitative variables used percentage. Once the variables were defined, univariate analysis was performed using the chi-square test and Mann-Whitney's U-test. Variables with a $p$ value < 0.2 in univariate analyses were entered into the logistic regression analysis. The threshold for statistical significance was 5%. Study data were collected and managed using REDCap (Research Electronic Data Capture) electronic data capture tools hosted at BCH (23).

# RESULTS

## Patient Features

The clinical and pathological information of the two groups is summarized in **Table 1**. More than 96% of patients are ECOG 0-1. In the recurrence group, we had four patients diagnosed with endometrial adenocarcinoma with squamous differentiation, whereas in the nonrecurrence group, we did not have any diagnosis of this histological subtype (p = 0.01). There was a higher prevalence of white patients in the recurrence group (94.1%) than in the nonrecurrence group (70.6%) (p = 0.075). Other clinical and pathological features were well balanced between the two groups.

Of the 51 samples that were sequenced for ProMisE, we observed a high frequency of inconclusive results due to the poor quality of the DNA obtained, hampering meaningful analysis. The assessment of MSI was inconclusive in one case, and among the other 50 cases, 12 (24%) were MSI-H. Of the 39 remaining samples for *POLE* sequencing, 18 were inconclusive, and only one (4.8%) was mutated [exon 9 – c.857C>G; p. (Pro286Arg)]. Concerning the 38 samples for *TP53* mutation analysis, 10 cases (66.7%) were wild-type, and five (33.3%) were mutated (**Supplementary Table 1**). There was no difference between the four groups of the ProMisE methodology and the increased chance of recurrence (p = 0.823).

## Gene Expression

Concerning the gene expression profile, 49 of the 51 cases (96%) were conclusive, leading to 16 recurrence and 33 nonrecurrence samples for further analysis. Two samples were excluded due to low-quality RNA. The expression profile based on unsupervised clustering showed 12 genes with differential RNA expression between the two groups studied (**Figure 1**). The *LEF1, PLA2G4A, DKK1, BMP4, FGF19, FN1, SMAD9*, and *DUSP4* genes showed increased RNA expression in the recurrence group, while *HIST1H3G, SIX1, TNF*, and *IL8* were downregulated compared to nonrecurrence group.

We next generated a ROC curve for each of the 12 genes described above to assess the performance of each gene to discriminate between the recurrence and nonrecurrence groups (**Table 2**). All 12 genes presented an AUC higher than 0.7.

**TABLE 1** | Clinical and pathological characteristics of patients with low- and intermediate-risk endometrial cancer.

| | | Recurrence (n=17) | Nonrecurrence (n=34) | *p* value |
|---|---|---|---|---|
| Age (mean)[a] | | 62.4 (46-77) | 62,8 (51-88) | 0.779 |
| FIGO staging (%)[b] | IA | 11 (64.7) | 22 (64.7) | 1.00 |
| | IB | 6 (35.3) | 12 (35.3) | |
| ECOG Performance Status (%)[b] | 0-1 | 16 (94.1) | 33 (97.0) | 1.00 |
| | 2 | 1 (5.9) | 1 (3.0) | |
| Ethnicity (%)[b] | White | 16 (94.1) | 24 (70.6) | **0.075** |
| | Nonwhite | 1 (5.9) | 10 (29.4) | |
| BMI (mean)[a] | | 31.42 (19.78-43.29) | 33.03 (18.67-52.71) | 0.873 |
| Smoking history[b] | Yes | 3 (17.6) | 4 (11.8) | 0.673 |
| | No | 14 (82.4) | 30 (88.2) | |
| Surgery | With lymphadenectomy | 6 (35.3) | 16 (47.1) | 0.424 |
| | Without lymphadenectomy | 11 (64.7) | 18 (52.9) | |
| Surgical route | Laparotomic | 8 (47.1) | 10 (29.4) | 0.233 |
| | Laparoscopic | 9 (52.9) | 24 (70.6) | |
| Tumor differentiation grade[b] | Grade 1 | 9 (52.9) | 22 (64.7) | 0.417 |
| | Grade 2 | 8 (47.1) | 12 (35.3) | |
| Histological subtype (%)[b] | Endometrioid | 13 (76.5) | 34 (100) | **0.010** |
| | Endometrioid with squamous differentiation | 4 (23.5) | 0 (0.0) | |
| Tumor size (mean – cm)[a] | | 4.5 (2.2-11.5) | 3.8 (1.0-7.0) | 0.219 |
| Endocervical invasion (%)[b] | Yes | 4 (23.5) | 7 (20.6) | 1.00 |
| | No | 13 (76.5) | 27 (79.4) | |
| LVSI (%)[b] | Yes | 3 (17.6) | 3 (8.8) | 0.387 |
| | No | 14 (82.4) | 31 (91.2) | |

*BMI, body mass index; ECOG, Eastern Cooperative Oncology Group; FIGO, International Federation of Gynecology and Obstetrics; LVSI, lymphovascular space invasion.*
[a]*Mann-Whitney test.*
[b]*Fisher's exact test.*
*Bold, significant values.*

To understand the crosstalk among the 12 genes, an interaction network was constructed and is depicted in **Figure 2**. Except for the *DUSP4* and *HIST1H3G* genes, interactions are known among the differentially expressed genes.

## Recurrence Risk Score

Based on the 12 differentially expressed genes, we applied logistic regression to build a recurrence risk score (RRS) and improve predictive performance. Through the backward stepwise logistic regression model, four genes with the best performance were selected: *FN1, DUSP4, LEF1,* and *SMAD9* (increased RNA expression in the recurrence cases). The RRS was calculated as the logit from the logistic regression as follows: RRS = -21.14 + 1.02**FN1* + 1.07**DUSP4* + 0.6211**LEF1* + 0.8832**SMAD9* (**Supplementary Table 2**).

Univariate analysis was performed to calculate the odds ratio (OR) for each gene and for the final score (**Table 3**). Cases with overexpression of the *FN1* gene had an OR of 3.3 for recurrence compared to cases without overexpression. In addition, the final gene score showed an OR of 2.7 for recurrence.

Moreover, the combination of the expression of the four genes showed an AUC of 0.93, a sensitivity of 100%, and a specificity of 72.7% to identify low- and intermediate-risk endometrial cancer with recurrence trough the RNA expression **(Figure 3).**

We performed a logistic regression analysis with the four differentially expressed genes score and two significant clinicopathological variables (ethnicity and histological subtype). The histological subtype variable was withdrawn from this model since one of its categories did not contain subjects (no endometrioid with squamous differentiation in the nonrecurrence group), resulting in no data conversion to the odds ratio value. Using a backward stepwise logistic regression technique, a new model was constructed with two parameters: four differentially expressed genes score (OR: 2.616; $p = 0.001$) and white ethnicity (OR: 0.299; $p = 0.342$).

# DISCUSSION

In this study, we characterized the expression profile of two distinct groups (recurrence and nonrecurrence) of low- and intermediate-risk endometrial cancer. Twelve genes were differentially expressed. After performed a logistic regression, four genes remained to define a possible RRS model, exhibiting an impressive AUC of 0.93, with a sensitivity of 100% and a specificity of 73%. To the best of our knowledge, this is the first study to identify a gene signature associated with recurrence in low- and intermediate-risk endometrial cancer.

The four genes are associated with important cancer pathways, namely, the MAPK/PI3K pathways (*FN1* and *DUSP4*), the Wnt pathway (*LEF1*), and the TGF pathway (*SMAD9*).

The Wnt/beta-catenin signaling pathway plays an essential role in tumorigenesis and recurrence in endometrial cancer. Two studies demonstrated the role of the beta-catenin/*CTNNB1* gene as a poor prognostic factor in low-risk endometrial cancer (24, 25). First, in a large study with 342 patients with low-grade and early-stage endometrial cancer through next-generation sequencing, the worst recurrence-free and overall survival was demonstrated in patients with *CTNNB1* and *TP53* mutations (24). In a case-control study similar to ours with recurrent stage I and grade 1 endometrioid endometrial cancers, Moroney et al. showed that *CTNNB1* mutations are present at higher rates in recurrent patients (25).

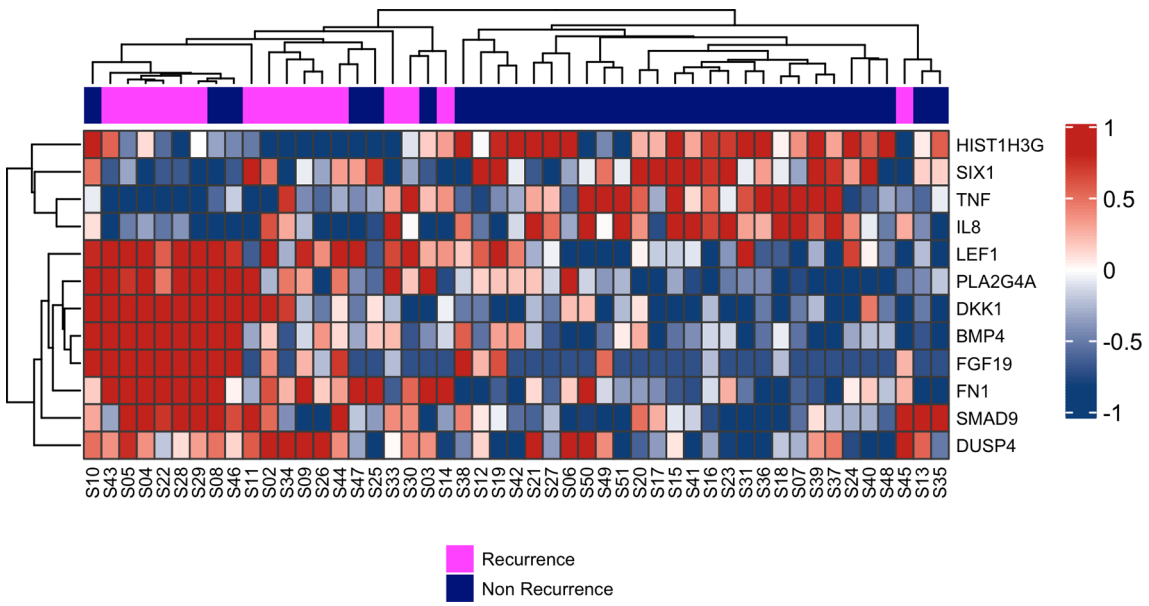


**FIGURE 1** | Hierarchical clustering of the 12 RNAs differentially expressed between patients who presented recurrence (pink) compared to those who did not relapse (purple). On the right side: gene expression scaling from dark blue (downregulated) to dark red (upregulated).

**TABLE 2** | Differentially expressed genes between the recurrence and nonrecurrence groups.

| Genes | Fold Change | Sensitivity[1] | Specificity[1] | AUC[2] |
|---|---|---|---|---|
| ***HIST1H3G*** | - 2.6 | 0.7575 | 0.8125 | 0.8219 |
| ***TNF*** | - 2.1 | 0.7272 | 0.6875 | 0.7613 |
| ***SIX1*** | - 2.1 | 0.7272 | 0.75 | 0.7575 |
| ***IL8*** | - 2.5 | 0.6363 | 0.6875 | 0.7045 |
| ***FN1*** | 3.0 | 0.8125 | 0.8181 | 0.8532 |
| ***DKK1*** | 5.3 | 0.6875 | 0.7575 | 0.7821 |
| ***DUSP4*** | 2.3 | 0.75 | 0.6969 | 0.7784 |
| ***PLA2G4A*** | 2.3 | 0.6875 | 0.8484 | 0.7575 |
| ***LEF1*** | 2.1 | 0.8125 | 0.7272 | 0.7547 |
| ***FGF19*** | 3.7 | 0.75 | 0.7272 | 0.7537 |
| ***SMAD9*** | 2.1 | 0.6875 | 0.8181 | 0.7348 |
| ***BMP4*** | 3.0 | 0.75 | 0.6363 | 0.7121 |

[1]*Sensitivity and specificity were determined by the Youden index.*
[2]*AUC, area under the curve.*

*LEF1* (lymphoid enhancer factor) is a nuclear transcription factor that interacts with beta-catenin to activate the Wnt pathway (26). The role of LEF1 protein overexpression in the carcinogenesis of endometrial cancer may be related to the modulation of cell surface adhesion proteins, influencing the prognosis of this tumor (27). A study with *LEF1* knockout mice demonstrated its importance in endometrial cancer carcinogenesis. The LEF1 protein is essential in uterine glandular formation, and its overexpression possibly influences the disordered growth of glandular cells and the development of cancer (28).

The MAPK/PI3K pathway is a central pathway in the tumorigenesis of several tumors, and it is even a target in breast cancer treatment (29). The role of *FN1*, which encodes fibronectin, and *DUSP4*, which encodes dual-specificity protein phosphatase 4, in endometrial cancer is not well understood. A recent study by Raglan et al. evaluated the TCGA proteomic data of 560 endometrial cancers and demonstrated that obese patients without cancer had upregulation of several proteins, including DUSP4 (30). Another recent study evaluated the predictive model of lymph node involvement in endometrial cancer using a combined proteomic and transcriptomic approach. The authors reported that high protein expression of fibronectin, cyclin D1, and tumor grade were associated with lymph node involvement. Moreover, overexpression of both *FN1* and *CCND1* (cyclin D1 encoded gene) genes correlated with greater potential for mesenchymal invasion (31).

The third pathway identified was TGF-β through the overexpression of the *SMAD9* gene. This gene belongs to the SMAD superfamily (Drosophila mothers against decapentaplegic protein) made up of important cytokines in the TGF-β family (32). *SMAD9* overexpression is associated with the prevalence of hamartomatous polyposis and is a prognostic factor for lung cancer (33, 34). So far, no studies have addressed its impact in endometrial cancer.

Analyzing the clinical and pathological features of this case-control study, having squamous differentiation in the histopathological diagnosis could be a risk factor for recurrence in this population, according to previously published studies (35, 36). Related to ethnicity, some studies have already shown less medical access in the nonwhite population in the USA impacting oncologic outcomes (37); however, demonstrated a risk due to ethnicity itself. In this study, there was a higher prevalence of white patients in the recurrence group.

Despite these notable findings, our study has some limitations, such as having a small sample size and a retrospective nature. The small number of cases can be explained by the excellent prognosis

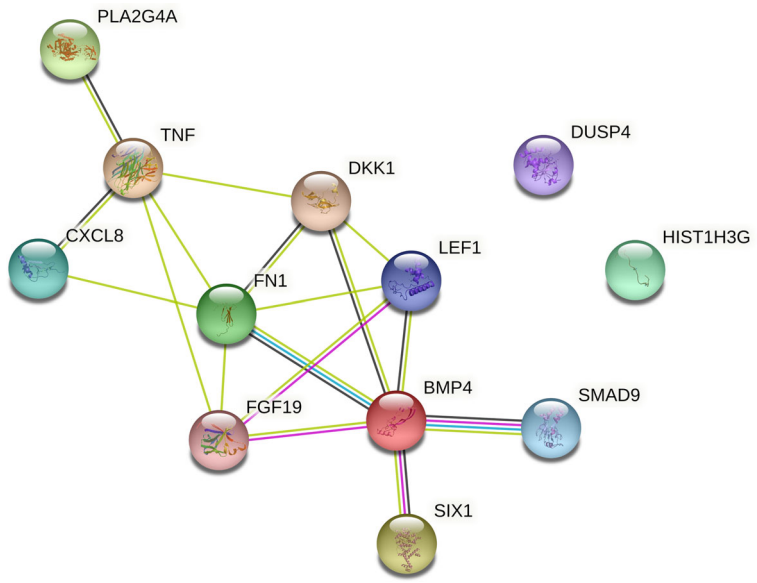


**FIGURE 2** | STRING interaction network of the 12 genes differentially expressed in the recurrence and nonrecurrence groups of patients [known interactions (light blue – from curated databases; purple – experimentally determined); predicted interactions (green, gene neighborhood; red, gene fusions; dark blue, gene cooccurrence); others (yellow, text mining; black, coexpression; gray, protein homology)].

**TABLE 3** | Selected genes predicting recurrence in low- and intermediate-risk endometrial cancer.

| Genes | Estimates | OR | 95% CI | | *p* value |
|---|---|---|---|---|---|
| | | | Lower | Upper | |
| ***FN1*** | 1.195 | 3.303 | 1.628 | 6.704 | 0.001 |
| ***DUSP4*** | 0.960 | 2.613 | 1.302 | 5.241 | 0.007 |
| ***LEF1*** | 0.818 | 2.266 | 1.187 | 4.325 | 0.013 |
| ***SMAD9*** | 0.831 | 2.295 | 1.223 | 4.309 | 0.010 |
| **Score** | 1.000 | 2.718 | 1.545 | 4.784 | 0.001 |

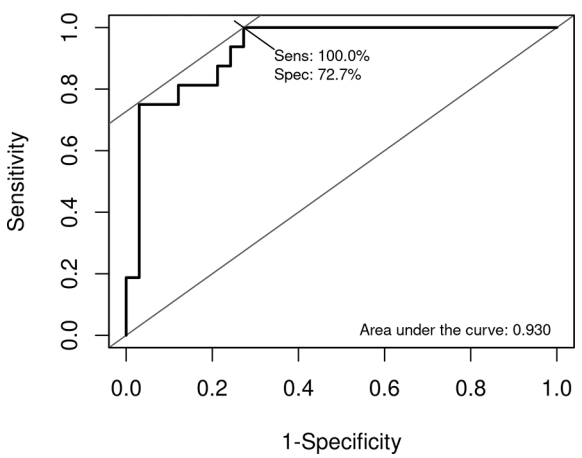


**FIGURE 3** | Receiver operating characteristic (ROC) curve of the recurrence risk score (RRS). Sensitivity and specificity were determined by the Youden index.

and low risk of recurrence in low- and intermediate-risk endometrial cancer patients. Therefore, validation of this 4-gene signature in a larger cohort is needed to confirm its predictive value. Moreover, it would be interesting to validate these 4 biomarkers by other methodologies, such as immunohistochemistry. On the other hand, our study has several strengths. First, the robustness of the NanoString methodology proved to be effective for gene expression evaluation in routine samples, even after many years of storage, up to 10 years in our study (38). Second, we evaluated a restricted subpopulation of endometrial cancer to detect risk factors for recurrence in this population. As this is a retrospective study, all patients who relapsed and their matched controls had their pathological reports reviewed by expert gynecologic oncology pathologists to minimize selection bias. Some studies have shown that gynecologic oncology has one of the highest rates of disagreement in the expert pathologist's report compared to the nonspecialized report (39, 40). In addition, this case-control study represents the experience of a reference cancer center hospital where well-defined treatment protocols minimize possible sample heterogeneity.

## CONCLUSION

For the first time, we identified a four-gene signature associated with recurrence in low and intermediate endometrial cancer. Additionally, the four genes (*FN1, DUSP4, LEF1,* and *SMAD9*) identified can shed light on the mechanisms of recurrence in endometrial cancer. This study can pave the way for personalized approaches of low- and intermediate-risk endometrial cancer.

## DATA AVAILABILITY STATEMENT

The datasets presented in this study can be found in online repositories. The names of the repository/repositories and accession number(s) can be found below: https://www.ncbi.nlm.nih.gov/geo/, GSE178671.

## ETHICS STATEMENT

The studies involving human participants were reviewed and approved by BCH Ethical Review Board in March 2017. Written informed consent for participation was not required for this study in accordance with the national legislation and the institutional requirements.

## AUTHOR CONTRIBUTIONS

Conception and design: DA, RMR, and RdR. Development of methodology: DA, RMR, and RdR. Acquisition of data: DA. Analysis and interpretation of data: DA, LS, AL, ML, GB, VS, GM, MB, AS, RMR, and RdR. Writing, review, and/or revision of the manuscript: DA, LS, AL, ML, GB, VS, GM, MB, AS, AE, JC, RMR, and RdR. Study supervision: RMR and RdR. All authors contributed to the article and approved the submitted version.

## ACKNOWLEDGMENTS

We thank Barretos Cancer Hospital and the Public Ministry of Labor Campinas (Research, Prevention, and Education of Occupational Cancer Project), Campinas, Brazil, for partially funding the present study. RMR is recipient of a CNPq productivity fellowship.

## SUPPLEMENTARY MATERIAL

The Supplementary Material for this article can be found online at: https://www.frontiersin.org/articles/10.3389/fonc.2021.729219/full#supplementary-material

## REFERENCES

1. Siegel RL, Miller KD, Fuchs HE, Jemal A. Cancer Statistics, 2021. *CA: Cancer J Clin* (2021) 71(1):7–33. doi: 10.3322/caac.21654
2. Smrz SA, Calo C, Fisher JL, Salani R. An Ecological Evaluation of the Increasing Incidence of Endometrial Cancer and the Obesity Epidemic. *Am J Obstet Gynecol* (2021) 224(5):506.e1–.e8. doi: 10.1016/j.ajog.2020.10.042
3. *Estimativa 2020: Incidência De Câncer No Brasil Rio De Janeiro: INCA - Instituto Nacional De Câncer José Alencar Gomes Da Silva* (2020). Available at: www.inca.gov.br/estimativa/2020/.
4. Bendifallah S, Canlorbe G, Raimond E, Hudry D, Coutant C, Graesslin O, et al. A Clue Towards Improving the European Society of Medical Oncology Risk Group Classification in Apparent Early Stage Endometrial Cancer? Impact of Lymphovascular Space Invasion. *Br J Cancer* (2014) 110 (11):2640–6. doi: 10.1038/bjc.2014.237
5. Bokhman JV. Two Pathogenetic Types of Endometrial Carcinoma. *Gynecol Oncol* (1983) 15(1):10–7. doi: 10.1016/0090-8258(83)90111-7
6. Kandoth C, Schultz N, Cherniack AD, Akbani R, Liu Y, Shen H, et al. Integrated Genomic Characterization of Endometrial Carcinoma. *Nature* (2013) 497(7447):67–73. doi: 10.1038/nature12113
7. Talhouk A, McConechy MK, Leung S, Li-Chang HH, Kwon JS, Melnyk N, et al. A Clinically Applicable Molecular-Based Classification for Endometrial Cancers. *Br J Cancer* (2015) 113(2):299–310. doi: 10.1038/bjc.2015.190
8. Stelloo E, Nout RA, Osse EM, Jürgenliemk-Schulz IJ, Jobsen JJ, Lutgens LC, et al. Improved Risk Assessment by Integrating Molecular and Clinicopathological Factors in Early-Stage Endometrial Cancer-Combined Analysis of the PORTEC Cohorts. *Clin Cancer Res* (2016) 22(16):4215–24. doi: 10.1158/1078-0432.CCR-15-2878
9. Deng F, Mu J, Qu C, Yang F, Liu X, Zeng X, et al. A Novel Prognostic Model of Endometrial Carcinoma Based on Clinical Variables and Oncogenomic Gene Signature. *Front Mol Biosci* (2020) 7:587822. doi: 10.3389/fmolb.2020.587822
10. Wang Z, Zhang J, Liu Y, Zhao R, Zhou X, Wang H. An Integrated Autophagy-Related Long Noncoding RNA Signature as a Prognostic Biomarker for Human Endometrial Cancer: A Bioinformatics-Based Approach. *BioMed Res Int* (2020) 2020:5717498. doi: 10.1155/2020/5717498
11. Chen B, Wang D, Li J, Hou Y, Qiao C. Screening and Identification of Prognostic Tumor-Infiltrating Immune Cells and Genes of Endometrioid Endometrial Adenocarcinoma: Based on the Cancer Genome Atlas Database and Bioinformatics. *Front Oncol* (2020) 10:554214. doi: 10.3389/fonc.2020.554214
12. Horeweg N, de Bruyn M, Nout RA. Prognostic Integrated Image-Based Immune and Molecular Profiling in Early-Stage Endometrial Cancer. *Cancer Immunol Res* (2020) 8(12):1508–19. doi: 10.1158/2326-6066.CIR-20-0149
13. Gomes I, Moreno DA, Dos Reis MB, da Silva LS, Leal LF, Gonçalves GM, et al. Low MGMT Digital Expression Is Associated With a Better Outcome of IDH1 Wildtype Glioblastomas Treated With Temozolomide. *J Neuro-Oncol* (2021) 151(2):135–44. doi: 10.1007/s11060-020-03675-6
14. Berardinelli GN, Scapulatempo-Neto C, Durães R, Antônio de Oliveira M, Guimarães D, Reis RM. Advantage of HSP110 (T17) Marker Inclusion for Microsatellite Instability (MSI) Detection in Colorectal Cancer Patients. *Oncotarget* (2018) 9(47):28691–701. doi: 10.18632/oncotarget.25611
15. Britton H, Huang L, Lum A, Leung S, Shum K, Kale M, et al. Molecular Classification Defines Outcomes and Opportunities in Young Women With Endometrial Carcinoma. *Gynecol Oncol* (2019) 153(3):487–95. doi: 10.1016/j.ygyno.2019.03.098
16. Campanella NC, Silva EC, Dix G, de Lima Vazquez F, Escremim de Paula F, Berardinelli GN, et al. Mutational Profiling of Driver Tumor Suppressor and Oncogenic Genes in Brazilian Malignant Pleural Mesotheliomas. *Pathobiology* (2020) 87(3):208–16. doi: 10.1159/000507373
17. Rosa MN, Evangelista AF, Leal LF, De Oliveira CM, Silva VAO, Munari CC, et al. Establishment, Molecular and Biological Characterization of HCB-514: A Novel Human Cervical Cancer Cell Line. *Sci Rep* (2019) 9(1):1913. doi: 10.1038/s41598-018-38315-7
18. Team RC. *R: A Language and Environment for Statistical Computing* (2019). Available at: https://wwwR-projectorg/ (Accessed 06 February 2021).
19. Waggott D, Chu K, Yin S, Wouters BG, Liu FF, Boutros PC. Nanostringnorm: An Extensible R Package for the Pre-Processing of Nanostring mRNA and MiRNA Data. *Bioinf (Oxf Engl)* (2012) 28(11):1546–8. doi: 10.1093/bioinformatics/bts188
20. Gu Z, Eils R, Schlesner M. Complex Heatmaps Reveal Patterns and Correlations in Multidimensional Genomic Data. *Bioinf (Oxf Engl)* (2016) 32(18):2847–9. doi: 10.1093/bioinformatics/btw313
21. Szklarczyk D, Gable AL, Lyon D, Junge A, Wyder S, Huerta-Cepas J, et al. STRING V11: Protein-Protein Association Networks With Increased Coverage, Supporting Functional Discovery in Genome-Wide Experimental Datasets. *Nucleic Acids Res* (2019) 47(D1):D607–d13. doi: 10.1093/nar/gky1131
22. Robin X, Turck N, Hainard A, Tiberti N, Lisacek F, Sanchez JC, et al. Proc: An Open-Source Package for R and s+ to Analyze and Compare ROC Curves. *BMC Bioinf* (2011) 12:77. doi: 10.1186/1471-2105-12-77
23. Harris PA, Taylor R, Thielke R, Payne J, Gonzalez N, Conde JG. Research Electronic Data Capture (Redcap)–a Metadata-Driven Methodology and Workflow Process for Providing Translational Research Informatics Support. *J Biomed Inf* (2009) 42(2):377–81. doi: 10.1016/j.jbi.2008.08.010
24. Kurnit KC, Kim GN, Fellman BM, Urbauer DL, Mills GB, Zhang W, et al. CTNNB1 (Beta-Catenin) Mutation Identifies Low Grade, Early Stage

Endometrial Cancer Patients at Increased Risk of Recurrence. *Modern Pathol* (2017) 30(7):1032–41. doi: 10.1038/modpathol.2017.15
25. Moroney MR, Davies KD, Wilberger AC, Sheeder J, Post MD, Berning AA, et al. Molecular Markers in Recurrent Stage I, Grade 1 Endometrioid Endometrial Cancers. *Gynecol Oncol* (2019) 153(3):517–20. doi: 10.1016/j.ygyno.2019.03.100
26. McMellen A, Woodruff ER, Corr BR, Bitler BG, Moroney MR. Wnt Signaling in Gynecologic Malignancies. *Int J Mol Sci* (2020) 21(12):4272. doi: 10.3390/ijms21124272
27. Hsu YT, Osmulski P, Wang Y, Huang YW, Liu L, Ruan J, et al. Epcam-Regulated Transcription Exerts Influences on Nanomechanical Properties of Endometrial Cancer Cells That Promote Epithelial-to-Mesenchymal Transition. *Cancer Res* (2016) 76(21):6171–82. doi: 10.1158/0008-5472.CAN-16-0752
28. Shelton DN, Fornalik H, Neff T, Park SY, Bender D, DeGeest K, et al. The Role of LEF1 in Endometrial Gland Formation and Carcinogenesis. *PloS One* (2012) 7(7):e40312. doi: 10.1371/journal.pone.0040312
29. André F, Ciruelos EM, Juric D, Loibl S, Campone M, Mayer IA, et al. Alpelisib Plus Fulvestrant for PIK3CA-Mutated, Hormone Receptor-Positive, Human Epidermal Growth Factor Receptor-2-Negative Advanced Breast Cancer: Final Overall Survival Results From SOLAR-1. *Ann Oncol* (2021) 32 (2):208–17. doi: 10.1016/j.annonc.2020.11.011
30. Raglan O, Assi N, Nautiyal J, Lu H, Gabra H, Gunter MJ, et al. Proteomic Analysis of Malignant and Benign Endometrium According to Obesity and Insulin-Resistance Status Using Reverse Phase Protein Array. *Trans Res* (2020) 218:57–72. doi: 10.1016/j.trsl.2019.12.003
31. Berg HF, Ju Z, Myrvold M, Fasmer KE, Halle MK, Hoivik EA, et al. Development of Prediction Models for Lymph Node Metastasis in Endometrioid Endometrial Carcinoma. *Br J Cancer* (2020) 122(7):1014–22. doi: 10.1038/s41416-020-0745-6
32. Dai ZT, Wang J, Zhao K, Xiang Y, Li JP, Zhang HM, et al. Integrated TCGA and GEO Analysis Showed That SMAD7 Is an Independent Prognostic Factor for Lung Adenocarcinoma. *Medicine* (2020) 99(44):e22861. doi: 10.1097/MD.0000000000022861
33. Ngeow J, Yu W, Yehia L, Niazi F, Chen J, Tang X, et al. Exome Sequencing Reveals Germline SMAD9 Mutation That Reduces Phosphatase and Tensin Homolog Expression and is Associated With Hamartomatous Polyposis and Gastrointestinal Ganglioneuromas. *Gastroenterology* (2015) 149(4):886–9.e5. doi: 10.1053/j.gastro.2015.06.027
34. Gao L, Tian Q, Wu T, Shi S, Yin X, Liu L, et al. Reduction of MiR-744 Delivered by NSCLC Cell-Derived Extracellular Vesicles Upregulates SUV39H1 to Promote NSCLC Progression *via* Activation of the Smad9/BMP9 Axis. *J Trans Med* (2021) 19(1):37. doi: 10.1186/s12967-020-02654-9
35. Andrade DAP, da Silva VD, Matsushita GM, de Lima MA, Vieira MA, Andrade C, et al. Squamous Differentiation Portends Poor Prognosis in Low and Intermediate-Risk Endometrioid Endometrial Cancer. *PloS One* (2019) 14 (10):e0220086. doi: 10.1371/journal.pone.0220086
36. Misirlioglu S, Guzel AB, Gulec UK, Gumurdulu D, Vardar MA. Prognostic Factors Determining Recurrence in Early-Stage Endometrial Cancer. *Eur J Gynaecol Oncol* (2012) 33(6):610–4.
37. Kaspers M, Llamocca E, Quick A, Dholakia J, Salani R, Felix AS. Black and Hispanic Women are Less Likely Than White Women to Receive Guideline-Concordant Endometrial Cancer Treatment. *Am J Obstetrics Gynecol* (2020) 223(3):398.e1–.e18. doi: 10.1016/j.ajog.2020.02.041
38. Leal LF, Evangelista AF, de Paula FE, Caravina Almeida G, Carloni AC, Saggioro F, et al. Reproducibility of the Nanostring 22-Gene Molecular Subgroup Assay for Improved Prognostic Prediction of Medulloblastoma. *Neuropathol: Off J Jpn Soc Neuropathol* (2018) 38(5):475–83. doi: 10.1111/neup.12508
39. Manion E, Cohen MB, Weydert J. Mandatory Second Opinion in Surgical Pathology Referral Material: Clinical Consequences of Major Disagreements. *Am J Surg Pathol* (2008) 32(5):732–7. doi: 10.1097/PAS.0b013e31815a04f5
40. de Boer SM, Wortman BG, Bosse T, Powell ME, Singh N, Hollema H, et al. Clinical Consequences of Upfront Pathology Review in the Randomised PORTEC-3 Trial for High-Risk Endometrial Cancer. *Ann Oncol* (2018) 29 (2):424–30. doi: 10.1093/annonc/mdx753

**Conflict of Interest:** The authors declare that the research was conducted in the absence of any commercial or financial relationships that could be construed as a potential conflict of interest.

**Publisher's Note:** All claims expressed in this article are solely those of the authors and do not necessarily represent those of their affiliated organizations, or those of the publisher, the editors and the reviewers. Any product that may be evaluated in this article, or claim that may be made by its manufacturer, is not guaranteed or endorsed by the publisher.

frontiers in Oncology

ORIGINAL RESEARCH
published: 29 October 2021
doi: 10.3389/fonc.2021.757678

# Identification of miR-499a-5p as a Potential Novel Biomarker for Risk Stratification in Endometrial Cancer

*Gloria Ravegnini[1]*, Antonio De Leo[2,3,4], Camelia Coada[5,6], Francesca Gorini[1], Dario de Biase[1,2], Claudio Ceccarelli[2], Giulia Dondi[2,5,7], Marco Tesei[2,7], Eugenia De Crescenzo[2,5,7], Donatella Santini[2,8], Angelo Gianluca Corradini[8], Giovanni Tallini[2,3,4], Patrizia Hrelia[1], Pierandrea De Iaco[2,5,7], Sabrina Angelini[1†] and Anna Myriam Perrone[2,5,7*†]*

[1] Department of Pharmacy and Biotechnology (FaBiT), University of Bologna, Bologna, Italy, [2] Centro di Studio e Ricerca delle Neoplasie Ginecologiche (CSR), University of Bologna, Bologna, Italy, [3] Department of Experimental, Diagnostic and Specialty Medicine, Alma Mater Studiorum-University of Bologna, Bologna, Italy, [4] Molecular Pathology Laboratory, Istituto di Ricovero e Cura a Carattere Scientifico (IRCCS) Azienda Ospedaliero-Universitaria di Bologna/Azienda USL di Bologna, Bologna, Italy, [5] Department of Medical and Surgical Sciences (DIMEC), University of Bologna, Bologna, Italy, [6] Center for Applied Biomedical Research, Alma Mater Studiorum-University of Bologna, Bologna, Italy, [7] Division of Oncologic Gynecology Unit, IRCCS—Azienda Ospedaliero-Universitaria di Bologna, Bologna, Italy, [8] Pathology Unit, IRCCS Azienda Ospedaliero—Universitaria di Bologna, Bologna, Italy

**Introduction:** The Cancer Genome Atlas (TCGA) project identified four distinct prognostic groups in endometrial cancer (EC), among which two are correlated with an intermediate prognosis: the MisMatch Repair-deficient (MMRd) and the No Specific Molecular Profile (NSMP) groups. The two groups represent a heterogeneous subset of patients frequently harboring CTNNB1 alterations with distinctive clinicopathologic features. The study aimed to evaluate the miRNA expression in ECs to identify potential biomarkers of prognosis.

**Methods:** We analyzed miRNA expression in 72 ECs classified as MMRd or NSMP including 15 ECs with CTNNB1 mutations. In the discovery step, miRNA expression was evaluated in 30 cases through TaqMan miRNA arrays. Subsequently, four miRNAs were validated in the total cohort of ECs. The data were further tested in the TCGA cohort, and correlations with overall survival (OS) and progression-free interval (PFI) were evaluated.

**Results:** miR-499a-3p and miR-499a-5p resulted to be overexpressed in CTNNB1 mutant EC patients at intermediate risk. Similarly, in the TCGA cohort, miR-499a-3p and miR-499a-5p were differentially expressed between CTNNB1 mutant and wild-type patients ($p < 0.0001$). NSMP patients with low miR-499a-5p expression showed longer OS ($p = 0.03$, log-rank test). By combining miR-499a-3p or -5p expression levels with the CTNNB1 status, ECs with CTNNB1 mutation and lower miR-499a-5p expression showed better OS compared with the other subgroups ($p = 0.03$, log-rank test), among the NSMP patients. Moreover, in a multivariate analysis, combination of wild type CTNNB1 status and high miR-499a-5p expression was indipendently associated with high risk of death [HR (95%CI): 3.53 (1.1-10.5), $p = 0.02$].

OPEN ACCESS

**Edited by:**
*Alberto Farolfi, Istituto Scientifico Romagnolo per lo Studio e il Trattamento dei Tumori (IRCCS), Italy*

**Reviewed by:**
*Gregory Gard, Royal North Shore Hospital, Australia*
*Giacomo Corrado, Università Cattolica del Sacro Cuore, Italy*

***Correspondence:**
*Gloria Ravegnini*
*Gloria.ravegnini2@unibo.it*
*Anna Myriam Perrone*
*myriam.perrone@aosp.bo.it*

*†These authors have contributed equally to this work*

**Specialty section:**
*This article was submitted to Gynecological Oncology, a section of the journal Frontiers in Oncology*

**Received:** *12 August 2021*
**Accepted:** *30 September 2021*
**Published:** *29 October 2021*

**Citation:**
*Ravegnini G, De Leo A, Coada C, Gorini F, de Biase D, Ceccarelli C, Dondi G, Tesei M, De Crescenzo E, Santini D, Corradini AG, Tallini G, Hrelia P, De Iaco P, Angelini S and Perrone AM (2021) Identification of miR-499a-5p as a Potential Novel Biomarker for Risk Stratification in Endometrial Cancer. Front. Oncol. 11:757678. doi: 10.3389/fonc.2021.757678*

**Conclusion:** Our results suggest that the combination of CTNNB1 status and miR-499a-5p allows a better stratification of NSMP patients and could promote a personalization of the treatment in intermediate-risk patients.

**Keywords: endometrial cancer, miRNA—microRNA, MMRd, TCGA, prognostic biomarkers, personalized medicine, NSMP**

## INTRODUCTION

Endometrial cancer (EC) is the most common gynecological cancer, with an increasing incidence in Western countries ranging between 15 and 25 per 100,000 women (1, 2).

Historically, three distinct but overlapping EC classifications have been proposed to define prognosis (3): pathogenetic, histopathological, and molecular classification. However, despite their merits, the three classifications are not able to uniquely define the complexity and heterogeneity of the disease and present various issues. Histopathological parameters used alone to identify risk factors are not always easily reproducible, particularly in high-grade carcinomas and those with intratumoral heterogeneity (4–8).

To overcome this kind of problems, recently, The Cancer Genome Atlas (TCGA) endometrial collaborative project identified four distinct prognostic EC groups based on molecular alterations: (i) the ultramutated subtype that encompassed POLE exonuclease domain mutated (POLE) cases (excellent prognosis); (ii) the hypermutated subtype, characterized by MisMatch Repair deficiency (MMRd) (intermediate prognosis); (iii) the copy-number high subtype, with p53 abnormal/mutated features (p53abn) (poor prognosis); and (iv) the copy-number low subtype, also known as No Specific Molecular Profile (NSMP) (intermediate prognosis) (9). However, in order to translate the proposed TCGA scheme into clinical practice, two independent research groups proposed and validated surrogate markers (POLE mutation, microsatellite instability, and p53abn to improve the integration of the TCGA classification in the routine clinical practice (9–12). In 2021, the European Society of Gynecological Oncology (ESGO), the European Society for Radiotherapy and Oncology (ESTRO), and the European Society of Pathology (ESP) published updated guidelines for the determination of the risk group in EC, integrating both molecular and clinicopathological diagnostic variables, with the aim of improving patients' treatment (13).

The ESGO/ESTRO/ESP guidelines consider all POLE mutant ECs up to stage II to be at low risk of recurrence regardless of other ESMO risk parameters, and adjuvant treatments are deemed unnecessary in these cases. The p53abn group benefits from adjuvant therapy which is also expected to be aggressive independently of histology and different managements for these two entities may not be recommended. Within the MMRd and NSMP groups, which have an intermediate prognosis, FIGO grade, LVSI, and depth of myometrial invasion are critical factors for risk stratification. Thus, in these two groups, treatment continues to rely largely on conventional risk factors, and the choice of the most appropriate adjuvant therapies remains a challenge. MMRd ECs represent a heterogeneous group of cancers. A better stratification within this group to select therapies is needed in consideration that a subgroup of MMRd ECs exhibiting MLH1 promoter methylation presents a worse prognosis than other MMRd ECs (14). In the NSMP group, the absence of specific molecular signatures appears to be accompanied by a more heterogeneous biological behavior than the other TCGA groups. This group mainly includes low-grade endometrioid-type ECs characterized by alterations in PI3K/AKT and Wnt/β-catenin signaling pathways often with mutations on exon 3 of CTNNB1 (52%). Although a few studies have characterized the CTNNB1 alterations in EC (15, 16), its prognostic significance among NSMP ECs is not completely understood; moreover, it is not clear if CTNNB1 mutations could indicate a distinct molecular group (17). This shows that integration of different prognostic factors may serve to accurately define the risk classes, leading to a more precise characterization of ECs which are extremely heterogeneous and sometimes unclassifiable.

MicroRNAs (miRNAs) are small non-coding RNAs spanning between 18 and 25 nucleotides in length, which are able to regulate specific target genes at the posttranscriptional level by inhibiting their expression (18). Consequently, miRNAs deregulation can have a deep impact on key cellular processes which, in turn, could drive carcinogenesis or promote cancer progression. In recent years, many studies investigating miRNA expression level in EC have been published, shedding light on this heterogeneous disease (19). However, identifying novel potential diagnostic biomarkers remains an unmet clinical need, particularly within the EC patients with intermediate prognosis who represent the most difficult category to manage from a clinical point of view (i.e., NSMP and MMRd groups).

Based on the above, we aimed to characterize the miRNA expression level in these groups defined as at intermediate risk, considering the CTNNB1 status, in order to better stratify these patients. To do that, we first focused on the NSMP and MMRd EC patients comparing patients harboring, or not, CTNNB1 mutations; secondly, we tested our findings in the TCGA EC cohort to corroborate them.

## MATERIAL AND METHODS

### Tumor Specimen Collection

Starting from a cohort of 117 consecutive surgical EC specimens characterized and divided into four groups according to the molecular classification, we selected the ones identified as NSMP or MMRd. Formalin-fixed, paraffin-embedded (FFPE) primary tumors from 72 EC patients were included in the study. Tumor

samples were collected at the time of hysterectomy for EC; patients submitted to previous radiotherapy or chemotherapy treatment were excluded. FFPE specimens were retrieved from the archives of the departments of pathology of the IRCCS Azienda Ospedaliero-Universitaria of Bologna between 2014 and 2020. The selected blocks were used to assess histopathologic parameters, for immunohistochemical and molecular analyses, and were classified according to standard histopathologic criteria following the World Health Organization classification of tumors (20). The study was approved by the Institutional Review Board 189/2021/Oss/AOUBo, ClinicalTrials.gov Identifier: NCT04845425. **Supplementary Table S1** summarizes the main clinical and pathological features of the patients.

## Tissue Processing

All FFPE specimens were conserved in the Institution's pathology archives, and two expert pathologists examined tissue slides to confirm the EC diagnosis and to ensure the inclusion of more than 70% of cancer cells. When the percentage was not respected, tissue slides were macro-dissected to eliminate contamination of non-tumoral components and guarantee that at least 70% of the samples for the analysis were tumor cells indicated by the pathologist. RNA was isolated from FFPE (three to six sections >10 μm for each sample) by RecoverAll Total Nucleic Acid Isolation Kit (Ambion, Thermo Scientific) following the manufacturer's instructions. RNA integrity and quantification were evaluated using the 2100 Agilent Bioanalyzer. Mutation analysis was carried out as previously described (17).

## MiRNA Analysis

MiRNA expression was firstly evaluated in a discovery step comprising 30 ECs (discovery cohort), and the results were then validated in 72 ECs (n = 30 ECs overlapping with the discovery step + n = 42 new ECs, validation cohort).

## Discovery Step: miRNA Expression Profiling

The expression profiles of 384 miRNAs were analyzed in 30 primary tumors, of which 12 were NSMP CTNNB1 mutant ($CTNNB1^{mut}$), 11 NSMP CTNNB1- wild-type ($CTNNB1^{wt}$), and 7 MMRd. One nanogram of total RNA was reverse transcribed to cDNA, using TaqMan Advanced miRNA cDNA Synthesis Kit (Applied Biosystems, Thermo Scientific), which is specific for the detection and quantification of mature human miRNAs in biological samples. The cDNAs were then amplified using the Universal miR-Amp Primers and Master Mix to uniformly increase the amount of cDNA for each target, maintaining the relative differential expression levels. The cDNA was loaded into the TaqMan Array Advanced miRNA array pool A and run in a 7900HT Fast PCR System (Applied Biosystems).

## Validation of the Profiling Results by qRT-PCR

miRNA expression levels of miR-187-3p (assay ID # 477941_mir), miR-325 (assay ID # 478025_mir), miR-499a-3p (assay ID # 478948_mir), and miR-499a-5p (assay ID # 478139_mir) were evaluated by qRT_PCR through TaqMan Advanced miRNA Assay (Thermo Fisher Scientific). miR-16-5p (assay ID # 477860_mir, Thermo Fisher Scientific) was used as the internal reference (21), after the literature review and assessment of its stability in our study cohort. The analysis was conducted in all the 72 EC patients. miRNA expression was evaluated according to standard TaqMan Advanced miRNA assay protocol and run in a 7900HT Fast PCR System (Applied Biosystems). Each TaqMan Advanced miRNA assay was run in triplicate.

## Statistical Analysis

miRNA data were analyzed with SDS RQ Software version 2.4 and with a Thermo Fisher Cloud app (Thermo Fisher Scientific); miRNAs with Ct values ≥ 38 were considered as not expressed and excluded from further analysis. The relative expression levels were quantified using the $2^{-\Delta\Delta Ct}$ method using miR-16-5p as reference (22). Statistical significance was estimated using the non-parametric Mann–Whitney–Wilcoxon test. This non-parametric test allows problems related to equal variance, normality assumption, or those regarding the use of frequencies to be obviated. A p-value < 0.05 was considered statistically significant.

## Validation of the Results in the TCGA Cohort

MAF files for the UCEC TCGA project were downloaded and explored using the R (version 4.1.0) packages TCGAbiolinks and maftools. The selection of pathogenic CTNNB1 and p53 mutations was done considering the pathogenicity prediction by both PolyPhen and SIFT scoring systems. UCEC-curated molecular subtypes derived from the TCGA marker paper were retrieved from synapse through TCGAbiolinks (9, 23, 24). For expression analysis, sample-level log2 miRSeq and mRNASeq expression values were retrieved using the FireBrowse RESTful API (25). For clinical variables, the progression-free interval (PFI) and overall survival (OS) were used as outcome variables, as recommended by the PanCanAtlas Publications NCI Genomic Data Commons guidelines (https://www.cell.com/cell/fulltext/S0092-8674(18)30229-0). The NSMP EC subgroup was selected by the exclusion of POLE, MMRd, and p53-mutated tumors.

For each miRNA analyzed, the cohort of UCEC patients was divided into two groups based on the expression level of the miRNA of interest using the median expression value as a threshold. Statistical analysis was carried out using the GraphPad Prism 8 and SPSS v20 software. Comparisons between groups were conducted using the two-tailed Student's t-test. Kaplan–Meier curves were plotted for the OS and PFI while the statistical significance was assessed using the log-rank test. For multivariate analysis, the COX proportional hazards model was used. A p value <0.05 was considered statistically significant.

The general workflow of the paper is presented in **Supplementary Figure 1**.

# RESULTS

## Discovery Step: miRNA Expression Profiling

We analyzed miRNA expression profiling in the NSMP group (n = 23) comparing the CTNNB1 mutant (n = 12) and the CTNNB1 wild-type (n = 11) cases.

This comparison highlighted a significant upregulation of two miRNAs, namely, miR-499a-3p (p = 0.0002; padj = 0.023) and miR-499a-5p (p = 0.00009; padj = 0.013) in the CTNNB1$^{mut}$ subgroup.

Subsequently, given the similar intermediate prognosis usually observed in MMRd ECs, we included seven consecutive additional MMRd cases, all CTNNB1$^{wt}$, in our discovery step.

miRNA expression profiling was thus evaluated on a total of 30 cases with intermediate risk, of which 12 were NSMP CTNNB1$^{mut}$, 11 NSMP CTNNB1$^{wt}$, and 7 MMRd. We compared the cases with CTNNB1 mutation (n = 12) with the remaining cases, irrespective of NSMP or MMRd molecular group (n = 18). The results showed that 39 miRNAs presented a statistically significant deregulation, as reported in **Supplementary Table S2**. The top two deregulated miRNAs were again miR-499a-3p and miR-499a-5p.

The miRNet tool was used to perform pathway-enriched analysis; the results are reported in **Supplementary Table S3**.

## Validation of the Profiling Results by qRT-PCR

Based on the p-value and on Ampscore, - a value released by the Thermo Fisher Cloud app which evaluates the goodness of RT-PCR amplification, - we selected four miRNAs to validate in 72 samples. Validation was performed in the NSMP cohort alone as well as in the NSMP + MMRd cohort. **Figure 1** shows the results.

In the NSMP ECs, miR-499a-3p and miR-499a-5p maintained the statistical significance between CTNNB1$^{wt}$ and CTNNB1$^{mut}$ patients (miR-499a-3p, p = 0.0008; miR-499a-5p p < 0.0001; **Figure 1**). As expected, based on the profiling data, miR-187-3p and miR-325 were not significantly deregulated between the two subgroups.

Regarding the extended cohort including NSMP and MMRd patients together, miR-187-3p did not maintain the statistical significance, whereas the other three miRNAs confirmed the differential expression between EC samples harboring the CTNNB1 mutation and the wild-type ones. In particular, miR-325 was downregulated in the CTNNB1$^{mut}$ ECs compared with the CTNNB1$^{wt}$ cases (p = 0.012), whereas miR-499a-3p and miR-499a-5p were both upregulated in CTNNB1$^{mut}$ ECs with respect to CTNNB1$^{wt}$ patients (p < 0.0001 for both). No association between miRNA expression and clinical parameters reported in **Table 1** was observed.

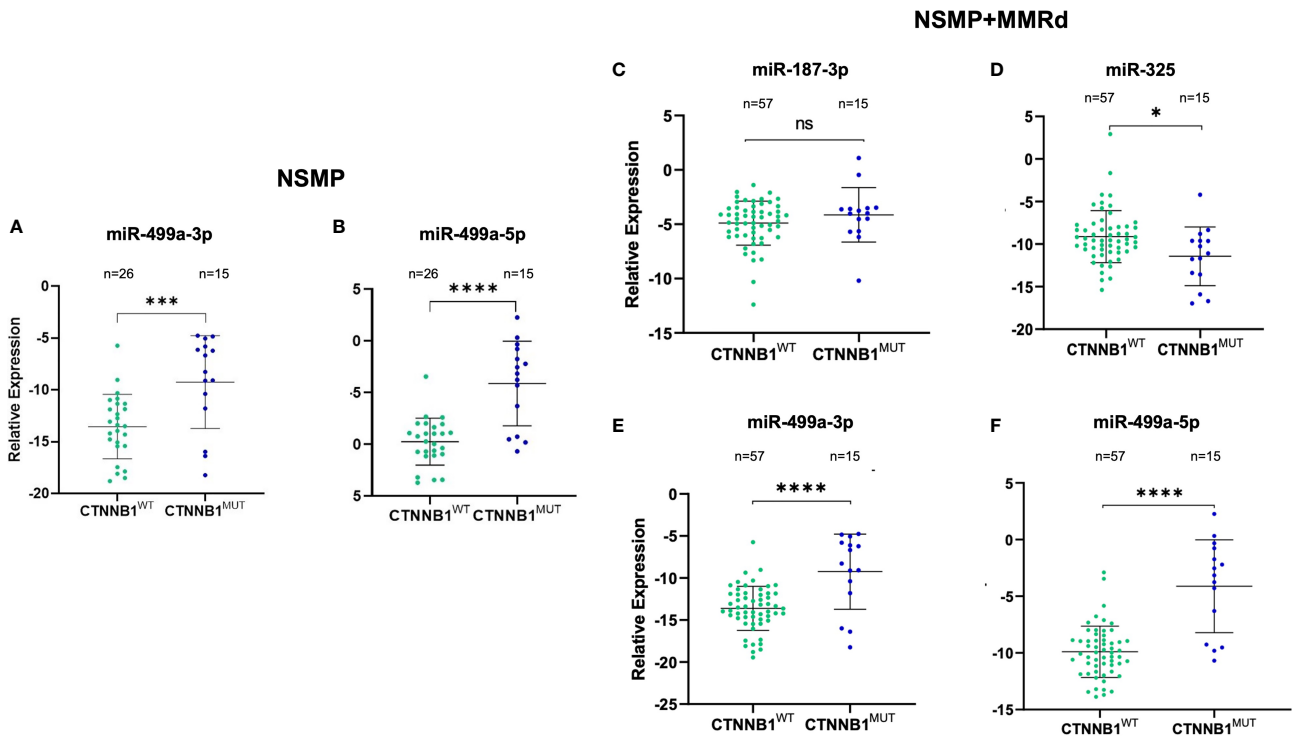


**FIGURE 1** | Validation of miR-499a-3p and 499a-5p in the NSMP ECs (n = 41) **(A, B)**, validation of miR-187-3p **(C)**, miR-325 **(D)**, miR-499a-3p **(E)**, and 499a-5p **(F)** in the 72 EC samples (NSMP + MMRd). ns, not significant (p > 0.05); *p < 0.05; ***p < 0.001; ****p < 0.0001.

## Validation of the Results in the TCGA EC Cohort

To corroborate our data, we further validated the results in an independent cohort of ECs. To do that, we analyzed the TCGA cohort of EC, stratifying the patients based on the CTNNB1 mutation. We were able to retrieve the data for 151 EC cases, of which 91 were NSMP and 60 MMRd. Of note, out of all miRNAs, miR-325 expression in the TCGA ECs could not be assessed. As we did for our cohort, we first analyzed miRNA expression considering only the NSMP cases, and subsequently, we included the MMRd cases. As shown in **Figures 2A, B**, miR-187-3p resulted to be significantly deregulated in both NSMP cohort alone and including the MMRd ($p = 0.004$ and $p = 0.049$, respectively). With regard to miR-499a-3p and -5p, the statistical significance was maintained in both the cohorts analyzed (**Figures 2C–F**). The chi-square test was used to assess the distribution of high/low miRNA expression based on the CTNNB1 mutational status (**Figure 3**). As clearly shown, the CTNNB1 mutant ECs presented a significant enrichment of tumors with high expression of the two miRNAs in NSMP alone and in NSMP+ MMRd cohorts.

**TABLE 1** | Characteristics of the study cohort.

| | N = 72 (%) |
|---|---|
| **Age** | |
| <50 | 6 (8.3) |
| >50 | 66 (91.7) |
| **BMI** | |
| <25 | 25 (34.7) |
| >25 | 47 (65.3) |
| **Histotype** | |
| E | 62 (86.1) |
| I-DED | 8 (11.1) |
| S | 2 (2.8) |
| CS | 0 |
| CCC | 0 |
| **ESMO risk** | |
| Low risk | 14 (19.4) |
| Intermediate risk | 5 (6.9) |
| High-intermediate risk | 31 (43.1) |
| High risk | 22 (30.6) |
| **Grading** | |
| Low | 55 (76.4) |
| High | 17 (23.6) |
| **FIGO stage** | |
| IA | 45 (62.5) |
| IB–II | 13 (18.1) |
| III–IV | 14 (19.4) |
| **LVI** | |
| Absent | 25 (34.72) |
| Focal | 23 (31.94) |
| Massive | 23 (31.94) |
| Missing | 1 (1.39) |
| **TCGA classification** | |
| NSMP | 41 (56.9) |
| MSI | 31 (43.9) |

*BMI, body mass index; E, endometrioid; I-DED, de-differentiated; S, serous; CS, carcinosarcoma; CCC, clear cell carcinoma; LVI, lymphovascular invasion.*

## Prognostic Impact of miR-499a on TCGA EC Cohort

Given the small sample size of our study group and the limited number of events, we evaluated a possible association between miR-187-3p, miR-499a and OS and PFI in the TCGA EC cohort. First, we considered the expression of the two miRNAs in both NSMP and NSMP + MMRd cohorts. Based on miRNA expression, we divided the patients in two groups (high and low expression) using the median value of the specific miRNA as a cutoff. No significant associations were identified with miR-187-3p. The median values for miR-499a-3p and -5p were -1.19 and -1.25, respectively. Interestingly, miR-499a-5p was significantly associated with OS in the NSMP group ($p=0.03$, log-rank test). In particular, ECs with a lower miR-499a-5p expression showed better OS when compared to the patients with higher levels (**Figure 4**). In order to exclude other factors which may influence OS in the NSMP subgroup and to strengthen the prognostic value of miR499a-5p, we considered other clinical factors which can have an impact on patient outcome, such as tumor stage and grade. The COX proportional hazards model was used, and variables reaching significance in the univariate analysis were included in the multivariate model. Both high level of miR499a-5p [HR (95% CI): 3.96 (1.1–14.7), $p = 0.04$] and high tumor grade [HR (95% CI): 5.7 (1.7–18.9), $p = 0.004$] were independent predictors of poor survival in EC patients.

In the NSMP+ MMRd cohort, the same trend was observed, but without reaching a statistical significance ($p = 0.13$). PFI was not associated with miR-499a-5p expression neither in the NSMP group ($p = 0.39$) nor in the NSMP + MMRd ($p = 0.49$) group. MiR-499a-3p did not show any significant correlation (**Supplementary Figure 2**).

Finally, we combined miR-499a-3p and -5p expression levels (low or high) with the CTNNB1 mutational status (mutant or wt). The combination of miR-499a-3p and CTNNB1 status did not reveal any significant correlation with OS and PFI in NSMP alone or NSMP + MMRd cohorts (**Supplementary Figure 3**). On the contrary, CTNNB1 mutant ECs with lower miR-499a-5p expression showed better OS compared with the other subgroups, among the NSMP patients (**Figure 5**). Conversely, the combination of miR-499a-5p expression and CTNNB1 mutational status showed a significant difference in OS in the NSMP patients ($p=0.03$, log-rank test) (**Figure 5**). Specifically, ECs with no CTNNB1 mutations and high miR-499a-5p expression, showed shorter OS compared with the other groups [HR (95% CI): 3.99 (1.3–11.6), $p = 0.006$]. Moreover, in a multivariate analysis, the same combination of miRNA expression and CTNNB1 mutational status remained independently associated with higher risk of death [HR (95% CI): 3.53 (1.1–10.5), $p = 0.02$]. The same trend was observed in NSMP + MMRd patients, but without reaching statistical significance ($p = 0.37$). With regard to the PFI, even if no significant correlations were observed, CTNNB1 mutant ECs with low 499a-5p expression showed better PFI in NSMP alone and NSMP + MMRd combined groups ($p = 0.14$ and $p = 0.26$, respectively). The combination of miR-499a-5p and CTNNB1 mutational status allows for a better

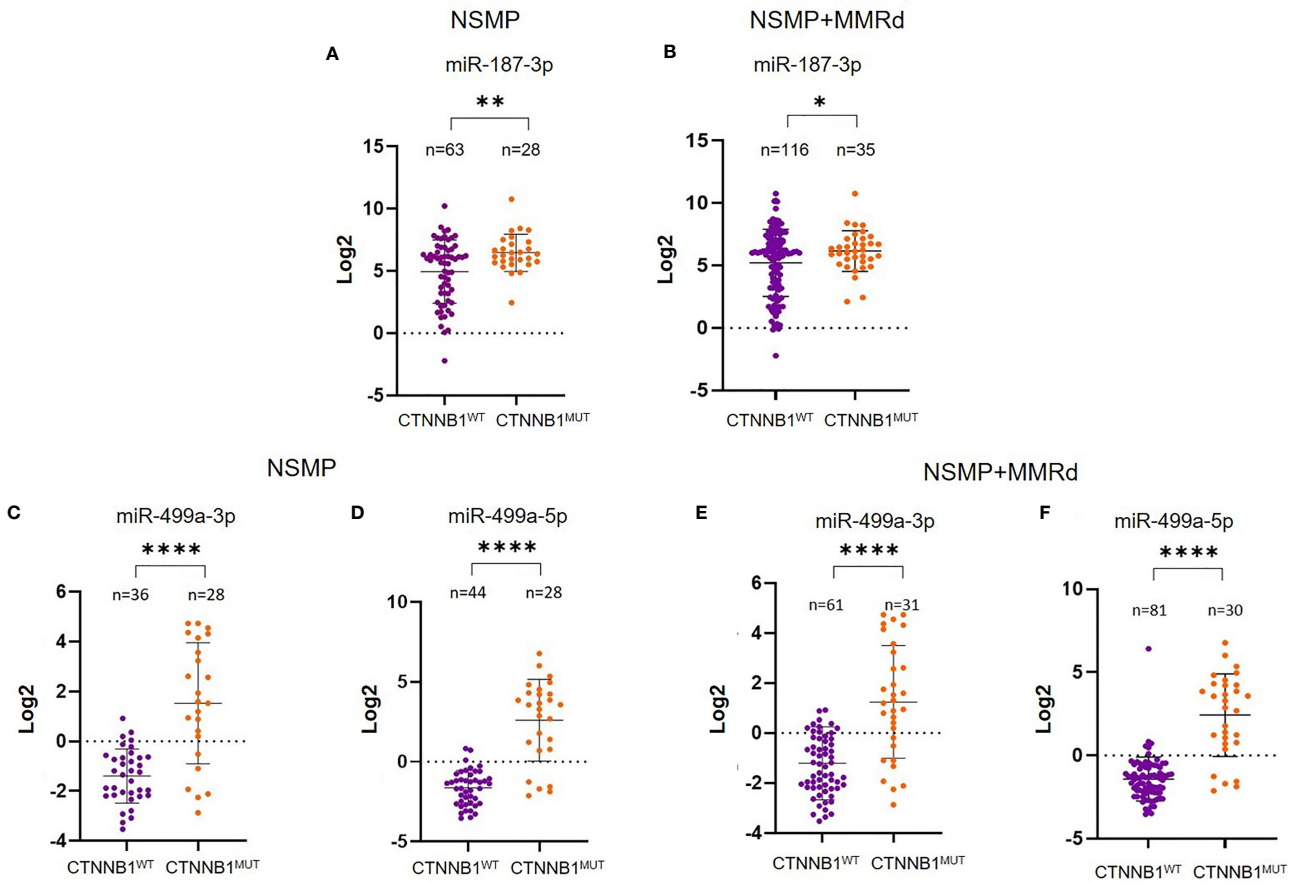


**FIGURE 2** | Analysis of miR-187-3p in the NSMP alone and in NSMP + MMRd TCGA cohorts **(A, B)**. Analysis of miR-499a-3p and miR-499a-5p in the TCGA NSMP alone **(C, D)** and in NSMP + MMRd EC groups **(E, F)**. *p < 0.05; **p < 0.01; ****p < 0.0001.

stratification of EC patients with respect to the CTNNB1 mutation alone (**Supplementary Figure 4**).

## DISCUSSION

In the last decade, several miRNAs have been described as potential biomarkers of EC prognosis or diagnosis. For example, among others, miR-34a was identified as able to stratify patients at high risk of recurrence (26) and reduced miR-497-5p levels were reported in high-grade ECs compared with low-grade Ecs (27). However, to the best of our knowledge, this is the first study to analyze miRNA expression in EC with the aim to obtain prognostic information in the intermediate-risk groups (i.e., NSMP and MMRd) of the molecular classification, trying to create subclassifications while taking into account the CTNNB1 mutational status.

In the attempt to better define this latter group, we first evaluated the miRNA expression profile in CTNNB1$^{mut}$ ECs compared with the CTNNB1$^{wt}$ NSMP ones. To this purpose, we analyzed the miRNA expression profile in 23 EC cases, identifying miR-499a-3p and 5p as significantly upregulated miRNAs in the CTNNB1$^{mut}$ cases when compared with the wt ones. However, considering that in literature the NSMP EC subgroup appears to be similar to the MMRd group at the prognosis level, we included seven additional MMRd patients.

Based on the results, we selected four miRNAs to validate in 72 EC samples and we observed a high statistical significance for miR-499a-3p and -5p. Finally, to corroborate our data, we analyzed the TCGA EC cohort, stratifying the patients based on the CTNNB1 mutation. In agreement with our results, the CTNNB1$^{mut}$ patients showed a higher expression of both miR-499a-3p and -5p in NSMP ECs as well as among the NSMP/MMRd patients. We further analyzed the survival rate in terms of OS and PFI with regard to the two-miRNA level. We did not perform this analysis in our study cohort due to the limited number of samples and events which, from a statistical point of view, will not give strong results. In fact, considering the MSI and NSMP groups, the time needed for the development of such events is a limiting factor and requires a statistical power that we did not have; therefore, at this time, validation of our results in the TCGA cohort appeared more appropriate.

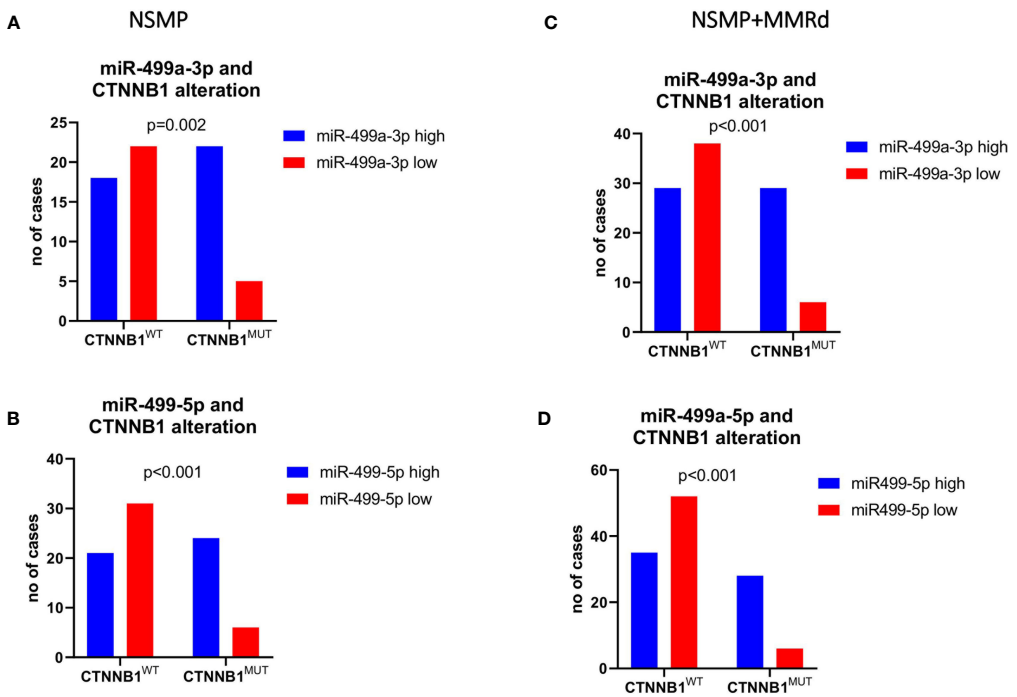


**FIGURE 3** | Chi-square test was used to test the distribution of low/high miR-499a-3p **(A, C)** and 5p **(B, D)** expression across the CTNNB1-mutated *versus* wild-type patients' subgroups.

Based on miRNA expression, the patients were divided into two groups (high and low expression) using the median of their expression level as a cutoff. MiR-499a-5p was significantly associated with OS, showing that NSMP patients with a lower expression have a prolonged survival. Conversely, the high level of miR-499a-5p was an independent predictor of poor survival.

The same correlation was observed when miRNA level and CTNNB1 status were combined. Indeed, NSMP patients with no CTNNB1 mutations and high miR-499a-5p expression had an increased risk of death.

MiR-499a-3p and 499a-5p belong to the miR-499 family, together with miR-499b. Human miR-499 is located in intron 19 of the *MYH7B* gene and it is composed of two genes, miR-499a and miR-499b. Those are located in sense (miR-499a) and antisense (miR-499b) DNA chains of the same region and transcribed in antiparallel directions (28). Data about miR-499b are missing, whereas several reports on miR-499a dysregulation have recently been published. Interestingly, a previous work by Zhang et al. showed a link between miR-499a and the Wnt/β-catenin signaling pathway. In particular, the authors demonstrated that overexpression of miR-499a activated β-catenin in cardiac differentiation. With regard to cancer, a few recent studies have tried to clarify the roles of miR-499a. However, it is not surprising that the results were contradictory among the analyzed tumor types because, as well established, the precise function of a single miRNA is strongly dependent on the specific biological context. Li et al. demonstrated that overexpressed miR-499 inhibited non-small cell lung cancer growth by suppressing cell proliferation and promoting apoptosis (29). On the contrary, Liu et al. showed that in colorectal cancer (CRC), miR-499 acts as an onco-mir by targeting two tumor suppressor genes, FOXO4 and PDCD4. Thus, overexpression of miR-499 is associated with advanced CRC stage and with cellular invasion and tumor metastasis in *in vitro* CRC models. In our results, a lower expression of the miRNA was associated with better survival in NSMP patients. Even if a clear mechanism has not been investigated, an interesting explanation could be related to the APC gene. Physiologically, APC acts as a scaffold in the β-catenin destruction complex, so it tightly regulates the Wnt pathway activity (30). APC is a target of miR-499a-5p based on TargetScan prediction, and its upregulation could promote inhibition of APC which, in turn, is less efficient in regulating the β-catenin level (31). Consequently, β-catenin can translocate in the nucleus and activate the Wnt pathway which fosters carcinogenesis. Thus, the higher miR-499a-5p expression could raise the APC inhibition which, consecutively, will be less effective in regulating the cytoplasmatic β-catenin destruction. **Figure 6** shows the proposed mechanism. The CTNNB1 mutations by themselves are classically associated with nuclear translocation and activation of Wnt/β-catenin signaling (15). Interestingly, these mutations are usually found in heterozygosity (17, 32, 33) and, thus, it is reasonable to suppose that miR-499a-5p could play a role in CTNNB1 wild-type cells. Basically, higher miR-499a-5p expression represents an advantage for the tumor cells which may activate transcription of pro-tumorigenic genes besides normal CTNNB1. This could explain why a lower expression of miR-499a-5p resulted to be associated with a better

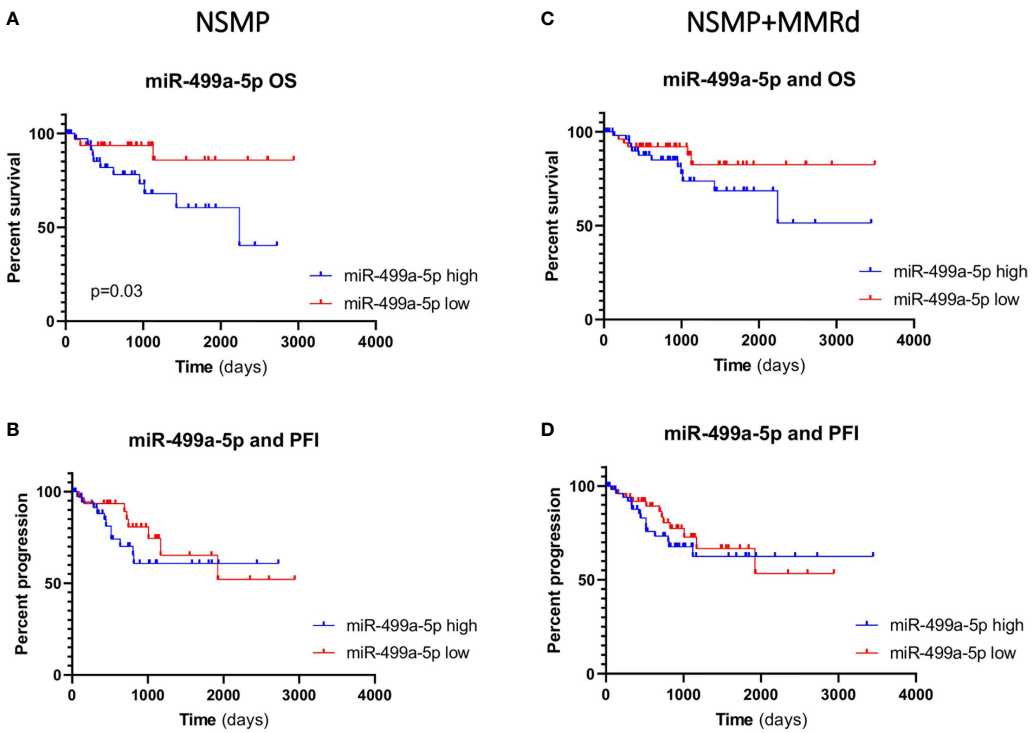


**FIGURE 4** | Kaplan–Meier estimates of overall survival **(A, C)** and progression-free interval **(B, D)** in NSMP alone and NSMP + MMRd groups, based on miR-499a-5p expression.

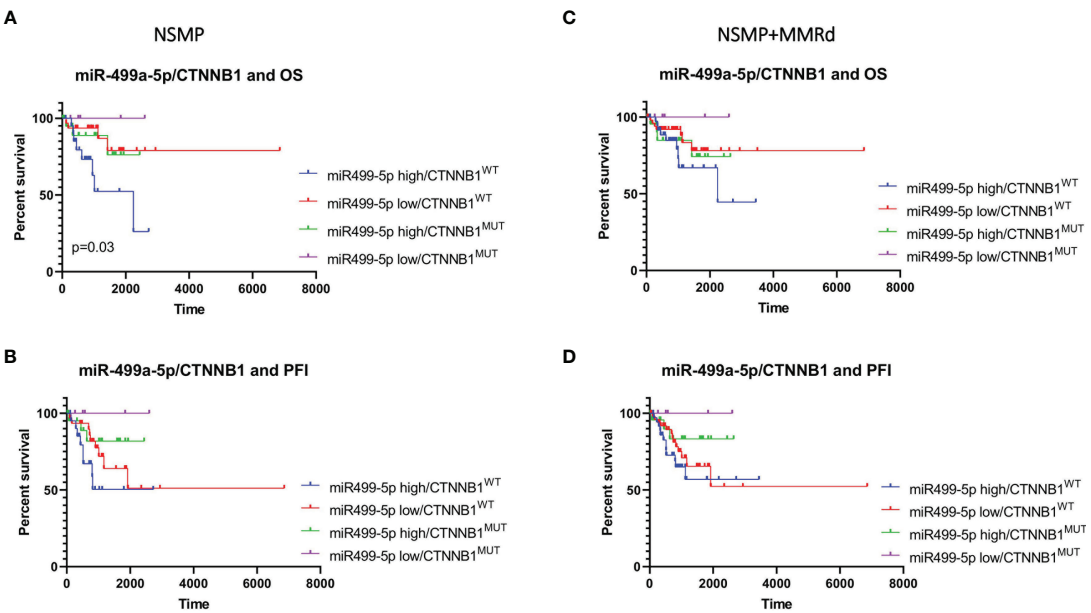


**FIGURE 5** | Kaplan–Meier estimates of OS **(A, C)** and PFI **(B, D)** in NSMP alone and NSMP + MMRd groups, based on the combination of miR-499a-5p expression and CTNNB1 status.

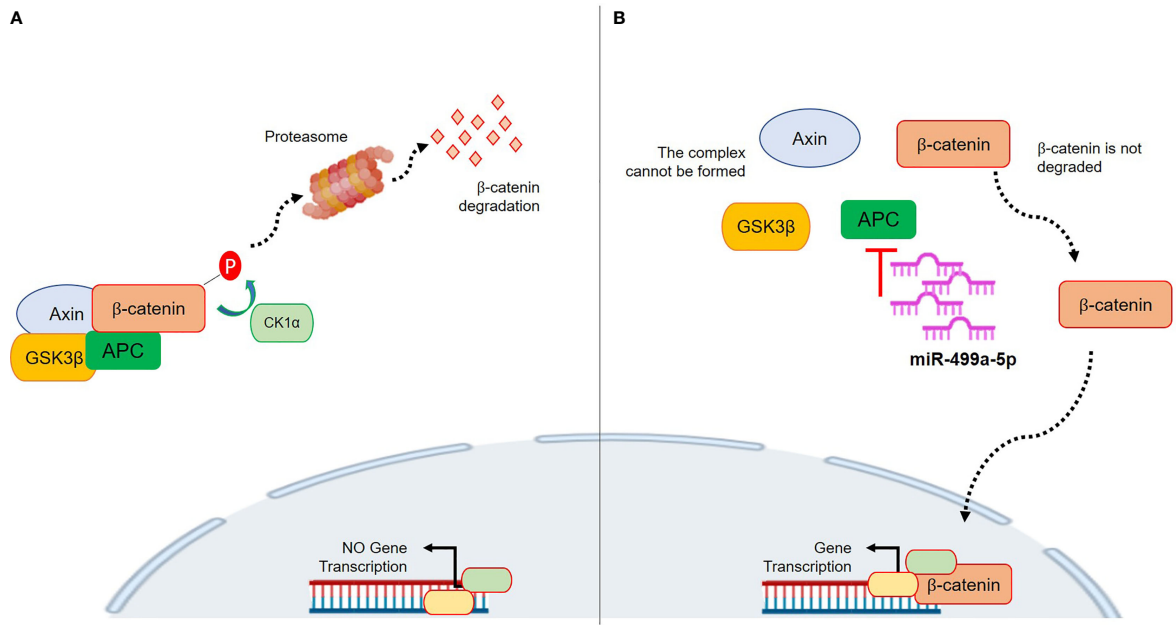


**FIGURE 6** | Proposed mechanism of action of miR-499a-5p within the Wnt/β-catenin pathway. **(A)** The complex formed by AXIN, CK1α, GSK3β, and APC phosphorylates β-catenin, which subsequently undergoes the ubiquitin-proteasomal degradation. This prevents its nuclear translocation and pro-tumor gene transcription. **(B)** miR-499a-5p targets APC. High expression of miR-499a-5p promotes APC inhibition, thus preventing the AXIN/CK1α/GSK3β/APC complex formation. Without complex, β-catenin is not degraded, and it can translocate in the nucleus where it promotes gene transcription.

outcome in NSMP patients; however, functional studies are needed in order to test this hypothesis. Our work has several strengths; first, the sample size of NSMP and MMRd patients is numerically important considering the incidence of this tumor. Second, the data were corroborated in the TCGA cohort, an independent and well-described group of EC patients. In the TCGA data, the Illumina platform was used to assess the miRNA expression, whereas we used the RT-PCR-based array and assays; accordingly, two different techniques were exploited to investigate miRNA levels. Third, our cohort was highly homogeneous from a molecular point of view, and this allowed us to limit potential biases; finally, all the patients were homogeneously treated according to ESMO risk classifications. However, there are some limits to consider; among these, we have to include the retrospective design of the study which, however, was essential to creating a model that could be prospectively validated in larger and independent cohorts and possibly on blood samples to assess the validity of the miRNA as a liquid prognostic biomarker. We did not analyze the two miRNAs in the other TCGA groups (i.e., POLE and p53abn groups) because we focused our attention on the NSMP and MMRd ECs in which TCGA had the smallest impact as regards the definition of therapy. Indeed, the classic pathological parameters with all their limitations, defined by ESGO/ESTRO/ESP guidelines, continue to be the gold standard for the therapy selection. Unfortunately, we could not perform any functional validations of our model due to the lack of commercial cell lines with no mutations on p53 or without microsatellite instability.

In conclusion, to the best of our knowledge, we showed, for the first time, that specific miRNAs are associated with the molecular subgroups proposed by the TCGA. miR-499a-5p, in particular, may represent a novel independent prognostic biomarker in NSMP ECs and, if validated in an independent cohort of patients, could improve the current classification and promote a more personalized management of those patients.

## DATA AVAILABILITY STATEMENT

The original contributions presented in the study are included in the article/**Supplementary Material**. Further inquiries can be directed to the corresponding authors.

## ETHICS STATEMENT

The studies involving human participants were reviewed and approved by 189/2021/Oss/AOUBo, ClinicalTrials.gov Identifier: NCT04845425. The patients/participants provided their written informed consent to participate in this study.

## AUTHOR CONTRIBUTIONS

Conceptualization, GR, ADL, and AMP. Methodology, GR, ADL, FG, and DdB. Validation, GR, FG, ADL, and AMP.

Formal analysis, GR, CaC, and ADL. Investigation, ADL, DdB, ClC, AMP, and PDI. Resources, AMP and PDI. Data curation, GR, ADL, FG, DdB, AMP, and ClC. Writing—original draft preparation, GR, AMP, ADL, and DdB. Writing—review and editing, GR, CaC, GT, DdB, PDI, AMP, GD, MT, DS, EDC, AGC, and PH. Supervision, GR, AMP, SA, and PDI. All authors contributed to the article and approved the submitted version.

## FUNDING

The work was supported by Fondazione Cassa di Risparmio in Bologna (Carisbo): project number #19094 to AMP.

## ACKNOWLEDGMENTS

GR was supported by a Fulbright Research Scholarship (year 2021). FG is supported by a fellowship from the Fondazione Cassa di Risparmio in Bologna (Carisbo).

## SUPPLEMENTARY MATERIAL

The Supplementary Material for this article can be found online at: https://www.frontiersin.org/articles/10.3389/fonc.2021.757678/full#supplementary-material

## REFERENCES

1. Allemani C, Matsuda T, Di Carlo V, Harewood R, Matz M, Nikšić M, et al. Global Surveillance of Trends in Cancer Survival 2000–14 (CONCORD-3): Analysis of Individual Records for 37 513 025 Patients Diagnosed With One of 18 Cancers From 322 Population-Based Registries in 71 Countries. *Lancet* (2018) 391:1023–75. doi: 10.1016/S0140-6736(17)33326-3
2. Ferlay J, Colombet M, Soerjomataram I, Dyba T, Randi G, Bettio M, et al. Cancer Incidence and Mortality Patterns in Europe: Estimates for 40 Countries and 25 Major Cancers in 2018. *Eur J Cancer* (2018) 103:356–87. doi: 10.1016/j.ejca.2018.07.005
3. Bell DW, Ellenson LH. Molecular Genetics of Endometrial Carcinoma. *Annu Rev Pathol* (2019) 14:339–67. doi: 10.1146/ANNUREV-PATHOL-020117-043609
4. Murali R, Soslow RA, Weigelt B. Classification of Endometrial Carcinoma: More Than Two Types. *Lancet Oncol* (2014) 15:e268–78. doi: 10.1016/S1470-2045(13)70591-6
5. Soslow RA, Tornos C, Park KJ, Malpica A, Matias-Guiu X, Oliva E, et al. Endometrial Carcinoma Diagnosis: Use of FIGO Grading and Genomic Subcategories in Clinical Practice: Recommendations of the International Society of Gynecological Pathologists. *Int J Gynecol Pathol* (2019) 38:S64–74. doi: 10.1097/PGP.0000000000000518
6. Colombo N, Preti E, Landoni F, Carinelli S, Colombo A, Marini C, et al. Endometrial Cancer: ESMO Clinical Practice Guidelines for Diagnosis, Treatment and Follow-Up. *Ann Oncol* (2013) 24:33–8. doi: 10.1093/annonc/mdt353
7. Gilks CB, Oliva E, Soslow RA. Poor Interobserver Reproducibility in the Diagnosis of High-Grade Endometrial Carcinoma. *Am J Surg Pathol* (2013) 37:874–81. doi: 10.1097/PAS.0b013e31827f576a
8. Perrone AM, Di Marcoberardino BB, Rossi MM, Pozzati FF, Pellegrini AA, Procaccini MM, et al. Laparoscopic Versus Laparotomic Approach to Endometrial Cancer. *Eur J Gynaecol Oncol* (2012) 33:376–81.
9. Getz G, Gabriel SB, Cibulskis K, Lander E, Sivachenko A, Sougnez C, et al. Integrated Genomic Characterization of Endometrial Carcinoma. *Nature* (2013) 497:67–73. doi: 10.1038/nature12113
10. Talhouk A, McConechy MK, Leung S, Li-Chang HH, Kwon JS, Melnyk N, et al. A Clinically Applicable Molecular-Based Classification for Endometrial Cancers. *Br J Cancer* (2015) 113:299–310. doi: 10.1038/bjc.2015.190
11. Talhouk A, McConechy MK, Leung S, Yang W, Lum A, Senz J, et al. Confirmation of ProMisE: A Simple, Genomics-Based Clinical Classifier for Endometrial Cancer. *Cancer* (2017) 123:802–13. doi: 10.1002/cncr.30496
12. Kommoss S, McConechy MK, Kommoss F, Leung S, Bunz A, Magrill J, et al. Final Validation of the ProMisE Molecular Classifier for Endometrial Carcinoma in a Large Population-Based Case Series. *Ann Oncol* (2018) 29:1180–8. doi: 10.1093/annonc/mdy058
13. Concin N, Matias-Guiu X, Vergote I, Cibula D, Mirza MR, Marnitz S, et al. ESGO/ESTRO/ESP Guidelines for the Management of Patients With Endometrial Carcinoma. *Int J Gynecol Cancer* (2021) 31:12–39. doi: 10.1136/ijgc-2020-002230
14. Pasanen A, Loukovaara M, Bützow R. Clinicopathological Significance of Deficient DNA Mismatch Repair and MLH1 Promoter Methylation in Endometrioid Endometrial Carcinoma. *Mod Pathol* (2020) 33:1443–52. doi: 10.1038/S41379-020-0501-8
15. Kurnit KC, Kim GN, Fellman BM, Urbauer DL, Mills GB, Zhang W, et al. CTNNB1 (Beta-Catenin) Mutation Identifies Low Grade, Early Stage Endometrial Cancer Patients at Increased Risk of Recurrence. *Mod Pathol* (2017) 30:1032–41. doi: 10.1038/MODPATHOL.2017.15
16. Liu Y, Patel L, Mills GB, Lu KH, Sood AK, Ding L, et al. Clinical Significance of CTNNB1 Mutation and Wnt Pathway Activation in Endometrioid Endometrial Carcinoma. *J Natl Cancer Inst* (2014) 106:1–8. doi: 10.1093/JNCI/DJU245.
17. De Leo A, de Biase D, Lenzi J, Barbero G, Turchetti D, Grillini M, et al. Arid1a and Ctnnb1/β-Catenin Molecular Status Affects the Clinicopathologic Features and Prognosis of Endometrial Carcinoma: Implications for an Improved Surrogate Molecular Classification. *Cancers (Basel)* (2021) 13:1–22. doi: 10.3390/cancers13050950
18. Calin GA, Croce CM. MicroRNA Signatures in Human Cancers. *Nat Rev Cancer* (2006) 6:857–66. doi: 10.1038/nrc1997
19. Di Leva G, Garofalo M, Croce CM. MicroRNAs in Cancer. *Annu Rev Pathol Mech Dis* (2014) 9:287–314. doi: 10.1146/annurev-pathol-012513-104715
20. IARC Publications. *Female Genital Tumours*. Available at: https://publications.iarc.fr/Book-And-Report-Series/Who-Classification-Of-Tumours/Female-Genital-Tumours-2020 (Accessed June 24, 2021). Website.
21. Schwarzenbach H, da Silva AM, Calin G, Pantel K. Data Normalization Strategies for MicroRNA Quantification. *Clin Chem* (2015) 61:1333–42. doi: 10.1373/CLINCHEM.2015.239459
22. Rinnerthaler G, Hackl H, Gampenrieder S, Hamacher F, Hufnagl C, Hauser-Kronberger C, et al. miR-16-5p Is a Stably-Expressed Housekeeping MicroRNA in Breast Cancer Tissues From Primary Tumors and From Metastatic Sites. *Int J Mol Sci* (2016) 17:156. doi: 10.3390/ijms17020156
23. Colaprico A, Silva TC, Olsen C, Garofano L, Cava C, Garolini D, et al. TCGAbiolinks: An R/Bioconductor Package for Integrative Analysis of TCGA Data. *Nucleic Acids Res* (2016) 44:e71. doi: 10.1093/NAR/GKV1507
24. Mounir M, Lucchetta M, Silva TC, Olsen C, Bontempi G, Chen X, et al. New Functionalities in the TCGAbiolinks Package for the Study and Integration of Cancer Data From GDC and GTEx. *PLoS Comput Biol* (2019) 15:e1006701. doi: 10.1371/JOURNAL.PCBI.1006701
25. Deng M, Brägelmann J, Kryukov I, Saraiva-Agostinho N, Perner S. FirebrowseR: An R Client to the Broad Institute's Firehose Pipeline. *Database* (2017) 2017:1–6. doi: 10.1093/DATABASE/BAW160
26. Corrado G, Laquintana V, Loria R, Carosi M, de Salvo L, Sperduti I, et al. Endometrial Cancer Prognosis Correlates With the Expression of L1CAM and Mir34a Biomarkers. *J Exp Clin Cancer Res* (2018) 37:1–10. doi: 10.1186/S13046-018-0816-1
27. Fridrichova I, Kalinkova L, Karhanek M, Smolkova B, Machalekova K, Wachsmannova L, et al. miR-497-5p Decreased Expression Associated With High-Risk Endometrial Cancer. *Int J Mol Sci* (2020) 22:1–18. doi: 10.3390/IJMS22010127

28. Chistiakov DA, Orekhov A, Bobryshev Y. Cardiac-Specific miRNA in Cardiogenesis, Heart Function, and Cardiac Pathology (With Focus on Myocardial Infarction). *J Mol Cell Cardiol* (2016) 94:107–21. doi: 10.1016/J.YJMCC.2016.03.015
29. Li M, Zhang S, Wu N, Wu L, Wang C, Lin Y. Overexpression of miR-499-5p Inhibits Non-Small Cell Lung Cancer Proliferation and Metastasis by Targeting VAV3. *Sci Rep* (2016) 6:1–10. doi: 10.1038/SREP23100
30. Parker TW, Neufeld KL. APC Controls Wnt-Induced β-Catenin Destruction Complex Recruitment in Human Colonocytes. *Sci Rep* (2020) 10:1–14. doi: 10.1038/s41598-020-59899-z
31. Zhou J, Zhang S, Sun X, Lou Y, Bao J, Yu J. Hyperoside Ameliorates Diabetic Nephropathy Induced by STZ *via* Targeting the miR-499-5p/APC Axis. *J Pharmacol Sci* (2021) 146:10–20. doi: 10.1016/J.JPHS.2021.02.005
32. Forbes SA, Beare D, Gunasekaran P, Leung K, Bindal N, Boutselakis H, et al. COSMIC: Exploring the World's Knowledge of Somatic Mutations in Human Cancer. *Nucleic Acids Res* (2015) 43:D805–11. doi: 10.1093/nar/gku1075
33. COSMIC V85 Released 08-M-18. CosmicCatalogue Of Somatic Mutations. In: *Cancer*. Available at: https://cancer.sanger.ac.uk/cosmic.

**Conflict of Interest:** The authors declare that the research was conducted in the absence of any commercial or financial relationships that could be construed as a potential conflict of interest.

frontiers in Oncology

ORIGINAL RESEARCH
published: 26 November 2021
doi: 10.3389/fonc.2021.753386

# Single-Cell RNA Sequencing Reveals Multiple Pathways and the Tumor Microenvironment Could Lead to Chemotherapy Resistance in Cervical Cancer

*Meijia Gu[1], Ti He[2], Yuncong Yuan[3,4], Suling Duan[1], Xin Li[5]* and Chao Shen[3,4]**

*[1] Key Laboratory of Combinatorial Biosynthesis and Drug Discovery, Ministry of Education, School of Pharmaceutical Sciences, Wuhan University, Wuhan, China, [2] Department of Scientific Research & Industrial Application, Beijing Microread Genetics Co., Ltd., Beijing, China, [3] College of Life Sciences, Wuhan University, Wuhan, China, [4] China Center for Type Culture Collection, Wuhan University, Wuhan, China, [5] Department of Gynecology 2, Renmin Hospital of Wuhan University, Wuhan, China*

OPEN ACCESS

**Edited by:**
*Robert Vierkant,*
*Mayo Clinic, United States*

**Reviewed by:**
*Ying Li,*
*Mayo Clinic, United States*
*Syed S. Islam,*
*King Faisal Specialist Hospital & Research Centre, Saudi Arabia*

***Correspondence:**
*Chao Shen*
*shenchao@whu.edu.cn*
*Xin Li*
*lixinwhu@189.cn*

**Specialty section:**
*This article was submitted to Gynecological Oncology, a section of the journal Frontiers in Oncology*

**Received:** *04 August 2021*
**Accepted:** *27 October 2021*
**Published:** *26 November 2021*

**Citation:**
*Gu M, He T, Yuan Y, Duan S, Li X and Shen C (2021) Single-Cell RNA Sequencing Reveals Multiple Pathways and the Tumor Microenvironment Could Lead to Chemotherapy Resistance in Cervical Cancer. Front. Oncol. 11:753386. doi: 10.3389/fonc.2021.753386*

**Background:** Cervical cancer is one of the most common gynecological cancers worldwide. The tumor microenvironment significantly influences the therapeutic response and clinical outcome. However, the complex tumor microenvironment of cervical cancer and the molecular mechanisms underlying chemotherapy resistance are not well studied. This study aimed to comprehensively analyze cells from pretreated and chemoresistant cervical cancer tissues to generate a molecular census of cell populations.

**Methods:** Biopsy tissues collected from patients with cervical squamous cell carcinoma, cervical adenocarcinoma, and chronic cervicitis were subjected to single-cell RNA sequencing using the 10× Genomics platform. Unsupervised clustering analysis of cells was performed to identify the main cell types, and important cell clusters were reclustered into subpopulations. Gene expression profiles and functional enrichment analysis were used to explore gene expression and functional differences between cell subpopulations in cervicitis and cervical cancer samples and between chemoresistant and chemosensitive samples.

**Results:** A total of 24,371 cells were clustered into nine separate cell types, including immune and non-immune cells. Differentially expressed genes between chemoresistant and chemosensitive patients enriched in the phosphoinositide 3-kinase (PI3K)/AKT pathway were involved in tumor development, progression, and apoptosis, which might lead to chemotherapy resistance.

**Conclusions:** Our study provides a comprehensive overview of the cancer microenvironment landscape and characterizes its gene expression and functional difference in chemotherapy resistance. Consequently, our study deepens the insights into cervical cancer biology through the identification of gene markers for diagnosis, prognosis, and therapy.

**Keywords: single-cell RNA sequencing, cervical cancer, tumor microenvironment, chemotherapy resistance, multiple pathways**

## INTRODUCTION

As the fourth most common gynecological malignant tumor, cervical cancer is a leading cause of cancer-related deaths among women and poses a serious threat to the health of women worldwide (1). In 2018, approximately 570,000 new cases of cervical cancer and 311,000 deaths from this cancer were reported (1). Paclitaxel, cisplatin, carboplatin, or a combination of these agents is the front-line treatment for cervical cancer (2). However, the efficacy of current chemotherapeutic agents is limited, with relatively low response rates of 29%–63% because of chemotherapy resistance (3). The combination of paclitaxel and cisplatin is one of the most commonly utilized regimens in the metastatic disease setting (4). However, in actual clinical treatment, tumor cells often develop resistance.

The tumor microenvironment (TME) comprises various cell types [such as fibroblasts, endothelial cells (ECs), and immune cells] and extracellular components (such as cytokines, hormones, extracellular matrix, and growth factors), which surround tumor cells as a vascular network. The TME not only plays a pivotal role during tumor initiation, progression, and metastasis, but it also has profound effects on therapeutic efficacy. TME-mediated chemotherapy resistance is a result of complex crosstalk between tumor cells and their surrounding environment (5, 6).

For example, the TME and therapeutic response can be induced by soluble factors secreted by tumors. The adhesion of tumor cells to stromal fibroblasts can also affect responses to chemotherapy (7), and immune cells also play an important role in improving and obstructing therapeutic efficacy (7). The interaction between chemotherapy sensitivity and TME is a complex phenomenon. Cancers can develop remarkable resistance to various treatments that target different molecular pathways (8).

Research studies have shown that the cellular and molecular mechanisms underlying the development of resistance are multifactorial and include genetic and epigenetic alterations, cell detoxification, and abnormal drug efflux and accumulation (9, 10). However, the molecular mechanisms underlying the occurrence and development of resistance are poorly understood. Thus, there is an urgent need to identify the basic factors that determine chemotherapy resistance in cancer.

Previous studies on molecular mechanisms and chemotherapy resistance in cervical cancer patients have focused mainly on bulk genomic or transcriptome profiling methods and *in-situ* hybridization techniques (11–13). Consequently, studies of chemoresistance mechanisms based on the signatures of distinct cell populations are obscure (10–12). Single-cell RNA sequencing (scRNA-seq) techniques have emerged as a powerful tool for analyzing the spectrum of cell populations in tissues. Furthermore, these techniques have been widely used for elucidating the complex subpopulations in tissues of organs such as the lung (14), heart (15), and brain (16), as well as in various cancers including melanoma (17), ovarian (18), and colon (19) cancers (20, 21).

Although studies have used scRNA-seq on the cervix uteri (22) and drug-resistant cell lines (12), to the best of our knowledge, scRNA-seq profiling of human cervical cancer tissues has not been reported to date. Although scRNA-seq is increasingly being adopted, its application to tumors has been limited to several types, but not cervical cancer. Because of this limited elucidation of human tumors and the lack of TME profiling, the intratumoral transcriptomic heterogeneity of the most common cancer in women is largely unknown.

Exploring the molecular mechanism of chemotherapy resistance is important in the development of strategies to overcome tumor resistance and provides a theoretical basis for reversing tumor resistance and improving cancer chemotherapy efficacy. The development of chemotherapy combinations that could simultaneously target tumor cells and the microenvironment may represent a solution to overcome chemotherapy resistance. This study aimed to analyze cells from pretreated and chemoresistant cervical cancer tissues at a much higher scale, to generate a molecular census of cell populations.

Furthermore, we sought to uncover the cell heterogeneity using unbiased scRNA-seq techniques. Consequently, we performed an scRNA-seq survey of 23,444 cells from five tissues from pretreated cervical cancer patients and constructed a single-cell transcriptome atlas for early malignancy of cervical cancer (**Figure 1**). Our study provides novel insights into the heterogeneity of cervical cancer at the single-cell level and will serve as a valuable resource for understanding chemotherapy resistance mechanisms in tumor progression.

## MATERIALS AND METHODS

### Patients and Tumor Specimens

Four female patients with a pathologic diagnosis of cervical cancer and one female patient diagnosed with cervicitis were enrolled at Renmin Hospital of Wuhan University, Wuhan (**Table 1**). All enrolled patients signed the written consent, and this study was approved by the Institutional Review Board (IRB) of Renmin Hospital of Wuhan University (IRB no. WDRY2021-K014). Fresh tumor samples (at least 1.5 $cm^3$) were surgically resected from all enrolled patients. None of the patients were treated with chemotherapy prior to tissue sample collection. After sample resection, three of the four cervical cancer patients were treated with chemotherapy, and one patient was a responder and the two were resistant to chemotherapy.

**Abbreviations:** CBP, carboplatin; CA, cervical adenocarcinoma; CE, chronic cervicitis; CQ, cervical squamous cell carcinoma; DEGs, differentially expressed genes; ECs, endothelial cells; FAP, fibroblast activating protein; FDR, false discovery rate; GO, Gene Ontology; HGF, hepatocyte growth factor; KEGG, Kyoto Encyclopedia of Genes and Genomes; PCA, principal component analysis; PDL1, programmed cell death ligand 1; PDL2, programmed cell death ligand 2; PLD1, phospholipase D1; PLVAP, plasmalemmal vesicle-associated protein; scRNA-seq, single-cell RNA sequencing; SDF1, stromal cell-derived factor 1; *t*-SNE, t-distributed stochastic neighbor embedding; TME, tumor microenvironment; UMI, unique molecular identifiers; VEGF, vascular endothelial growth factor.

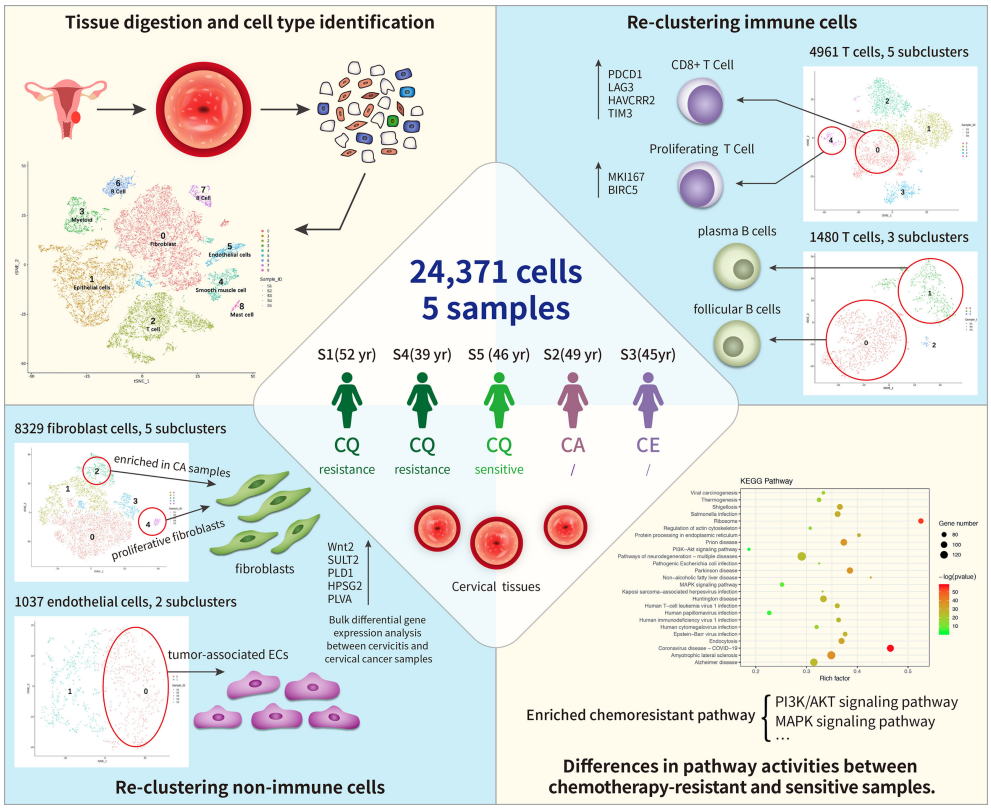


**FIGURE 1** | Single-cell transcriptome regulatory network of the tumor microenvironment (TME) and chemoresistance in cervical cancer. In total, 24,371cells were clustered into nine separate cell types, including immune cells (T cells, B cells, and myeloid) and non-immune cells [fibroblast cells and endothelial cells (ECs), epithelial cells, and smooth muscle cells]. Among these, fibroblast cells formed five distinct subtypes, and cluster 4 (C4) contained proliferative fibroblast cells enriched in cancer samples. ECs comprised two subclusters: C0 corresponded to tumor-associated ECs. T and B cells formed five and three subclusters, respectively, where C1 of T cells expressed higher levels of immune checkpoint molecules (PDCD1) than the other clusters did and C4 highly expressed proliferating cancer marker genes, *MKI167* and *BIRC5*. Subpopulations of B cells were not strongly affected by drug resistance. Differentially expressed genes (DEGs) between chemoresistant and chemosensitive patients were enriched in phosphoinositide 3-kinase (PI3K)/AKT pathway involved in tumor development, progression, and apoptosis, which might lead to chemoresistance.

## Human Cervical Cancer Tissue Cell Dissociation

All fresh cervical cancer tissues were transferred from the operating room to the dissociation laboratory in cold Hank's balanced salt solution (HBSS) medium supplemented with 1% penicillin–streptomycin within 30 min. Samples were gently washed in phosphate-buffered saline (PBS) after removing the adipose tissue and minced into pieces of approximately 1 $mm^3$ using an Iris scissors. Enzymatic digestion was performed using the MACS tumor dissociation kit (Miltenyi Biotec) according to

**TABLE 1** | Clinical information of the five patients.

| | Patient 1 | Patient 2 | Patient 3 | Patient 4 | Patient 5 |
|---|---|---|---|---|---|
| **Sex** | Female | Female | Female | Female | Female |
| **Age** | 52 | 49 | 45 | 39 | 46 |
| **Chemotherapy before sampling** | No | No | No | No | No |
| **Chemotherapy drug** | PTX + CBP | No | No | PTX + CBP | PTX + CBP |
| **Clinical AJCC** | Squamous-cell carcinoma (IIA2) | Adenocarcinoma | Cervicitis | Squamous-cell carcinoma (IIA2) | Squamous-cell carcinoma (IIA2) |
| **Drug tolerance** | Primary resistance | Non-chemotherapy | Non-chemotherapy | Primary resistance | Non-resistance |
| **Other information** | / | / | / | / | / |
| **HPV infection** | 31 (+) | 18 (+) | Negative | Negative | 18 (+) |

*PTX, paclitaxel; CBP, carboplatin; HPV, human papillomavirus.*

the instructions of the manufacturer. The cell suspension was further filtered through a 40-μm cell-strainer (BD) and centrifuged at 400*g* for 10 min to remove the cell aggregates. After removing the supernatant, the pelleted cells were resuspended in 2 ml red blood cell lysis buffer (SolarBio), and then resuspended in PBS with 10% fetal bovine serum (FBS). The viability of the obtained single-cell suspension was detected using a hemocytometer with trypan blue (0.4%, 420301, Gibco).

## Single-Cell RNA Capturing, Library Preparation, and Sequencing

All single-cell capturing and downstream library construction were performed using the 10× Chromium Single Cell platform (Single Cell 3 library and Gel Bead kit v.3). Briefly, the cell suspensions at a concentration of 1,000 cells/μl were loaded into a 10x Genomics microfluidics chip and encapsulated with barcoded gel beads to generate gel beads in emulsion (GEM).

Reverse transcription of generated droplets was performed at 53°C for 45 min. cDNA was amplified for 12 cycles total on T100 Thermal Cycler (Bio-Rad). Then, RT-cDNA was recovered using Recovery Agent provided by 10× Genomics and purified with DynaBeads MyOne Silane Beads (Thermo Fisher Scientific) as outlined in the user guide. Subsequently, purified cDNAs were amplified and cleaned up with the SPRIselect Reagent Kit (Beckman Coulter, USA). Quantification of constructed libraries of each sample was detected using a Qubit2.0 Fluorometer (Invitrogen) before pooling. Pooled libraries were sequenced to a depth of an average of 50,000 reads per cell on a NovaSeq 6000 sequencer (Illumina, San Diego) at 2 × 150 bp sequencing model (23–25).

## scRNA-Seq Data Analysis

scRNA-seq raw data were demultiplexed to FASTQ files (observed average read depth per cell was ~1.6 million reads) and aligned to an indexed ensembl_92-GRCh38.92 RefSeq genome to generate gene expression matrices using 10× Genomics pipeline CellRanger v.2.1.0 (25). The number of unique molecular identifiers (UMIs), the number of genes, and the percentage of mitochondrial genes were examined for quality control. Cells expressing <500 or >4,000 genes (potential cell duplets) and gene expression not detected in fewer than three cells were trimmed from the library.

Cells containing >10% mitochondrial genes were also discarded because of their poor cell viability (**Table S1**). We detected 92,675 genes in 21,433 cells from five samples. After data normalization, variably expressed genes were normalized and scaled, where single-cell gene counts were normalized to the total gene counts presented in that cell at a normalized expression between a low cutoff of 0.0125 and a high cutoff of 3 and a quantile-normalized variance >0.5, using the Seurat R package. The resulting gene expression values were transformed into a log space.

## Major Cell-Type Clustering

Principal component analysis (PCA) was used to reduce the dimensionality of the results of variably expressed genes based on the JackStraw function. Then, the first 10 principal components were selected as a statistically significant input for further two-dimensional visualization using *t*-distributed stochastic neighbor embedding (*t*-SNE) plots (RunTSNE function, the default setting). Cell clusters were annotated and identified to known cell types using specific marker genes identified using the Seurat "FindAllMarkers" function with the default setting (26).

## Marker Gene and Cell-Type Identification

Cluster-specific genes were acquired using the Seurat native FindMarkers function with a log-fold change threshold of 0.25. Receiver operating characteristic (ROC) analysis was used to identify cell markers. To further characterize these cell types in each cluster, we used the automated annotation tool SingleR (27) and manually checked using known cell surface markers based on related references.

## Identification of Differential Gene Expression and Cell Function in Different Samples

Differential expression analysis was performed after normalization and removal of the batch effects of total genes from the specific cluster from different samples. The function of *FindAllMarkers* wrapped in the R package of Seurat was used to identify differentially expressed genes for each of cell clusters compared to others. Then, the functions of *FindIntegrationAnchors* and *IntegrateData* wrapped in the R package of Seurat were employed to remove the batch effect referred to the standard procedure. We detected differentially expressed genes (DEGs) with a false discovery rate (FDR) <10e-6 and abs (log2 ratio) >2. Gene Ontology (GO) and Kyoto Encyclopedia of Genes and Genomes (KEGG) pathway analyses were performed to investigate the cell functional status. DEGs and molecular regulators in the clusters were investigated using GO and KEGG pathway analyses, respectively. GO and KEGG terms with an FDR <0.05 were considered significantly enriched (28).

# RESULTS

## Single-Cell Profiling of Cervical Cancer and Chronic Cervicitis Tissues

The single-cell atlas of the cervical tissues was characterized using five biopsy samples comprising three cervical squamous cell carcinomas (CQ), one cervical adenocarcinoma (CA), and one chronic cervicitis (CE). Two of the CQ patients were chemoresistant, one was chemosensitive, and three were infected with human papillomavirus. Each sample was processed to isolate single cells without prior selection of cell types, and then we performed scRNA-seq using a 10× Genomics Chromium platform to generate RNA-seq data. After quality filtering, 24,371 high-quality cells from five cervical biopsy samples with a median of 1,303–2,214 genes per cell were analyzed (**Figure 2**). Subsequently, the cells were further identified to be nine separate cell types, including fibroblast cells (34.17%), epithelial cells (24.07%), smooth muscle cells (4.3%), ECs (4.26%), and immune cells (33.2%).

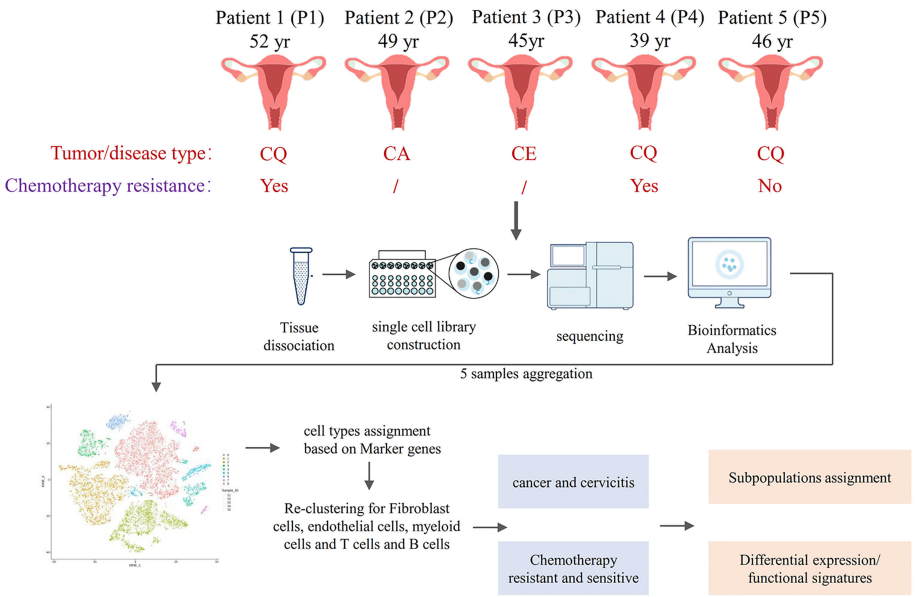


**FIGURE 2** | Overview of single-cell RNA sequencing (scRNA-seq) using cervical cancer and cervicitis biopsy samples.

The main cell types were identified based on gene expression patterns obtained using dimensionality reduction and unsupervised cell clustering with the described Seurat pipeline. Based on the marker genes of each cell cluster, nine distinct cell clusters were assigned to known cell lineages, which mainly comprised immune and non-immune cells (**Figure 3A**). The *t*-SNE plot also showed distinct clustering according to the tumor origin (**Figure 3B**). The heatmap showed differentially expressed marker genes in nine clusters (**Figure 3C**).

The proportions and composition of cell types varied among the different samples. The CA samples clustered with CE samples and mainly comprised fibroblast cells, accounting for 84.7% and 63.4% of the total cells. In contrast, the corresponding CQ werepredominantly epithelial and immune cells with almost no fibroblasts and ECs. Immune cells mainly consisted of B cells [CD20 (MS4A1) and CD79A] (26, 29, 30), myeloid cells (IL1B) (29), T cells (CD3D, CD2) (29–31), and mast cells (MS4A2) (29). The non-immunecell lineages comprised fibroblasts (DCN, LUM, and COL1A2) (26, 32, 33), epithelial cells (KRT, SLPI, and SFN) (32, 34), smooth muscle cells (MYL9, CALD1, and RGS5) (35, 36), andECs [VMF, ENG, and fms-related receptor tyrosine kinase 1 (FLT1)] (26) (**Figures 3D–F**).

## Reclustering and Differential Gene Profiles of Fibroblast and ECs in Cervicitis and Cervical Cancer Samples

We detected 8,329 fibroblast cells among the five samples and most were found in the CA and the CE samples, which accounted for 95.1% of the total fibroblast cells of the five samples (**Figure 4A**). To gain a better understanding of these cell types, we performed a reclustering of 8,329 fibroblasts and 1,037 ECs and assigned each of these subclusters based on known cell markers.

In our study, five distinct subtypes of fibroblast cells were identified. Cluster 0 (C0), C1, and C3 contained cells from all samples, but C2 and C4 were strongly enriched in the CA sample (**Figure 4B**). C0 and C3 were similar, corresponding to cells expressing extracellular matrix (ECM) molecules, such as collagen type III alpha 1 chain (COL3A1), COL6A3, and COL1A1, and these cells represent a population of collagen-generating fibroblasts. C1 demonstrated differential activation of FOS, heat shock protein 90 (HSP90s), and ETS-related gene-1 (ERG1).

Cells in C2 exhibited differentially elevated expression of genes involved in translation initiation [ribosomal protein L10 (RPL10) and RPS3] (37) and iron metabolism regulation [ferritin light chains (FTLs)] (38). The final subpopulation C4 was speculated to be a group of proliferative fibroblast cells, which has not been previously recognized, based on the expression of a relatively high level of proliferative genes such as the *S100* (*s100B*) and *CDH19* genes (18, 39) (**Figure 4C**).

To better understand the differential gene expression profiles between cervicitis and cervical cancer samples, bulk differential gene expression analysis was performed for cervical cancer and cervicitis samples. The two-tailed Wilcoxon rank-sum test, which is implemented in R, was used to conduct the bulk differential gene expression analysis. The volcano map (**Figure 4D**) and the heat map (**Figure 4E**) showed significant diversity in the expressed genes across the two samples.. For example, wnt2, a member of the WNT gene family, is highly expressed in cervical cancer samples, and WNT signaling is normally involved in the development and progression of various cancers.

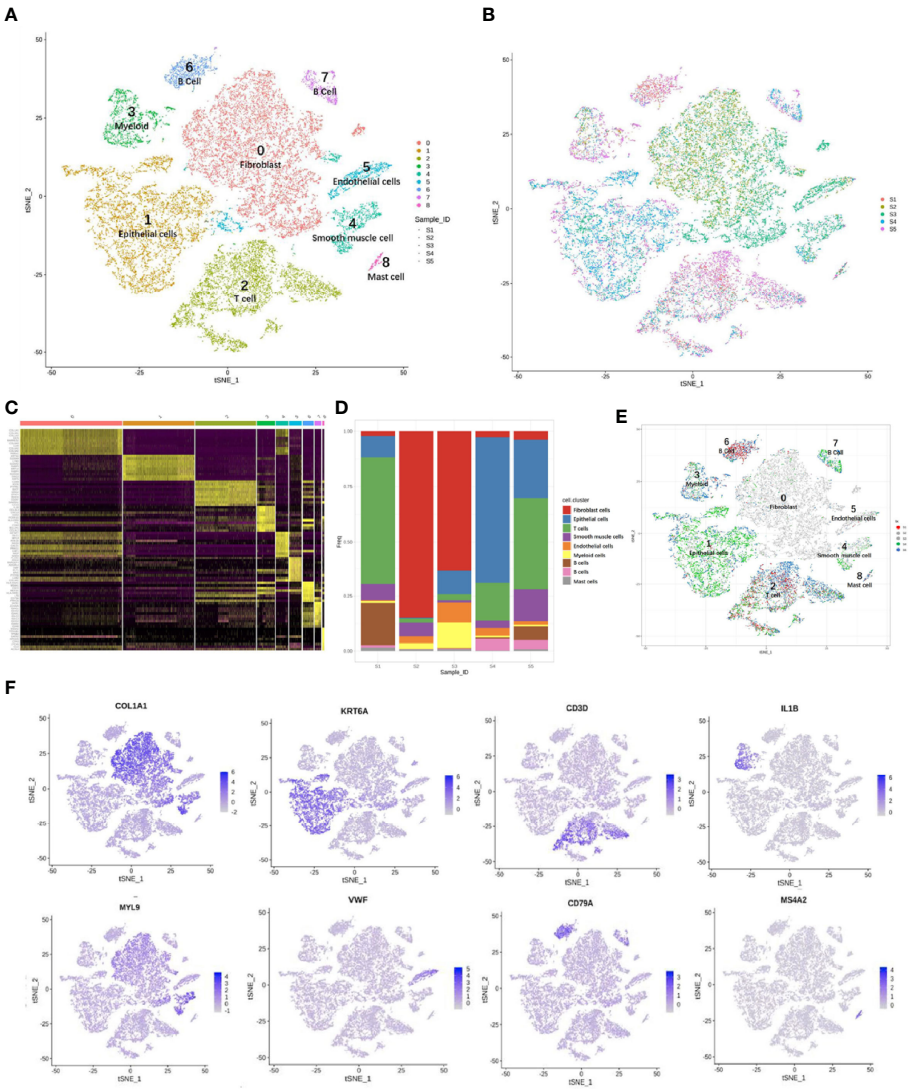


**FIGURE 3** | Overview of 24,371 cells from five cervical cancer tissues. *t*-Distributed stochastic neighbor embedding (*t*-SNE) plots displaying 24,371 cell profiles with each cell color-coded for **(A)** associated cell type and **(B)** its sample origin. **(C)** Heatmap shows differentially expressed marker genes (rows) in nine clusters. Yellow and dark purple: high and low expression, respectively. **(D)** Proportions of cells in each sample. **(E)** *t*-SNE plots displaying 24,371 cell profiles with color-coded sample origins. Samples 2 and 3 are gray. **(F)** *t*-SNE plot color-coded for marker gene expression (gray to white to blue) for *COL1A2* (cluster 0, C0), *KRT6A* (C1), *CD3D* (C2), *IL1B* (C3), *MYL9* (C4), *VWF* (C5), *CD79A* (C6 and C7), and *MS4A2* (C8).

We also found that the extracellular sulfatase, SULT2, was highly expressed in the cancer samples, which is consistent with the findings of other studies (40). Upregulation of *SULF2* gene expression is associated with proliferation, invasion, and migration of cervical cancer cells by its regulation of the extracellular signal-related kinase (ERK)/AKT signaling pathway (41). The ECM is important in tumor genesis and progression and fibroblast-activating protein (FAP), which plays a crucial role in ECM production and remodeling genes and is highly upregulated in tumor fibroblast cells (42).

C4 mainly contained proliferative fibroblast cells, which were mostly from the CA sample. Furthermore, we studied the gene profiles and performed functional enrichment, which demonstrated that several crucial genes were upregulated or downregulated in this cluster. The functional enrichment analysis results indicated that C4 was enriched in cell adhesion molecule binding and collagen-binding growth factor binding in molecular functions (**Figure 4F**).

As shown in **Figures 5A–C**, the 1,037 ECs were clustered in two separate subclusters. C0 corresponded to tumor-associated [heparan sulfate proteoglycan 2 (HPSG2) and plasmalemmal vesicle-associated protein (PLVAP)] and C1 ECs were blood ECs (FLT). Cells from sample 2 were spread in C0 but not in C1. PLVAP is located in the fenestral diaphragm and is considered to play a role in the passage of proteins through the fenestrae (43, 44). The generation of *Plvap*-deficient mice has highlighted the

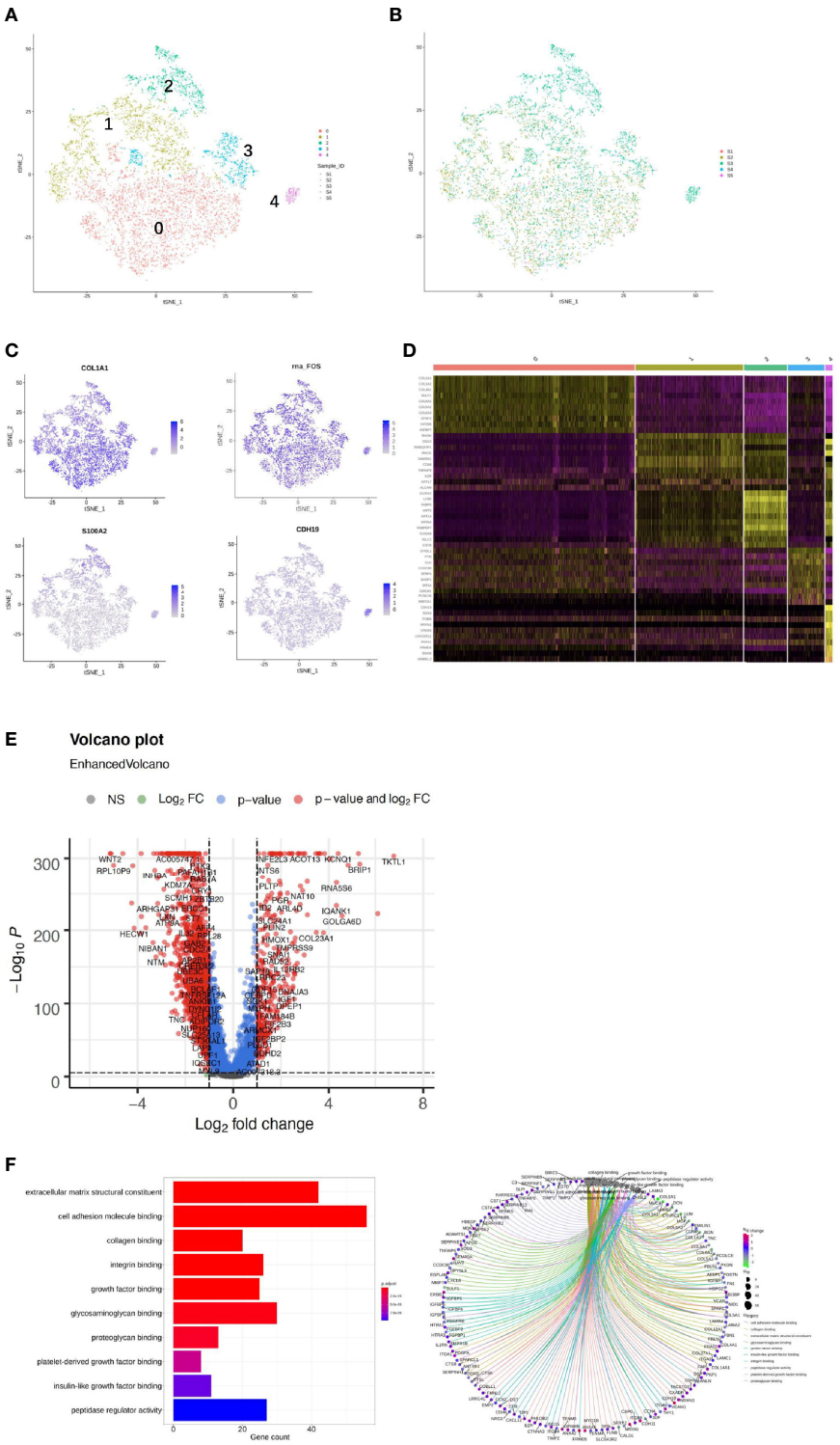


**FIGURE 4** | Single-cell RNA sequencing (scRNA) profiles of fibroblast cell lineages. Reclustering of 8,329 fibroblast cells color-coded by **(A)** clusters and **(B)** sample origin (right). **(C)** *t*-Distributed stochastic neighbor embedding (*t*-SNE) plot color-coded for marker gene expression (gray to white to blue) for *COLIAI*, *FOS*, *S100A2*, and *CDH19*. **(D)** Heatmap shows differentially expressed marker genes (rows) in five clusters. Yellow and dark purple: high and low expression, respectively. **(E)** Volcano plot shows differentially expressed marker genes between cervicitis and cervical cancer samples. **(F)** Differences in pathway activities of cells between cluster 1 (C1), C2, C3, and C4.

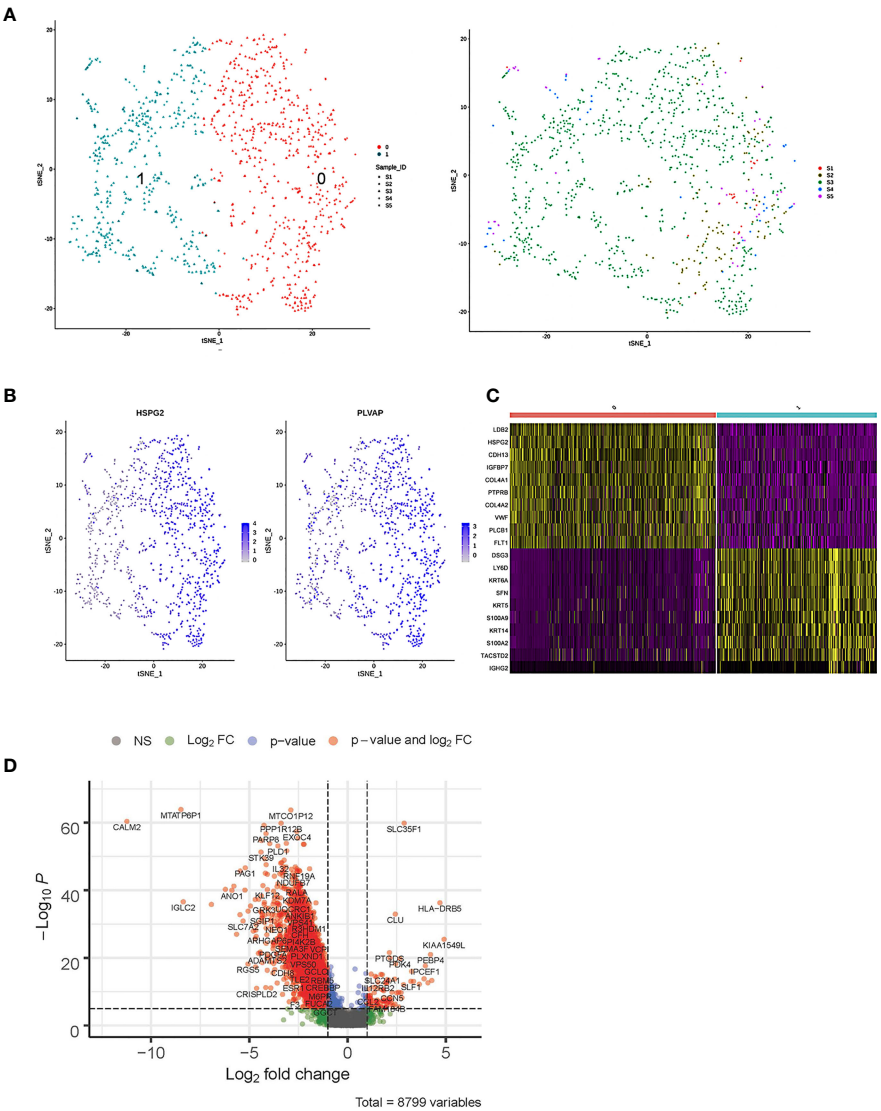


**FIGURE 5** | Single-cell RNA sequencing (scRNA) profiles of endothelial cell (EC) lineages. **(A)** Reclustering of 1,037 fibroblast cells, color-coded by clusters (left) or sample origin (right). **(B)** *t*-Distributed stochastic neighbor embedding (*t*-SNE) plot color-coded for marker gene expression (gray to white to blue) of *HPSG2* and *PLVAP*. **(C)** Heatmap shows differentially expressed marker genes (rows) in two clusters. Yellow and dark purple: high and low expression, respectively. **(D)** Volcano plot shows differentially expressed marker genes between cervicitis and cervical cancer samples.

structural role of PLVAP in the maintenance of size-selective permeability in fenestrated endothelia (45, 46). Moreover, *Plvap*-deficient mice that survived postnatally showed growth retardation (46).

The bulk differential gene expression analysis between cervicitis and cervical cancer samples showed that several cancer marker genes, which have been reported in various malignant tumors responsible for angiogenesis, metastasis, and invasion, were significantly elevated in cancer ECs (**Figure 5D**). For example, we detected elevated levels of phospholipase D1 (PLD1), a key enzyme involved in lipid metabolism, indicating that abnormal lipid metabolism might be involved in the tumorigenesis and progression of cervical cancer (47, 48).

## Acquired Resistance Was Associated With Differential Immune Cell Subpopulation Distribution and mRNA Expression

Both adaptive immune cells (T and B lymphocytes) and innate immune cells (such as macrophages, mast cells, neutrophils, dendritic cells, and natural killer cells) have critical roles in the TME and are considered to interact with tumor cells by direct contact or through different chemokine and cytokine signaling pathways that regulate the response of tumors to therapy. To explore the diversity of immune cells in cervical cancer, we extracted 4,961 T cells, 1,480 B cells, and 1,476 myeloid cells from three individual CQ patients and reclustered them (**Figures 6**, **7**). Furthermore, the main T-cell clusters could be

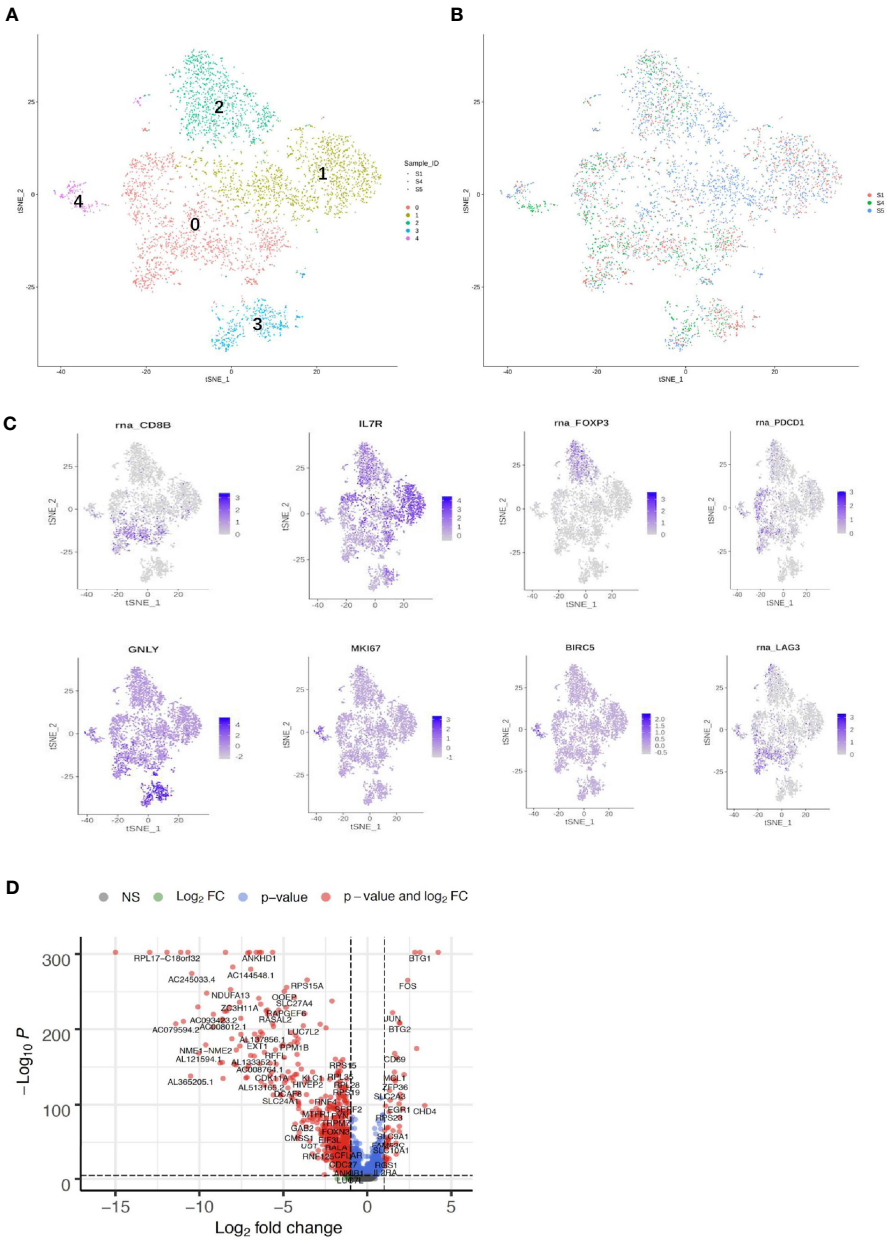


**FIGURE 6** | Single-cell RNA sequencing (scRNA) profiles of T-cell lineages. Reclustering of 4,961 T cells color-coded by **(A)** clusters and **(B)** sample origin (right). **(C)** *t*-Distributed stochastic neighbor embedding (*t*-SNE) plot color-coded for marker gene expression (gray to white to blue) for *CD8*+ (cluster 0, C0), *CD4*+ (C1), *IL2A* (C2), *GNLY* (C3), *MKI167*, and *BIRC2* (C4). **(D)** Volcano plot shows differentially expressed marker genes (rows) between chemoresistant patients and chemosensitive samples.

classified into five subpopulations designated as T0–T4, which were cytotoxic CD8+ T cells (CD8A+ and CD8B), CD4+ T cells [CD4+ and interleukin 7R (IL7R)], regulatory T cells [IL2RA, forkhead box protein P3 (FOXP3), tumor necrosis factor receptor superfamily, member 4 (TNFRSF4)], natural killer cells [killer cell lectin-like receptor C1 (KLRC1), X-C motif chemokine ligand 1/2 (XCL1/2), and granulysin (GNLY)], and proliferating T cells [marker of proliferation Ki-67 (MKI67) and baculoviral IAP repeat containing 5 (BIRC5), **Figure 5A**] (26, 29). Cells from all clusters were detected in all patients. Cells from all five clusters were detected in both chemoresistant and chemosensitive patients, except for C1, which was predominantly derived from chemoresistant patients. It is worth noting that there were high levels of immune checkpoint molecules, including approved target programmed cell death 1 (PDCD1) and other targets that are currently undergoing clinical

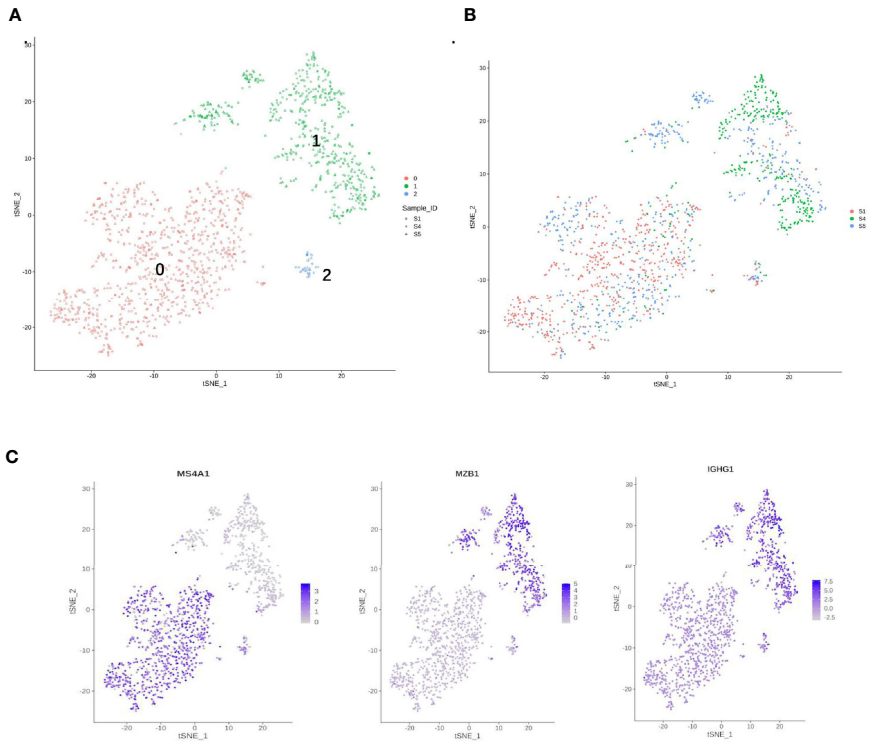


**FIGURE 7** | Single-cell RNA sequencing (scRNA) profiles for B-cell lineages. **(A)** Reclustering of 1,480 B cells, color-coded by their cluster. **(B)** Its sample origin. **(C)** *t*-SNE plot color-coded for marker gene expression (gray to white to blue) for MS4A1 (cluster 0), MZB1, and IGHG1 (cluster 1).

trials [lymphocyte activating 3 (LAG3) and hepatitis A virus cellular receptor 2/T-cell immunoglobulin and mucin domain-3 (HAVCR2/TIM3)] (49), indicating that the cytotoxic activities of CD8+ are significantly curtailed by high-level expression of the checkpoint gene. The robust CD8+ response was confirmed to play a critical role in a mammary tumor model treated with a HER2 inhibitor (50). Additionally, the average expression of the proliferating cancer marker genes, *MKI167* and *BIRC5*, was significantly enriched in C4 (**Figure 6D**). These two cancer marker genes, *MKI167* and *BIRC5*, have been reported to be highly expressed in cervical cancer in many studies, where they are associated with the cell cycle pathway and cell apoptosis inhibition, respectively, and are both involved in breast cancer pathogenesis (51–53).

B cells (1,480) were detected and reclustering from C6 and C7 revealed three subclusters, and cell type assignments were performed based on known marker genes. C0 corresponded to follicular B cells based on marker MS4A1, whereas C1 corresponded to plasma B cells based on MZB1, CD38, and IGHG1 (**Figures 7A, C**) (29, 54). C2 contained lower quality B cells and showed no B-cell markers; thus, it was not further analyzed. One sample was mostly from patient 4, and two others were mostly from patients 1 and 5. The *t*-SNE profile failed to show the separation of subclusters between chemoresistant and chemosensitive patients, indicating that the B-cell subpopulation was not strongly affected by drug resistance.

## DEG Pathways Between Chemoresistant and Chemosensitive Patients

To investigate the enriched functions of DEGs between chemoresistant and chemosensitive samples, signaling pathway analysis was performed among subpopulations of epithelial, T, and B cells. In total, 3,157, 1,399, and 1,141 DEGs were annotated into 327, 312, and 312 pathways for epithelial, T, and B cells, respectively, in the KEGG database (**Tables S2**–**S4**). The top 25 annotation results, which were classified according to the pathway types, are shown in **Figure 8**. Several signaling pathways that are closely correlated with chemotherapy were enriched in all three subpopulations, including the PI3K/AKT and mitogen-activated protein kinase (MAPK) signaling pathways. The PI3K/AKT signaling pathway is involved in tumor development, progression, cellular survival, and apoptosis, and its correlation with chemoresistance has been presented in numerous studies (55–57) and cervical cancer (12). Another chemotherapy resistance-associated pathway, the MAPK signaling pathway, was significantly enriched and upregulated in chemoresistant patients and is responsible for the regulation of cell migration, survival, proliferation, and progression (58). Activation of survival pathways involving PI3K/Akt and MAPK caused by integrins and soluble factors secreted in the TME results in elevated expression of anti-apoptotic proteins, leading to cell viability and drug resistance (7).

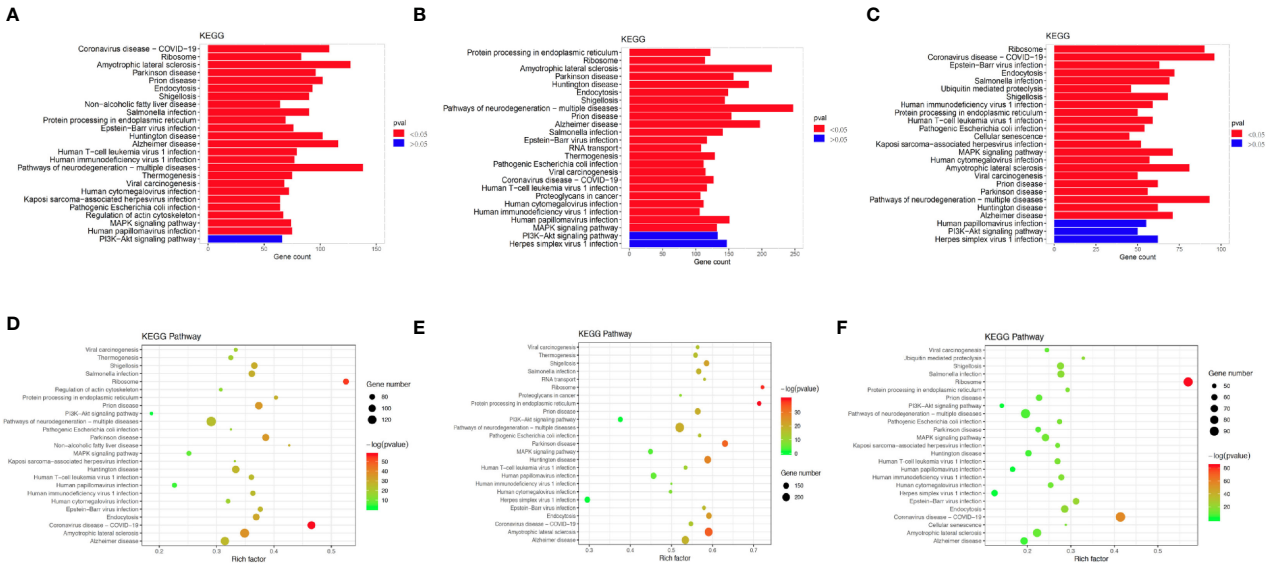


**FIGURE 8** | Differences in pathway activities scored using Kyoto Encyclopedia of Genes and Genomes (KEGG) database between chemoresistant and chemosensitive samples. Top 25 differentially expressed genes (DEGs) enriched KEGG functional annotation on **(A)** epithelial, **(B)** T, and **(C)** B cells. The *x*-axis indicates the number of genes annotated to pathway and proportion of all DGEs, and the *y*-axis shows KEGG metabolic pathway. Red bar ($p < 0.05$). Scatter plot of the top 25 DEGs enriched in the KEGG pathway on **(D)** epithelial, **(E)** T, and **(F)** B cells. Each circle indicates a KEGG pathway. Ordinate is log10 (*Q* value), color-coded from green to orange to red. Circle sizes indicate enrichment level of DEGs in pathway. *Q* value: *p*-value after multiple hypothesis tests.

## DISCUSSION

Advanced scRNA-seq technology has allowed the comprehensive investigation of tumor heterogeneity gene expression differences with single-cell resolution. Although scRNA-seq profiles of other gynecological cancers, including breast and ovarian cancers, have been extensively studied (18, 34, 59), profiles of the microenvironment of cervical cancer, particularly with respect to chemotherapy resistance, have not been demonstrated. To the best of our knowledge, this is one of the first few studies to comprehensively characterize a single-cell atlas of cervical cancer patients in China and worldwide (60).

Here, we present a comprehensive catalog of cell types and subtypes, including fibroblast, endothelial, and immune cells in CQ, adenocarcinoma, and non-tumorous CE biopsy samples at single-cell resolution. In this study, we isolated 24,371 cells from five cervical biopsy samples and identified nine separate cell types, including fibroblast, epithelial, smooth muscle, and immune cells as well as ECs. Then, we subclustered the main cell types into different subpopulations based on the expression of the marker gene. We then studied pathway signatures and activities of distinct subpopulations that represent different biological and molecular entities between cervical cancer and cervicitis samples, and assessed the differential gene expression and signaling pathways between chemoresistant and chemosensitive cervical cancer patients.

Fibroblasts are considered a heterogeneous population in many cancers, but the extent of heterogeneity remains unclear, especially in cervical cancer because they are difficult to culture and highly dependent on context (26). Furthermore, fibroblasts are a large source of growth factors and cytokines, including stromal cell-derived factor 1 (SDF1), hepatocyte growth factor (HGF), and vascular endothelial growth factor (VEGF), which all promote tumor growth and contribute to chemotherapy resistance (61–63). Although most clusters were composed of cells originating from different samples, the fibroblast cells and ECs were observably enriched in CA and CE patients.

The significant shift might have occurred because the condition of the patients who provided the cervical squamous cell carcinoma samples was likely more serious, which would result in the recruitment of more immune cells to exert their antitumor function. In addition, upregulated expression of WNT2 in tumor fibroblast cells, which was observed in this study, could also result in tumor growth and promotion of invasion by activating the canonical WNT/β-catenin signaling pathway (64, 65). A previous study also revealed that downregulating WNT2 significantly suppressed cell motility and invasion and reversed epithelial–mesenchymal transition (EMT) progression in cervical cancer (66).

By comparing the differential gene expression in fibroblasts and ECs between cervical cancer and cervicitis patients, we found that several cancer marker genes, which have been reported in various malignant tumors responsible for angiogenesis, metastasis, and invasion, *via* various metabolic pathways related to cervical cancer, were significantly elevated in cancer ECs. For instance, genes involved in translation initiation such as *RPL10* and *RPS3* (37) and iron metabolism regulation such as *FTLs* (38), which have been reported to be involved in increased cell viability, migration, and invasion in different cancers, were elevated in the identified C2. This observation indicates that

these cells are highly active and associated with tumorigenesis. In addition, the differential activation of FOS, HSP90s, and ERG1 exhibited by the cells in C1 indicated a strong correlation with myogenesis and fibrosis (37, 67).

Tumor cells have been reported to trigger the immunosuppressive activities of tumor-associated ECs that influence therapeutic responses (68). ECs selectively permit transmigration of immunosuppressive myeloid cells from the blood to the tumor, thereby impairing antitumor immune responses (69). Moreover, ECs involved in the TME may also suppress T-cell function through the expression of different inhibitory molecules, such as programmed cell death ligand 1 (PDL1) and PDL2 (70).

Checkpoint immunotherapy is rarely used in cervical cancer, and there is a poor understanding of the outcome of immunotherapy. The results of this study were consistent with this phenomenon, and we found that the immune checkpoint molecules, PDCD1, LAG3, and HAVCR2, were highly expressed in CD8+ cells. This observation indicates that cytotoxicity was inhibited by high checkpoint expression (54) and that immunotherapy could also be useful in cervical cancer by targeting these pathways. This result is in agreement with the good clinical results observed in immunotherapy of cervical cancer (71).

The results of the analysis of differentially enriched signaling pathways did not show significant differences in chemoresistant patients. However, the PI3K/AKT pathway enriched most DEGs, which suggests that the activation state of this common pathway, which is involved in tumor development, progression, and apoptosis, might contribute to the development of resistance to chemotherapy in cervical cancer patients. Inhibition of certain components of the PI3K/AKT and MAPK pathways not only enhances chemotherapy efficacy in cervical cancer, but also has the potential to overcome resistance (72, 73).

There are some limitations to our study that need to be addressed in future studies. First, because sample collection was challenging, the number of samples in this study was relatively small, especially the chemoresistant and chemosensitive samples, which indicates that our observations cannot reflect the comprehensive profiles of the TME and generalize the gene expression differences in cervical cancer and its chemoresistant features.

## CONCLUSION

In conclusion, we comprehensively described the profiles of immune and non-immune cells in cervical cancer and cervicitis samples at single-cell resolution. Furthermore, we compared the distinctive features of signaling pathways among subpopulations from chemoresistant and chemosensitive samples in this study. Our results of the analysis of extensive bioinformatics data demonstrated the scope and potential impact of heterogeneity and suggest that single-cell profiling could identify and characterize clinically important subpopulations to develop successful targeted treatments. Our findings also indicated the need for comprehensive single-cell gene profiling and characterization of heterogeneous tumors such as chemoresistant cervical cancer. Finally, by assessing the cell subpopulations, differential gene expression between chemoresistant and chemosensitive samples, and distinct signaling pathways, we expect that our findings will provide novel and deeper insights into human cervical cancer and facilitate the advancement of its diagnosis and treatment.

## DATA AVAILABILITY STATEMENT

The original contributions presented in the study are included in the article/**Supplementary Material**. Further inquiries can be directed to the corresponding authors.

## ETHICS STATEMENT

The studies involving human participants were reviewed and approved by the Institutional Review Board of Renmin Hospital of Wuhan University (Institutional Review Board no. WDRY2021-K014). The patients/participants provided their written informed consent to participate in this study.

## AUTHOR CONTRIBUTIONS

Conceived and designed the experiments: CS, XL, and MG. Acquired the data: MG, TH, YY, and SD. Analyzed and interpreted the data: MG, TH, and YY. Drafted the manuscript: MG and TH. Obtained funding: CS. Supervised the study: CS and XL. All authors contributed to the article and approved the submitted version.

## FUNDING

This work was made possible by the financial support of the National Science and Technology Infrastructure Grant (NSTI-CR14-19) to CS.

## ACKNOWLEDGMENTS

We would like to thank Professor Congyi Zheng for his helpful suggestions regarding sample sources. We also thank all the individuals who participated in this study and donated samples.

## SUPPLEMENTARY MATERIAL

The Supplementary Material for this article can be found online at: https://www.frontiersin.org/articles/10.3389/fonc.2021.753386/full#supplementary-material

## REFERENCES


1. Arbyn M, Weiderpass E, Bruni L, de Sanjose S, Saraiya M, Ferlay J, et al. Estimates of Incidence and Mortality of Cervical Cancer in 2018: A Worldwide Analysis. *Lancet Glob Health* (2020) 8(2):e191–203. doi: 10.1016/S2214-109X(19)30482-6
2. Rosen VM, Guerra I, McCormack M, Nogueira-Rodrigues A, Sasse A, Munk VC, et al. Systematic Review and Network Meta-Analysis of Bevacizumab Plus First-Line Topotecan-Paclitaxel or Cisplatin-Paclitaxel Versus Non-Bevacizumab-Containing Therapies in Persistent, Recurrent, or Metastatic Cervical Cancer. *Int J Gynecol Cancer* (2017) 27(6):1237–46. doi: 10.1097/IGC.0000000000001000
3. Kitagawa R, Katsumata N, Shibata T, Kamura T, Kasamatsu T, Nakanishi T, et al. Paclitaxel Plus Carboplatin Versus Paclitaxel Plus Cisplatin in Metastatic or Recurrent Cervical Cancer: The Open-Label Randomized Phase III Trial Jcog0505. *J Clin Oncol* (2015) 33(19):2129–35. doi: 10.1200/JCO.2014.58.4391
4. Markman M. Advances in Cervical Cancer Pharmacotherapies. *Expert Rev Clin Pharmacol* (2014) 7(2):219–23. doi: 10.1586/17512433.2014.884924
5. Quail DF, Joyce JA. Microenvironmental Regulation of Tumor Progression and Metastasis. *Nat Med* (2013) 19(11):1423–37. doi: 10.1038/nm.3394
6. Hanahan D, Coussens LM. Accessories to the Crime: Functions of Cells Recruited to the Tumor Microenvironment. *Cancer Cell* (2012) 21(3):309–22. doi: 10.1016/j.ccr.2012.02.022
7. Wu T, Dai Y. Tumor Microenvironment and Therapeutic Response. *Cancer Lett* (2017) 387:61–8. doi: 10.1016/j.canlet.2016.01.043
8. Gottesman MM, Ludwig J, Xia D, Szakacs G. Defeating Drug Resistance in Cancer. *Discovery Med* (2006) 6(31):18–23.
9. Cadron I, Van Gorp T, Amant F, Leunen K, Neven P, Vergote I. Chemotherapy for Recurrent Cervical Cancer. *Gynecol Oncol* (2007) 107 (1 Suppl 1):S113–8. doi: 10.1016/j.ygyno.2007.07.004
10. Siddik ZH. Cisplatin: Mode of Cytotoxic Action and Molecular Basis of Resistance. *Oncogene* (2003) 22(47):7265–79. doi: 10.1038/sj.onc.1206933
11. Rhodes DR, Chinnaiyan AM. Integrative Analysis of the Cancer Transcriptome. *Nat Genet* (2005) 37(Suppl):S31–7. doi: 10.1038/ng1570
12. Wang Y, Liu L, Chen Z. Transcriptome Profiling of Cervical Cancer Cells Acquired Resistance to Cisplatin by Deep Sequencing. *Artif Cells Nanomed Biotechnol* (2019) 47(1):2820–9. doi: 10.1080/21691401.2019.1637882
13. Fan Z, Cui H, Yu H, Ji Q, Kang L, Han B, et al. MiR-125a Promotes Paclitaxel Sensitivity in Cervical Cancer Through Altering STAT3 Expression. *Oncogenesis* (2016) 5:e223. doi: 10.1038/oncsis.2016.21
14. Guo X, Zhang Y, Zheng L, Zheng C, Song J, Zhang Q, et al. Global Characterization of T Cells in Non-Small-Cell Lung Cancer by Single-Cell Sequencing. *Nat Med* (2018) 24(7):978–85. doi: 10.1038/s41591-018-0045-3
15. Gladka MM, Molenaar B, de Ruiter H, van der Elst S, Tsui H, Versteeg D, et al. Single-Cell Sequencing of the Healthy and Diseased Heart Reveals Cytoskeleton-Associated Protein 4 as a New Modulator of Fibroblasts Activation. *Circulation* (2018) 138(2):166–80. doi: 10.1161/CIRCULATIONAHA.117.030742
16. Ofengeim D, Giagtzoglou N, Huh D, Zou C, Yuan J. Single-Cell RNA Sequencing: Unraveling the Brain One Cell at a Time. *Trends Mol Med* (2017) 23(6):563–76. doi: 10.1016/j.molmed.2017.04.006
17. Fattore L, Ruggiero CF, Liguoro D, Mancini R, Ciliberto G. Single Cell Analysis to Dissect Molecular Heterogeneity and Disease Evolution in Metastatic Melanoma. *Cell Death Dis* (2019) 10(11):827. doi: 10.1038/s41419-019-2048-5
18. Shih AJ, Menzin A, Whyte J, Lovecchio J, Liew A, Khalili H, et al. Identification of Grade and Origin Specific Cell Populations in Serous Epithelial Ovarian Cancer by Single Cell RNA-Seq. *PloS One* (2018) 13(11): e0206785. doi: 10.1371/journal.pone.0208778
19. Bian S, Hou Y, Zhou X, Li X, Yong J, Wang Y, et al. Single-Cell Multiomics Sequencing and Analyses of Human Colorectal Cancer. *Science* (2018) 362 (6418):1060–3. doi: 10.1126/science.aao3791
20. Xu J, Liao K, Yang X, Wu C, Wu W, Han S. Using Single-Cell Sequencing Technology to Detect Circulating Tumor Cells in Solid Tumors. *Mol Cancer* (2021) 20(1):104. doi: 10.1186/s12943-021-01392-w
21. Xu Y, Su GH, Ma D, Xiao Y, Shao ZM, Jiang YZ. Technological Advances in Cancer Immunity: From Immunogenomics to Single-Cell Analysis and Artificial Intelligence. *Signal Transduct Target Ther* (2021) 6(1):312. doi: 10.1038/s41392-021-00729-7
22. Devitt K, Hanson SJ, Tuong ZK, McMeniman E, Soyer HP, Frazer IH, et al. Single-Cell RNA Sequencing Reveals Cell Type-Specific HPV Expression in Hyperplastic Skin Lesions. *Virology* (2019) 537:14–9. doi: 10.1016/j.virol.2019.08.007
23. Xie T, Wang Y, Deng N, Huang G, Taghavifar F, Geng Y, et al. Single-Cell Deconvolution of Fibroblast Heterogeneity in Mouse Pulmonary Fibrosis. *Cell Rep* (2018) 22(13):3625–40. doi: 10.1016/j.celrep.2018.03.010
24. Januszyk M, Chen K, Henn D, Foster DS, Borrelli MR, Bonham CA, et al. Characterization of Diabetic and Non-Diabetic Foot Ulcers Using Single-Cell RNA-Sequencing. *Micromachines (Basel)* (2020) 11(9):815–30. doi: 10.3390/mi11090815
25. Macosko EZ, Basu A, Satija R, Nemesh J, Shekhar K, Goldman M, et al. Highly Parallel Genome-Wide Expression Profiling of Individual Cells Using Nanoliter Droplets. *Cell* (2015) 161(5):1202–14. doi: 10.1016/j.cell.2015.05.002
26. Lambrechts D, Wauters E, Boeckx B, Aibar S, Nittner D, Burton O, et al. Phenotype Molding of Stromal Cells in the Lung Tumor Microenvironment. *Nat Med* (2018) 24(8):1277–89. doi: 10.1038/s41591-018-0096-5
27. Aran D, Looney AP, Liu L, Wu E, Fong V, Hsu A, et al. Reference-Based Analysis of Lung Single-Cell Sequencing Reveals a Transitional Profibrotic Macrophage. *Nat Immunol* (2019) 20(2):163–72. doi: 10.1038/s41590-018-0276-y
28. Chen EY, Tan CM, Kou Y, Duan Q, Wang Z, Meirelles GV, et al. Enrichr: Interactive and Collaborative HTML5 Gene List Enrichment Analysis Tool. *BMC Bioinf* (2013) 14:128. doi: 10.1186/1471-2105-14-128
29. Cai Y, Dai Y, Wang Y, Yang Q, Guo J, Wei C, et al. Single-Cell Transcriptomics of Blood Reveals a Natural Killer Cell Subset Depletion in Tuberculosis. *EBioMedicine* (2020) 53:102686. doi: 10.1016/j.ebiom.2020.102686
30. Zhao J, Guo C, Xiong F, Yu J, Ge J, Wang H, et al. Single Cell RNA-Seq Reveals the Landscape of Tumor and Infiltrating Immune Cells in Nasopharyngeal Carcinoma. *Cancer Lett* (2020) 477:131–43. doi: 10.1016/j.canlet.2020.02.010
31. Chen YP, Yin JH, Li WF, Li HJ, Chen DP, Zhang CJ, et al. Single-Cell Transcriptomics Reveals Regulators Underlying Immune Cell Diversity and Immune Subtypes Associated With Prognosis in Nasopharyngeal Carcinoma. *Cell Res* (2020) 30(11):1024–42. doi: 10.1038/s41422-020-0374-x
32. McCray T, Moline D, Baumann B, Vander Griend DJ, Nonn L. Single-Cell RNA-Seq Analysis Identifies a Putative Epithelial Stem Cell Population in Human Primary Prostate Cells in Monolayer and Organoid Culture Conditions. *Am J Clin Exp Urol* (2019) 7(3):123–38.
33. He H, Suryawanshi H, Morozov P, Gay-Mimbrera J, Del Duca E, Kim HJ, et al. Single-Cell Transcriptome Analysis of Human Skin Identifies Novel Fibroblast Subpopulation and Enrichment of Immune Subsets in Atopic Dermatitis. *J Allergy Clin Immunol* (2020) 145(6):1615–28. doi: 10.1016/j.jaci.2020.01.042
34. Nguyen QH, Pervolarakis N, Blake K, Ma D, Davis RT, James N, et al. Profiling Human Breast Epithelial Cells Using Single Cell RNA Sequencing Identifies Cell Diversity. *Nat Commun* (2018) 9(1):2028. doi: 10.1038/s41467-018-04334-1
35. Muhl L, Genove G, Leptidis S, Liu J, He L, Mocci G, et al. Single-Cell Analysis Uncovers Fibroblast Heterogeneity and Criteria for Fibroblast and Mural Cell Identification and Discrimination. *Nat Commun* (2020) 11(1):3953. doi: 10.1038/s41467-020-18511-8
36. Liu X, Chen W, Li W, Li Y, Priest JR, Zhou B, et al. Single-Cell RNA-Seq of the Developing Cardiac Outflow Tract Reveals Convergent Development of the Vascular Smooth Muscle Cells. *Cell Rep* (2019) 28(5):1346–61.e4. doi: 10.1016/j.celrep.2019.06.092
37. Zhao Q, Eichten A, Parveen A, Adler C, Huang Y, Wang W, et al. Single-Cell Transcriptome Analyses Reveal Endothelial Cell Heterogeneity in Tumors and Changes Following Antiangiogenic Treatment. *Cancer Res* (2018) 78 (9):2370–82. doi: 10.1158/0008-5472.CAN-17-2728
38. Shi J, Zhang L, Zhou D, Zhang J, Lin Q, Guan W, et al. Biological Function of Ribosomal Protein L10 on Cell Behavior in Human Epithelial Ovarian Cancer. *J Cancer* (2018) 9(4):745–56. doi: 10.7150/jca.21614
39. Xu H, Zhong L, Deng J, Peng J, Dan H, Zeng X, et al. High Expression of ACE2 Receptor of 2019-Ncov on the Epithelial Cells of Oral Mucosa. *Int J Oral Sci* (2020) 12(1):8. doi: 10.1038/s41368-020-0074-x

40. Lindsay J, Wang LL, Li Y, Zhou SF. Structure, Function and Polymorphism of Human Cytosolic Sulfotransferases. *Curr Drug Metab* (2008) 9(2):99–105. doi: 10.2174/138920008783571819
41. Jiang T, Chen ZH, Chen Z, Tan D. SULF2 Promotes Tumorigenesis and Inhibits Apoptosis of Cervical Cancer Cells Through the ERK/AKT Signaling Pathway. *Braz J Med Biol Res* (2020) 53(2):e8901. doi: 10.1590/1414-431x20198901
42. Walker C, Mojares E, Del Rio Hernandez A. Role of Extracellular Matrix in Development and Cancer Progression. *Int J Mol Sci* (2018) 19(10):3028–59. doi: 10.3390/ijms19103028
43. Stan RV, Kubitza M, Palade GE. PV-1 Is a Component of the Fenestral and Stomatal Diaphragms in Fenestrated Endothelia. *Proc Natl Acad Sci USA* (1999) 96(23):13203–7. doi: 10.1073/pnas.96.23.13203
44. Hamilton BJ, Tse D, Stan RV. Phorbol Esters Induce PLVAP Expression *via* VEGF and Additional Secreted Molecules in MEK1-Dependent and P38, JNK and PI3K/Akt-Independent Manner. *J Cell Mol Med* (2019) 23(2):920–33. doi: 10.1111/jcmm.13993
45. Stan RV, Tse D, Deharvengt SJ, Smits NC, Xu Y, Luciano MR, et al. The Diaphragms of Fenestrated Endothelia: Gatekeepers of Vascular Permeability and Blood Composition. *Dev Cell* (2012) 23(6):1203–18. doi: 10.1016/j.devcel.2012.11.003
46. Herrnberger L, Seitz R, Kuespert S, Bosl MR, Fuchshofer R, Tamm ER. Lack of Endothelial Diaphragms in Fenestrae and Caveolae of Mutant Plvap-Deficient Mice. *Histochem Cell Biol* (2012) 138(5):709–24. doi: 10.1007/s00418-012-0987-3
47. Wang XX, Liao Y, Hong L, Zeng Z, Yuan TB, Xia X, et al. Tissue Microarray Staining Reveals PLD1 and Sp1 Have a Collaborative, Pro-Tumoral Effect in Patients With Osteosarcomas. *Oncotarget* (2017) 8(43):74340–7. doi: 10.18632/oncotarget.20605
48. Kolanjiappan K, Manoharan S, Kayalvizhi M. Measurement of Erythrocyte Lipids, Lipid Peroxidation, Antioxidants and Osmotic Fragility in Cervical Cancer Patients. *Clin Chim Acta* (2002) 326(1-2):143–9. doi: 10.1016/S0009-8981(02)00300-5
49. Pardoll DM. The Blockade of Immune Checkpoints in Cancer Immunotherapy. *Nat Rev Cancer* (2012) 12(4):252–64. doi: 10.1038/nrc3239
50. Hannesdottir L, Tymoszuk P, Parajuli N, Wasmer MH, Philipp S, Daschil N, et al. Lapatinib and Doxorubicin Enhance the Stat1-Dependent Antitumor Immune Response. *Eur J Immunol* (2013) 43(10):2718–29. doi: 10.1002/eji.201242505
51. Zhang P, Yang M, Zhang Y, Xiao S, Lai X, Tan A, et al. Dissecting the Single-Cell Transcriptome Network Underlying Gastric Premalignant Lesions and Early Gastric Cancer. *Cell Rep* (2020) 30(12):4317. doi: 10.1016/j.celrep.2020.03.020
52. Elango R, Alsaleh KA, Vishnubalaji R, Manikandan M, Ali AM, Abd El-Aziz N, et al. MicroRNA Expression Profiling on Paired Primary and Lymph Node Metastatic Breast Cancer Revealed Distinct microRNA Profile Associated With LNM. *Front Oncol* (2020) 10:756. doi: 10.3389/fonc.2020.00756
53. Dai JB, Zhu B, Lin WJ, Gao HY, Dai H, Zheng L, et al. Identification of Prognostic Significance of BIRC5 in Breast Cancer Using Integrative Bioinformatics Analysis. *Biosci Rep* (2020) 40(2):BSR20193678. doi: 10.1042/BSR20193678
54. Baker D, Marta M, Pryce G, Giovannoni G, Schmierer K. Memory B Cells Are Major Targets for Effective Immunotherapy in Relapsing Multiple Sclerosis. *EBioMedicine* (2017) 16:41–50. doi: 10.1016/j.ebiom.2017.01.042
55. LoPiccolo J, Blumenthal GM, Bernstein WB, Dennis PA. Targeting the PI3K/Akt/mTOR Pathway: Effective Combinations and Clinical Considerations. *Drug Resist Updat* (2008) 11(1-2):32–50. doi: 10.1016/j.drup.2007.11.003
56. Cassinelli G, Zuco V, Gatti L, Lanzi C, Zaffaroni N, Colombo D, et al. Targeting the Akt Kinase to Modulate Survival, Invasiveness and Drug Resistance of Cancer Cells. *Curr Med Chem* (2013) 20(15):1923–45. doi: 10.2174/09298673113209990106
57. Steelman LS, Navolanic P, Chappell WH, Abrams SL, Wong EW, Martelli AM, et al. Involvement of Akt and mTOR in Chemotherapeutic- and Hormonal-Based Drug Resistance and Response to Radiation in Breast Cancer Cells. *Cell Cycle* (2011) 10(17):3003–15. doi: 10.4161/cc.10.17.17119
58. Achkar IW, Abdulrahman N, Al-Sulaiti H, Joseph JM, Uddin S, Mraiche F. Cisplatin Based Therapy: The Role of the Mitogen Activated Protein Kinase Signaling Pathway. *J Transl Med* (2018) 16(1):96. doi: 10.1186/s12967-018-1471-1
59. Kawano M, Mabuchi S, Matsumoto Y, Sasano T, Takahashi R, Kuroda H, et al. The Significance of G-CSF Expression and Myeloid-Derived Suppressor Cells in the Chemoresistance of Uterine Cervical Cancer. *Sci Rep* (2015) 5:18217. doi: 10.1038/srep18217
60. Li C, Guo L, Li S, Hua K. Single-Cell Transcriptomics Reveals the Landscape of Intra-Tumoral Heterogeneity and Transcriptional Activities of ECs in CC. *Mol Ther Nucleic Acids* (2021) 24:682–94. doi: 10.1016/j.omtn.2021.03.017
61. Paraiso KH, Smalley KS. Fibroblast-Mediated Drug Resistance in Cancer. *Biochem Pharmacol* (2013) 85(8):1033–41. doi: 10.1016/j.bcp.2013.01.018
62. Erez N, Glanz S, Raz Y, Avivi C, Barshack I. Cancer Associated Fibroblasts Express Pro-Inflammatory Factors in Human Breast and Ovarian Tumors. *Biochem Biophys Res Commun* (2013) 437(3):397–402. doi: 10.1016/j.bbrc.2013.06.089
63. Fukumura D, Xavier R, Sugiura T, Chen Y, Park EC, Lu N, et al. Tumor Induction of VEGF Promoter Activity in Stromal Cells. *Cell* (1998) 94(6):715–25. doi: 10.1016/S0092-8674(00)81731-6
64. Logan CY, Nusse R. The Wnt Signaling Pathway in Development and Disease. *Annu Rev Cell Dev Biol* (2004) 20:781–810. doi: 10.1146/annurev.cellbio.20.010403.113126
65. Clevers H. Wnt/beta-Catenin Signaling in Development and Disease. *Cell* (2006) 127(3):469–80. doi: 10.1016/j.cell.2006.10.018
66. Zhou Y, Huang Y, Cao X, Xu J, Zhang L, Wang J, et al. WNT2 Promotes Cervical Carcinoma Metastasis and Induction of Epithelial-Mesenchymal Transition. *PloS One* (2016) 11(8):e0160414. doi: 10.1371/journal.pone.0160414
67. Sontake V, Wang Y, Kasam RK, Sinner D, Reddy GB, Naren AP, et al. Hsp90 Regulation of Fibroblast Activation in Pulmonary Fibrosis. *JCI Insight* (2017) 2(4):e91454. doi: 10.1172/jci.insight.91454
68. Turley SJ, Cremasco V, Astarita JL. Immunological Hallmarks of Stromal Cells in the Tumour Microenvironment. *Nat Rev Immunol* (2015) 15 (11):669–82. doi: 10.1038/nri3902
69. Talmadge JE, Gabrilovich DI. History of Myeloid-Derived Suppressor Cells. *Nat Rev Cancer* (2013) 13(10):739–52. doi: 10.1038/nrc3581
70. Rodig N, Ryan T, Allen JA, Pang H, Grabie N, Chernova T, et al. Endothelial Expression of PD-L1 and PD-L2 Down-Regulates CD8+ T Cell Activation and Cytolysis. *Eur J Immunol* (2003) 33(11):3117–26. doi: 10.1002/eji.200324270
71. Wendel Naumann R, Leath CA3rd. Advances in Immunotherapy for Cervical Cancer. *Curr Opin Oncol* (2020) 32(5):481–7. doi: 10.1097/CCO.0000000000000663
72. Kim D, Dan HC, Park S, Yang L, Liu Q, Kaneko S, et al. AKT/PKB Signaling Mechanisms in Cancer and Chemoresistance. *Front Biosci* (2005) 10:975–87. doi: 10.2741/1592
73. Brognard J, Clark AS, Ni Y, Dennis PA. Akt/protein Kinase B Is Constitutively Active in Non-Small Cell Lung Cancer Cells and Promotes Cellular Survival and Resistance to Chemotherapy and Radiation. *Cancer Res* (2001) 61 (10):3986–97.


**Conflict of Interest:** TH is employed by the company Beijing Microread Genetics Co., Ltd.

The remaining authors declare that the research was conducted in the absence of any commercial or financial relationships that could be construed as a potential conflict of interest.

**Publisher's Note:** All claims expressed in this article are solely those of the authors and do not necessarily represent those of their affiliated organizations, or those of the publisher, the editors and the reviewers. Any product that may be evaluated in this article, or claim that may be made by its manufacturer, is not guaranteed or endorsed by the publisher.

frontiers in Oncology

ORIGINAL RESEARCH
published: 22 December 2021
doi: 10.3389/fonc.2021.756011

# Adipose-Derived Stem Cells Facilitate Ovarian Tumor Growth and Metastasis by Promoting Epithelial to Mesenchymal Transition Through Activating the TGF-β Pathway

*Xiaowu Liu[1,2], Guannan Zhao[2,3], Xueyun Huo[4], Yaohong Wang[5], Gabor Tigyi[6], Bing-Mei Zhu[7], Junming Yue[2,3]* and Wenjing Zhang[8]**

*[1] Department of Urology, The First Affiliated Hospital of China Medical University, Shenyang, China, [2] Department of Pathology and Laboratory Medicine, The University of Tennessee Health Science Center, Memphis, TN, United States, [3] Center for Cancer Research, College of Medicine, The University of Tennessee Health Science Center, Memphis, TN, United States, [4] School of Basic Medical Sciences, Capital Medical University, Beijing, China, [5] Department of Pathology, Immunology, and Microbiology, Vanderbilt University Medical Center, Nashville, TN, United States, [6] Department of Physiology, College of Medicine, The University of Tennessee Health Science Center, Memphis, TN, United States, [7] Regenerative Medicine Research Center, West China Hospital, Sichuan University, Chengdu, China, [8] Department of Genetics, Genomics & Informatics, College of Medicine, The University of Tennessee Health Science Center, Memphis, TN, United States*

OPEN ACCESS

**Edited by:**
*Robert Vierkant, Mayo Clinic, United States*

**Reviewed by:**
*Dong-Joo (Ellen) Cheon, Albany Medical College, United States*
*Enes Taylan, Mount Sinai Hospital, United States*

***Correspondence:**
*Wenjing Zhang*
*wzhang67@uthsc.edu*
*Junming Yue*
*jyue@uthsc.edu*

**Specialty section:**
*This article was submitted to Gynecological Oncology, a section of the journal Frontiers in Oncology*

**Received:** *09 August 2021*
**Accepted:** *29 November 2021*
**Published:** *22 December 2021*

**Citation:**
*Liu X, Zhao G, Huo X, Wang Y, Tigyi G, Zhu B-M, Yue J and Zhang W (2021) Adipose-Derived Stem Cells Facilitate Ovarian Tumor Growth and Metastasis by Promoting Epithelial to Mesenchymal Transition Through Activating the TGF-β Pathway. Front. Oncol. 11:756011. doi: 10.3389/fonc.2021.756011*

Adipose-derived stem cells (ADSC) are multipotent mesenchymal stem cells derived from adipose tissues and are capable of differentiating into multiple cell types in the tumor microenvironment (TME). The roles of ADSC in ovarian cancer (OC) metastasis are still not well defined. To understand whether ADSC contributes to ovarian tumor metastasis, we examined epithelial to mesenchymal transition (EMT) markers in OC cells following the treatment of the ADSC-conditioned medium (ADSC-CM). ADSC-CM promotes EMT in OC cells. Functionally, ADSC-CM promotes OC cell proliferation, survival, migration, and invasion. We further demonstrated that ADSC-CM induced EMT *via* TGF-β growth factor secretion from ADSC and the ensuing activation of the TGF-β pathway. ADSC-CM-induced EMT in OC cells was reversible by the TGF-β inhibitor SB431542 treatment. Using an orthotopic OC mouse model, we also provide the experimental evidence that ADSC contributes to ovarian tumor growth and metastasis by promoting EMT through activating the TGF-β pathway. Taken together, our data indicate that targeting ADSC using the TGF-β inhibitor has the therapeutic potential in blocking the EMT and OC metastasis.

**Keywords: adipose-deprived stem cell, ovarian cancer, metastasis, epithelial to mesenchymal transition (EMT), TGF-β**

## INTRODUCTION

Ovarian cancer (OC) is the most lethal gynecological malignancy worldwide, because of its early dissemination in the peritoneal cavity, late detection, and high recurrence rate (1). Most patients are diagnosed at advanced stages with poor prognosis and significant mortality. OC metastasizes *via* pelvic dissemination directly from the primary tumor to peritoneal organs, which is usually asymptomatic at the early stage (2).

The tumor microenvironment (TME) plays a critical role in tumor progression and metastasis, which is becoming a potential therapeutic target (3). TME is composed of fibroblast, mesenchymal stromal cells (MSC), immune cells, blood vessels, and extracellular matrix. MSC has been shown to play different roles in different cancers, including colon, breast, pancreatic, and lung cancer. The influences of MSC on cancers are controversial. MSC in the TME have been shown to promote the aggressive malignant phenotypes of various solid cancers, including colon cancer (4) and breast cancer (5). However, MSC also showed inhibitory effects in lung cancer (6) and liver cancer (7).

Adipose-derived stem cells (ADSC) are residents in adipose tissue and share most multipotency features of MSC. ADSC can differentiate into adipocyte, osteoblast, chondrocyte, myocyte, and lineages. Several studies have demonstrated the interplay between ADSC and cancer cells (8). Intravenous-injected ADSC can promote breast cancer growth and metastasis in a mouse model (9). The effects of ADSC in promoting tumor metastasis have also been observed in pancreatic, prostate, endometrial, and lung cancers (10–14). Human ADSC promotes invasion of breast cancer cells by producing CCL5 *in vitro* (15). ADSC also shows enhanced adipogenic differentiation in breast cancer (16). ADSC increase OC cell proliferation, migration, and chemoresistance (17–19). The conditioned medium (CM) of ADSC alters the proteomic profile of OC cell lines *in vitro* and expression of thymosin beta 4 X-linked (TMSB4X) in OC cells increased significantly, which promoted OC progression (20). Inhibition of TMSB4X attenuated the protumor effects of ADSCs (20). ADSC were reported to promote autophagy through activating the STAT3 signaling pathway (21). ADSC promote cancer progression by differentiating into cancer-associate fibroblast (CAF) or cancer-associate adipocytes (CAA) (22, 23) and facilitating CSC self-renewal (24). In addition, ADSC promote OC chemoresistance *via* inhibiting the cleavage of caspase-3 and inducing the platinum accumulation in OC cells (25, 26). Although, most studies showed protumor effects of ADSC on OC. The inhibitory effects of ADSC on OC progression was also reported, co-culturing ADSC with OC cells inhibited OC cell invasion induced apoptosis (27). ADSC-CM blocked cell cycle and induced apoptosis in OC cell lines (28).

Epithelial to mesenchymal transition (EMT) contributes to malignant tumor progression. ADSC promotes EMT in different tumors, including lung cancer, breast cancer, and glioma (29–31). In the present study, we assessed the effects of ADSC on OC metastasis using CM from ADSC *in vitro* and in an orthotopic OC mouse model *in vivo*. Here, we demonstrate that ADSC contributes to OC metastasis by promoting EMT at least in part *via* activating the TGF-β pathway.

## MATERIAL AND METHODS

### Cell Culture and Preparation of CM

Ovarian cancer cell lines OVCAR3 and OVCAR8 were purchased from NCI and cultured in 10% RPMI1640 medium with 10% FBS (Hyclone, Logan, UT, USA), 100 U/ml penicillin, and 100 μg/ml streptomycin (Invitrogen, Carlsbad, CA, USA). We selected OVCAR3 and OVCAR8 based on their properties inducing OC tumor metastasis and p53 mutational status. Both OVCAR3 and OVCAR8 have endogenous p53 mutations, whereas OVCAR3 is nonmetastatic in contrast to OVCAR8 that is aggressively metastatic *in vivo*. Human ADSC were purchased from Lonza (Basel, Switzerland) and cultured in MEM-α, nucleosides, GlutaMAX™ medium (MEM) supplemented with FBS, penicillin, and streptomycin. All cells were tested negative for mycoplasma using luciferase reporter assay (Lonza) and authenticated using the short tandem repeat analysis by ATCC (Manassas, VA, USA). CM was prepared when ADSC reached passages 3–6 and 80%–90% confluence. After the medium was changed into fresh complete medium (with or without serum) and culturing for additional 24 h, the medium was collected as ADSC-CM following centrifugation at 300×*g* for 5 min and filtration through 0.22 μm filter and stored at −80°C for the subsequent experiments.

### Characterization of ADSC by Flow Cytometry

ADSC at the third passage were collected by 0.25% trypsin-EDTA (Gibco, Grand Island, NY, USA), washed in PBS and resuspended in PBS at a concentration of $1 \times 10^6$ cells/ml. The cells were then blocked with 0.5% bovine serum albumin (BSA) (Sigma-Aldrich, St. Louis, MO, USA) at 4°C for 20 min, followed by additional 30 min incubation at 4°C in the dark with one of the following antibodies: anti-CD44-FITC (1:50), anti-CD73-PE (1:50), anti-CD105-BV421 (1:100), anti-CD31-APC-Cy™7 (1:100), anti-CD45-APC (1:100), and anti-CD90-PerCP-Cy™5.5 (1:50). All antibodies were purchased from BD Biosciences (San Jose, CA, USA). The cells were subsequently washed in 1 ml 0.2% BSA and centrifuged at 500×*g* for 5 min. Antibody binding was detected using a Bio-Rad ZE5 cell analyzer (Bio-Rad, Hercules, CA, USA) and analyzed using the FlowJo® software.

### MTT Assay

OVCAR3 and OVCAR8 cells (2,000 cells/well) were seeded into 96-well plates. After culturing for 24 h, the medium was substituted with fresh complete culture medium (control) or serum containing ADSC-CM. The MTT reagent (10 μl) was added at the end of the indicated time points (1-, 3-, and 5d) and incubated for 4 h, before 100 μl detergent reagent was added. Subsequently, the plates were incubated at room temperature in the dark for 2 h and the absorbance was measured at 570 nm.

### Cell Colony Formation Assay

OVCAR3 and OVCAR8 cells were plated into 6-well plates at the concentration of 400 cells/well and cultured with control medium or serum-containing ADSC-CM for 14 days. The cell

colonies were fixed with methanol and stained with crystal violet before being imaged and counted.

## Cell Migration Assay

A modified Transwell™ chamber (BD Falcon, San Jose, CA, USA) with an 8.0-μm pore size was used for the cell migration assay. OVCAR3 and OVCAR8 cells ($2 \times 10^5$) were suspended in 300 μl of serum-free medium and seeded into the Transwell chamber; control medium or serum-containing ADSC-CM was added into the lower chamber of the 24-well plates. Following 6-h incubation, the cells on the upper side of the chamber membrane were removed with cotton swabs, while the migrated cells on the lower side of the membranes were fixed with methanol and stained with crystal violet. Images were taken at ×10 magnification, and cells in at least three different fields of view were counted.

## Cell Invasion Assay

The 24-well Tumor Invasion System (BD BioSciences, San Jose, CA, USA), which were precoated with Matrigel (BD BioCoat™), were used for cell invasion assay. OVCAR3 or OVCAR8 cells ($2 \times 10^5$) were seeded in serum-free medium onto upper chamber, and control medium or ADSC-CM were used as a chemoattractant and added into the lower chamber. After incubating for 12 h, the Transwell inserts following fixation with methanol for 20 min were stained with hematoxylin and eosin for 10 min. Pictures were taken at ×10 magnification, and the cells were counted in at least three different fields.

## Measurement of TGF-β in ADSC-CM

The quantitation of TGF-β1 in serum-free ADSC-CM was performed by using Fast Human TGF-β1 ELISA Kit (Tribioscience, Sunnyvale, CA, USA) following the manufacturer's instructions. ADSC-CM were collected after changing the serum-free medium for 6-, 12-, 24-, and 48 h, respectively.

## Western Blot

OC cells were collected with RIPA buffer (Thermo Scientific, Rockford, IL, USA) containing 1% Halt Proteinase Inhibitor Cocktail (Thermo Scientific). A total of 30 μg protein/lane were loaded onto 10% SDS-PAGE gels and transferred onto PVDF membranes. The blots were blocked with 5% blocking buffer (nonfat milk) at room temperature for 1 h and incubated at 4°C overnight with the primary antibodies against phospho-SMAD2 (p-SMAD2, 1:500 #18338S), SMAD2/3 (1:1,000, #8685S), E-cadherin (1:1,000, #3195S), N-cadherin (1:1,000, #13116S), vimentin (1:1,000, #5741S) (Cell Signaling, Danvers, MA, USA), cytokeratin 7 (1:1,000, #ab181598, Abcam, Cambridge, MA, USA), and GAPDH (1:1,000,#G9545; Sigma-Aldrich, St. Louis, MO, USA). The membranes were washed with PBST and incubated with horseradish peroxidase-conjugated secondary antibodies (1:10,000, goat anti-rabbit, #sc-2004; goat anti-mouse, sc-2005; Santa Cruz, Dallas, TX, USA) at room temperature for 1 h. Protein bands were visualized using chemiluminescence by exposing on X-ray film. The films were scanned and analyzed by Image J.

## SMAD-Dependent Reporter Gene Luciferase Assay

OVCAR3 and OVCAR8 cells were transduced with the lentiviral vector pGF-SMAD2/3/4-mCMV-luciferase-EF1a-puro (System Biosciences, CA) containing SMAD2/3/4 transcriptional response elements (TRE). The medium was changed to control medium (serum-free) or ADSC-CM (serum-free) and incubated for 12 h and treated with 6 ng/ml TGF-β for additional 12 h to activate SMAD2/3/4 pathway. For some groups, the cells were also treated with the TGF-β antagonist at 10 μM SB431542 (Sigma-Aldrich, #S4317) (St. Louis, MO, USA) or vehicle for 24 h. Luciferase activity was measured using Dual-Luciferase Reporter Assay System (Promega, Madison, WI, USA) and normalized by comparing with the control or vehicle-treated group.

## Orthotopic Ovarian Cancer Mouse Model

To track ovarian tumor growth and metastasis *in vivo*, OVCAR 8 cells labeled with luciferase (OVCAR8-Luc2) were used in an orthotopic OC mouse model. 2-month-old immunocompromised NOD.Cg Prkdcscid Il2rgtm1Wjl/SzJ (NSG) female mice (Jackson Laboratory) were intrabursally inoculated with $5 \times 10^5$ cells. Then the 20 mice were randomized into four groups 1-week postinoculation and treated with either 1) control medium, 2) serum-free ADSC-CM, 3) SB431542 plus control medium, or 4) SB431542 plus serum-free ADSC-CM *via* peritoneal injection. SB431542 was peritoneally injected with a dose of (10 mg/kg body weight). Mice were treated daily for 5 days a week and for 3 weeks. Tumor growth and metastasis were observed by Xenogen Bioimaging system once a week. All mice were sacrificed at 4 weeks after cell injection. Primary ovarian and metastatic tumors were collected for histology and western blot to determine p-SMAD2 and EMT markers protein levels. All animal experiments were performed in accordance with the protocol approved by the Institutional Animal Care and Use Committee of the University of Tennessee Health Science Center.

## Statistical Analysis

At least three independent experiments in sample triplicate were performed. Data are presented as mean ± SD and Student's *t*-test was performed using GraphPad Prism 8 (GraphPad, San Diego, CA, USA) to determine significant differences between the treatment and control groups. $p < 0.05$ was considered significant.

# RESULTS

## ADSC Promotes OC Cell Growth, Migration, and Invasion

ADSC were characterized by examining specific marker gene expression using flow cytometry. As shown in **Supplementary Figure S1**, CD44, CD73, CD90, and CD105 are expressed while CD31 and CD45 are absent in ADSC.

To assess how ADSC affect OC cell functions, we examined the OC cell proliferation and survival following treatment using ADSC-CM or control medium. ADSC-CM significantly

increased OC cell proliferation compared with the control medium at all three time points (1, 3, and 5 days) in both OVCAR3 and OVCAR8 cells (**Figures 1A, B**). ADSC-CM also significantly promote OC cell survival as shown by cell colony formation assay (**Figures 1C, D**).

We also examined cell migration and invasion using the Transwell plates to determine whether ADSC contribute to OC invasiveness and found that ADSC-CM significantly increased cell migration (**Figures 1E, F**) and invasion in both OVCAR3 and OVCAR8 cells (**Figures 1G, H**).

## ADSC Promotes EMT by Activating the TGF-β Signaling Pathway in OC Cells

We have shown previously that TGF-β promotes EMT and contributes to OC tumor cell invasion (32). To understand the mechanisms on how ADSC contribute to OC growth and metastasis, extending our earlier observations, we examined whether ADSC affect EMT phenotypic switch through TGF-β pathway. We determined expression of EMT marker proteins in both OVCAR3 and OVCAR8 following treatment with ADSC-CM for different periods (0, 24, and 48 h). We found that ADSC-CM increased the expression of the mesenchymal markers N-cadherin and vimentin whereas, inhibited the expression of epithelial markers E-cadherin and cytokeratin-7 e in a time-dependent manner in both OC cell lines (**Figures 2A, B**), indicating that ADSC facilitates the EMT of OC cells. Changes in cell morphology are shown in **Supplementary Figure S2**. After treatment with ADSC-CM, some OC cells showed spindle-like shapes.

To explore whether TGF-β signaling pathway is involved in the ADSC-CM-induced EMT, we detected expression of p-SMAD2 and total SMAD2 in OVCAR3 and OVCAR8 cells at different time points after ADSC-CM treatment. We found that ADSC-CM enhanced p-SMAD2 level without changing the total

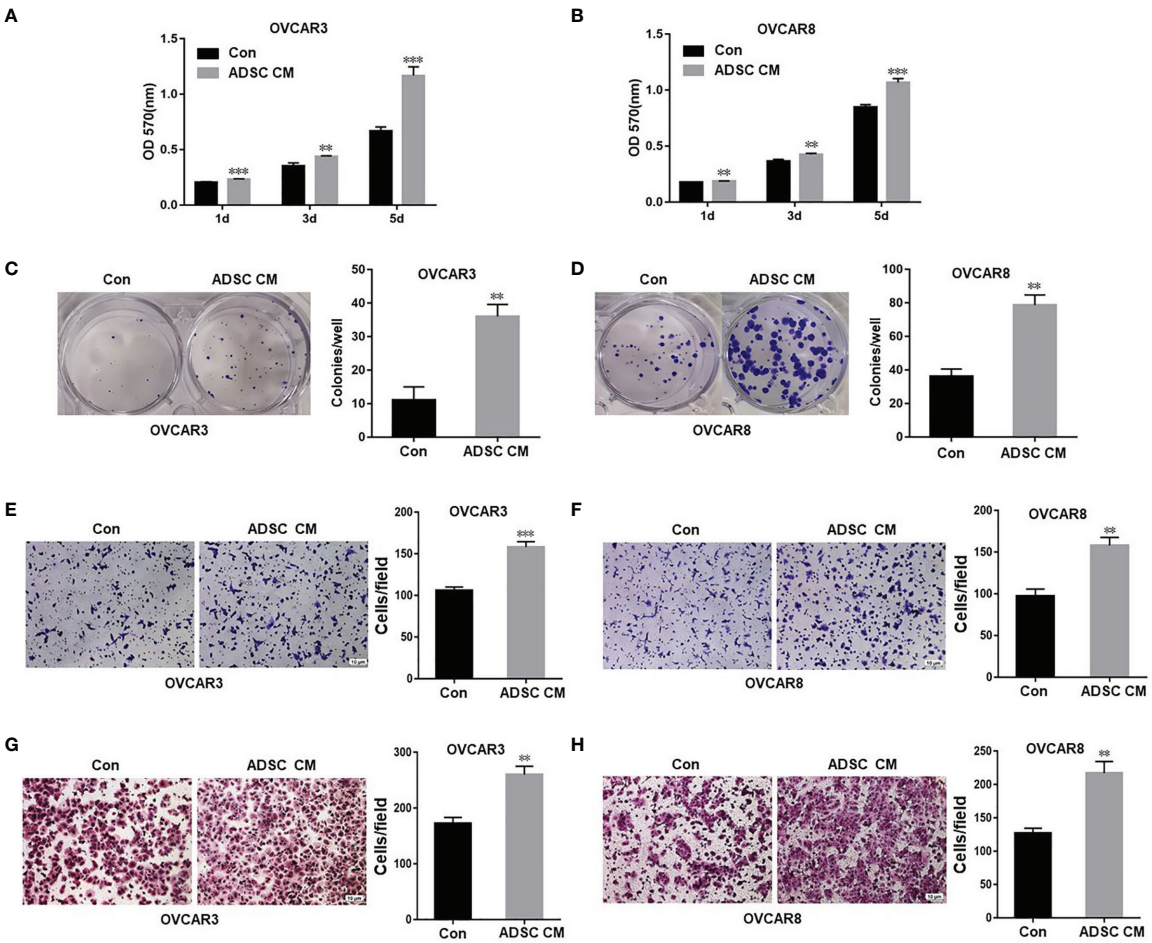


**FIGURE 1** | ADSC promote cell growth, migration, and invasion in ovarian cancer cells. **(A, B)** MTT assay was performed to detect the cell proliferation in OVCAR3 **(A)** and OVCAR8 **(B)** cells at different time points, following treatment with ADSC-CM or control medium. **(C, D)** Cell colony formation assay was performed to determine cell survival in OVCAR3 **(C)** and OVCAR8 **(D)** cells treated with ADSC-CM or control medium. **(E, F)** Cell migration in OVCAR3 **(E)** and OVCAR8 **(F)** cells treated with ADSC-CM or control medium performed using Transwell plates. **(G, H)** Cell invasion in OVCAR3 **(G)** and OVCAR8 **(H)** cells treated with ADSC-CM or control medium examined using Matrigel-coated plates. Data represent the mean ± SD of three independent experiments. $^{**}p < 0.01$, $^{***}p < 0.001$ compared with the control group.

SMAD2 expression (**Figures 2C, D**). We further validated this finding by applying SMAD-dependent reporter gene luciferase assay. ADSC-CM significantly increased SMAD2/3/4 transcriptional activity in both OVCAR3 and OVCAR8 cells (**Figures 2E, F**). Since ADSC-CM activates the TGF-β pathway, we decided to examine whether ADSC indeed secret TGF-β into ADSC-CM using ELISA assay. We found that TGF-β1 in ADSC-CM increased significantly at 6 h, reaching its peak levels between 24 and 48 h (**Figure 2G**). Our data indicate that ADSC promotes EMT phenotypic switch by activating the TGF-β pathway in OC cells.

## Inhibition of TGF-β Pathway Blocks ADSC-Induced OC Cell Survival, Migration, and Invasion

Adipocytes in omentum contribute to OC metastasis. ADSC can differentiate into multiple cancer-associated cell types including adipocytes, fibroblasts, and endothelial cells. Targeting ADSC in omentum as major cell type in OC TME has great therapeutic potentials. Therefore, we tested whether inhibition of TGF-β pathway activated by ADSC affects OC function. We treated OVCAR3 and OVCAR8 cells with 10 μM TGF-β receptor inhibitor SB431542 for 24 h and then added ADSC-CM into culture for different time points (0, 24, and 48 h). ADSC activation of SMAD2 phosphorylation in OC cells was significantly inhibited by SB431542 (**Figures 3A, B**). We also validated this finding using SMAD-dependent reporter gene luciferase assay. Similarly, ADSC-induced SMAD2/3/4 transcriptional activity was significantly inhibited by SB431542 treatment (**Figures 3C, D**). Next, we tested whether SB431542 treatment of the OC cells affected the ADSC-CM-induced EMT phenotypic switch. We found that SB431542 significantly reduced EMT in OC cells induced by ADSC as shown by the downregulation of mesenchymal markers and upregulation of epithelial markers compared with vehicle-treated cells (**Figures 3E, F**). In addition, ADSC-induced OC cell proliferation, cell colony formation, migration, and invasion were also significantly inhibited by SB431542 (**Figures 3G–N**). Our results indicate that targeting the TGF-β pathway can effectively inhibit ADSC-induced OC cell growth, migration, and invasion.

## ADSC Promotes Primary Tumor Growth and Metastasis in an Orthotopic OC Mouse Model

To test whether ADSC promote ovarian tumor progression and metastasis *in vivo* using the orthotopic OC mouse model we described before (33), we intrabursally injected OVCAR8 cells

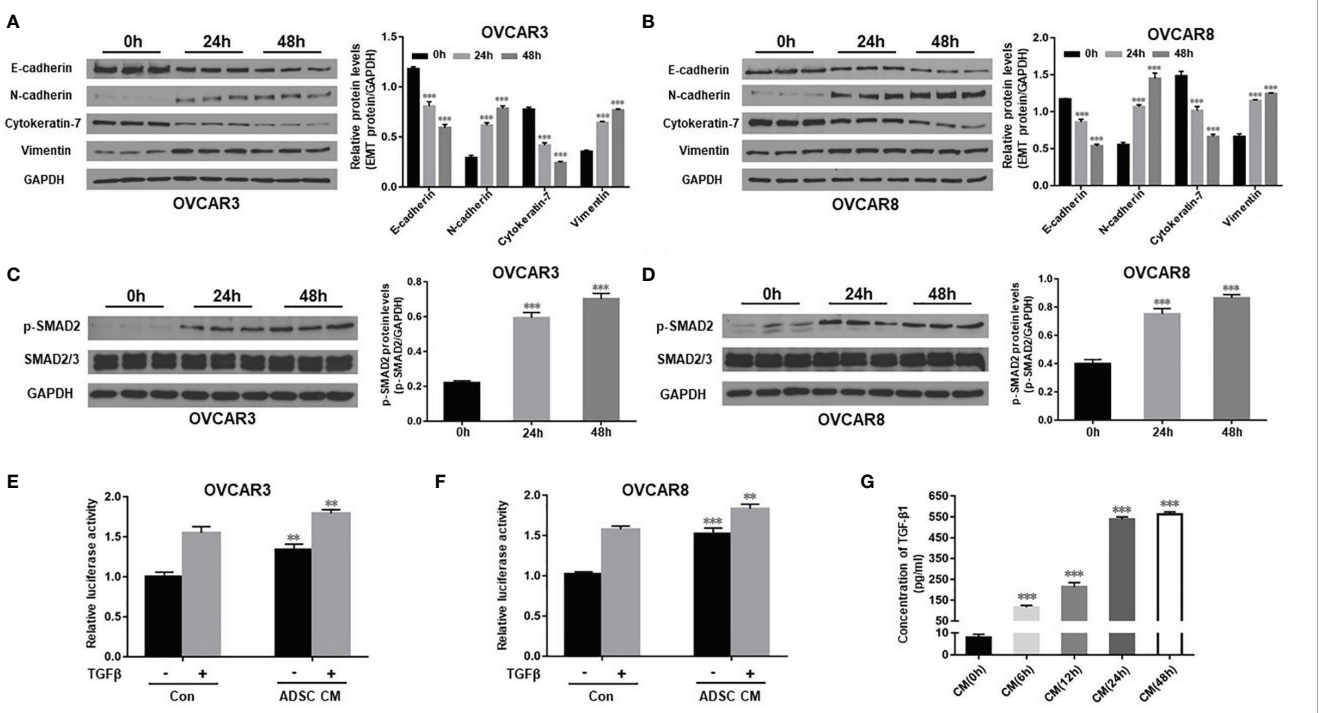


**FIGURE 2** | ADSC promotes EMT by activating the TGF-β signaling pathway in OC cells. **(A, B)** Western blot analysis of EMT markers in both OVCAR3 **(A)** and OVCAR8 **(B)** cells following treatment with ADSC-CM for different time durations (0, 24, and 48 h). Right, the quantification analysis of the blots. **(C, D)** Western blot analysis of the p-SMAD2 and SMAD2/3 expression in both OVCAR3 **(C)** and OVCAR8 **(D)** cells following treatment with ADSC-CM for different time durations. Right, the quantification analysis of the blots. **(E, F)** Luciferase activity in OVCAR3 **(E)** and OVCAR8 **(F)** cells following ADSC-CM treatment for 24 h, then 6 ng/ml TGF-β treatment for 12 h. **(G)** ELISA analysis of ADSC-CM collected at different time points to detect the concentrations of TGF-β1. Data represent the mean ± SD of three independent experiments. $^{**}p < 0.01$, $^{***}p < 0.001$ compared with the control group.

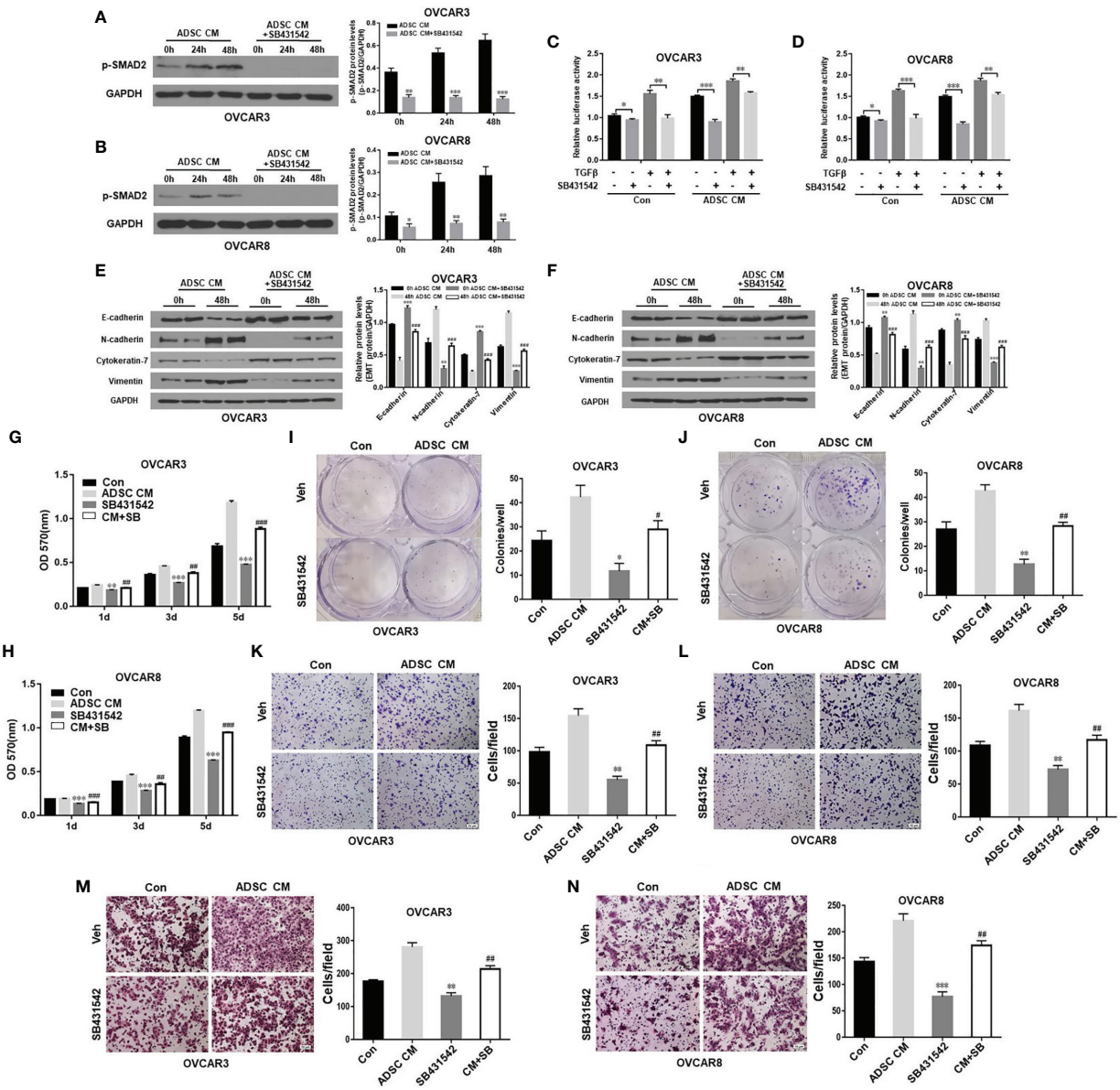


**FIGURE 3** | Inhibition of TGF-β pathway antagonizes ADSC-induced OC growth, migration, and invasion. **(A, B)** Western blot analysis of the p-SMAD2 expression in both OVCAR3 **(A)** and OVCAR8 **(B)** cells treated with 10 μM SB431542 for 24 h and then ADSC-CM for different time durations. Right, the quantification analysis of the blots. **(C, D)** Luciferase activity in OVCAR3 **(C)** and OVCAR8 **(D)** cells following ADSC-CM treatment for 24 h, SB431542 treatment for 24 h, then 6 ng/ml TGF-β treatment for 12 h. **(E, F)** Western blot analysis of EMT markers in both OVCAR3 **(E)** and OVCAR8 **(F)** following treatment with ADSC-CM and SB431542 (10 μM) for 48 h. Right, the quantification analysis of the blots. **(G, H)** MTT assay was performed to detect the cell proliferation ability of OVCAR3 **(G)** and OVCAR8 **(H)** cells at different time points following ADSC-CM and SB431542 (10 μM) treatment. **(I, J)** Cell colony formation assay determined cell survival in OVCAR3 **(I)** and OVCAR8 **(J)** cells following ADSC-CM and SB431542 (5 μM) treatment. **(K, L)** Cell migration in OVCAR3 **(K)** and OVCAR8 **(L)** cells treated with ADSC-CM or control medium following SB431542 (10 μM) treatment 24 h performed using Transwell plates. **(M, N)** Cell invasion in OVCAR3 **(M)** and OVCAR8 **(N)** cells treated with ADSC-CM or control medium following SB431542 (10 μM) treatment for 24 h using Matrigel-coated plates. Data represent the mean ± SD of three independent experiments. $^{*}p < 0.05$, $^{**}p < 0.01$, $^{***}p < 0.001$ compared with the corresponding control group; $^{\#}p < 0.05$, $^{\#\#}p < 0.01$, $^{\#\#\#}p < 0.001$ compared with the corresponding ADSC-CM group.

labeled with luciferase into immunocompromised NSG female mice, and then treated mice with ADSC-CM and SB431542. OC primary tumors and metastases were significantly higher in mice treated with ADSC-CM compared with control medium. Moreover, progression of the primary tumors was significantly lower in mice treated with SB43152 compared with vehicle as shown by bioluminescent intensity (**Figure 4A**). Histologic examination confirmed OC growth in the ovaries of the mice

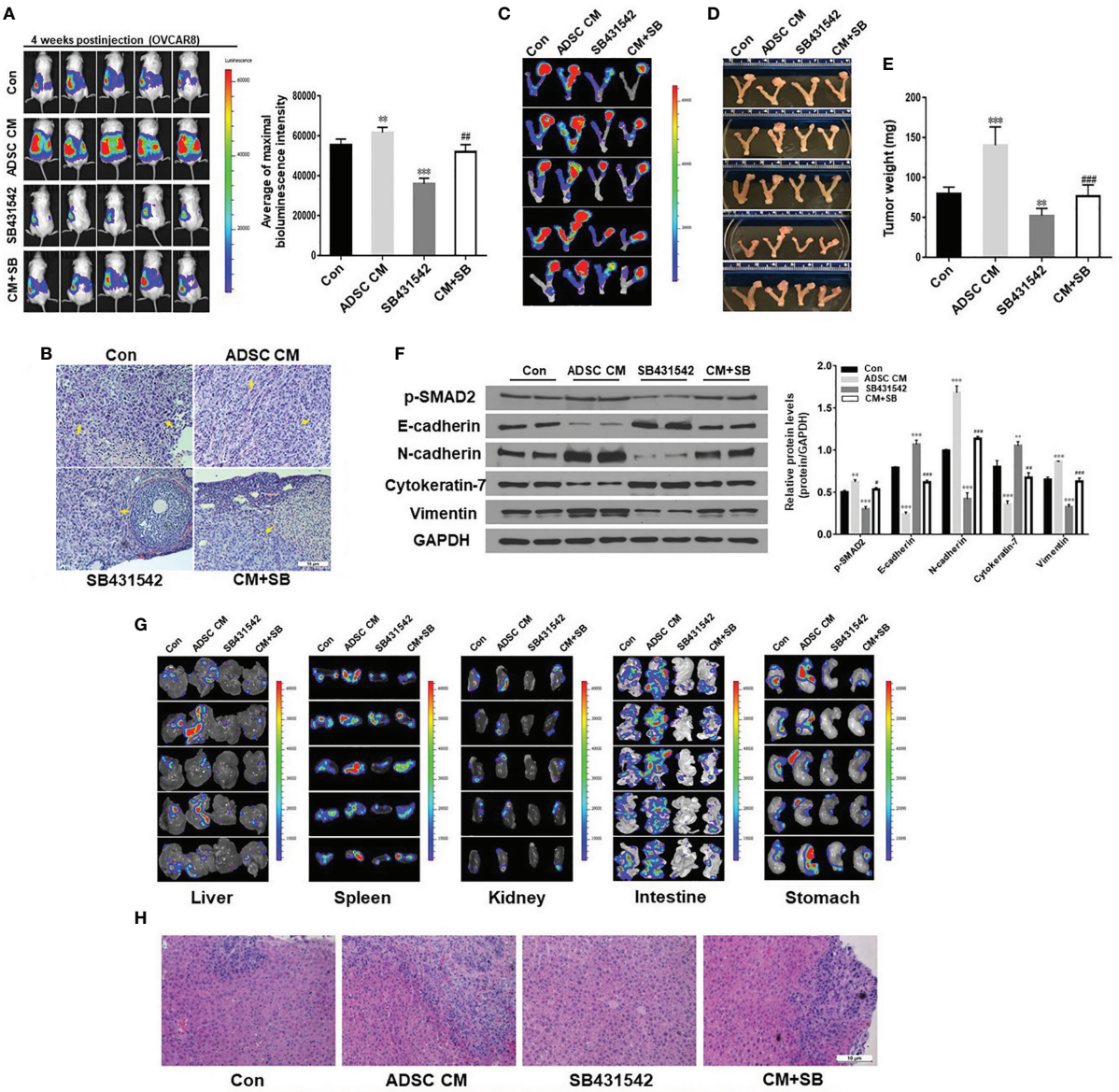


**FIGURE 4** | ADSC enhance primary ovarian tumor growth and metastasis in an orthotopic ovarian cancer mouse model. **(A)** Live animal imaging of primary tumors in ovaries of mice at 4 weeks following intrabursal injection of OVCAR8 cells. Right, the quantitative bioluminescence intensities. **(B)** H&E staining of primary tumor in ovaries. There are high-grade serous carcinomas involving the ovarian stroma. No normal ovary structure could be seen in the control and ADSC-CM groups. Tumors are indicated by yellow arrows. **(C)** Primary tumors in ovaries of mice were identified by live animal imaging. **(D, E)** Tumors in ovaries of mice were dissected, imaged **(D)**, and weighed **(E)**. **(F)** Western blot analysis of p-SMAD2 and EMT markers in primary ovarian tumors. Right, the quantification analysis of the blots. **(G)** Metastatic tumors in liver, spleen, kidney, intestine, and stomach of xenografted mice were identified by live animal imaging. **(H)** H&E staining of metastatic tumors in livers of xenografted mice. Data represent the mean ± SD of three independent experiments. $^{**}p < 0.01$, $^{***}p < 0.001$ compared with the control group. $^{\#}p < 0.05$, $^{\#\#}p < 0.01$, $^{\#\#\#}p < 0.001$ compared with the corresponding ADSC-CM group.

(**Figure 4B**). All 4 groups showed malignant epithelial tumor with serous differentiation, nest, or solid/glandular growth and moderate to severe nuclear atypia. Cytologically, tumor cells showed prominent nuclear atypia, characterized by highly pleomorphic, irregular nuclear contours, and variably conspicuous nucleoli.

Consistent with bioluminescence results, a significant difference in tumor weight among four groups was observed (**Figures 4C–E**). ADSC-CM significantly stimulated tumor growth in ovaries, and ADSC-CM-induced tumor growth was significantly suppressed by SB431542. We also examined p-SMAD2 and EMT markers in primary ovarian tumors using Western blot. ADSC-CM treatment increased expression of p-SMAD2, N-cadherin, and vimentin and reduced the expression of E-cadherin and cytokeratin-7 (**Figure 4F**).

ADSC-induced EMT marker expression was significantly inhibited by SB431542 treatment (**Figure 4F**). We then examined tumor metastasis in multiple peritoneal organs and tumors were found in liver, spleen, kidney, intestine, and stomach (**Figures 4G, H**). ADSC-CM treatment significantly promoted tumor dissemination in these organs, which was significantly reduced by SB431542 treatment. Taken together, our results show that ADSC-CM significantly enhances primary ovarian tumor growth and metastasis by promoting EMT and activating the TGF-β pathway in an orthotopic OC mouse model.

## DISCUSSION

In the present study, we investigated whether ADSC contributes to OC growth and metastasis by using the transfer of ADSC-CM. Our data indicate that ADSC-CM promotes OC growth and metastasis at least partially *via* promoting EMT and activating the TGF-β pathway. ADSC-CM enhances OC cell proliferation, migration, and invasion. Consistent with the role of TGF-β, pharmacological inhibition of TGF-β signaling pathway antagonizes the effects of ADSC-CM on OC function and tumor metastasis. These findings indicate that ADSC-derived TGF-β is a major regulator of OC TME, which contributes to OC tumor progression and metastasis. These findings strongly suggest that TGF-β signaling can be targeted to improve the therapeutic outcomes in OC patients.

Previous studies showed that ADSC play important roles in the interaction between TME and tumor progression by secreting soluble factors and exosomes, including breast cancer, head and neck cancer, and osteosarcoma (34–38). Coculture with ADSC or treatment with ADSC-CM increased metalloproteinase (MMP) 2/9 expression and activated STAT3 transcription factor in osteosarcoma cells, therefore promoted osteosarcoma cell proliferation and invasion (35). Human ADSC secreted CSCL1/8 in contacting with breast cancer cells and then promoted angiogenesis and tumor growth of breast cancer (36). Coculture of human ADSC and head/neck cancer cells showed elevated MMP 2/9 expression and stimulated migration of cancer cells but had no effect on cancer cell growth (38). ADSC from omentum of OC cancer patients induced OC cell growth, migration, and chemoresistance (17). Another study reported that coculture of omentum ADSC and OC cells promoted OC cell proliferation and invasion *via* increased MMP secretion of cancer cells (18). Proteomic analysis of OC cells after treatment with ADSC-CM identified TMSB4X as a factor that mediates protumor effect of ADSC (20). Our findings are consistent with the previous reports that ADSC-CM enhances growth and metastasis of OC both *in vitro* and *in vivo* (18, 20). However, here we show an additional and different molecular mechanism by demonstrating that ADSC-derived TGF-β activates EMT, which in turn contributes to OC progression and metastasis.

We show here that ADSC promotes EMT in OC cells. Consistent with this study, ADSC-CM has also been shown to stimulate EMT in glioma cells (29), lung cancer cells (30), and breast cancer cells (31), suggesting that the ADSC may play a pivotal and general role in tumor metastasis by promoting EMT. EMT is well-known to be associated with tumor metastasis and chemoresistance (39, 40). Our findings indicate that ADSC can also promote OC growth and metastasis through stimulation of EMT. We previously showed that TGF-β promotes EMT in OC (32). Here, we detected TGF-β secreted from cultured ADSC by ELISA assay, which can activate TGF-β signaling in the OC cells. Using a TGF-βR½ inhibitor, SB431542, we show for the first time that blocking of TGF-β pathway attenuates the promotion effects of ADSC on the OC growth and metastasis *in vitro* and *in vivo*. Thus, our findings demonstrate that ADSC can promote OC progression through promoting EMT *via* activation of TGF-β signaling.

Although we demonstrated that ADSC-CM promote OC progression and metastasis by activating the TGF-β pathway, there are multiple growth factors secreted from ADSC and multiple signaling pathways might be involved in the interaction between ADSC and OC. It is essential to identify those growth factors or adipokines secreted from ADSC through the proteomic approach to further understand the importance of ADSC in OC metastasis. In addition, we tested the therapeutic effects of TGF-β inhibitor in OC mouse models; however, it is important to further test whether TGF-β inhibitor has synergistic effects in enhancing the chemotherapy drugs in OC mouse models.

In conclusion, ADSC residing in the TME contributes to OC growth and metastasis, at least in part through promoting EMT and activating the TGF-β signaling. These findings not only help us understand the importance of ADSC in the TME of OC but also provide experimental evidence to target ADSC in TME for the treatment of OC and potentially of several other aggressive cancers.

## DATA AVAILABILITY STATEMENT

The original contributions presented in the study are included in the article/**Supplementary Material**. Further inquiries can be directed to the corresponding authors.

## ETHICS STATEMENT

The animal study was reviewed and approved by the Institutional Animal Care and Use Committee (IACUC) at the University of Tennessee Health Science Center.

## AUTHOR CONTRIBUTIONS

XL, GZ, and XH performed experiments. WZ and JY designed experiments and wrote the manuscript. WZ, JY, GT, YW, and B-MZ edited the manuscript. All authors read and approved the final version.

## FUNDING

This study was supported by a grant 1R21CA216585-01A1 from NCI and a CORNET Award of UTHSC to YJ and a grant CA-092160-21 from NCI to TG.

## SUPPLEMENTARY MATERIAL

The Supplementary Material for this article can be found online at: https://www.frontiersin.org/articles/10.3389/fonc.2021.756011/full#supplementary-material

## REFERENCES

1. Nash Z, Menon U. Ovarian Cancer Screening: Current Status and Future Directions. *Best Pract Res Clin Obstet Gynaecol* (2020) 65:32–45. doi: 10.1016/j.bpobgyn.2020.02.010
2. Lengyel E. Ovarian Cancer Development and Metastasis. *Am J Pathol* (2010) 177:1053–64. doi: 10.2353/ajpath.2010.100105
3. Luo Z, Wang Q, Lau WB, Lau B, Xu L, Zhao L, et al. Tumor Microenvironment: The Culprit for Ovarian Cancer Metastasis? *Cancer Lett* (2016) 377:174–82. doi: 10.1016/j.canlet.2016.04.038
4. Shinagawa K, Kitadai Y, Tanaka M, Sumida T, Kodama M, Higashi Y, et al. Mesenchymal Stem Cells Enhance Growth and Metastasis of Colon Cancer. *Int J Cancer* (2010) 127:2323–33. doi: 10.1002/ijc.25440
5. Albarenque SM, Zwacka RM, Mohr A. Both Human and Mouse Mesenchymal Stem Cells Promote Breast Cancer Metastasis. *Stem Cell Res* (2011) 7:163–71. doi: 10.1016/j.scr.2011.05.002
6. Liu T, Zhu K, Ke C, Yang S, Yang F, Li Z, et al. Mesenchymal Stem Cells Inhibited Development of Lung Cancer Induced by Chemical Carcinogens in a Rat Model. *Am J Transl Res* (2017) 9:2891–900.
7. Yulyana Y, Ho IA, Sia KC, Newman JP, Toh XY, Endaya BB, et al. Paracrine Factors of Human Fetal MSCs Inhibit Liver Cancer Growth Through Reduced Activation of IGF-1r/PI3K/Akt Signaling. *Mol Ther* (2015) 23:746–56. doi: 10.1038/mt.2015.13
8. Zhang W, Torres-Rojas C, Yue J, Zhu BM. Adipose-Derived Stem Cells in Ovarian Cancer Progression, Metastasis, and Chemoresistance. *Exp Biol Med (Maywood)* (2021) 246(16):1810–15. doi: 10.1177/15353702211023846
9. Muehlberg FL, Song YH, Krohn A, Pinilla SP, Droll LH, Leng X, et al. Tissue-Resident Stem Cells Promote Breast Cancer Growth and Metastasis. *Carcinogenesis* (2009) 30:589–97. doi: 10.1093/carcin/bgp036
10. Ji SQ, Cao J, Zhang QY, Li YY, Yan YQ, Yu FX. Adipose Tissue-Derived Stem Cells Promote Pancreatic Cancer Cell Proliferation and Invasion. *Braz J Med Biol Res* (2013) 46:758–64. doi: 10.1590/1414-431X20132907
11. Prantl L, Muehlberg F, Navone NM, Song YH, Vykoukal J, Logothetis CJ, et al. Adipose Tissue-Derived Stem Cells Promote Prostate Tumor Growth. *Prostate* (2010) 70:1709–15. doi: 10.1002/pros.21206
12. Klopp AH, Zhang Y, Solley T, Amaya-Manzanares F, Marini F, Andreeff M, et al. Omental Adipose Tissue-Derived Stromal Cells Promote Vascularization and Growth of Endometrial Tumors. *Clin Cancer Res* (2012) 18:771–82. doi: 10.1158/1078-0432.CCR-11-1916
13. Zhang Y, Daquinag A, Traktuev DO, Amaya-Manzanares F, Simmons PJ, March KL, et al. White Adipose Tissue Cells Are Recruited by Experimental Tumors and Promote Cancer Progression in Mouse Models. *Cancer Res* (2009) 69:5259–66. doi: 10.1158/0008-5472.CAN-08-3444
14. Heo SC, Lee KO, Shin SH, Kwon YW, Kim YM, Lee CH, et al. Periostin Mediates Human Adipose Tissue-Derived Mesenchymal Stem Cell-Stimulated Tumor Growth in a Xenograft Lung Adenocarcinoma Model. *Biochim Biophys Acta* (2011) 1813:2061–70. doi: 10.1016/j.bbamcr.2011.08.004
15. Pinilla S, Alt E, Abdul Khalek FJ, Jotzu C, Muehlberg F, Beckmann C, et al. Tissue Resident Stem Cells Produce CCL5 Under the Influence of Cancer Cells and Thereby Promote Breast Cancer Cell Invasion. *Cancer Lett* (2009) 284:80–5. doi: 10.1016/j.canlet.2009.04.013
16. Weigand A, Boos AM, Tasbihi K, Beier JP, Dalton PD, Schrauder M, et al. Selective Isolation and Characterization of Primary Cells From Normal Breast and Tumors Reveal Plasticity of Adipose Derived Stem Cells. *Breast Cancer Res* (2016) 18:32. doi: 10.1186/s13058-016-0688-2
17. Nowicka A, Marini FC, Solley TN, Elizondo PB, Zhang Y, Sharp HJ, et al. Human Omental-Derived Adipose Stem Cells Increase Ovarian Cancer Proliferation, Migration, and Chemoresistance. *PLoS One* (2013) 8:e81859. doi: 10.1371/journal.pone.0081859
18. Chu Y, Tang H, Guo Y, Guo J, Huang B, Fang F, et al. Adipose-Derived Mesenchymal Stem Cells Promote Cell Proliferation and Invasion of Epithelial Ovarian Cancer. *Exp Cell Res* (2015) 337:16–27. doi: 10.1016/j.yexcr.2015.07.020
19. Hass R, Otte A. Mesenchymal Stem Cells as All-Round Supporters in a Normal and Neoplastic Microenvironment. *Cell Commun Signal* (2012) 10:26. doi: 10.1186/1478-811X-10-26
20. Chu Y, You M, Zhang J, Gao G, Han R, Luo W, et al. Adipose-Derived Mesenchymal Stem Cells Enhance Ovarian Cancer Growth and Metastasis by Increasing Thymosin Beta 4x-Linked Expression. *Stem Cells Int* (2019) 2019:9037197. doi: 10.1155/2019/9037197
21. Chu Y, Wang Y, Li K, Liu M, Zhang Y, Li Y, et al. Human Omental Adipose-Derived Mesenchymal Stem Cells Enhance Autophagy in Ovarian Carcinoma Cells Through the STAT3 Signalling Pathway. *Cell Signal* (2020) 69:109549. doi: 10.1016/j.cellsig.2020.109549
22. Cho JA, Park H, Lim EH, Kim KH, Choi JS, Lee JH, et al. Exosomes From Ovarian Cancer Cells Induce Adipose Tissue-Derived Mesenchymal Stem Cells to Acquire the Physical and Functional Characteristics of Tumor-Supporting Myofibroblasts. *Gynecol Oncol* (2011) 123:379–86. doi: 10.1016/j.ygyno.2011.08.005
23. Cho JA, Park H, Lim EH, Lee KW. Exosomes From Breast Cancer Cells can Convert Adipose Tissue-Derived Mesenchymal Stem Cells Into Myofibroblast-Like Cells. *Int J Oncol* (2012) 40:130–8. doi: 10.3892/ijo.2011.1193
24. Coffman LG, Choi YJ, McLean K, Allen BL, di Magliano MP, Buckanovich RJ. Human Carcinoma-Associated Mesenchymal Stem Cells Promote Ovarian Cancer Chemotherapy Resistance *via* a BMP4/HH Signaling Loop. *Oncotarget* (2016) 7:6916–32. doi: 10.18632/oncotarget.6870
25. Wen Y, Guo Y, Huang Z, Cai J, Wang Z. Adipose–derived Mesenchymal Stem Cells Attenuate Cisplatin–Induced Apoptosis in Epithelial Ovarian Cancer Cells. *Mol Med Rep* (2017) 16:9587–92. doi: 10.3892/mmr.2017.7783
26. Sookram J, Zheng A, Linden KM, Morgan AB, Brown SA, Ostrovsky O. Epigenetic Therapy can Inhibit Growth of Ovarian Cancer Cells and Reverse Chemoresistant Properties Acquired From Metastatic Omentum. *Int J Gynaecol Obstetr* (2019) 145:225–32. doi: 10.1002/ijgo.12800
27. Khalil C, Moussa M, Azar A, Tawk J, Habbouche J, Salameh R, et al. Anti-Proliferative Effects of Mesenchymal Stem Cells (MSCs) Derived From Multiple Sources on Ovarian Cancer Cell Lines: An *In-Vitro* Experimental Study. *J Ovarian Res* (2019) 12:70. doi: 10.1186/s13048-019-0546-9
28. Reza A, Choi YJ, Yasuda H, Kim JH. Human Adipose Mesenchymal Stem Cell-Derived Exosomal-miRNAs Are Critical Factors for Inducing Anti-Proliferation Signalling to A2780 and SKOV-3 Ovarian Cancer Cells. *Sci Rep* (2016) 6:38498. doi: 10.1038/srep38498
29. Iser IC, Ceschini SM, Onzi GR, Bertoni AP, Lenz G, Wink MR. Conditioned Medium From Adipose-Derived Stem Cells (ADSCs) Promotes Epithelial-To-Mesenchymal-Like Transition (EMT-Like) in Glioma Cells *In Vitro*. *Mol Neurobiol* (2016) 53:7184–99. doi: 10.1007/s12035-015-9585-4
30. Park YM, Yoo SH, Kim SH. Adipose-Derived Stem Cells Induced EMT-Like Changes in H358 Lung Cancer Cells. *Anticancer Res* (2013) 33:4421–30.
31. Wu S, Wang Y, Yuan Z, Wang S, Du H, Liu X, et al. Human Adipose–Derived Mesenchymal Stem Cells Promote Breast Cancer MCF7 Cell Epithelial –Mesenchymal Transition by Cross Interacting With the TGF–β/Smad and PI3K/AKT Signaling Pathways. *Mol Med Rep* (2019) 19:177–86. doi: 10.3892/mmr.2018.9664
32. Chen Z, Wang Y, Liu W, Zhao G, Lee S, Balogh A, et al. Doxycycline Inducible Kruppel-Like Factor 4 Lentiviral Vector Mediates Mesenchymal to Epithelial Transition in Ovarian Cancer Cells. *PLoS One* (2014) 9:e105331. doi: 10.1371/journal.pone.0105331
33. Zhao G, Zhang W, Dong P, Watari H, Guo Y, Pfeffer LM, et al. EIF5A2 Controls Ovarian Tumor Growth and Metastasis by Promoting Epithelial to

Mesenchymal Transition *via* the TGFbeta Pathway. *Cell Biosci* (2021) 11:70. doi: 10.1186/s13578-021-00578-5
34. Baasse A, Juerss D, Reape E, Manda K, Hildebrandt G. Promoting Effects of Adipose-Derived Stem Cells on Breast Cancer Cells Are Reversed by Radiation Therapy. *Cytotechnology* (2018) 70:701–11. doi: 10.1007/s10616-017-0172-6
35. Wang Y, Chu Y, Yue B, Ma X, Zhang G, Xiang H, et al. Adipose-Derived Mesenchymal Stem Cells Promote Osteosarcoma Proliferation and Metastasis by Activating the STAT3 Pathway. *Oncotarget* (2017) 8:23803–16. doi: 10.18632/oncotarget.15866
36. Wang Y, Liu J, Jiang Q, Deng J, Xu F, Chen X, et al. Human Adipose-Derived Mesenchymal Stem Cell-Secreted CXCL1 and CXCL8 Facilitate Breast Tumor Growth By Promoting Angiogenesis. *Stem Cells* (2017) 35:2060–70. doi: 10.1002/stem.2643
37. Koellensperger E, Bonnert LC, Zoernig I, Marme F, Sandmann S, Germann G, et al. The Impact of Human Adipose Tissue-Derived Stem Cells on Breast Cancer Cells: Implications for Cell-Assisted Lipotransfers in Breast Reconstruction. *Stem Cell Res Ther* (2017) 8:121. doi: 10.1186/s13287-017-0579-1
38. Rowan BG, Lacayo EA, Sheng M, Anbalagan M, Gimble JM, Jones RK, et al. Human Adipose Tissue-Derived Stromal/Stem Cells Promote Migration and Early Metastasis of Head and Neck Cancer Xenografts. *Aesthet Surg J* (2016) 36:93–104. doi: 10.1093/asj/sjv090
39. Bilyk O, Coatham M, Jewer M, Postovit LM. Epithelial-To-Mesenchymal Transition in the Female Reproductive Tract: From Normal Functioning to Disease Pathology. *Front Oncol* (2017) 7:145. doi: 10.3389/fonc.2017.00145
40. Song IH, Kim KR, Lim S, Kim SH, Sung CO. Expression and Prognostic Significance of Epithelial-Mesenchymal Transition-Related Markers and Phenotype in Serous Ovarian Cancer. *Pathol Res Pract* (2018) 214:1564–71. doi: 10.1016/j.prp.2018.07.016

**Conflict of Interest:** The authors declare that the research was conducted in the absence of any commercial or financial relationships that could be construed as a potential conflict of interest.

**Publisher's Note:** All claims expressed in this article are solely those of the authors and do not necessarily represent those of their affiliated organizations, or those of the publisher, the editors and the reviewers. Any product that may be evaluated in this article, or claim that may be made by its manufacturer, is not guaranteed or endorsed by the publisher.

frontiers in Oncology

REVIEW
published: 07 January 2022
doi: 10.3389/fonc.2021.744257

# Ovarian Biomechanics: From Health to Disease

*Chenchen Sun*[1†], *Xiaoxu Yang*[1†], *Tianxiao Wang*[1†], *Min Cheng*[2*] *and Yangyang Han*[1*]

[1] School of Life Science and Technology, Weifang Medical University, Weifang, China, [2] Department of Physiology, Weifang Medical University, Weifang, China

Biomechanics is a physical phenomenon which mainly related with deformation and movement of life forms. As a mechanical signal, it participates in the growth and development of many tissues and organs, including ovary. Mechanical signals not only participate in multiple processes in the ovary but also play a critical role in ovarian growth and normal physiological functions. Additionally, the involvement of mechanical signals has been found in ovarian cancer and other ovarian diseases, prompting us to focus on the roles of mechanical signals in the process of ovarian health to disease. This review mainly discusses the effects and signal transduction of biomechanics (including elastic force, shear force, compressive stress and tensile stress) in ovarian development as a regulatory signal, as well as in the pathological process of normal ovarian diseases and cancer. This review also aims to provide new research ideas for the further research and treatment of ovarian-related diseases.

**Keywords: ovary, biomechanics, signal transduction, ovarian cancer, follicle development**

OPEN ACCESS

***Edited by:***
*R. Steven Conlan, Swansea University, United Kingdom*

***Reviewed by:***
*Lewis Webb Francis, Swansea University, United Kingdom*
*Andrea Gazze, Swansea University, United Kingdom*

***Correspondence:**
*Yangyang Han*
*hanyy@wfmc.edu.cn*
*Min Cheng*
*mincheng@wfmc.edu.cn*

*†These authors have contributed equally to this work*

***Specialty section:***
*This article was submitted to Gynecological Oncology, a section of the journal Frontiers in Oncology*

***Received:*** *20 July 2021*
***Accepted:*** *13 December 2021*
***Published:*** *07 January 2022*

***Citation:***
*Sun C, Yang X, Wang T, Cheng M and Han Y (2022) Ovarian Biomechanics: From Health to Disease. Front. Oncol. 11:744257. doi: 10.3389/fonc.2021.744257*

The mammalian ovary is a major reproductive organ, ensuring various functions essential to the reproductive process. Its most obvious role is the production and release of functional female gametes, oocytes. Growing evidence indicates that the growth and development of the ovary, as well as the malignant process, are accompanied by changes in biomechanical characteristics, but only superficially. Here, we review the roles of biomechanics in normal ovarian development and ovarian diseases, aiming to provide new insights into understanding the mechanisms of ovarian biomechanics.

**Abbreviations:** IGFR, insulin-like growth factor I receptor; FBN3, fibrillin 3; GDF 9, factor 9; BMP 15, bone morphogenetic protein 15; TGF, transforming growth factor; BM, basement membrane; HP, hydrostatic pressure; PI3K, phosphoinositide 3-kinase; YAP, Yes-associated protein; CCN, connective tissue growth factors; FSH, Follicle-stimulating hormone; IGF, insulin-like growth factors; PDMS, polydimethylsiloxane; DSL, Delta, Srrate, Lag2; LLC, large latent complex; Mfs, myofi broblasts; HA, hyaluronic acid; GAGs, glycosaminoglycans; 3D, three-dimensional; AKT, protein kinase B; RPS6, ribosomal protein S6; ERK, extracellular regulated protein kinases; SHP2, Src-homology-2-containing phosphotyrosine phosphatase; ECM , Extracellular matrix; Col, collagen; Alg, alginate; MVC, microvibration culture; PARP, poly (ADP-ribose) polymerase; Myo-II, nonmuscle myosin II; HBO1, histone acetyltransferase; PCOS, Polycystic ovary syndrome; IVA, in vitro activation; e-cadherin, Epithelial (E)3-cadherin; n-cadherin, Neural (N)-cadherin; MMP-14, Membrane type 1 matrix metalloprotein.

## FOLLICLE DEVELOPMENT AND MECHANICAL FACTORS

As one of the main reproductive organs of the female reproductive system, the growth and development of the ovary are extremely complex processes involving the participation of multiple regulatory mechanisms, regulatory factors and effect factors. Additionally, some studies have suggestion that mechanical factors are involved in normal ovarian development and the malignant process of ovarian cancer in mammals and play vital roles (1–5). Based on the role of biomechanical factors in the growth and development of various tissues and organs of the human body, their influence on the cell and tissue levels of bone (6), muscle (7), intestine (8), joints (9) and other organs has been studied in depth. Additionally, location shifts and tissue remodeling occur during follicle formation, suggesting that extracellular matrix (ECM) plays an important role in follicle development and that the mechanics involved in the process of ovarian growth and development have gradually attracted increased attention (10, 11).

### Change in the Mechanical Environment During Follicle Development

The follicle is the fundamental function tissue of mammalian ovary. According to their morphological and functional characteristics, follicles can be divided into primordial, primary, secondary, and mature follicles. Human follicle development begins in the fetal period, from the primal follicle to the primary follicle transition. Primordial follicles are composed by oocytes and pre-granular cells which are single spindle-shaped layer like (12). When stimulated by biological signals, the primordial follicles are recruited into the growth pool, and the shape of granular cells transform from spindle-flat to cubic thus form primary follicles. Later, granular cells proliferate from monolayer to multiple layers with appearance of fluid cavities with different sizes which further synthesize follicular cavities, and at that time, secondary follicles are formed (13).Further, the secondary follicles develop to antral follicles under the regulation of follicle-stimulating hormones (FSH) and finally arrive the ovulatory preparation period (**Figure 1A**). Overall, the follicles development process is mainly comprised the increased number of granulosa cells and the enlargement of oocytes.

In the process of follicles development, some factors were confirmed to involved this. For example, growth factor 9 (GDF 9), bone morphogenetic protein 15 (BMP 15) and BMP 6 were thought to be involved in the recruitment of primordial follicles (16, 17), and GDF 9 and BMP 15 were involved in the regulation of oocyte maturation and the function of granulosa cell (17); Furthermore, Vendola K et al. (18) found that insulin-like growth factor I receptor (IGFR) was increased in oocytes after androgen treatment, which stimulated the activation of primordial follicles and the formation of primary follicles (18).

In all stages of follicle development, mechanical factors are involved, affecting the entire process. Normal ovarian structure is divided into two parts: the cortex and the medulla. Different structural areas provide different hardness environments for primordial follicles: the ovarian cortex comprises connective tissue, which occupies most of the ovary; however, the medulla is located in the center of the ovary and comprises loose connective tissue (19). In general, the rigidity of the cortex is greater than that of the medulla, providing a rigid environment for the complete

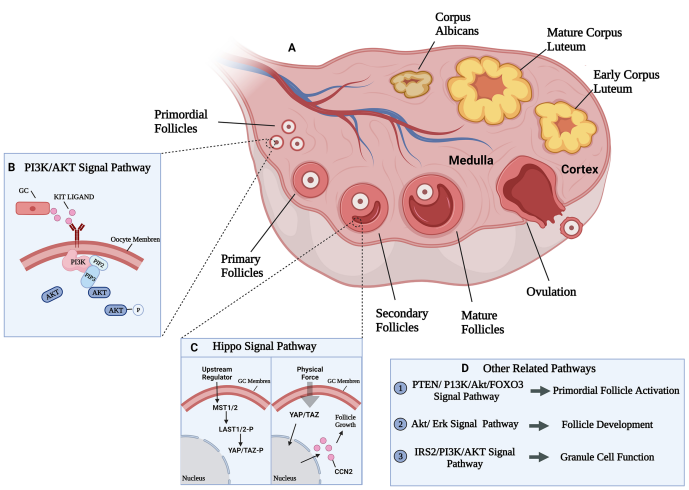


**FIGURE 1** | Ovarian developmental processes and some of the mechanical pathways involved. **(A)** The growth and development process of follicle and related signal pathways. Follicle development goes through primordial, primary, secondary, and mature follicles four stages. **(B)** PI3K/AKT signal pathway participate in primordial follicles activation. PI3K was activated by growth factor KIT LIGAND (KL) and converted phosphatidylinositol 4,5-bisphosphate (PIP2) into phosphatidylinositol 3,4,5-trisphosphate (PIP3) at the cell membrane, leading to AKT phosphorylation and activation, eventually lead to primordial follicles activation (14). **(C)** Activated state of Hippo signaling in granulosa cells (left). Uncharacterized upstream factors stimulate the Hippo signaling cascade (MST1/2 and LATS1/2) to phosphorylate and restrict the activition of two transcriptional coactivators (YAP and TAZ). Disruption of Hippo signaling in granulosa cells (right). Physical force disrupt the Hippo signaling cascade by translocating un-phosphorylated YAP/TAZ into the nucleus to bind the TEAD transcriptional factors, thus induce expression of CCN which are involved in granulosa cell proliferation and survival, leading to follicle growth (15). **(D)** Other related signal pathways in follicle development.

preservation of primordial follicles. With the production of secondary follicles, the rigid environment of the ovarian cortex limits the maturation and expansion of the follicles, and the secondary follicles then transfer from the cortex to the medulla to obtain a softer environment (20). Additionally, in the process of follicles development, the zona pellucida consisted with the mucopolysaccharide which secreted by granular cells became thickened, and the structure became denser, it suggested that the matrix environment which surround granulosa cells has changed. As early as 1996, a study compared the activation ratio of primordial follicles *in vivo* to primordial follicles *in vitro* in cattle and found that the activation of primordial follicles *in vitro* was significantly better, implying that the ovarian matrix environment plays a particular role in the activation and growth of follicles (21). Felder S et al. (22) used the pore structure formed by a macroporous alginate (Alg) scaffold to simulate the physical environment of the ovarian cortex, regulate the development of follicles, and successfully promote the growth of ovarian primitive follicles *in vitro* (22), suggesting that the internal mechanical structure of the ovary may affect the development of the ovary.

In the process of follicle activation and development, the expression of genes that regulate matrix hardness is in a particular dynamic state. The fibrillin 3 (FBN3) gene regulates the expression of extracellular matrix (ECM) -related proteins and fibrin, uses the transforming growth factor β (TGF-β) signaling pathway to indirectly affect the function of fibroblasts in the matrix, and regulates the production and deposition of collagen (Col) in normal and fibrotic tissues (23). In the early stage of follicle development, during the transition from primordial to primary follicles, FBN3 is expressed in the stromal area around the follicle (24), implying that this gene may regulate the content of collagen to regulate the mechanical environment around the follicle, thereby affecting follicle development.

Not only the above influence factors, some literatures demonstrated that the biomechanics of basement membrane (BM) affected the development of follicles. The BM regulates and maintains the morphology of the epithelium, and its structure changes in different follicular development periods. Chlasta J et al. (25) found that in late follicular development, the follicular morphology changes from cuboidal to squamous or columnar increase the density and growth of follicular fibers then resulting the increased stiffness of BM caused by the embedded of follicular fibers. This change in stiffness creates areas with alternating soft and hard biomechanics which furthermore maintain the follicular morphology (25). Additionally, pre-ovulatory follicles are separated from the ovaries and placed under hydrostatic pressure (HP), and an increase in the number of mature oocytes, indicating that HP promotes oocyte maturation and follicle development (26). The effect of the mechanical environment on the follicle is not limited to the internal environment of the ovary but is in a state where follicle development can be regulated at all times.

## Mechanical Signal Regulation in Follicle Development

The influence of mechanical factors on follicle development is finally realized through the regulation of well-known classical mechanical pathways, such as PI3K or Hippo pathways. Researchers have demonstrated that phosphoinositide 3-kinase (PI3K)signaling pathway stimulation induced the activation of the primordial follicle pool that can lead to rapid depletion of the pool and subfertility (27, 28) (**Figure 1B**). In the ovary, most primitive follicles are in dormant state, while when the follicles transfer from stiffer cortex to softer medulla area, the stimulation of Hippo signaling may slow down the growth of follicles (29). Meanwhile, other studies confirmed that Hippo mechanical signal in the follicles near the cortex may be blocked because of the destruction of the highly rigid microenvironment, resulting in increased Yes-associated protein (YAP) activity and connective tissue (CCN) growth factors secretion, resulting in activation and maturation of primordial follicles and follicle development (15, 30) (**Figure 1C**).

Moreover, studies also confirmed the major regulation of Akt and Erk signaling pathways in follicle growth and development (**Figure 1D**). Ryan K et al. (31) found that inhibition of Akt and Erk pathways inhibit the stimulatory actions of follicle-stimulating hormone (FSH) and insulin-like growth factors (IGF), and thus influence the growth of cultured follicle cells *in vitro* using the inhibitor of Akt or Erk (31). Besides, decreasing the activation of Akt resulted the lower synthesis of estradiol and progesterone and thus slowing down granulosa cell development (32). The combination of ovarian fragmentation and Akt stimulant increases the production of secondary follicles and pre-ovulatory follicles, and trigger actin polymerization and block Hippo signaling (33), it is suggested that Akt and Hippo signaling pathways may interactive in follicles development.

# MECHANICAL CHARACTERISTICS OF ECM AND FOLLICLE DEVELOPMENT

The ECM exists in all tissues and organs and comprises mainly water, protein (collagens, elastin, fibronectin, laminins, and several other glycoproteins) and polysaccharides (34). Not only acts as physical supporting role, ECM also has crucial roles because of its special structure. Specifically speaking, various receptors are found on the ECM that mediate different physiological processes. Besides, the ECM of different tissues or organs has a specific structural composition and heterogeneity (35). Studies have showed that in the early stage of stem cell differentiation and early embryonic development, the content of elastin, collagen, BM protein and laminin, increase, providing suitable rigidity for the growth and development (36). Furthermore, similarity function was found in ovary.

## Changes in the Mechanical Characteristics of the ECM During Follicle Development

Changes of ECM elasticity can produce mechanical signals, and such signals not only change the biological characteristic of ECM, but also result in changes of stress fibers and cytoskeleton, which may further regulate the activity level of YAP/TAZ (37). YAP/TAZ is then activated and transferred to

nucleus and combines with transcription factors to regulate gene expression (38, 39). Other research found that stiffer rigidity of ECM activates TGF-β, and this activation is mediated by the high contractility produced by a-ama-positive stress fibers *via* integrins to the large latent complex (LLC), which releases TGF-β1 when anchored in the stiff ECM. This activation acts to induce myofibroblasts (Mfs) differentiation, which then regulate normal physiological processes of cells or pathological fibrosis, but with reduced activation of TGF-β1 compared to softer matrices (40, 41).

The preservation of oocytes depends on the ovarian environment. Oocytes are in dormant state in the ovary, and the surrounding granular cells and ECM are the main sources of mechanical stress on oocytes. Specificity speaking, the abundant of actin filaments in granular cells produce pressure on oocytes to keep them in dormant state, and the fibronectin and collagen type IV in cortical ECM region which around the perifollicular area also maintain the dormant state. Nagamatsu G et al. (42) found that the number of activated oocytes increased after using collagenase type IV and trypsin to elimination collagen type IV and fibronectin, and the number of large oocytes (>50 μm in diameter) also increased under similar condition (42), demonstrated the crucial role of ECM in maintain oocytes' dormant state.

Following the activation of follicle development, the mechanical microenvironment of ECM appears to be different. Human prepubertal ECM is stiffer caused by the higher percentage of thick collagen fibers in prepubertal ovary, and further reason is the decreased elasticity of thick collagen fibers make ECM less compliant and more rigid (20). Combining the mechanical characteristics of follicle development, the stiffer prepubertal ECM environment may provide suitable environment for preservation of primordial follicles.

Excepting the collagen, ECM also has other components, such as hyaluronic acid (HA) and elastin, while their changes will also lead to the mechanical changes of ECM. HA is a glycosaminoglycan, and as the main component of the ECM, it is widely confirmed that the changes of HA will alter the mechanical properties of ECM (43–45). Besides, HA also plays a certain role in cell differentiation and cell growth (46), promoting muscle cell proliferation and other physiological functions (47). During follicle development, high concentrations of low-molecular-weight hyaluronic acid can cause abnormal meiotic abnormalities and abnormal aging of oocytes (48), and it may also due to the mechanical changes of ECM. As another major component of ECM, the content of elastin also changes in different stages of ovarian development. The synthesis of elastin in the adult ovary gradually stops, and the content is lower than that in the prepubertal ovarian elastin (20). Considering the important role of elastin in mechanical homeostasis (49, 50), the changes of elastin synthesis may alter the mechanical properties of ECM and then play a role in ovarian development.

## ECM Simulation of Ovarian Development *In Vitro*

In order to research the influence of ECM on ovarian development, many studies have attempted to use biological materials with different properties to create a suitable physical environment for ovarian development to achieve ovarian culture *in vitro*. For example, researchers commonly used biological materials, such as hyaluronic acid and Alg, form a matrix environment with different stiffnesses to support follicle development. Kim et al. (51) constructed a 3D culture of ovarian follicles and found that Alg which has harder rigidity limiting follicle development compared with the hydrogel formed by hyaluronic acid which has softer rigidity (51). He et al. (52) produced a new ECM materials composed of different concentration collagen and Alg, and found that compared with the softer ECM composition (0.5% collagen core and 2% Alg shell), ovarian tissue cultured on stiffer ECM composition (0.5% Col plus 0.5% Alg as the core and 2% oxidized alginate shell) produced at least 10% higher estradiol, and the development rate of bionic ovarian micro-tissues was also increased (52), indicating the mechanical characteristic of ECM played a major role in ovarian development.

Furthermore, the mechanical microvibration culture (MVC) system was used to culture human immature oocytes *in vitro* and successfully obtained normal mature oocytes with development potential comparable to mature oocytes (53). During the construction of the above ovarian *in vitro* culture ECM model, the development of the ovary was simulated by changing the ratio of the construction materials, showing that different ECM structures have different effects on the developmental rate of the ovary. Confirm the importance of the ECM mechanical environment in the normal development of the ovary, and to further understand the role of the ECM in ovarian development, indicating that it is necessary to further explore the specific mechanism by which the ECM mechanical environment regulates ovarian development.

# OVARIAN CANCER AND BIOMECHANICS

As a global problem, ovarian cancer is no longer regarded as a single disease but as a heterogeneous disease with different histological subtypes and different identifiable risk factors, origin cells, molecular and clinical features and treatments (54). Among them, epithelial ovarian cancer has the highest incidence, accounting for approximately 90% of ovarian cancer (55). Ovarian cancer is usually diagnosed at an advanced stage because of the lack of an effective early screening strategy. However, with the continuous research and progress of genetic testing based on personal or family history, ethnic background or other demographic characteristics, some individuals with a high risk of ovarian cancer, such as those with germline mutations in BRCA1 or BRCA2, have been identified. However, we did not see any improvements in mortality rates (56). Presently, ovarian cancer treatment is dominated by surgery and platinum chemotherapy. Angiogenesis inhibitors, poly (ADP-ribose) polymerase (PARP) inhibitors and immunotherapy (cytotoxic T lymphocyte antigen 4 and PD-1) have updated the treatment model of ovarian cancer to a certain extent, while most of them are still in preclinical trials (57). Effective methods of prevention and early screening as well as promising new treatment models

remain to be explored, and the study of biomechanics has shown potential in this field.

## Elastic Changes of Ovarian Cancer Cells

Studies have shown that ovarian cancer cells are different from normal cells and healthy cells in growth, adhesion, morphology and cytoskeleton structure (58, 59). This finding is partly due to cell biomechanics (elastic and viscous behavior), the study of which is crucial to the development of disease treatments and detection methods. Cell biomechanics is an important part of biology. It involves the study of cell membrane, cytoskeleton deformation, elastic constant, viscoelasticity, adhesion and other mechanical properties under mechanical load, and the effects of mechanical factors on cell growth, development, maturation, proliferation, senescence and death and its mechanism. It is the basis and key point to reveal the life activities of cells. As more physical properties of cells are investigated, such as growth, adhesion, morphology and cytoskeleton structure we mentioned above are all physical properties, different properties may become potentially powerful tools for cancer diagnosis and treatment. Many research groups have calculated the elastic modulus of cancer cells and believe that cancer cells are "softer" or deform faster than healthy, untransformed cancer cells (60, 61). Ovarian cancer is no exception. Although the characterization of information concerning the mechanical properties of human malignant and benign ovarian cells trails that of other cancers because of the lack of advanced detection methods, with the continuous progress of technology, such as ultrasonic elastography and magnetic resonance elastography, a series of studies have also shown a significant relationship between the viscoelasticity and biological properties of ovarian cancer cells.

Ketene et al. (62) relied on the spontaneous transformation of epithelial cells on the surface of mouse ovaries in cell culture and established a primary cell model of progressive ovarian cancer in C57BL/6 mice (62). The results showed an obvious transfer pattern in the early, middle and late transformation of the cell line. When the same cell line changes from the benign to invasive stage, an increasing number of hypoelastic cells are found in the cell population. This high invasiveness, high mobility, low elasticity and viscosity may be related to significant differences in cytoskeletal structure (63).

Both the cell changes in different periods and the properties of different pathological types of ovarian cancer cells have been quantified. The elastic modulus of mucinous ovarian cancer, serous ovarian cancer, mature teratoma and endometriosis was quantitatively classified by atomic force microscopy. Ansardamavandi et al. (64) mechanically characterized human ovarian tissues with four distinct pathological conditions: mucinous, serous, and mature teratoma tumors, and non-tumorous endometriosis by using atomic force microscopy. Mechanical elasticity profiles were quantified and the resultant data were categorized using K-means clustering method, as well as fuzzy C-means, to evaluate elastic moduli of cellular and non-cellular parts of diseased tissues and compare them among four disease conditions. Samples were stained by hematoxylin-eosin staining to further study the content of different locations of tissues. They found that pathological state vastly influenced the mechanical properties of the ovarian tissues. Significant alterations among elastic moduli of both cellular and non-cellular parts were observed. Mature teratoma tumors commonly composed of multiple cell types and heterogeneous ECM structure showed the widest range of elasticity profile and the stiffest average elastic modulus of 14 kPa. Samples of serous tumors were the softest tissues with elastic modulus of only 400 Pa for the cellular part and 5 kPa for the ECM. Tissues of other two diseases were closer in mechanical properties as mucinous tumors were insignificantly stiffer than endometriosis in cellular part, 1300 Pa compared to 1000 Pa, with the ECM average elastic modulus of 8 kPa for both. In short, The higher incidence of carcinoma out of teratoma and serous tumors may be related to the intense alteration of mechanical features of the cellular and ECM, serving as a potential risk factor which necessitates further investigation (64). A similar outcome was found in a study by Chen et al. (65) the elasticity and viscosity of ovarian cancer cells OVCAR-3 (1195.72 ± 122.94Pa) and HO-8910 (996.27 ± 52.56Pa) were significantly lower than those of human ovarian surface epithelial cells (2160.94 ± 167.77 Pa) (65). Further detection showed that the migration/invasion ability of OVCAR-3 and HO-8910 cells was significantly higher than that of the control group.

Based on the effective phenotypic changes, that is, the physical structure is sufficient to affect the behavior of cancer cells, exploration of the mechanism of "low cellular elasticity-high metastasis risk" was also gradually conducted. Differences in focal adhesion signals (higher FAK expression) and Rho/ROCK activity (increased RhoA activity) suggest that they are involved in biomechanically driven cellular responses (66), KRAS (67), nonmuscle myosin II (Myo-II) (68), and histone acetyltransferase (HBO1) (69) have also been studied to change the mechanical phenotype of ovarian cancer cells through signal transduction (**Figure 2**), and the change of cellular elasticity was measured directly by atomic force microscopy. Thereby changing the metastatic tendency of ovarian cancer. According to this physiological characteristic, the discovery and application of selenium nanoparticles (70) and gold nanoparticles (71), which can change the mechanical characteristics of the cell membrane, may provide a new idea for ovarian cancer treatment.

## Ovarian Cancer and Shear Stress

Whether because of the continuous peristalsis of the gastrointestinal system or exposure to the ascites environment, the surface of the ovary is exposed to peritoneal pressure and shear force, creating a mechanical microenvironment for the ovarian cancer cells (72). The study of the effect of shear stress on the occurrence and development of ovarian cancer is accompanied by the progress of corresponding experiments and mathematical models; particularly, there is a need for computer simulation models to improve our understanding of the physiological stress that occurs in the peritoneal cavity. Because the movement of the body is directly related to the level of shear stress experienced by floating and attached ovarian cancer, these complex interactions must be modeled and analyzed using hydrodynamic systems (73).

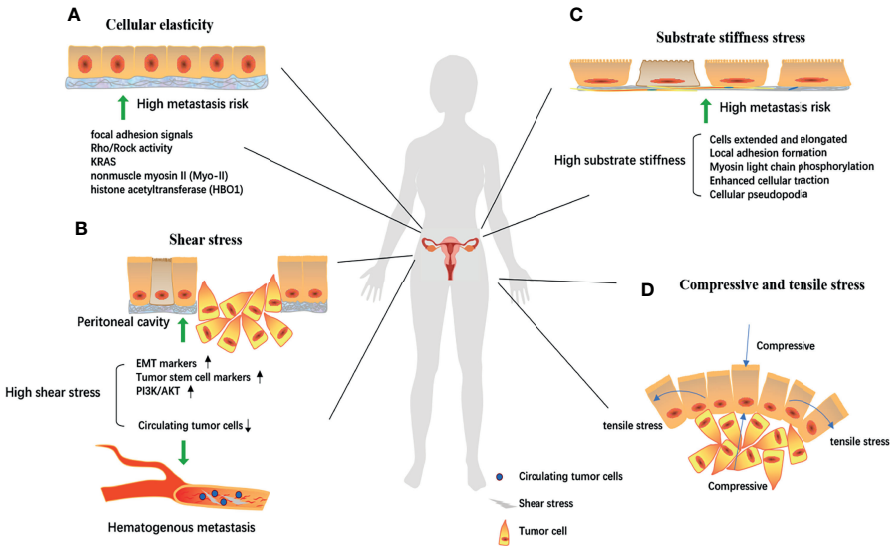


**FIGURE 2** | The biomechanical mechanism of ovarian cell canceration and metastasis. **(A)** Focal adhesion signals, Rho/Rock activity, KRAS, nonmuscle myosin II (Myo-II), histone acetyltransferase (HBO1) could reduce cell elasticity through signal transduction, thereby increasing the risk of metastasis; Under high shear environment, the epithelial-mesenchymal transformation and tumor stem cell markers are significantly expressed. **(B, C)** The abnormal activation of the PI3K/Akt pathway significantly increases the malignancy of cells. While in hematogenous metastasis, high shear stress destroyed circulating tumor cells and prevented cancer metastasis; Local adhesion formation, myosin light chain phosphorylation, enhanced cell traction, and cellular pseudopodia produced by extracellular matrix tissue increase substrate stiffness, gradually stretch and elong the cells, thereby making ovarian cancer cells have a high risk of metastasis. **(D)** Proliferation of ovarian cancer cells will produce tension stress and compressive stress on the cells around the developing mass and the increase of these two stress will further increase the invasion ability of tumor cells. EMT, epithelial-mesenchymal transformation.

The *in vitro* progression model of ovarian cancer is widely used in the study of shear stress. Hyler et al. (74) conducted experiments to test the different metastatic potentials of mouse ovarian cancer cell lines under the influence of low-level shear stress (74). Benign to highly invasive epithelial cell lines of ovarian cancer were used. OCE1 (healthy person) and SKOV3 (human ovarian clear cell adenocarcinoma) cells were exposed to fluid shear stress < 1 dyne/cm2 on a rotating plate for 12 days. Even with low-intensity shear, genomic changes were observed in the treated cells. Shear stress may not only be a contributing factor to the progression of ovarian cancer but also a key factor in benign cell deterioration, which leads to changes in the mechanical phenotype of cells and is associated with the risk of ovarian cancer metastasis (**Figure 2**). Specifically, after exposure to three consecutive 96 h (288 h total) fluid shear stress, a significant increase in CREST-positive (chromosome mis-segregation) micronuclei was observed in all cell lines ($p < 0.001$), as well as low levels of CREST-negative (DNA fragments) micronuclei observed in SKOV-3 (0.4% ± 0.1%) cells. Besides, in non-tumorigenic MOSE-E cells, fluid shear stress may promote the generation of tetraploid cells by inducing defective cell division. Researchers also studied spheroid formation, which reflects a more metastatic phenotype, for it was related to change of cytoskeleton organization. The tumorigenic cells lines (SKOV-3) responded to fluid shear stress by detaching and forming aggregates or spheroids. SKOV-3 spheroids grew in diameter from 139.5 ± 10.6μm to 208.6 ± 87.8μm after repeated passaging and were able to re-attach to the culture dishes with a moderate adherent monolayer outgrowth. A model that mimics peritoneal fluid pressure and shear stress caused by continuous peristalsis of the gastrointestinal system was constructed by Avraham-Chakim et al. (75) based on fluid-induced wall shear stress exposure in epithelial ovarian cancer (75). The authors used OVCAR-3 cell line, cultured them in a simulated physiological environment, applied wall shear forces of 0.5, 1.0, and 1.5 dyne/cm2 on the cell surface, and then studied the changes in mechanical indexes, such as the cytoskeleton and actin. Formation of a thick filamentous network of stress fibers was observed in cells exposed to shear stress, compared with control cultures in which actin was present mainly in the peripheral areas of the cell. There was a linear relationship between the magnitude of wall shear stresses and the level of stress fibers formation and that the level of stress fibers formation depended on the magnitude of shear stress. Furthermore, the formation of stress fibers also leads to cell elongation. These conditions occur during the occurrence and development of tumors. For example, a similar outcome of shear stress induced actin-tubulin remodeling was also observed in metastatic esophageal cancer cells (76). It suggests that stress fibers may be associated with the development of ovarian cancer.

The development and metastasis of ovarian cancer caused by increased shear stress must be accompanied by potential cellular and molecular mechanisms. Researchers have noticed this and performed a series of studies on the related mechanisms. Ip CK et al. (77) found that epithelial-mesenchymal transformation and expression of tumor stem cell markers can be obtained when

ovarian cancer cells grow under fluid shear stress, indicating a significant increase in the degree of malignancy of ovarian cancer cells (77). The same results were also observed in Rizvi's et al. study (78). Additionally, these cells developed significant chemotherapy resistance to cisplatin and paclitaxel, a finding that may be attributed to abnormal activation of the PI3K/Akt pathway.

However, during process of hematogenous metastasis, the opposite results was found. High shear stress destroyed circulating tumor cells and prevented cancer metastasis. Studies have shown that a high shear stress of 60 dyne/cm2 during intensive exercise can kill more than 90% of circulating tumor cells within 4 hours. Compared with the low shear stress of 15 dyne/cm2 at rest, long-term high shear stress treatment effectively reduces the survival rate of highly metastatic and drug-resistant cancer cells (79). The killing effect of this high shear stress on cancer cells can be blocked by platelets (80). Specifically, when platelets are under shear stress, lactate dehydrogenase is significantly decreased, indicating that the nondestructive cycle time of cancer cells is prolonged *in vivo*.

The reverse effect of this shear stress in the process of *in vitro* and hematogenous metastasis is an interesting and contradictory discovery, suggesting the dual mechanism of shear stress in a complex body environment: on the one hand, continuous shear stress can cause changes in the cell genome and mechanical phenotype, leading to the deterioration of normal cells and metastasis of cancer cells; on the other hand, high shear stress can destroy cancer cells in the circulatory system and reduce the risk of cancer metastasis. Future research should be more targeted, specifically describing the mechanism of shear stress under different environmental conditions.

## Ovarian Cancer and Substrate Stiffness Stress

The ECM provides physical support for tissues, organs and signaling pathways through integrins and other membrane receptors (81). This characteristic also determines its key position during tumor metastasis. A series of studies have been performed to understand the interaction between the occurrence and development of cancer cells and the physical properties of the substrate (76–80).

Cells are very sensitive to substrate stiffness and texture. To explore the cell response to these two types of input in a precisely controlled way, Park et al. (82) analyzed the substrate response of Chinese hamster ovary cells to different stiffnesses (from 1.8 MPa to 1.1 GPa). With increasing substrate stiffness, the cells gradually extended and elongated in a dependent manner (82). This change was partly attributed to local adhesion formation, myosin light chain phosphorylation and enhanced cellular traction (83), as well as cellular pseudopodia produced by ECM tissue under strong substrate stiffness (84), which is a prelude to metastasis. The increase in substrate stiffness may be closely related to the distant metastasis of ovarian cancer cells (**Figure 2**). The epithelial-mesenchymal transformation pathway (85) and the Rho/ROCK pathway (86) may play important regulatory roles.

## Ovarian Cancer and Compressive and Tensile Stress

Ovarian cancer cells are subjected to a series of compression and stretch stimuli that contribute to mechanical transduction. On the one hand, as ovarian cancer expands, it produces tension on the cells around the developing mass; on the other hand, the cells are exposed to chronic loads from abdominal cavity, surrounding cell displacement and growth-induced stress (87). We can understand that when the body surface is swollen, inflammatory exudation or congestion will produce a squeezing force on the skin, and the skin will also have a counteracting squeezing force on the inside, which is compressive stress. Meanwhile, the normal surface of the skin expands and the muscle fibers pull each other, resulting in tensile stress (**Figure 2**). Relatively few studies have investigated the tensile stress of ovarian-specific cells (88). The regulation of the RhoA/ROCK signaling cascade seems to be critical and further plays an important role in vascular endothelial growth factor-mediated angiogenesis (89).

Studies on the effect of compressive stress on cancer progression have found a trend toward late invasion and metastasis phenotypes. Klymenko et al. (87) used an *in vitro* model system to simulate the effects of static pressure on four ovarian cell lines under ascites pressure for 6 or 24 hours. The enhancement of invasive ability was accompanied by an increase pressure, and the expression of genes related to epithelial-mesenchymal transformation and dispersion of multicellular aggregates was regulated by compressive stress to varying degrees. It was noteworthy that the expression of Epithelial (E) 3-cadherin (e-cadherin) and neural (N)-cadherin (n-cadherin) were changed under static pressure, further affect cell-cell and cell-matrix adhesion, while no changes of cell proliferation related signaling pathways were observed (87). Burkhalter et al. (88) proposed that integrin induced e-cadherin internalization and activated β-catenin, thus co-regulated intercellular linkage mainly according to Wnt/β-catenin signaling pathway in ovarian cancer invasion and metastasis. And further investigate indicated that these influences might cause by the changed expression of membrane type 1 matrix metalloproteinases (MMP-14) (88). In general, the response of Wnt signaling pathway under compressive and tensile stress may be one of the potential molecular mechanisms in ovarian cancer invasion and metastasis. In a similar study, Novak et al. (90) encapsulated high-grade serous ovarian cancer cell lines in simulated ECM hydrogels containing agarose collagen and type I collagen, and used a 3D compression bioreactor to observe the effects of compressive stress on ovarian cancer cells under limited cyclic or static pressure for 24 and 72 hours, respectively. Compression stimulation not only significantly increased the proliferation and invasion of ovarian cancer cells but also caused chemotherapy resistance in ovarian cancer cells, which may be attributed to the abnormal activation of CDC42 (90). Notably, whether the stem cell characteristics of ovarian cancer cells will appear under compressive stress and promote development and metastasis warrants further study.

### Biological Characteristics of Ovarian Cancer Spheroids

Multicellular spheroids (MCS) also need to be mentioned. Ovarian cancer cells typically spread and metastasize within the abdominal cavity, where ascites promotes this process. Metastatic ascites contains MCS, which reduces the sensitivity of the body to chemotherapy (91). Through *in vivo* lineage tracing, the researchers found that MCS appeared preferentially from collective detachment, rather than aggregation in the abdomen (92). MCS usually appears as "blastuloid" spheroids after maturation, with a smooth profile and immotile cells (93). It is a dynamic structure composed of proliferating, non-proliferating and hypoxic regions. The spheroid neither binds nor allows cells to penetrate (94). This form can keep the internal cells from being damaged by external forces such as shear stress, and maintain phenotypic heterogeneity during dissemination (92).

## BENIGN OVARIAN DISEASES AND BIOMECHANICS

### Polycystic Ovary Syndrome

Polycystic ovary syndrome (PCOS) is a common endocrine disorder with many pathological manifestations, such as hormone disorders, insulin resistance, and ovarian dysfunction (oligoovulation, anovulation or polycystic ovary). Among them, insulin resistance may cause infertility (95); when the two pathological characteristics of hyperandrogenism and ovarian dysfunction are met, it can be diagnosed as PCOS (24).

With the restoration of Hippo signal transduction in the ovary, the growth of follicles slows down. Therefore, CCN growth factor treatment of these patients or topical application of actin polymerization drugs may offset the impact of Hippo on the ovaries and provide potential treatments for patients with PCOS. Additionally, the high androgenic properties of PCOS may be caused by a rigid biomechanical environment. In a mouse model, androgens secreted by follicles in a harder and denser Alg substrate were present at higher levels (96).

The dense collagenous and thickened ovarian cortex may create a biomechanically forbidden environment and change the mechanical signals in the ovary (29). Forbidden environment means the stiff cortical region, which could decrease local Hippo signaling, leading to overactivity of YAP, increased CCN growth factor secretion, stromal cell proliferation, and thecal cell hyperplasia. The follicles of patients with PCOS have polycystic ovaries with an increase in matrix hypertrophy; the granular cell substrate is thickened, and the electron density in the zona pellucida formed by secondary follicles increases. Ovarian drilling is often used for clinical treatment, and the mechanical forces generated in the process cause changes in the ovarian endocrine level, especially an luteinizing hormone decline (97, 98). Presently, a mechanobiology-based treatment that ruptures the ovarian cortex through *in vitro* activation (IVA) temporarily interrupts the Hippo pathway and promotes the secondary development of follicles. Compared with traditional surgical treatment, this mechanical biological therapy reduces damage to the ovaries (15).

### Ovarian Insufficiency

Ovarian insufficiency is a key fertility defect characterized by impaired expected follicular reserve (99). This defect occurs when the existing primordial follicles are depleted or inhibited in activation (100), and its pathophysiological mechanism has not yet been determined. Studies have shown that by obtaining primordial follicles in the ovarian cortex, autologous transplantation after the activation of mechanical destruction *in vitro* can stimulate their development into preantral follicles (101). Additionally, the interaction between the Akt pathway and mechanical signals is crucial for follicle activation, and this understanding has been applied to some treatments that may maintain female fertility.

## CONCLUSION

As a complex and relatively stable system, the development of ovaries and follicles has a profound impact on female fertility and human reproductive potential, and its entire biological behavior is mediated by the participation of biomechanics. Follicle maturation, ovarian development, and the occurrence and development of ovarian cancer all involve extensive interventions of mechanical signals. The elucidation of biomechanics is critical for enhancing our understanding of the pathophysiology of ovaries and follicles. Future research is expected to further characterize biomechanics and related signal transduction pathways.

## AUTHOR CONTRIBUTIONS

CS and XY wrote most of the manuscript. TW wrote parts of the manuscript and revised the manuscript. MC provided all supporting for this review. YH provided the concept and organized members to discuss the manuscript. All authors contributed to the article and approved the submitted version.

## FUNDING

The present study was supported by the National Natural Science Foundation of China (grant numbers: 81501683) and the Natural Science Foundation of Shandong Province (grant No. ZR2019MH047, ZR2015HL057).

## ACKNOWLEDGMENTS

The authors thank the lab members for their in-depth discussions and careful reading of this review.

## REFERENCES


1. Huang X, Yang X, Sun C, Huang S, Cheng M, Han Y. Biophysical Signal Transduction in Cancer Cells: Understanding Its Role in Cancer Pathogenesis and Treatment. *Biochim Biophys Acta Rev Cancer* (2020) 1874(2):188402. doi: 10.1016/j.bbcan.2020.188402
2. Hartanti MD, Hummitzsch K, Irving-Rodgers HF, Bonner WM, Copping KJ, Anderson RA, et al. Morphometric and Gene Expression Analyses of Stromal Expansion During Development of the Bovine Fetal Ovary. *Reprod Fertil Dev* (2019) 31(3):482–95. doi: 10.1071/rd18218
3. Stansfield FJ, Nöthling JO, Allen WR. Growth and Development of the Ovary and Small Follicle Pool From Mid Fetal Life to Pre-Puberty in the African Elephant (Loxodonta Africana). *BMC Vet Res* (2012) 8:119. doi: 10.1186/1746-6148-8-119
4. Takmaz O, Asoglu MR, Yuksel B, Gungor M, Tokat F, Kayhan KC, et al. Ovarian Incision Enhances Folliculogenesis: A Rat Model. *J Obstet Gynaecol Res* (2020) 46(10):2043–9. doi: 10.1111/jog.14373
5. McKenzie AJ, Hicks SR, Svec KV, Naughton H, Edmunds ZL, Howe AK. The Mechanical Microenvironment Regulates Ovarian Cancer Cell Morphology, Migration, and Spheroid Disaggregation. *Sci Rep* (2018) 8(1):7228. doi: 10.1038/s41598-018-25589-0
6. Moalli MR, Caldwell NJ, Patil PV, Goldstein SA. An *In Vivo* Model for Investigations of Mechanical Signal Transduction in Trabecular Bone. *J Bone Miner Res* (2000) 15(7):1346–53. doi: 10.1359/jbmr.2000.15.7.1346
7. Tidball JG. Mechanical Signal Transduction in Skeletal Muscle Growth and Adaptation. *J Appl Physiol (Bethesda Md: 1985)* (2005) 98(5):1900–8. doi: 10.1152/japplphysiol.01178.2004
8. Basson MD. Paradigms for Mechanical Signal Transduction in the Intestinal Epithelium. Category: Molecular, Cell, and Developmental Biology. *Digestion* (2003) 68(4):217–25. doi: 10.1159/000076385
9. Mow VC, Wang CC, Hung CT. The Extracellular Matrix, Interstitial Fluid and Ions as a Mechanical Signal Transducer in Articular Cartilage. *Osteoarthr Cartil* (1999) 7(1):41–58. doi: 10.1053/joca.1998.0161 PubMedPMID:10367014
10. Berkholtz CB, Shea LD, Woodruff TK. Extracellular Matrix Functions in Follicle Maturation. *Semin Reprod Med* (2006) 24(4):262–9. doi: 10.1055/s-2006-948555
11. Gougeon A. Human Ovarian Follicular Development: From Activation of Resting Follicles to Preovulatory Maturation. *Ann Endocrinol* (2010) 71 (3):132–43. doi: 10.1016/j.ando.2010.02.021
12. Rimon-Dahari N, Yerushalmi-Heinemann L, Alyagor L, Dekel N. Ovarian Folliculogenesis. *Results Probl Cell Differ* (2016) 58:167–90. doi: 10.1007/978-3-319-31973-5_7
13. Fortune JE, Cushman RA, Wahl CM, Kito S. The Primordial to Primary Follicle Transition. *Mol Cell Endocrinol* (2000) 163(1-2):53–60. doi: 10.1016/s0303-7207(99)00240-3
14. Devos M, Grosbois J Interaction Between PI3K/AKT and Hippo Pathways During *In Vitro* Follicular Activation and Response to Fragmentation and Chemotherapy Exposure Using a Mouse Immature Ovary Model. *Biology of Reproduction* (2020) 102(3):717–29.
15. Kawashima I, Kawamura K. Regulation of Follicle Growth Through Hormonal Factors and Mechanical Cues Mediated by Hippo Signaling Pathway. *Syst Biol Reprod Med* (2018) 64(1):3–11. doi: 10.1080/19396368.2017.1411990
16. Drummond AE. TGFbeta Signalling in the Development of Ovarian Function. *Cell Tissue Res* (2005) 322(1):107–15. doi: 10.1007/s00441-005-1153-1
17. Juengel JL, McNatty KP. The Role of Proteins of the Transforming Growth Factor-Beta Superfamily in the Intraovarian Regulation of Follicular Development. *Hum Reprod Update* (2005) 11(2):143–60. doi: 10.1093/humupd/dmh061
18. Vendola K, Zhou J, Wang J, Famuyiwa OA, Bievre M, Bondy CA. Androgens Promote Oocyte Insulin-Like Growth Factor I Expression and Initiation of Follicle Development in the Primate Ovary. *Biol Reprod* (1999) 61(2):353–7. doi: 10.1095/biolreprod61.2.353
19. Matsuzaki S. Mechanobiology of the Female Reproductive System. *Reprod Med Biol* (2021) 20(4):371–401. doi: 10.1002/rmb2.12404
20. Ouni E, Bouzin C, Dolmans MM, Marbaix E, Pyr Dit Ruys S, Vertommen D, et al. Spatiotemporal Changes in Mechanical Matrisome Components of the Human Ovary From Prepuberty to Menopause. *Hum Reprod (Oxford England)* (2020) 35(6):1391–410. doi: 10.1093/humrep/deaa100
21. Wandji SA, Srsen V, Voss AK, Eppig JJ, Fortune JE. Initiation *In Vitro* of Growth of Bovine Primordial Follicles. *Biol Reprod* (1996) 55(5):942–8. doi: 10.1095/biolreprod55.5.942
22. Felder S, Masasa H, Orenbuch A, Levaot N, Shachar Goldenberg M, Cohen S. Reconstruction of the Ovary Microenvironment Utilizing Macroporous Scaffold With Affinity-Bound Growth Factors. *Biomaterials* (2019) 205:11–22. doi: 10.1016/j.biomaterials.2019.03.013
23. Raja-Khan N, Urbanek M, Rodgers RJ, Legro RS. The Role of TGF-β in Polycystic Ovary Syndrome. *Reprod Sci (Thousand Oaks Calif)* (2014) 21 (1):20–31. doi: 10.1177/1933719113485294
24. Puttabyatappa M, Padmanabhan V. Ovarian and Extra-Ovarian Mediators in the Development of Polycystic Ovary Syndrome. *J Mol Endocrinol* (2018) 61(4):R161–r84. doi: 10.1530/jme-18-0079
25. Chlasta J, Milani P, Runel G, Duteyrat JL. Variations in Basement Membrane Mechanics Are Linked to Epithelial Morphogenesis. *Development* (2017) 144(23):4350–62. doi: 10.1242/dev.152652
26. Rashidi Z, Azadbakht M, Khazaei M. Hydrostatic Pressure Improves *In-Vitro* Maturation of Oocytes Derived From Vitrified-Warmed Mouse Ovaries. *Iran J Reprod Med* (2012) 10(3):257–64. doi: 10.1016/j.ajog.2012.02.008
27. Reddy P, Zheng W, Liu K. Mechanisms Maintaining the Dormancy and Survival of Mammalian Primordial Follicles. *Trends Endocrinol Metab* (2010) 21(2):96–103. doi: 10.1016/j.tem.2009.10.001
28. Adhikari D, Zheng W, Shen Y, Gorre N, Hämäläinen T, Cooney AJ, et al. Tsc/mTORC1 Signaling in Oocytes Governs the Quiescence and Activation of Primordial Follicles. *Hum Mol Genet* (2010) 19(3):397–410. doi: 10.1093/hmg/ddp483
29. Hsueh AJ, Kawamura K, Cheng Y, Fauser BC. Intraovarian Control of Early Folliculogenesis. *Endocr Rev* (2015) 36(1):1–24. doi: 10.1210/er.2014-1020
30. Grosbois J, Demeestere I. Dynamics of PI3K and Hippo Signaling Pathways During *In Vitro* Human Follicle Activation. *Hum Reprod (Oxford England)* (2018) 33(9):1705–14. doi: 10.1093/humrep/dey250
31. Ryan KE, Glister C, Lonergan P, Martin F, Knight PG, Evans AC. Functional Significance of the Signal Transduction Pathways Akt and Erk in Ovarian Follicles: *In Vitro* and *In Vivo* Studies in Cattle and Sheep. *J Ovarian Res* (2008) 1(1):2. doi: 10.1186/1757-2215-1-2
32. Yang L, Lv Q, Liu J, Qi S, Fu D. miR-431 Regulates Granulosa Cell Function Through the IRS2/PI3K/AKT Signaling Pathway. *J Reprod Dev* (2020) 66 (3):231–9. doi: 10.1262/jrd.2019-155
33. Kawamura K, Cheng Y, Suzuki N, Deguchi M, Sato Y, Takae S, et al. Hippo Signaling Disruption and Akt Stimulation of Ovarian Follicles for Infertility Treatment. *Proc Natl Acad Sci USA* (2013) 110(43):17474–9. doi: 10.1073/pnas.1312830110
34. Theocharis AD, Skandalis SS, Gialeli C, Karamanos NK. Extracellular Matrix Structure. *Adv Drug Deliv Rev* (2016) 97:4–27. doi: 10.1016/j.addr.2015.11.001
35. Frantz C, Stewart KM, Weaver VM. The Extracellular Matrix at a Glance. *J Cell Sci* (2010) 123(Pt 24):4195–200. doi: 10.1242/jcs.023820
36. Padhi A, Nain AS. ECM in Differentiation: A Review of Matrix Structure, Composition and Mechanical Properties. *Ann Biomed Eng* (2020) 48 (3):1071–89. doi: 10.1007/s10439-019-02337-7
37. Piccolo S, Dupont S, Cordenonsi M. The Biology of YAP/TAZ: Hippo Signaling and Beyond. *Physiol Rev* (2014) 94(4):1287–312. doi: 10.1152/physrev.00005.2014
38. Muncie JM, Weaver VM. The Physical and Biochemical Properties of the Extracellular Matrix Regulate Cell Fate. *Curr Top Dev Biol* (2018) 130:1–37. doi: 10.1016/bs.ctdb.2018.02.002
39. Dupont S, Morsut L, Aragona M, Enzo E, Giulitti S, Cordenonsi M, et al. Role of YAP/TAZ in Mechanotransduction. *Nature* (2011) 474(7350):179–83. doi: 10.1038/nature10137
40. Wipff PJ, Rifkin DB, Meister JJ, Hinz B. Myofibroblast Contraction Activates Latent TGF-Beta1 From the Extracellular Matrix. *J Cell Biol* (2007) 179 (6):1311–23. doi: 10.1083/jcb.200704042

41. Cox TR, Erler JT. Remodeling and Homeostasis of the Extracellular Matrix: Implications for Fibrotic Diseases and Cancer. *Dis Models Mech* (2011) 4 (2):165–78. doi: 10.1242/dmm.004077
42. Nagamatsu G, Shimamoto S, Hamazaki N. Mechanical Stress Accompanied With Nuclear Rotation Is Involved in the Dormant State of Mouse Oocytes. *Sci Adv* (2019) 5(6):eaav9960. doi: 10.1126/sciadv.aav9960
43. Ferrer GG, Sanmartin-Masia E, Poveda-Reyes S. Extracellular Matrix-Inspired Gelatin/Hyaluronic Acid Injectable Hydrogels. *Int J Polym Mater* (2017) 66(6):280–8. doi: 10.1080/00914037.2016.1201828
44. Unal DB, Caliari SR, Lampe KJ. 3D Hyaluronic Acid Hydrogels for Modeling Oligodendrocyte Progenitor Cell Behavior as a Function of Matrix Stiffness. *Biomacromolecules* (2020) 21(12):4962–71. doi: 10.1021/acs.biomac.0c01164
45. Deegan DB, Zimmerman C, Skardal A, Atala A, Shupe TD. Stiffness of Hyaluronic Acid Gels Containing Liver Extracellular Matrix Supports Human Hepatocyte Function and Alters Cell Morphology. *J Mech Behav Biomed Mater* (2015) 55:87–103. doi: 10.1016/j.jmbbm.2015.10.016
46. Collins MN, Birkinshaw C. Hyaluronic Acid Based Scaffolds for Tissue Engineering–A Review. *Carbohydr Polym* (2013) 92(2):1262–79. doi: 10.1016/j.carbpol.2012.10.028
47. Silva Garcia JM, Panitch A, Calve S. Functionalization of Hyaluronic Acid Hydrogels With ECM-Derived Peptides to Control Myoblast Behavior. *Acta Biomater* (2019) 84:169–79. doi: 10.1016/j.actbio.2018.11.030
48. Rowley JE, Amargant F, Zhou LT, Galligos A, Simon LE, Pritchard MT, et al. Low Molecular Weight Hyaluronan Induces an Inflammatory Response in Ovarian Stromal Cells and Impairs Gamete Development *In Vitro*. *Int J Mol Sci* (2020) 21(3):1036. doi: 10.3390/ijms21031036
49. Lillie MA, Armstrong TE, Gérard SG, Shadwick RE, Gosline JM. Contribution of Elastin and Collagen to the Inflation Response of the Pig Thoracic Aorta: Assessing Elastin's Role in Mechanical Homeostasis. *J Biomech* (2012) 45(12):2133–41. doi: 10.1016/j.jbiomech.2012.05.034
50. Cocciolone AJ, Hawes JZ, Staiculescu MC, Johnson EO, Murshed M, Wagenseil JE. Elastin, Arterial Mechanics, and Cardiovascular Disease. *Am J Physiol Heart Circ Physiol* (2018) 315(2):H189–h205. doi: 10.1152/ajpheart.00087.2018
51. Kim EJ, Yang C, Lee J, Youm HW, Lee JR, Suh CS, et al. The New Biocompatible Material for Mouse Ovarian Follicle Development in Three-Dimensional *In Vitro* Culture Systems. *Theriogenology* (2020) 144:33–40. doi: 10.1016/j.theriogenology.2019.12.009
52. He X. Microfluidic Encapsulation of Ovarian Follicles for 3D Culture. *Ann Biomed Eng* (2017) 45(7):1676–84. doi: 10.1007/s10439-017-1823-7
53. Yang SH, Hur YS, Yoon SH, Jung JH, Lim JH, Ko Y. A Comparison of Embryonic Development and Clinical Outcomes Between *In Vitro* Oocytes Maturation Using Micro-Vibration System and *In Vivo* Oocytes Maturation in Polycystic Ovarian Syndrome Patients. *Gynecol Obstet Invest* (2020) 85 (3):252–8. doi: 10.1159/000507441
54. Matulonis UA, Sood AK, Fallowfield L, Howitt BE, Sehouli J, Karlan BY. Ovarian Cancer. *Nat Rev Dis Primers* (2016) 2:16061. doi: 10.1038/nrdp.2016.61
55. Oswald AJ, Gourley C. Low-Grade Epithelial Ovarian Cancer: A Number of Distinct Clinical Entities? *Curr Opin Oncol* (2015) 27(5):412–9. doi: 10.1097/cco.0000000000000216
56. Jacobs IJ, Menon U, Ryan A, Gentry-Maharaj A, Burnell M, Kalsi JK, et al. Ovarian Cancer Screening and Mortality in the UK Collaborative Trial of Ovarian Cancer Screening (UKCTOCS): A Randomised Controlled Trial. *Lancet (London England)* (2016) 387(10022):945–56. doi: 10.1016/s0140-6736(15)01224-6
57. Yang C, Xia BR, Zhang ZC, Zhang YJ, Lou G, Jin WL. Immunotherapy for Ovarian Cancer: Adjuvant, Combination, and Neoadjuvant. *Front Immunol* (2020) 11:577869. doi: 10.3389/fimmu.2020.577869
58. Asch BB, Kamat BR, Burstein NA. Interactions of Normal, Dysplastic, and Malignant Mammary Epithelial Cells With Fibronectin *In Vivo* and *In Vitro*. *Cancer Res* (1981) 41(6):2115–25. doi: 10.1016/0304-3835(81)90102-6
59. Chakraborty J, Von Stein GA. Pleomorphism of Human Prostatic Cancer Cells (DU 145) in Culture–the Role of Cytoskeleton. *Exp Mol Pathol* (1986) 44(2):235–45. doi: 10.1016/0014-4800(86)90074-2
60. Cross SE, Jin YS, Rao J, Gimzewski JK. Nanomechanical Analysis of Cells From Cancer Patients. *Nat Nanotechnol* (2007) 2(12):780–3. doi: 10.1038/nnano.2007.388
61. Cross SE, Jin YS, Tondre J, Wong R, Rao J, Gimzewski JK. AFM-Based Analysis of Human Metastatic Cancer Cells. *Nanotechnology* (2008) 19 (38):384003. doi: 10.1088/0957-4484/19/38/384003
62. Ketene AN, Schmelz EM, Roberts PC, Agah M. The Effects of Cancer Progression on the Viscoelasticity of Ovarian Cell Cytoskeleton Structures. *Nanomed Nanotechnol Biol Med* (2012) 8(1):93–102. doi: 10.1016/j.nano.2011.05.012
63. Nikkhah M, Strobl JS, De Vita R, Agah M. The Cytoskeletal Organization of Breast Carcinoma and Fibroblast Cells Inside Three Dimensional (3-D) Isotropic Silicon Microstructures. *Biomaterials* (2010) 31(16):4552–61. doi: 10.1016/j.biomaterials.2010.02.034
64. Ansardamavandi A, Tafazzoli-Shadpour M. An AFM-Based Nanomechanical Study of Ovarian Tissues With Pathological Conditions. *Int J Nanomedicine* (2020) 15:4333–50. doi: 10.2147/ijn.s254342
65. Chen M, Zeng J, Ruan W, Zhang Z, Wang Y, Xie S, et al. Examination of the Relationship Between Viscoelastic Properties and the Invasion of Ovarian Cancer Cells by Atomic Force Microscopy. *Beilstein J Nanotechnol* (2020) 11:568–82. doi: 10.3762/bjnano.11.45
66. Sarwar M, Sykes PH, Chitcholtan K, Alkaisi MM, Evans JJ. The Extracellular Topographical Environment Influences Ovarian Cancer Cell Behaviour. *Biochem Biophys Res Commun* (2019) 508(4):1188–94. doi: 10.1016/j.bbrc.2018.12.067
67. Ogishima J, Taguchi A, Kawata A, Kawana K, Yoshida M, Yoshimatsu Y, et al. The Oncogene KRAS Promotes Cancer Cell Dissemination by Stabilizing Spheroid Formation *via* the MEK Pathway. *BMC Cancer* (2018) 18(1):1201. doi: 10.1186/s12885-018-4922-4
68. Aranjuez G, Burtscher A, Sawant K, Majumder P, McDonald JA. Dynamic Myosin Activation Promotes Collective Morphology and Migration by Locally Balancing Oppositional Forces From Surrounding Tissue. *Mol Biol Cell* (2016) 27(12):1898–910. doi: 10.1091/mbc.E15-10-0744
69. Quintela M, Sieglaff DH, Gazze AS, Zhang A, Gonzalez D, Francis L, et al. HBO1 Directs Histone H4 Specific Acetylation, Potentiating Mechano-Transduction Pathways and Membrane Elasticity in Ovarian Cancer Cells. *Nanomed Nanotechnol Biol Med* (2019) 17:254–65. doi: 10.1016/j.nano.2019.01.017
70. Toubhans B, Gazze SA, Bissardon C, Bohic S, Gourlan AT, Gonzalez D, et al. Selenium Nanoparticles Trigger Alterations in Ovarian Cancer Cell Biomechanics. *Nanomed Nanotechnol Biol Med* (2020) 29:102258. doi: 10.1016/j.nano.2020.102258
71. Ali MRK, Wu Y. Nuclear Membrane-Targeted Gold Nanoparticles Inhibit Cancer Cell Migration and Invasion. *ACS Nano* (2017) 11(4):3716–26. doi: 10.1021/acsnano.6b08345
72. Tan DS, Agarwal R, Kaye SB. Mechanisms of Transcoelomic Metastasis in Ovarian Cancer. *Lancet Oncol* (2006) 7(11):925–34. doi: 10.1016/s1470-2045(06)70939-1
73. Novak C, Horst E, Mehta G. Review: Mechanotransduction in Ovarian Cancer: Shearing Into the Unknown. *APL Bioeng* (2018) 2(3):031701. doi: 10.1063/1.5024386
74. Hyler AR, Baudoin NC, Brown MS, Stremler MA, Cimini D, Davalos RV, et al. Fluid Shear Stress Impacts Ovarian Cancer Cell Viability, Subcellular Organization, and Promotes Genomic Instability. *PloS One* (2018) 13(3): e0194170. doi: 10.1371/journal.pone.0194170
75. Avraham-Chakim L, Elad D, Zaretsky U, Kloog Y, Jaffa A, Grisaru D. Fluid-Flow Induced Wall Shear Stress and Epithelial Ovarian Cancer Peritoneal Spreading. *PloS One* (2013) 8(4):e60965. doi: 10.1371/journal.pone.0060965
76. Lawler K, O'Sullivan G, Long A, Kenny D. Shear Stress Induces Internalization of E-Cadherin and Invasiveness in Metastatic Oesophageal Cancer Cells by a Src-Dependent Pathway. *Cancer Sci* (2009) 100(6):1082–7. doi: 10.1111/j.1349-7006.2009.01160.x
77. Ip CK, Li SS, Tang MY, Sy SK, Ren Y, Shum HC, et al. Stemness and Chemoresistance in Epithelial Ovarian Carcinoma Cells Under Shear Stress. *Sci Rep* (2016) 6:26788. doi: 10.1038/srep26788
78. Rizvi I, Gurkan UA, Tasoglu S, Alagic N, Celli JP, Mensah LB, et al. Flow Induces Epithelial-Mesenchymal Transition, Cellular Heterogeneity and Biomarker Modulation in 3D Ovarian Cancer Nodules. *Proc Natl Acad Sci USA* (2013) 110(22):E1974–83. doi: 10.1073/pnas.1216989110
79. Regmi S, Fu A, Luo KQ. High Shear Stresses Under Exercise Condition Destroy Circulating Tumor Cells in a Microfluidic System. *Sci Rep* (2017) 7:39975. doi: 10.1038/srep39975

80. Egan K, Cooke N, Kenny D. Living in Shear: Platelets Protect Cancer Cells From Shear Induced Damage. *Clin Exp Metastasis* (2014) 31(6):697–704. doi: 10.1007/s10585-014-9660-7
81. Lu P, Weaver VM, Werb Z. The Extracellular Matrix: A Dynamic Niche in Cancer Progression. *J Cell Biol* (2012) 196(4):395–406. doi: 10.1083/jcb.201102147
82. Park J, Kim HN, Kim DH, Levchenko A, Suh KY. Quantitative Analysis of the Combined Effect of Substrate Rigidity and Topographic Guidance on Cell Morphology. *IEEE Trans Nanobioscience* (2012) 11(1):28–36. doi: 10.1109/tnb.2011.2165728
83. McKenzie AJ, Hicks SR, Svec KV. The Mechanical Microenvironment Regulates Ovarian Cancer Cell Morphology, Migration, and Spheroid Disaggregation. *Sci Rep* (2018) 8(1):7228. doi: 10.1038/s41598-018-25589-0
84. Pal A, Haliti P, Dharmadhikari B, Qi W, Patra P. Manipulating Extracellular Matrix Organizations and Parameters to Control Local Cancer Invasion. *IEEE/ACM Trans Comput Biol Bioinform* (2020) 18(6):2566–76. doi: 10.1109/tcbb.2020.2989223
85. Lee S, Yang Y, Fishman D, Banaszak Holl MM, Hong S. Epithelial-Mesenchymal Transition Enhances Nanoscale Actin Filament Dynamics of Ovarian Cancer Cells. *J Phys Chem B* (2013) 117(31):9233–40. doi: 10.1021/jp4055186
86. McGrail DJ, Kieu QM, Dawson MR. The Malignancy of Metastatic Ovarian Cancer Cells is Increased on Soft Matrices Through a Mechanosensitive Rho-ROCK Pathway. *J Cell Sci* (2014) 127(Pt 12):2621–6. doi: 10.1242/jcs.144378
87. Klymenko Y, Wates RB, Weiss-Bilka H, Lombard R, Liu Y, Campbell L, et al. Modeling the Effect of Ascites-Induced Compression on Ovarian Cancer Multicellular Aggregates. *Dis Model Mech* (2018) 11(9):dmm034199. doi: 10.1242/dmm.034199
88. Burkhalter RJ, Symowicz J, Hudson LG, Gottardi CJ, Stack MS. Integrin Regulation of Beta-Catenin Signaling in Ovarian Carcinoma. *J Biol Chem* (2011) 286(26):23467–75. doi: 10.1074/jbc.M110.199539
89. Bryan BA, Dennstedt E, Mitchell DC, Walshe TE, Noma K, Loureiro R, et al. RhoA/ROCK Signaling is Essential for Multiple Aspects of VEGF-Mediated Angiogenesis. *FASEB J* (2010) 24(9):3186–95. doi: 10.1096/fj.09-145102
90. Novak CM, Horst EN, Lin E, Mehta G. Compressive Stimulation Enhances Ovarian Cancer Proliferation, Invasion, Chemoresistance, and Mechanotransduction *via* CDC42 in a 3D Bioreactor. *Cancers (Basel)* (2020) 12(6):1521. doi: 10.3390/cancers12061521
91. Casagrande N, Borghese C, Agostini F. In Ovarian Cancer Multicellular Spheroids, Platelet Releasate Promotes Growth, Expansion of ALDH+ and CD133+ Cancer Stem Cells, and Protection Against the Cytotoxic Effects of Cisplatin, Carboplatin and Paclitaxel. *Int J Mol Sci* (2021) 22(6):3019. doi: 10.3390/ijms22063019
92. Al Habyan S, Kalos C, Szymborski J, McCaffrey L. Multicellular Detachment Generates Metastatic Spheroids During Intra-Abdominal Dissemination in Epithelial Ovarian Cancer. *Oncogene* (2018) 37(37):5127–35. doi: 10.1038/s41388-018-0317-x
93. Langthasa J, Sarkar P, Narayanan S, Bhagat R, Vadaparty A, Bhat R. Extracellular Matrix Mediates Moruloid-Blastuloid Morphodynamics in Malignant Ovarian Spheroids. *Life Sci Alliance* (2021) 4(10):e202000942. doi: 10.26508/lsa.202000942
94. Matte I, Legault CM, Garde-Granger P, Laplante C, Bessette P, Rancourt C, et al. Mesothelial Cells Interact With Tumor Cells for the Formation of Ovarian Cancer Multicellular Spheroids in Peritoneal Effusions. *Clin Exp Metastasis* (2016) 33(8):839–52. doi: 10.1007/s10585-016-9821-y
95. He FF, Li YM. Role of Gut Microbiota in the Development of Insulin Resistance and the Mechanism Underlying Polycystic Ovary Syndrome: A Review. *J Ovarian Res* (2020) 13(1):73. doi: 10.1186/s13048-020-00670-3
96. West ER, Xu M, Woodruff TK, Shea LD. Physical Properties of Alginate Hydrogels and Their Effects on *In Vitro* Follicle Development. *Biomaterials* (2007) 28(30):4439–48. doi: 10.1016/j.biomaterials.2007.07.001
97. Hendriks ML, König T, Soleman RS, Korsen T, Schats R, Hompes PG, et al. Influence of Ovarian Manipulation on Reproductive Endocrinology in Polycystic Ovarian Syndrome and Regularly Cycling Women. *Eur J Endocrinol* (2013) 169(4):503–10. doi: 10.1530/eje-13-0334
98. Karagül M, Aktaş S, Coşkun Yılmaz B, Yılmaz M, Orekici Temel G. GDF9 and BMP15 Expressions and Fine Structure Changes During Folliculogenesis in Polycystic Ovary Syndrome. *Balkan Med J* (2018) 35 (1):43–54. doi: 10.4274/balkanmedj.2016.1110
99. Navarro-Pando JM, Bullón P, Cordero MD, Alcocer-Gómez E. Is AMP-Activated Protein Kinase Associated to the Metabolic Changes in Primary Ovarian Insufficiency? *Antioxid Redox Signal* (2020) 33(15):1115–21. doi: 10.1089/ars.2020.8144
100. Kawashima I, Kawamura K. Disorganization of the Germ Cell Pool Leads to Primary Ovarian Insufficiency. *Reproduction (Cambridge England)* (2017) 153(6):R205–r13. doi: 10.1530/rep-17-0015
101. Cordeiro CN, Christianson MS, Selter JH, Segars JH Jr. *In Vitro* Activation: A Possible New Frontier for Treatment of Primary Ovarian Insufficiency. *Reprod Sci (Thousand Oaks Calif)* (2016) 23(4):429–38. doi: 10.1177/1933719115625842


**Conflict of Interest:** The authors declare that the research was conducted in the absence of any commercial or financial relationships that could be construed as a potential conflict of interest.

**Publisher's Note:** All claims expressed in this article are solely those of the authors and do not necessarily represent those of their affiliated organizations, or those of the publisher, the editors and the reviewers. Any product that may be evaluated in this article, or claim that may be made by its manufacturer, is not guaranteed or endorsed by the publisher.

frontiers in Oncology

REVIEW
published: 25 January 2022
doi: 10.3389/fonc.2021.720622

# Approaches Toward Targeting Matrix Metalloproteases for Prognosis and Therapies in Gynecological Cancer: MicroRNAs as a Molecular Driver

*Anuradha Pandit*[1†], *Yasmin Begum*[1†], *Priyanka Saha*[2], *Amit Kumar Srivastava*[2] *and Snehasikta Swarnakar*[1*]

[1] *Infectious Diseases & Immunology Division, CSIR-Indian Institute of Chemical Biology, Kolkata, India,* [2] *Cancer Biology & Inflammatory Disorder Division, CSIR-Indian Institute of Chemical Biology, Kolkata, India*

OPEN ACCESS

**Edited by:**
*Sarah M Temkin, National Institutes of Health (NIH), United States*

**Reviewed by:**
*Dong-Joo (Ellen) Cheon, Albany Medical College, United States*
*Dinesh Ahirwar, The Ohio State University, United States*

***Correspondence:**
*Snehasikta Swarnakar*
*snehasiktaiicbidi@gmail.com*

[†]*These authors have contributed equally to this work and share first authorship*

**Specialty section:**
*This article was submitted to Gynecological Oncology, a section of the journal Frontiers in Oncology*

**Received:** *04 June 2021*
**Accepted:** *30 December 2021*
**Published:** *25 January 2022*

**Citation:**
*Pandit A, Begum Y, Saha P, Srivastava AK and Swarnakar S (2022) Approaches Toward Targeting Matrix Metalloproteases for Prognosis and Therapies in Gynecological Cancer: MicroRNAs as a Molecular Driver. Front. Oncol. 11:720622. doi: 10.3389/fonc.2021.720622*

Gene expression can be regulated by small non-coding RNA molecules like microRNAs (miRNAs) which act as cellular mediators necessary for growth, differentiation, proliferation, apoptosis, and metabolism. miRNA deregulation is often observed in many human malignancies, acting both as tumor-promoting and suppressing, and their abnormal expression is linked to unrestrained cellular proliferation, metastasis, and perturbation in DNA damage as well as cell cycle. Matrix Metalloproteases (MMPs) have crucial roles in both growth, and tissue remodeling in normal conditions, as well as in promoting cancer development and metastasis. Herein, we outline an integrated interactive study involving various MMPs and miRNAs and also feature a way in which these communications impact malignant growth, movement, and metastasis. The present review emphasizes on important miRNAs that might impact gynecological cancer progression directly or indirectly *via* regulating MMPs. Additionally, we address the likely use of miRNA-mediated MMP regulation and their downstream signaling pathways towards the development of a potential treatment of gynecological cancers.

**Keywords: microRNA, gynecological cancer, matrix metalloprotease (MMP), EMT, metastasis**

## BACKGROUND

Gynecological malignancies, like cervical, ovarian, and endometrial cancers, account significantly for most of the global cancer load, where cervical cancer (CC) accounts to be the fourth most prevalent malignancy among women, along with ovarian cancer (OC) comprising 4.4% of the entire cancer-related mortality among women (1). In 2018, endometrial cancer (EC) was reported to have caused 382,069 cases and 89,929 deaths globally (1). The percentage of women over 65 diagnosed with cancer is projected to increase dramatically over the next decade (2). As a result, there is already a significant unmet therapeutic need in the field for successful treatments of gynecological malignancies.

Gynecological cancers have a high mortality rate due to the diagnosis at late stages in addition to multi-drug resistance, impaired apoptotic pathway, inhibition of the immune system, and aberrant

**Abbreviations:** miRNAs, microRNAs; MMP, matrix metalloprotease; ECM, extracellular matrix; CC, cervical cancer; OC, ovarian cancer; EOC, epithelial ovarian cancer; EMT, epithelial-mesenchymal transition; AGO, Argonaute.

MMP production (3, 4). Extracellular matrix (ECM) remodeling is crucial for maintaining extracellular microenvironment homeostasis and tissue turnover. Tumor cells must be able to disrupt the surrounding ECM to proliferate, invade, and metastasize. Uncontrolled tumor proliferation, tissue remodeling, inflammation, cellular invasion, and metastasis are all consequences of abnormal ECM proteolysis. Matrix metalloproteases (MMPs) are enzymes capable of degrading multiple ECM components, leading to wound healing, tissue repair, embryonic development (5). Rampant MMP expression has been associated with tumor aggressiveness, metastasis, and vascularization and is correlated with late diagnosis in various malignancies such as lung, prostate, colon, breast, and pancreatic cancers (6–10). MMP expression is closely monitored by many regulatory mechanisms, which include zymogen activation, compartmentalization, endogenously produced tissue inhibitors of metalloproteases (TIMPs), and miRNAs.

miRNAs are endogenously produced non-coding RNA elements responsible for gene silencing by degrading target mRNA. They are frequently altered during tumorigenesis and their ability to regulate various genes has made them an attractive candidate for cancer therapeutics (11). Dysregulation of both MMP and miRNA levels is a pronounced feature of gynecological cancers (12–14). The involvement of miRNAs to regulate the expression of the MMP gene has recently received a lot of attention. MMP regulation by various miRNAs may affect cancer progression. Moreover, the functional relevance of miRNA-mediated MMP regulation in malignancies might be explored further by examining the post-transcriptional regulation system controlling MMP gene expression. The current study focuses on the mechanisms controlling MMP expression by miRNAs in gynecological cancers and also aims to come up with a strategy to assist miRNAs targeting MMPs for diagnosis and therapeutic intervention.

## miRNA BIOGENESIS

Numerous small RNAs have been evolved to negatively regulate undesired genetic elements and transcripts (15). miRNAs are the most dominating group of small RNAs having a length of ~22 nucleotides and are generated by RNase III proteins namely Dicer and Drosha (16). miRNA functions as a guide by targeting specific mRNAs at its 3'untranslated region (3'UTR) region usually by base-pairing thereby inducing RNA silencing (17) and AGO proteins act as the effector proteins recruiting factors that induce mRNA deadenylation, translational repression, and mRNA degradation (18).

Because each miRNA affects a vast number of mRNAs, the miRNA biogenesis pathway has a pivotal role in gene regulation as well as their networks. Throughout the last decade, miRNAs have been revealed to play important roles in tumor cell recruitment, progression, and metastasis (19). The miR 17-92 cluster expression, which cooperated with MYC to induce cancer growth in a B cell lymphoma mouse model, was the very first example (20). Certain miRNA also functions as tumor suppressors, for instance, the let 7 family suppresses tumor development and metastasis *via* targeting key oncogenic genes like high-mobility group AT-hook 2 (HMGA2), members of the RAS family (NRAS, KRAS, and HRAS), and MYC (21–23). As a result, cancer-related variations in the expression profiles of miRNA are emerging as promising diagnostic markers as well as the targets, for therapeutics, that are frequently linked to tumor growth and overall survival (19). Although particular miRNAs possess either an oncogenic or tumor-suppressive effect, multiple reports suggested a decreased miRNA expression universally in cancerous cells in contrast to healthy cells, implying that miRNA synthesis may be disrupted during tumorigenesis (24, 25).

Most of the miRNA genes are transcribed as pri-miRNA, made up of a hairpin loop structure which consists of a sequence of miRNA, by RNA polymerase II (Pol II) either as intronic clusters in the pre-mRNAs or as individual genetic elements, encoded within long non-coding RNAs (26). The biogenesis of miRNAs is carried out in two steps, first processed inside the nuclei and then in the cytoplasm (26, 27). DROSHA, an RNase type III enzyme, along with other related proteins comprises the microprocessor complex which catalyzes the nuclear event (26). This nuclear processing event leads to the synthesis of pre-miRNAs, which are ~70 nucleotides stem-loop-like precursor miRNAs that are then exported to the cytosol through the Exportin-5 (XPO-5) export receptor (28). The pre-miRNAs are later catalyzed in the cytosol by DICER, another RNase type III enzyme, which leads to miRNA duplex formation. These miRNA duplexes are then incorporated into RISC (RNA-Induced Silencing complex) along with another protein namely Argonaute (AGO), where only a single strand is chosen to form the mature miRNA (**Figure 1**) (29).

Also, there is a non-canonical miRNA biogenesis pathway that also produces functional miRNAs. Such as mirtrons which are produced through the pre-mRNA splicing process, while certain other miRNAs are produced from small nucleolar RNA (snoRNA) precursors, $m^7G$ pre-miRNA/Exportin1 pathway, t-RNA derived pathway, etc (16). Mirtrons are miRNAs, a byproduct of intron splicing, made by a non-canonical route that skips the Drosha cleavage step. Mirtrons go through lariat-debranching by DBR1, a debranching enzyme, then enter the conventional route at the exportin-5 level, therefore known as canonical mirtrons (**Figure 1**) (30).

Phosphorylation, ubiquitination, and sumoylation are some of the post-translational modifications of miRNA processing factors that can influence DGCR8, DROSHA, and/or DICER complex components. In another report, it was revealed that the regulation of miRNA biogenesis can also happen in a cell density-dependent manner (26).

## ROLE OF MMPs IN CANCER

MMPs are endopeptidases monitoring ECM's physiological turnover and remodeling. While collagens, gelatins, proteoglycans, and elastin are among their substrates, they

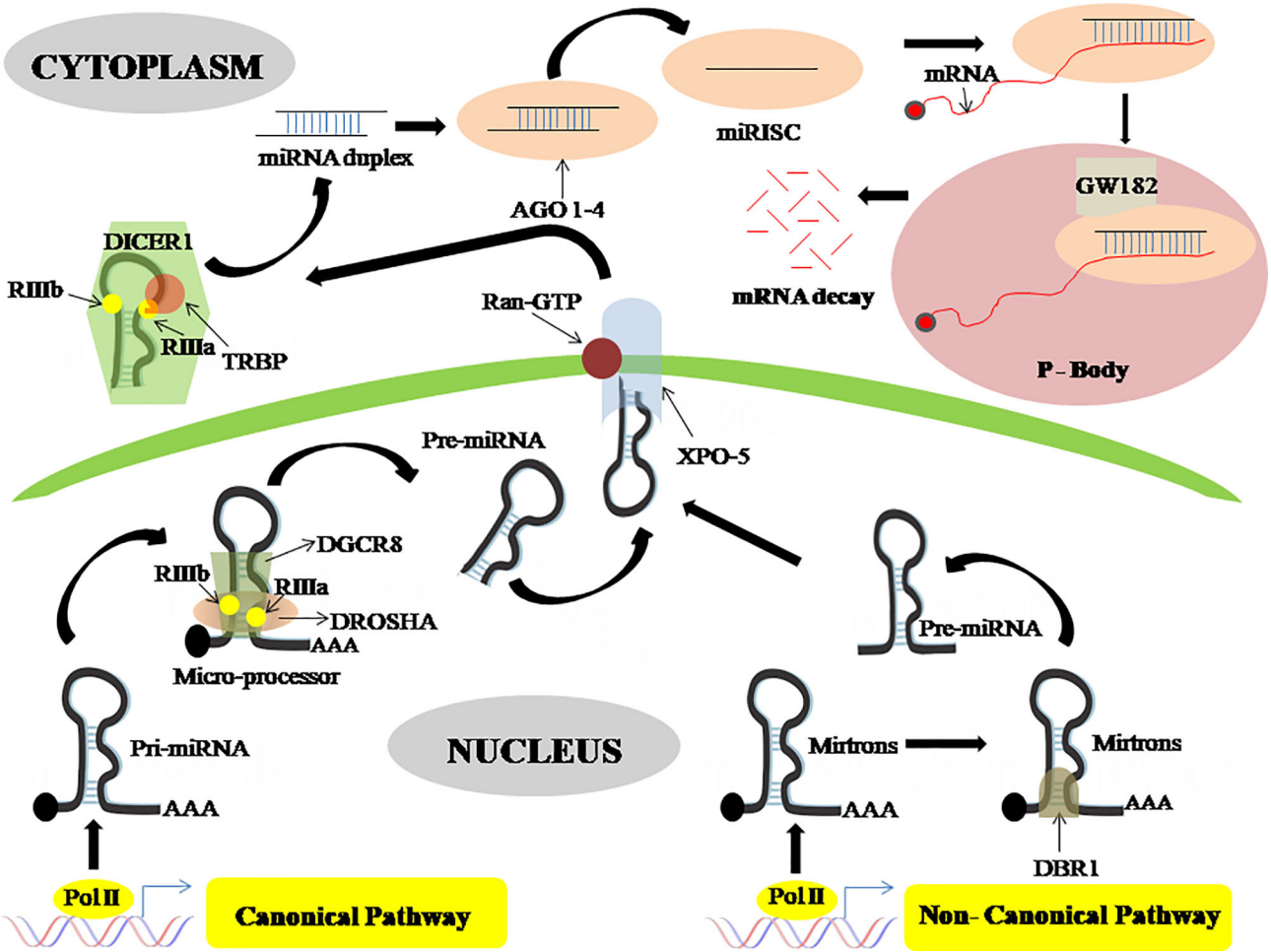


**FIGURE 1** | MicroRNA biogenesis through a canonical and non-canonical pathway. In the canonical pathway the pri-miRNA is processed by DROSHA and DGCR8 to form pre-miRNA which then is exported to the cytoplasm *via* exportin-5, wherein the cytoplasm this pre-miRNA is processed by DICER-1 which gives rise to miRNA duplex. This miRNA duplex is then incorporated into RISC together with an argonaute protein to form mature miRNA. This mature miRNA then binds with an mRNA in the processing body where mRNA decay happens. On the contrary, in the non-canonical pathway, the pre-miRNA is generated from mitrons by DBR1. This pre-miRNA is transported by exportin-5 and enters the canonical pathway. DROSHA, Class 2 ribonucleaseIIIenzyme; DGCR8, DiGeorge syndrome critical region 8 gene; DBR1, Debranching enzyme; XPO-5, Exportin-5; DICER, ribonucleaseIIIenzyme; AGO, Argonaute protein; RISC, RNA-Induced Silencing complex; P-Body, Processing Body.

have a wide range of effects on many other proteins (31). Because MMPs digest a diverse array of substrates, their actions have a major impact on the extracellular environment, and if left uncontrolled, can lead to unnecessary ECM degradation (32, 33). MMPs consist of a predomain, catalytic domain, hemopexin domain and prodomain. MMPs are secreted as pro-enzymes, which are made inactive by interacting with a cysteine-sulphydryl group in the N-terminal (pro) domain with the zinc ion in the catalytic domain. The elimination of this association is known as the "cysteine switch," and it is triggered by pro-hormone convertases (furin) (34). Another level of MMP regulation is performed by TIMPs that bind to the MMP catalytic site and regulate proteolytic activity. Nonspecific antagonists such as 2-macroglobulin, thrombospondin-1, and -2 can also inhibit MMPs (35). MMPs are divided into Collagenases, Gelatinases, Stromelysins, Matrilysin and membrane-type and non-classified MMPs subtypes. MMPs are crucial in the biochemical interplay between tumor and stroma. Stromal cells produce the majority of MMPs in the tumor microenvironment, bringing about ECM cleavage, thereby forming a path for cell movement from the tumor niche into adjoining areas and also releasing several bioactive compounds. Interaction of tumor cells with neighboring stromal cells is critical in facilitating cancer initiation and progression. Tumor cells secrete growth factors such as VEGF, EGF, FGF, interleukins, and IFN, which stimulate surrounding cells in the tumor tissues to release MMPs, allowing tumor cells to migrate (36, 37).

## MMPs in Cell Growth

Cancer cells are known for their uncontrolled proliferation. The tumor reaches this state in one of two ways: by being self-sufficient in growth-promoting signals or developing immunity to antigrowth signals. Cellular proliferation can be unchecked as a result of MMPs cleaving growth factor binding proteins, increasing their bioavailability, or activating growth factor receptors (38, 39). TGF-β It is activated by proteases like MMP-9, -2, -14, which leads to increased invasion and metastasis (40, 41). MMP-1 is found in stromal and epithelial cancer cells of invasive carcinomas and regulates cervical tumorigenesis and lymph node metastasis *via* the PPAR signaling pathway (42, 43). MMP-7 is implicated in cell proliferation, migration, and invasion, possibly through the wnt/catenin pathway (44, 45). Activation of the PKC pathway led to an increase in MMP-7 and 10 in cancer cells, indicating their involvement in cell proliferation and migration in OC (46). MMP-2 was shown to participate in OC cell proliferation *via* p38/MAPK pathway (47).

## MMPs in Apoptosis

Fas ligand binds to extracellular receptors like Fas receptors and activates intracellular caspases, resulting in the degradation of subcellular compartments, thus halting malignant spread. MMP activity inhibits apoptosis in malignant cells, by cleaving pro-apoptotic ligands or receptors (48).In human OC cells, downregulation of MMP-9 was shown to induce apoptosis and prevent proliferation (49). In another study, MMP-2 increased cell proliferation and reduced apoptosis in OVCAR3 (ovarian cancer cell line) cells, thereby lowering the effect of chemotherapeutic drugs on tumor cells (50).

## MMPs in Invasion and Metastasis

The tumor cells will subsequently enter the circulation and spread throughout the body by modulating MMP production (51). MMP-2 and -9 are the most prominent MMPs modulating cancer cell invasion. In both OC and CC, MMP-2 and -9 are implicated in cancer cell invasion and metastasis and are associated with poor survival (52, 53). Furthermore, MMP-2 promotes the attachment of metastatic OC cells to peritoneal surfaces by cleaving ECM and increasing their binding to integrin, as well as the OC cells' propensity to metastasize (54). Similarly, in CC, an association of MMP-2 activation with αvβ3 integrin/MT1-MMP/TIMP-2 has been implicated in tumor cell migration (55). MMP-7 is the primary MMP linked with invasion and metastasis in EC (56). MMP-7 is also overexpressed in ovarian serous cancer tissues, where it increases cellular invasiveness by activating MMP-2 and -9 or by IGFBP breakdown, enhancing IGF concentration and cancer cell proliferation (57, 58).

## MMPs in Angiogenesis

The role of MMPs in angiogenesis is dependent on the neighboring environment, such as substrate abundance and MMP expression time points during angiogenesis (59). MMP-2 is a widely known influencer of vascularization during cancer development. In OC, MMP-2 expression was increased *via* PI3K/Akt and NFκB pathways, enhancing endothelial progenitor cell proliferation (60). Activation of PAR-1 *via* MMP-1 causes OC cells to secrete multiple angiogenic factors, resulting in cell proliferation, endothelial tube formation, and migration (61, 62). MMP-9 has a role in the release of VEGF from tumors (63). OC cells implanted into $Mmp9^{-/-}$ nude mice showed significantly lower levels of VEGF in tumors, thereby contributing to angiogenesis (64).

# REGULATION OF MMPs BY miRNAs

Considerable interest is seen in investigating post-transcriptional regulations of MMPs by miRNAs in recent times. Bioinformatics analyses have identified several miRNAs binding sites at the 3'UTR of MMP transcripts, thereby inducing mRNA instability or translational repression (11, 65). Studies have shown the participation of miRNA in regulating MMP gene expression thereby playing a key role in migration, differentiation, apoptosis, etc (66–68). These miRNAs either promote or repress malignant phenotype, acting as either oncogenic or tumor-suppressor, respectively. Oncogenic miRNAs (OncomiRs) are overexpressed in cancers whereas tumor-suppressor miRNA is downregulated, thereby leading to the onset of carcinogenesis, metastasis, and poor survival. However, there are conflicting pieces of evidence as if a miRNA behaves like an oncogene or tumor-suppressor in the tumor microenvironment. This review wishes to directly examine the effects of miRNAs towards MMP regulation in gynecological cancer development and disease progression (**Table 1**).

## OncomiRs

Several oncogenic miRNAs were found to be linked with gynecological cancer development and are involved in cell migration, angiogenesis, apoptosis, etc. (73, 78). Each miRNA has many different targets and modulate different signaling pathways in different cancer types (75, 99). The endogenous inhibitors of MMPs are known as tissue inhibitors of matrix metalloproteases (TIMPs). Disruption of MMPs/TIMPs balance occurs during multiple pathological conditions including cancer. In CC, miR-106a downregulates TIMP-2 through direct binding to its 3'-UTR region resulting in the induction of MMP-2 as well as MMP-9 expression and subsequently promoting cellular invasion, and migration (69). Alteration of TIMP-2 expression partly eradicates the invasion, migration, and MMP-2/9 expression in CC cells (34). Similarly, in HPV-induced CC, miR-21down-regulates TIMP-3, PTEN, and STAT3 expressions (61). Additionally, in uterine endometrial stromal sarcoma, miR-21 decreases the level of PTEN by directly binding to 3'UTR, leading to increased proliferation, invasion, decreased apoptosis, and metastatic potential thereby upregulating MMP-2 and -9 (73, 78). Epithelial-to-mesenchymal transition (EMT) is a crucial feature of cancer enabling cells to acquire mobility and translocate to distant sites. miR-183 promotes cellular proliferation and EMT in uterine EC by inhibiting CPEB1 expression and up-regulating MMP-9 expression. Studies

**TABLE 1** | Oncogenic and tumor suppressor miRNAs regulating MMPs during development of gynecological cancers.

| Disease | microRNA | ExpressionLevel | MMPs Involved | Binding | Function(s) | References |
|---|---|---|---|---|---|---|
| Cervical Cancer | miR-1246 | Upregulated | 2/9 | Indirect | Induces proliferation, tumor growth, cell migration, invasion, metastasis and EMT. | (69–72) |
| | miR-106a | Upregulated | | Indirect | | |
| | miR-183 | Downregulated | | Direct | | |
| | miR200b | Downregulated | | Indirect | | |
| Cervical Cancer | miR-21 | Upregulated | 2/9 | Indirect | Increased STAT3 decreased TIMP-3 and PTEN expression leading to cell invasion. | (73) |
| Cervical Cancer | miR-195-5p | Downregulated | 14 | Direct | Promotes proliferation and invasion by directly binding of miR-195-5p to 3'UTR of MMP-14 and modulating TNF-α pathway | (74) |
| Endometrial Cancer | miR-183 | Upregulated | 2/9 | Direct | Promotes cell proliferation and invasion. | (75–77) |
| | miR-130b | Upregulated | | Indirect | | |
| Uterine Endometrial Stromal Carcinoma | miR-21 | Upregulated | 2 | Indirect | Induces cell invasion and wound healing. | (78) |
| | miR-31 | Downregulated | | Indirect | | |
| | miR-145 | Upregulated | | Indirect | | |
| | miR-195 | Upregulated | | Indirect | | |
| Ovarian Cancer | miR-92 | Upregulated | 2/9 | Indirect | Promotes migration and angiogenesis by inhibiting VHL and upregulating HIF1α pathway genes. | (79, 80) |
| | miR-210 | Upregulated | | Indirect | | |
| Ovarian Cancer | miR-205 | Upregulated | 2/10 | Indirect | Promotes invasion *via* inhibiting TCF-21. | (81) |
| Endometrial Adenocarcinoma | miR-410 | Downregulated | 14 | Direct | Promotes tumor formation. | (13, 82) |
| Endometrial Cancer | miR-195 | Downregulated | 2/9 | Indirect | Promotes EMT by targeting GPER/PI3K/AKT. | (83) |
| Endometrial Endometroid Carcinoma | mir-22 | Downregulated | 2/9 | Indirect | Induces cell proliferation and invasion. | (84) |
| Endometrial Cancer | miR-320a | Downregulated | 3/9 | Indirect | Inhibits TGFβ-induced EMT. | (85) |
| | miR-340-5p | Downregulated | | Indirect | | |
| Ovarian Cancer | miR-574-3p | Downregulated | 9 | Indirect | Promotes migration and invasion, inhibiting AKT, FAK and c-Src by targeting EGFR. | (86) |
| Ovarian Cancer | miR-29b | Downregulated | 2 | Direct | Induces cell migration by regulating crosstalk between OC cells and fibroblast. | (12, 87) |
| Ovarian Cancer | miR-1236-3p | Downregulated | 2 | Indirect | Promotes proliferation and invasion and EMT *via* VEGF. | (88) |
| Ovarian Cancer | miR-16 | Downregulated | 2/9 | Indirect | Promotes migration and invasion *via* Wnt/β-catenin signaling pathway. | (89) |
| Ovarian Cancer | miR let-7d-5p | Downregulated | 2/9 | Indirect | Promotes proliferation by regulating p53 signaling pathway *via* HMGA1. | (90) |
| Ovarian Cancer | miR-1273g-3p | Downregulated | 2/9 | Indirect | Regulation of TNF-α and COL1A1. | (91) |
| Ovarian Cancer | miR-199a-5p | Downregulated | 2/9 | Indirect | Promotes cellular growth, proliferation and invasion *via* NF-κB pathway. | (92, 93) |
| | miR-9 | Downregulated | | Indirect | | |
| Ovarian Cancer | miR-122 | Downregulated | 2/14 | Indirect | Promotes EMT by targeting P4HA1. | (94) |
| Ovarian Cancer | miR-130b-3p | Downregulated | 2/9 | Indirect | Promotes EMT, cellular attachment and proliferation | (50, 95) |
| | miR-200 | Downregulated | | Indirect | through TGF-β signaling pathway. | |
| Ovarian Cancer | miR-17 | Downregulated | 2 | Indirect | Promotes metastasis by regulating integrin α5 and β1. | (96) |
| Ovarian Cancer | miR-340 | Downregulated | 2/9 | Indirect | Promotes metastasis and inhibits apoptosis *via* NF-x03BA;B1 activation. | (97) |
| Ovarian Cancer | miR-543 | Downregulated | 7 | Direct | Promotes invasion by direct binding of miR-543 to 3'-UTR of MMP-7. | (98) |

revealed CPEB1 and MMP-9 as the direct target of miR-183, also a binding region for 3'UTR of MMP-9 is found at the seed region of miR-183 (75, 76).

Von Hippel Lindau (VHL), a tumor suppressor, targets HIF1α/2α by ubiquitination involving E3 ligase to proteasomal degradation. Loss of VHL results in the accumulation of HIF1α inside the nuclei and expression of HIF target genes which subsequently leads to oncogenesis (100). In OC, miR-92 inhibits VHL, which in turn de-repress HIF-1α. HIF-1α, in turn, stimulates VEGF by acting as a transcription factor together with p300 and p-STAT3 (99). Similarly, miR-210 is another important miRNA activated during the hypoxic condition and has a role in DNA damage response, mitochondrial metabolism, cellular proliferation, angiogenesis, and apoptotic cell death. Loss of VHL in OC stabilizes HIF-1α which in turn stimulates miR-210 expression inducing tumor aggressiveness (79).

DNA methylation/histone acetylation forms a complex framework for epigenetic regulation during cancer development. An altered methylation pattern is seen in cancer cells, both globally and CpG islands in the promoter region (101), leading to aberrant gene activity during tumorigenesis. In EC, different levels of miR-130b expression and its CpG methylation were linked to MMP-2/9 expression and EMT-

related genes. Reversing miR-130b promoter hypermethylation decreased EC cell malignancy, suggesting that CpG island hypermethylation-mediated miRNA silencing contributes to carcinogenesis and is related to aggressive tumor behavior *via* increased MMP-2/9 expression, however, the mechanism behind the regulation of MMP expression by this miRNA is still unknown (77).

## Tumor Suppressor miRNAs

Tumor suppressor miRNAs are under-expressed during cancer progression and regulate cancer development by downregulating genes involved in tumorigenesis. The majority of ECs are accompanied by abnormal hormone signaling, where estrogen receptor α (ERα) behaves as oncogenic stimuli (102). Estrogen induction regulates cellular proliferation and subsequent invasion in EC and is accompanied by a downregulation of miR-22 in ER-α positive cell lines. Transfected miR-22 mimics into endometrial cells reduced the release of MMP-9 and MMP-2 thereby reversing 17β-estradiol (E2)-mediated progression of the cell cycle, cellular proliferation, and invasiveness of ERα-positive EC cells (84).

miR-200 family members have an enormous function in multiple cancer types (103–106). miR-200b plays a key role in regulating EMT and is correlated with cancer growth, proliferation, drug resistance in numerous diseases (107, 108). Cytoskeletal remodeling is the central event in the metastatic spread of cancerous cells. Actin structures facilitate cell migration and invasion, disruption of which leads to increased metastatic spread (109). In CC, miR-200b can suppress RhoE function, which regulates actin cytoskeleton and cell migration by altering cell motility by targeting MMP-9 thus suppressing EMT (70). Another report showed that downregulation of miR-200 family expression by TGFβ induced MMP-2, -9, and fibronectin 1 production and stimulated cancer cell attachment to human primary mesothelial cells (110). Catalpol induces miR-200 expression which sequentially inhibits MMP-2 expression levels, decreases cell proliferation, and accelerates apoptosis in OC cells (50). Similarly, TGFβ1 induced EMT was linked with decreased miR-320a and increased MMP-3 and -9 expressions in EC cells. Excessive expression of miR-320a or miR-340-5p substantially inhibited HEC-1A (endometrial adenocarcinoma cell line) cell invasion and migration through its binding to eIF4E mRNA 3'-UTR and diminished TGF-1-induced EMT properties (85). Another report suggested the involvement of miR-130b-3p in EMT, invasion, migration in cancer various types, mainly *via* the TGFβ pathway (111, 112). In OC overexpression of CMPK, cytidine nucleoside monophosphate kinase is seen, and CMPK knockdown dramatically decreases the cellular proliferation, invasion, and migration, along with MMP-9/-2 expression in epithelial OC. Downregulation of miR-130b-3p is seen in EOC which upregulates CMPK *via* the TGF-β signaling pathway (95).

Rak et al. showed a higher MMP-14 expression in endometrial adenocarcinoma tissue with a decrease in miR-410 level, suggesting a regulatory effect of miR-410 in modulating EC cell progression although the mechanism is largely unknown (13). Studies in odontoblast cells suggest the presence of a probable binding site for miR-410 on 3'UTR of MMP-14 (82). In lung cancer, miR-410 has a tumor-suppressive role by inducing apoptosis through downregulating JAK/STAT3/SOCS3 signaling pathway (113). Another miRNA, miR-195 has tumor-suppressive nature which negatively regulates cellular proliferation, migration, invasion, and promotes apoptosis (114–116). miR-195 overexpression ectopically decreased the viability, migration, and invasiveness of the endometrial carcinoma cell lines, along with the TIMP-2 upregulation and MMP-2/9 downregulation. miR-195 targets GPER (G protein-coupled estrogen receptor) and reduced the phosphorylation levels of PI3K/AKT, thus negatively regulating EMT in endometrial carcinoma (83). miR-195 also suppresses CC cellular proliferation, invasion, and migration through the TNF-pathway. The MMP-14 3'UTR binds to miR-195-5p directly through which its expression is directly inhibited. MMP-14 can modulate the expression of TNF-α. A downregulated miR-195-5p and an upregulated MMP-14 were noticed in CC (74).

miR-574-3p has an enormous role in cancer progression, EMT, metastasis, invasion, and chemosensitivity (117, 118). In epithelial OC, it inhibits the activation of AKT, FAK, c-Src, and MMP-9 by negatively regulating EGFR, inhibiting the cell invasion, and migration, and also increasing EOC cell sensitivity to paclitaxel and cisplatin (86). Different patterns of Let-7 family miRNAs were found in multiple cancers. In OC, let-7d-5p induces cell apoptosis and rescues chemosensitivity to cisplatin by targeting HMGA1 directly and thereby regulating the p53 pathway, MMP-2 and -9, and apoptotic pathway (90).

miR-17 is a highly conserved 6-membered gene cluster and is shown to have numerous roles in various pathways (119–121). In OC cells, it is seen to be downregulated thereby suppressing its inhibitory action of peritoneal metastasis *via* targeting integrin α5 and β1 and MMP-2 expression. miR-17 specifically binds to the α5 and β1 integrins 3'UTR region directly and decreases their expression. The addition of miR-17 to OC cells *in vitro* showed a significant decrease in adhesion and invasion (96). miR-29b is dysregulated in various cancers. It has a tumor-suppressing role in OC and is seen to be involved in tumor malignancy. It increases the α-SMA (mesenchymal cell markers) expression in fibroblasts which is a component of the cellular microenvironment that contributes to tumor malignancy by getting hyperactive and acquiring CAF (cancer-associated fibroblast) profile during carcinogenesis. These fibroblasts downregulate miR-29b expression in SKOV3 cells (ovarian cancer cell line), resulting in an increased invasion and migration. miR-29b can potentially target MMP-2 which is also found to be upregulated in OC (12). Studies in lung cancer metastasis also revealed the presence of a binding site of miR-29b at the MMP-2 3'UTR region through which it downregulates MMP-2 expression (87).miR-543 has been seen to be dysregulated in many cancers. It regulates proliferation, migration/invasion, EMT, metastasis, and many other pathways (122–124). miR-543 suppresses MMP-7 gene translation *via* the direct binding of MMP-7 3'-UTR whereas placental growth factor (PLGF), an angiogenic factor, represses the inhibitory action of miR-543 activating the MMP-7 mediated EMT and invasion in OC (98). Certain miRNAs have a dual role in carcinogenesis.

Although previously stated that miR-183 is oncogenic, it is also seen to possess a tumor-suppressive function. In CC tissues, miR-183 expression was notably reduced whereas MMP-9 expression was elevated. The addition of miR-183 in-vitro resulted in a reduced invasion and migration of CC cell lines, *via* directly targeting MMP-9 and reduction of metastatic capability. A presence of a possible binding site of miR-183 was found at the 3'UTR regions of the MMP-9 gene (71).

## PREDICTING THE ROLE OF MMPs IN CANCER SIGNALING PATHWAYS

To have a better understanding of the functions of MMPs and their regulation in cancer, an interaction plot has been created in String database (http://www.string-db.org) and analyzed in *Cytoscape ver 3.8.1.* Initially, miRwalk and miRmap database were used to find the miRNA and understand the regulating MMPs in gynecological cancer. The MMPs and their correlated genes were selected with k mean value of 0.23, neighborhood active interaction source, with a minimum confidence score of 0.45 and minimum stringency. As shown in **Figure 2**, MMP-9, -3, -7 and -2 are considered hub genes since most of the protein-protein interactions are seen among them. MMP-9, -7, -3, -2, -8 and -14 also show proximity to each other, hence they are correlated in each other's biochemical activity. A significant positive correlation is also seen in MMPs interacting with genes viz; ADAM17, PLAUR, TGFB1, SERPINE1, STAT3, EGF and TIMP. Results showed a positive correlation with genes involved in tumorigenesis and extracellular matrix proteins (125–130). IGF1, VEGFA, STAT3, PLG, ACAN and TIMP-2 were found to directly regulate with MMP-3, MMP-9 and MMP-7, respectively (**Figure 2**).

Screening of the miRNA was performed from the miRNA library and enrichment analysis was performed to understand the cellular activity and biochemical pathways in the form of a heat map showing the association of miRNAs involved in signaling pathways was created in miRpath (https://tools4mirs.org/software/target_functional_analysis/mirtar/). Recent evidence suggests the participation of miRNA in regulating MMP gene expression and is associated with key physiological pathways like TGF β, Rap1, Toll-like, Hippo, B cell and T cell receptor signaling pathway (131–136) (**Figure 3**). miRNAs regulate the actin cytoskeleton, which works synergistically on MMP regulation during cancer growth and metastasis (137, 138). As seen from th heatmap, among the miRNAs reported to regulate MMPs in gynecological cancer, miR-199-5p, miR-21-5p, miR-145-5p and miR-29b-3p have shown the highest

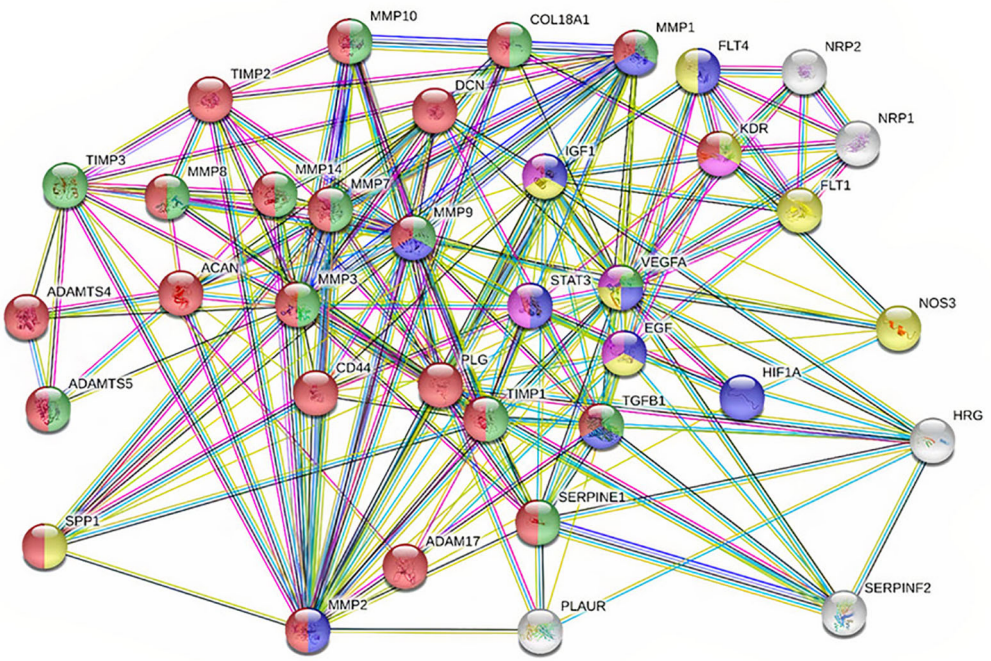


**FIGURE 2** | PPI network showing 36 associated proteins in cancer. The nodes are each candidate. Edges represent their interactions. The divisions with nodes are the shared functions. Blue symbolizes those that have a function in cell proliferation. Green and Red are the ones regulating ECM. Yellow are those with proliferation and angiogenesis.

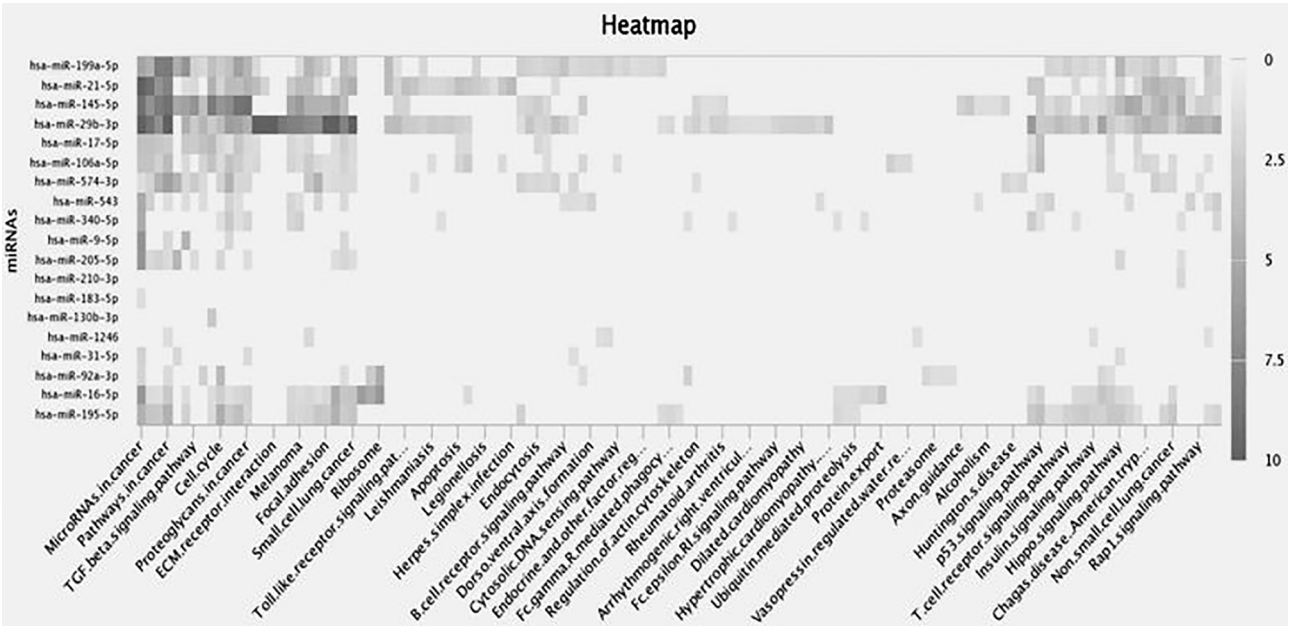


**FIGURE 3** | Heat map depicts differential expression of miRNAs in various biological processes. Rows represent enrichment results for the target miRNAs whereas columns show biochemical pathways. Each highlighted miRNA is correlated to the adjacent biological process in the black color gradient. The color of individual fields represents P-value of the enrichment results. The dark shade shows a strong correlation between miRNA and the target pathways, the light shades correspond to weaker ones, whereas transparent area explains no role of miRNA in that process.

correlation with cancer-related signaling pathways (**Figure 3**). miR-145-5p and miR-21-5p are associated with *TGF βand Hippo signaling pathway* whereas miR-29b-3p regulates *FAK pathway, Insulin pathway* and *p53 signaling pathway*, along with ECM receptor interactions and is also shown to play a crucial role in small cell lung cancer and melanoma (**Figure 3**). From literature studies, we found that miR-29b directly binds to MMP -2 3'UTR and regulates their expression in OC (12). Prudent manipulation of these miRNAs can therefore regulate MMP production in cancer cells and can act as antitumor agents.

## miRNA-BASED ANTI-CANCER THERAPEUTIC STRATEGIES

miRNA-based therapeutic protocols for regulating gene expression can be divided into two main strategies: miRNA anti-sense therapy and miRNA replacement therapy. Inhibition of oncomiRs synthesis can be achieved by using miRNA inhibitors or oligomers and, on the other hand, enhancement of miRNA activity can be achieved by replacement of oncomiRs with the viral vector-mediated introduction of tumor suppressor miRNAs in a cell-specific manner for reprogramming target cells. Strategies to inhibit oncomiRs biogenesis by small-molecule inhibitors, antagomiRs, miRNA sponges, miRNA masking and approaches for replacement of miRNAs, including lentiviral vectors, tumor-suppressor miRNA mimics, CRISPR/Cas-like genome editing tools, are currently being investigated as potential cancer therapeutics.

Locked nucleic acid (LNA), a class of high-affinity bicyclic RNA analogs, can detect miRNA in tissues and inhibit their function *in vitro* and *in vivo* studies. *Miravirsen*, a short locked nucleic acid complementary to miR-122 (Roche/Santaris) is the world's first miRNA drug candidate in phase II clinical trials for hepatitis C virus treatment, along with RG-101, an N-acetylgalactosamine-conjugated anti-miR targeting miR-122 (139, 140). Furthermore, tumor suppressor miRNA replacement has been explored utilizing miRNA mimics/lentiviral vectors producing miRNA, which may influence endogenous miRNA expression (141–144). As an alternative to lentiviral vectors that show off-target effects, nonviral miRNA delivery techniques like polyethyleneimine (PEI)-based nanoparticles, liposomes, polymeric micelles, and dendrimers have been proposed. MRX34 was the first miRNA replacement therapy in modified liposomes to enter clinical trials, restoring a tumor suppressor miRNA, miR-34, with promising outcomes in stage I trials (139).

Several potential small molecule drugs targeting enzymes involved in miRNA biogenesis have been identified using comprehensive compound library screening. miR-21 is upregulated in most cancers and suppression of PTEN by miR-21 can contribute to chemoresistance *via* activating the Akt/ERK pathways (145). Screening for small molecules modulating miR-21 activity resulted in the discovery of a novel etheramide backbone which led to a reduction in CC cell proliferation and tumor growth, as well as the activation of apoptosis by activating caspase-3/7 (145).

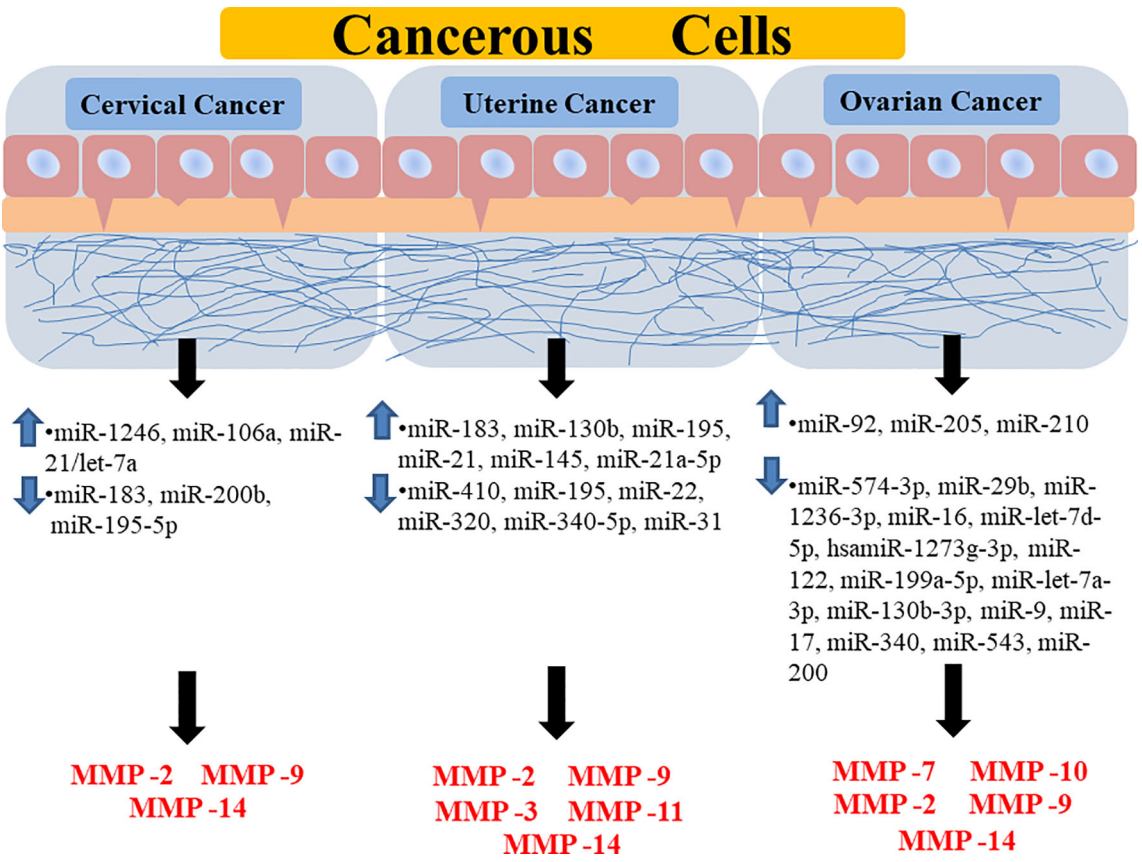


**FIGURE 4** | Diagrammatic representation showing the regulation of different MMPs through different miRNAs in various forms of gynecological cancer. It is showing how the upregulation or downregulation of certain miRNAs is promoting the expression of certain MMPs in a specific type of gynecological cancer. Highlighted miRNAs are highly correlated to major signaling pathways and target MMP-9/2 activities. MMP, Matrix Metalloprotease; miR, MicroRNA.

miRNA sponges are artificial transcripts containing several complementary binding sites for one or more miRNA of interest and can block the activity of multiple miRNAs sharing the same seed sequence. miR-9 reduced the expression of KLF17, CDH1, and LASS2 (tumor suppressor genes). A DNA sponge with four miR-9 binding sites was demonstrated to effectively inhibit miR-9 activity, restoring natural expression of KLF17, CDH1, and LASS2 (146). Researchers are also focusing on utilizing CRISPR/Cas9 gene-editing system for miRNAs inhibition. In human colon cancer cell lines targeting of miR-17/miR-200c/miR-141 loci was done using CRISPR/Cas9 resulting in decreased levels of mature miRNA and low off-target effects (147).

Combination strategies based on the co-administration of miRNA targeting agents along with antitumor drugs have been observed to eradicate drug-resistant tumor cells to treatment and have greater anticancer effects. Nano-liposome-based delivery of miR-205 mimic was shown to sensitize the tumor to radiation therapy in breast cancer xenograft model (148). In another example, PDL1 expression in tumor cells was decreased when mir-34a mimics (MRX34) were combined with radiation (149). Therefore, combining miRNA replacement therapies with conventional anticancer drugs reveal excellent results and presents a novel possibility of chemotherapeutic treatment regimens.

The capacity to target several genes in a particular pathway and efficiently build novel therapeutic components are two advantages of miRNA-based treatment. Given that a single miRNA may regulate multiple MMPs and their downstream signaling pathways amplifies the scope of utilizing miRNAs to act as an attractive candidate for anticancer treatments. However, this also invites additional problems of non-specific target inhibition by miRNAs. Targeting MMPs has been clinically challenging due to the non-specificity and musculoskeletal toxicity of the inhibitors (150). Therefore, precision medicine designed to target the MMPs increased in a particular tumor in a patient might show a potential resolution for this issue.

Even though there are no FDA-approved miRNA therapy candidates for medical intervention to date, potential candidate drugs are in clinical development or are in phase I and II clinical studies (151). Nanoparticle-based, tissue-specific miRNA-drug delivery to a particular lesion in a patient, can improve solubility and efficacy of the medicine while avoiding contact with healthy tissues. Intratumoral injections of miRNA-based therapeutics

directly into the pathogenic site can improve bioavailability, target specificity, effectiveness, and reduce adverse effects in cancer-related diseases (152, 153). Computational deep-learning-based approaches for accurately predicting human miRNA targets at the site level in patients have enabled the use of huge multi-omics data and increased the robustness of prediction models. It is critical to design a good delivery mechanism with high specificity for targeting cells to execute miRNA replacement therapy. As a result, miRNA replacement therapy may be a unique and appealing treatment option for a variety of cancers, and it is vital to research how to carry the appropriate miRNA based on the kind of cancer.

## CONCLUSION AND FUTURE PROSPECTS

MMPs are powerful regulators of cellular proliferation, differentiation, angiogenesis, migration, and apoptosis. MMPs are appealing targets for the creation of selective inhibitors with high therapeutic potential. However, all of the clinical trials in advanced cancer patients with MMP inhibitors were unsuccessful. Numerous MMP inhibitors, including small molecules and blocking antibodies, have been produced as drug candidates to attenuate MMP production but most of their effects tend to be majorly nonspecific. Since MMPs contain similar active sites and play multiple crucial roles in important biological processes, making it is challenging to construct highly selective MMP inhibitors with low toxicities. Therefore, to increase the clinical utility of MMPs for tumor therapy, new MMP inhibitors should be able to individually regulate individual MMPs as well as manage a network of interlinked molecules. The ability of miRNAs to regulate potentially hundreds of genes in a cell-specific manner makes it a powerful target for anticancer treatment (**Figure 4**). Since miRNAs may target MMPs more selectively without interfering with the structural similarities of MMP catalytic domains, miRNA-mediated MMP regulation may lead to the creation of MMP inhibitors. Furthermore, miRNAs may target several molecules, often in the context of a network, making them particularly effective at controlling various biological processes essential to malignant tumors. Comprehensive inter-atomic analyses of miRNAs involved in regulating signaling pathways associated with cancer development and progression might aid in establishing druggable targets for antitumor treatment. Therefore, targeting such miRNA will not only help in understanding their functions but also the underlying cause of several gynecological disorders arising today. For probing miRNA-MMP as an anticancer treatment, proper validation and optimization of miRNA functional role are required in the clinical system, xenograft and orthotopic models to elucidate a detailed understanding of their efficacy in carcinogenesis and for their journey from bench to clinic. Pharmaceutical companies are constantly developing new miRNA-MMP therapies of low cytotoxicity and limited side effects. Whether new technologies targeting miRNAs that regulate MMPs can successfully be employed to delay or stop cancer progression remains to be seen.

## AUTHOR CONTRIBUTIONS

Authors AP and YB were responsible for constructing the title, performing literature study, writing, illustration, and table preparation. SS and AS had taken the initiative of the work and gave their feedback on the study. PS carried out in silico studies and critically reviewed the article. All authors contributed to manuscript revision, read, and approved the submitted version.

## FUNDING

AP and YB are recipients of CSIR and UGC Fellowship, Government of India, respectively. PS gratefully acknowledges the financial support of DBT-RA Program in Biotechnology and Life Sciences, Government of India.

## REFERENCES

1. Bray F, Ferlay J, Soerjomataram I, Siegel RL, Torre LA, Jemal A. Global Cancer Statistics 2018: GLOBOCAN Estimates of Incidence and Mortality Worldwide for 36 Cancers in 185 Countries. *CA Cancer J Clin* (2018) 68 (6):394–424. doi: 10.3322/caac.21492
2. Dumas L, Ring A, Butler J, Kalsi T, Harari D, Banerjee S. Improving Outcomes for Older Women With Gynaecological Malignancies. *Cancer Treat Rev* (2016) 50:99–108. doi: 10.1016/j.ctrv.2016.08.007
3. Ottevanger PB. Ovarian Cancer Stem Cells More Questions Than Answers. *Semin Cancer Biol* (2017) 44:67–71. doi: 10.1016/j.semcancer.2017.04.009
4. Medhin LB, Tekle LA, Achila OO, Said S. Incidence of Cervical, Ovarian and Uterine Cancer in Eritrea: Data From the National Health Laboratory, 2011-2017. *Sci Rep* (2020) 10(1):9099. doi: 10.1038/s41598-020-66096-5
5. Visse R, Nagase H. Matrix Metalloproteinases and Tissue Inhibitors of Metalloproteinases: Structure, Function, and Biochemistry. *Circ Res* (2003) 92(8):827–39. doi: 10.1161/01.RES.0000070112.80711.3D
6. Vizoso FJ, Gonzalez LO, Corte MD, Rodriguez JC, Vazquez J, Lamelas ML, et al. Study of Matrix Metalloproteinases and Their Inhibitors in Breast Cancer. *Br J Cancer* (2007) 96(6):903–11. doi: 10.1038/sj.bjc.6603666
7. Hsu CP, Shen GH, Ko JL. Matrix Metalloproteinase-13 Expression Is Associated With Bone Marrow Microinvolvement and Prognosis in Non-Small Cell Lung Cancer. *Lung Cancer* (2006) 52(3):349–57. doi: 10.1016/j.lungcan.2006.01.011
8. Peng WJ, Zhang JQ, Wang BX, Pan HF, Lu MM, Wang J. Prognostic Value of Matrix Metalloproteinase 9 Expression in Patients With non-Small Cell Lung Cancer. *Clin Chim Acta* (2012) 413(13-14):1121–6. doi: 10.1016/j.cca.2012.03.012
9. Zhang Q, Liu S, Parajuli KR, Zhang W, Zhang K, Mo Z, et al. Interleukin-17 Promotes Prostate Cancer via MMP7-Induced Epithelial-to-Mesenchymal Transition. *Oncogene* (2017) 36(5):687–99. doi: 10.1038/onc.2016.240
10. Kotepui M, Thawornkuno C, Chavalitshewinkoon-Petmitr P, Punyarit P, Petmitr S. Quantitative Real-Time RT-PCR of ITGA7, SVEP1, TNS1, LPHN3, SEMA3G, KLB and MMP13 mRNA Expression in Breast Cancer. *Asian Pac J Cancer Prev* (2012) 13(11):5879–82. doi: 10.7314/APJCP.2012.13.11.5879
11. Li L, Li H. Role of microRNA-Mediated MMP Regulation in the Treatment and Diagnosis of Malignant Tumors. *Cancer Biol Ther* (2013) 14(9):796–805. doi: 10.4161/cbt.25936
12. Medeiros M, Ribeiro AO, Lupi LA, Romualdo GR, Pinhal D, Chuffa LGA, et al. Mimicking the Tumor Microenvironment: Fibroblasts Reduce

miR-29b Expression and Increase the Motility of Ovarian Cancer Cells in a Co-Culture Model. *Biochem Biophys Res Commun* (2019) 516(1):96–101. doi: 10.1016/j.bbrc.2019.06.001
13. Rak B, Garbicz F, Paskal W, Pelka K, Marczewska JM, Wolosz D, et al. The Expression of MMP-14 and microRNA-410 in FFPE Tissues of Human Endometrial Adenocarcinoma. *Histol Histopathol* (2016) 31(8):911–20. doi: 10.14670/HH-11-728
14. Sun XY, Han XM, Zhao XL, Cheng XM, Zhang Y. MiR-93-5p Promotes Cervical Cancer Progression by Targeting THBS2/MMPS Signal Pathway. *Eur Rev Med Pharmacol Sci* (2019) 23(12):5113–21. doi: 10.26355/eurrev_201906_18175
15. Ghildiyal M, Zamore PD. Small Silencing RNAs: An Expanding Universe. *Nat Rev Genet* (2009) 10(2):94–108. doi: 10.1038/nrg2504
16. Ha M, Kim VN. Regulation of microRNA Biogenesis. *Nat Rev Mol Cell Biol* (2014) 15(8):509–24. doi: 10.1038/nrm3838
17. Bartel DP. MicroRNAs: Target Recognition and Regulatory Functions. *Cell* (2009) 136(2):215–33. doi: 10.1016/j.cell.2009.01.002
18. Huntzinger E, Izaurralde E. Gene Silencing by microRNAs: Contributions of Translational Repression and mRNA Decay. *Nat Rev Genet* (2011) 12(2):99–110. doi: 10.1038/nrg2936
19. Lin S, Gregory RI. MicroRNA Biogenesis Pathways in Cancer. *Nat Rev Cancer* (2015) 15(6):321–33. doi: 10.1038/nrc3932
20. He L, Thomson JM, Hemann MT, Hernando-Monge E, Mu D, Goodson S, et al. A microRNA Polycistron as a Potential Human Oncogene. *Nature* (2005) 435(7043):828–33. doi: 10.1038/nature03552
21. Kim HH, Kuwano Y, Srikantan S, Lee EK, Martindale JL, Gorospe M. HuR Recruits Let-7/RISC to Repress C-Myc Expression. *Genes Dev* (2009) 23 (15):1743–8. doi: 10.1101/gad.1812509
22. Johnson SM, Grosshans H, Shingara J, Byrom M, Jarvis R, Cheng A, et al. RAS Is Regulated by the Let-7 microRNA Family. *Cell* (2005) 120(5):635–47. doi: 10.1016/j.cell.2005.01.014
23. Kumar MS, Erkeland SJ, Pester RE, Chen CY, Ebert MS, Sharp PA, et al. Suppression of Non-Small Cell Lung Tumor Development by the Let-7 microRNA Family. *Proc Natl Acad Sci USA* (2008) 105(10):3903–8. doi: 10.1073/pnas.0712321105
24. Lu J, Getz G, Miska EA, Alvarez-Saavedra E, Lamb J, Peck D, et al. MicroRNA Expression Profiles Classify Human Cancers. *Nature* (2005) 435(7043):834–8. doi: 10.1038/nature03702
25. Thomson JM, Newman M, Parker JS, Morin-Kensicki EM, Wright T, Hammond SM. Extensive Post-Transcriptional Regulation of microRNAs and its Implications for Cancer. *Genes Dev* (2006) 20(16):2202–7. doi: 10.1101/gad.1444406
26. Michlewski G, Caceres JF. Post-Transcriptional Control of miRNA Biogenesis. *RNA* (2019) 25(1):1–16. doi: 10.1261/rna.068692.118
27. Hutvagner G, McLachlan J, Pasquinelli AE, Balint E, Tuschl T, Zamore PD. A Cellular Function for the RNA-Interference Enzyme Dicer in the Maturation of the Let-7 Small Temporal RNA. *Science* (2001) 293 (5531):834–8. doi: 10.1126/science.1062961
28. Lund E, Guttinger S, Calado A, Dahlberg JE, Kutay U. Nuclear Export of microRNA Precursors. *Science* (2004) 303(5654):95–8. doi: 10.1126/science.1090599
29. The Knowledge of Pharmacological Therapy of a Group of Calabrian Nurses. The Cultural Association of Nurses of Catanzaro and the Ospedale Di Matera Working Group. *Riv Inferm* (1992) 11(2):71–80.
30. Rorbach G, Unold O, Konopka BM. Distinguishing Mirtrons From Canonical miRNAs With Data Exploration and Machine Learning Methods. *Sci Rep* (2018) 8(1):7560. doi: 10.1038/s41598-018-25578-3
31. Tocchi A, Parks WC. Functional Interactions Between Matrix Metalloproteinases and Glycosaminoglycans. *FEBS J* (2013) 280(10):2332–41. doi: 10.1111/febs.12198
32. Mehana EE, Khafaga AF, El-Blehi SS. The Role of Matrix Metalloproteinases in Osteoarthritis Pathogenesis: An Updated Review. *Life Sci* (2019) 234:116786. doi: 10.1016/j.lfs.2019.116786
33. Scheau C, Badarau IA, Costache R, Caruntu C, Mihai GL, Didilescu AC, et al. The Role of Matrix Metalloproteinases in the Epithelial-Mesenchymal Transition of Hepatocellular Carcinoma. *Anal Cell Pathol (Amst)* (2019) 2019:9423907. doi: 10.1155/2019/9423907
34. Cui N, Hu M, Khalil RA. Biochemical and Biological Attributes of Matrix Metalloproteinases. *Prog Mol Biol Transl Sci* (2017) 147:1–73. doi: 10.1016/bs.pmbts.2017.02.005
35. Baker AH, Edwards DR, Murphy G. Metalloproteinase Inhibitors: Biological Actions and Therapeutic Opportunities. *J Cell Sci* (2002) 115(Pt 19):3719–27. doi: 10.1242/jcs.00063
36. Mannello F, Tonti G, Papa S. Matrix Metalloproteinase Inhibitors as Anticancer Therapeutics. *Curr Cancer Drug Targets* (2005) 5(4):285–98. doi: 10.2174/1568009054064615
37. Chambers AF, Matrisian LM. Changing Views of the Role of Matrix Metalloproteinases in Metastasis. *J Natl Cancer Inst* (1997) 89(17):1260–70. doi: 10.1093/jnci/89.17.1260
38. Dong H, Diao H, Zhao Y, Xu H, Pei S, Gao J, et al. Overexpression of Matrix Metalloproteinase-9 in Breast Cancer Cell Lines Remarkably Increases the Cell Malignancy Largely via Activation of Transforming Growth Factor Beta/SMAD Signalling. *Cell Prolif* (2019) 52(5):e12633. doi: 10.1111/cpr.12633
39. Bredin CG, Liu Z, Klominek J. Growth Factor-Enhanced Expression and Activity of Matrix Metalloproteases in Human Non-Small Cell Lung Cancer Cell Lines. *Anticancer Res* (2003) 23(6C):4877–84.
40. Massague J. TGFbeta in Cancer. *Cell* (2008) 134(2):215–30. doi: 10.1016/j.cell.2008.07.001
41. Dallas SL, Rosser JL, Mundy GR, Bonewald LF. Proteolysis of Latent Transforming Growth Factor-Beta (TGF-Beta)-Binding Protein-1 by Osteoclasts. A Cellular Mechanism for Release of TGF-Beta From Bone Matrix. *J Biol Chem* (2002) 277(24):21352–60. doi: 10.1074/jbc.M111663200
42. Behrens P, Rothe M, Florin A, Wellmann A, Wernert N. Invasive Properties of Serous Human Epithelial Ovarian Tumors Are Related to Ets-1, MMP-1 and MMP-9 Expression. *Int J Mol Med* (2001) 8(2):149–54. doi: 10.3892/ijmm.8.2.149
43. Tian R, Li X, Gao Y, Li Y, Yang P, Wang K. Identification and Validation of the Role of Matrix Metalloproteinase-1 in Cervical Cancer. *Int J Oncol* (2018) 52(4):1198–208. doi: 10.3892/ijo.2018.4267
44. Zhu L, Zheng X, Du Y, Xing Y, Xu K, Cui L. Matrix Metalloproteinase-7 may Serve as a Novel Biomarker for Cervical Cancer. *Onco Targets Ther* (2018) 11:4207–20. doi: 10.2147/OTT.S160998
45. Wang CH, Li YH, Tian HL, Bao XX, Wang ZM. Long non-Coding RNA BLACAT1 Promotes Cell Proliferation, Migration and Invasion in Cervical Cancer Through Activation of Wnt/Beta-Catenin Signaling Pathway. *Eur Rev Med Pharmacol Sci* (2018) 22(10):3002–9. doi: 10.26355/eurrev_201805_15057
46. Al-Alem LF, McCord LA, Southard RC, Kilgore MW, Curry TE Jr. Activation of the PKC Pathway Stimulates Ovarian Cancer Cell Proliferation, Migration, and Expression of MMP7 and MMP10. *Biol Reprod* (2013) 89(3):73. doi: 10.1095/biolreprod.112.102327
47. Wang F, Chang Z, Fan Q, Wang L. Epigallocatechin3gallate Inhibits the Proliferation and Migration of Human Ovarian Carcinoma Cells by Modulating P38 Kinase and Matrix Metalloproteinase2. *Mol Med Rep* (2014) 9(3):1085–9. doi: 10.3892/mmr.2014.1909
48. Meyer E, Vollmer JY, Bovey R, Stamenkovic I. Matrix Metalloproteinases 9 and 10 Inhibit Protein Kinase C-Potentiated, P53-Mediated Apoptosis. *Cancer Res* (2005) 65(10):4261–72. doi: 10.1158/0008-5472.CAN-04-2908
49. Pu Z, Zhu M, Kong F. Telmisartan Prevents Proliferation and Promotes Apoptosis of Human Ovarian Cancer Cells Through Upregulating PPARgamma and Downregulating MMP9 Expression. *Mol Med Rep* (2016) 13(1):555–9. doi: 10.3892/mmr.2015.4512
50. Gao N, Tian JX, Shang YH, Zhao DY, Wu T. Catalpol Suppresses Proliferation and Facilitates Apoptosis of OVCAR-3 Ovarian Cancer Cells Through Upregulating microRNA-200 and Downregulating MMP-2 Expression. *Int J Mol Sci* (2014) 15(11):19394–405. doi: 10.3390/ijms151119394
51. Khasigov PZ, Podobed OV, Gracheva TS, Salbiev KD, Grachev SV, Berezov TT. Role of Matrix Metalloproteinases and Their Inhibitors in Tumor Invasion and Metastasis. *Biochem (Mosc)* (2003) 68(7):711–7. doi: 10.1023/A:1025051214001
52. Davidson B, Goldberg I, Gotlieb WH, Kopolovic J, Ben-Baruch G, Nesland JM, et al. High Levels of MMP-2, MMP-9, MT1-MMP and TIMP-2 mRNA

Correlate With Poor Survival in Ovarian Carcinoma. *Clin Exp Metastasis* (1999) 17(10):799–808. doi: 10.1023/A:1006723011835
53. Cortez-Retamozo V, Etzrodt M, Newton A, Rauch PJ, Chudnovskiy A, Berger C, et al. Origins of Tumor-Associated Macrophages and Neutrophils. *Proc Natl Acad Sci* (2012) 109(7):2491–6. doi: 10.1073/pnas.1113744109
54. Kenny HA, Lengyel E. MMP-2 Functions as an Early Response Protein in Ovarian Cancer Metastasis. *Cell Cycle* (2009) 8(5):683–8. doi: 10.4161/cc.8.5.7703
55. Mitra A, Chakrabarti J, Chattopadhyay N, Chatterjee A. Membrane-Associated MMP-2 in Human Cervical Cancer. *J Environ Pathol Toxicol Oncol* (2003) 22(2):93–100. doi: 10.1615/jenvpathtoxoncol.v22.i2.20
56. Piura B, Rabinovich A, Huleihel M. Matrix Metalloproteinases and Their Tissue Inhibitors in Malignancies of the Female Genital Tract. *Harefuah* (2003) 142(11):786–91, 804.
57. Brun JL, Cortez A, Commo F, Uzan S, Rouzier R, Darai E. Serous and Mucinous Ovarian Tumors Express Different Profiles of MMP-2, -7, -9, MT1-MMP, and TIMP-1 and -2. *Int J Oncol* (2008) 33(6):1239–46.
58. Li Y, Jin X, Kang S, Wang Y, Du H, Zhang J, et al. Polymorphisms in the Promoter Regions of the Matrix Metalloproteinases-1, -3, -7, and -9 and the Risk of Epithelial Ovarian Cancer in China. *Gynecol Oncol* (2006) 101(1):92–6. doi: 10.1016/j.ygyno.2005.09.058
59. Guo H, Dai Y, Wang A, Wang C, Sun L, Wang Z. Association Between Expression of MMP-7 and MMP-9 and Pelvic Lymph Node and Para-Aortic Lymph Node Metastasis in Early Cervical Cancer. *J Obstet Gynaecol Res* (2018) 44(7):1274–83. doi: 10.1111/jog.13659
60. Su Y, Gao L, Teng L, Wang Y, Cui J, Peng S, et al. Id1 Enhances Human Ovarian Cancer Endothelial Progenitor Cell Angiogenesis via PI3K/Akt and NF-Kappab/MMP-2 Signaling Pathways. *J Transl Med* (2013) 11:132. doi: 10.1186/1479-5876-11-132
61. Wang FQ, Fisher J, Fishman DA. MMP-1-PAR1 Axis Mediates LPA-Induced Epithelial Ovarian Cancer (EOC) Invasion. *Gynecol Oncol* (2011) 120(2):247–55. doi: 10.1016/j.ygyno.2010.10.032
62. Agarwal A, Tressel SL, Kaimal R, Balla M, Lam FH, Covic L, et al. Identification of a Metalloprotease-Chemokine Signaling System in the Ovarian Cancer Microenvironment: Implications for Antiangiogenic Therapy. *Cancer Res* (2010) 70(14):5880–90. doi: 10.1158/0008-5472.CAN-09-4341
63. Belotti D, Paganoni P, Manenti L, Garofalo A, Marchini S, Taraboletti G, et al. Matrix Metalloproteinases (MMP9 and MMP2) Induce the Release of Vascular Endothelial Growth Factor (VEGF) by Ovarian Carcinoma Cells: Implications for Ascites Formation. *Cancer Res* (2003) 63(17):5224–9.
64. Huang S, Van Arsdall M, Tedjarati S, McCarty M, Wu W, Langley R, et al. Contributions of Stromal Metalloproteinase-9 to Angiogenesis and Growth of Human Ovarian Carcinoma in Mice. *J Natl Cancer Inst* (2002) 94 (15):1134–42. doi: 10.1093/jnci/94.15.1134
65. Duellman T, Warren C, Yang J. Single Nucleotide Polymorphism-Specific Regulation of Matrix Metalloproteinase-9 by Multiple miRNAs Targeting the Coding Exon. *Nucleic Acids Res* (2014) 42(9):5518–31. doi: 10.1093/nar/gku197
66. Wang X, Chen X, Sun L, Bi X, He H, Chen L, et al. MicroRNA34a Inhibits Cell Growth and Migration in Human Glioma Cells via MMP9. *Mol Med Rep* (2019) 20(1):57–64. doi: 10.3892/mmr.2019.10233
67. Karimi L, Zeinali T, Hosseinahli N, Mansoori B, Mohammadi A, Yousefi M, et al. miRNA-143 Replacement Therapy Harnesses the Proliferation and Migration of Colorectal Cancer Cells In Vitro. *J Cell Physiol* (2019) 234 (11):21359–68. doi: 10.1002/jcp.28745
68. Li Q, Zhao H, Chen W, Huang P, Bi J. Human Keratinocyte-Derived Microvesicle miRNA-21 Promotes Skin Wound Healing in Diabetic Rats Through Facilitating Fibroblast Function and Angiogenesis. *Int J Biochem Cell Biol* (2019) 114:105570. doi: 10.1016/j.biocel.2019.105570
69. Li X, Zhou Q, Tao L, Yu C. MicroRNA-106a Promotes Cell Migration and Invasion by Targeting Tissue Inhibitor of Matrix Metalloproteinase 2 in Cervical Cancer. *Oncol Rep* (2017) 38(3):1774–82. doi: 10.3892/or.2017.5832
70. Cheng YX, Chen GT, Chen C, Zhang QF, Pan F, Hu M, et al. MicroRNA-200b Inhibits Epithelial-Mesenchymal Transition and Migration of Cervical Cancer Cells by Directly Targeting RhoE. *Mol Med Rep* (2016) 13(4):3139–46. doi: 10.3892/mmr.2016.4933
71. Fan D, Wang Y, Qi P, Chen Y, Xu P, Yang X, et al. MicroRNA-183 Functions as the Tumor Suppressor via Inhibiting Cellular Invasion and Metastasis by Targeting MMP-9 in Cervical Cancer. *Gynecol Oncol* (2016) 141(1):166–74. doi: 10.1016/j.ygyno.2016.02.006
72. Chen J, Yao D, Zhao S, He C, Ding N, Li L, et al. MiR-1246 Promotes SiHa Cervical Cancer Cell Proliferation, Invasion, and Migration Through Suppression of its Target Gene Thrombospondin 2. *Arch Gynecol Obstet* (2014) 290(4):725–32. doi: 10.1007/s00404-014-3260-2
73. Shishodia G, Shukla S, Srivastava Y, Masaldan S, Mehta S, Bhambhani S, et al. Alterations in microRNAs miR-21 and Let-7a Correlate With Aberrant STAT3 Signaling and Downstream Effects During Cervical Carcinogenesis. *Mol Cancer* (2015) 14:116. doi: 10.1186/s12943-015-0385-2
74. Li M, Ren CX, Zhang JM, Xin XY, Hua T, Wang HB, et al. The Effects of miR-195-5p/MMP14 on Proliferation and Invasion of Cervical Carcinoma Cells Through TNF Signaling Pathway Based on Bioinformatics Analysis of Microarray Profiling. *Cell Physiol Biochem* (2018) 50(4):1398–413. doi: 10.1159/000494602
75. Xiong H, Chen R, Liu S, Lin Q, Chen H, Jiang Q. MicroRNA-183 Induces Epithelial-Mesenchymal Transition and Promotes Endometrial Cancer Cell Migration and Invasion in by Targeting CPEB1. *J Cell Biochem* (2018) 119 (10):8123–37. doi: 10.1002/jcb.26763
76. Ruan H, Liang X, Zhao W, Ma L, Zhao Y. The Effects of microRNA-183 Promots Cell Proliferation and Invasion by Targeting MMP-9 in Endometrial Cancer. *BioMed Pharmacother* (2017) 89:812–8. doi: 10.1016/j.biopha.2017.02.091
77. Li BL, Lu W, Lu C, Qu JJ, Yang TT, Yan Q, et al. CpG Island Hypermethylation-Associated Silencing of microRNAs Promotes Human Endometrial Cancer. *Cancer Cell Int* (2013) 13(1):44. doi: 10.1186/1475-2867-13-44
78. Ravid Y, Formanski M, Smith Y, Reich R, Davidson B. Uterine Leiomyosarcoma and Endometrial Stromal Sarcoma Have Unique miRNA Signatures. *Gynecol Oncol* (2016) 140(3):512–7. doi: 10.1016/j.ygyno.2016.01.001
79. Bavelloni A, Ramazzotti G, Poli A, Piazzi M, Focaccia E, Blalock W, et al. MiRNA-210: A Current Overview. *Anticancer Res* (2017) 37(12):6511–21. doi: 10.21873/anticanres.12107
80. Guo FJ, Shao YP, Wang YP, Jin YM, Liu SS, Wang QY. MIR-92 Stimulates VEGF by Inhibiting Von Hippel-Lindau Gene Product in Epithelial Ovarian Cancer. *J Biol Regul Homeost Agents* (2017) 31(3):615–24.
81. Wei J, Zhang L, Li J, Zhu S, Tai M, Mason CW, et al. MicroRNA-205 Promotes Cell Invasion by Repressing TCF21 in Human Ovarian Cancer. *J Ovarian Res* (2017) 10(1):33. doi: 10.1186/s13048-017-0328-1
82. Brodzikowska A, Gondek A, Rak B, Paskal W, Pelka K, Cudnoch-Jedrzejewska A, et al. Metalloproteinase 14 (MMP-14) and hsa-miR-410-3p Expression in Human Inflamed Dental Pulp and Odontoblasts. *Histochem Cell Biol* (2019) 152(5):345–53. doi: 10.1007/s00418-019-01811-6
83. Deng J, Wang W, Yu G, Ma X. MicroRNA195 Inhibits Epithelialmesenchymal Transition by Targeting G Proteincoupled Estrogen Receptor 1 in Endometrial Carcinoma. *Mol Med Rep* (2019) 20 (5):4023–32. doi: 10.3892/mmr.2019.10652
84. Li S, Hu R, Wang C, Guo F, Li X, Wang S. miR-22 Inhibits Proliferation and Invasion in Estrogen Receptor Alpha-Positive Endometrial Endometrioid Carcinomas Cells. *Mol Med Rep* (2014) 9(6):2393–9. doi: 10.3892/mmr.2014.2123
85. Zhang HH, Li R, Li YJ, Yu XX, Sun QN, Li AY, et al. Eif4erelated Mir320a and Mir3405p Inhibit Endometrial Carcinoma Cell Metastatic Capability by Preventing TGFbeta1induced Epithelialmesenchymal Transition. *Oncol Rep* (2020) 43(2):447–60. doi: 10.3892/or.2019.7437
86. Zhang P, Zhu J, Zheng Y, Zhang H, Sun H, Gao S. miRNA-574-3p Inhibits Metastasis and Chemoresistance of Epithelial Ovarian Cancer (EOC) by Negatively Regulating Epidermal Growth Factor Receptor (EGFR). *Am J Transl Res* (2019) 11(7):4151–65.
87. Wang H, Guan X, Tu Y, Zheng S, Long J, Li S, et al. MicroRNA-29b Attenuates non-Small Cell Lung Cancer Metastasis by Targeting Matrix Metalloproteinase 2 and PTEN. *J Exp Clin Cancer Res* (2015) 34:59. doi: 10.1186/s13046-015-0169-y
88. Li QH, Liu Y, Chen S, Zong ZH, Du YP, Sheng XJ, et al. Circ-CSPP1 Promotes Proliferation, Invasion and Migration of Ovarian Cancer Cells by Acting as a miR-1236-3p Sponge. *BioMed Pharmacother* (2019) 114:108832. doi: 10.1016/j.biopha.2019.108832

89. Li N, Yang L, Sun Y, Wu X. MicroRNA-16 Inhibits Migration and Invasion via Regulation of the Wnt/beta-Catenin Signaling Pathway in Ovarian Cancer. *Oncol Lett* (2019) 17(3):2631–8. doi: 10.3892/ol.2019.9923
90. Chen YN, Ren CC, Yang L, Nai MM, Xu YM, Zhang F, et al. MicroRNA Let7d5p Rescues Ovarian Cancer Cell Apoptosis and Restores Chemosensitivity by Regulating the P53 Signaling Pathway via HMGA1. *Int J Oncol* (2019) 54(5):1771–84. doi: 10.3892/ijo.2019.4731
91. Gunel T, Gumusoglu E, Dogan B, Ertem FB, Hosseini MK, Cevik N, et al. Potential Biomarker of Circulating hsa-miR-1273g-3p Level for Detection of Recurrent Epithelial Ovarian Cancer. *Arch Gynecol Obstet* (2018) 298 (6):1173–80. doi: 10.1007/s00404-018-4913-3
92. Liu X, Yao B, Wu Z. miRNA-199a-5p Suppresses Proliferation and Invasion by Directly Targeting NF-Kappab1 in Human Ovarian Cancer Cells. *Oncol Lett* (2018) 16(4):4543–50. doi: 10.3892/ol.2018.9170
93. Huang X, Teng Y, Yang H, Ma J. Propofol Inhibits Invasion and Growth of Ovarian Cancer Cells via Regulating miR-9/NF-kappaB Signal. *Braz J Med Biol Res* (2016) 49(12):e5717. doi: 10.1590/1414-431X20165717
94. Duan Y, Dong Y, Dang R, Hu Z, Yang Y, Hu Y, et al. MiR-122 Inhibits Epithelial Mesenchymal Transition by Regulating P4HA1 in Ovarian Cancer Cells. *Cell Biol Int* (2018) 42(11):1564–74. doi: 10.1002/cbin.11052
95. Zhou D, Zhang L, Sun W, Guan W, Lin Q, Ren W, et al. Cytidine Monophosphate Kinase Is Inhibited by the TGF-Beta Signalling Pathway Through the Upregulation of miR-130b-3p in Human Epithelial Ovarian Cancer. *Cell Signal* (2017) 35:197–207. doi: 10.1016/j.cellsig.2017.04.009
96. Gong C, Yang Z, Wu F, Han L, Liu Y, Gong W. miR-17 Inhibits Ovarian Cancer Cell Peritoneal Metastasis by Targeting ITGA5 and ITGB1. *Oncol Rep* (2016) 36(4):2177–83. doi: 10.3892/or.2016.4985
97. Li P, Sun Y, Liu Q. MicroRNA-340 Induces Apoptosis and Inhibits Metastasis of Ovarian Cancer Cells by Inactivation of NF-X03ba;B1. *Cell Physiol Biochem* (2016) 38(5):1915–27. doi: 10.1159/000445553
98. Song N, Liu H, Ma X, Zhang S. Placental Growth Factor Promotes Metastases of Ovarian Cancer Through MiR-543-Regulated MMP7. *Cell Physiol Biochem* (2015) 37(3):1104–12. doi: 10.1159/000430235
99. Guo F, Tian J, Lin Y, Jin Y, Wang L, Cui M. Serum microRNA-92 Expression in Patients With Ovarian Epithelial Carcinoma. *J Int Med Res* (2013) 41 (5):1456–61. doi: 10.1177/0300060513487652
100. Zhang S, Zhou X, Wang B, Zhang K, Liu S, Yue K, et al. Loss of VHL Expression Contributes to Epithelial-Mesenchymal Transition in Oral Squamous Cell Carcinoma. *Oral Oncol* (2014) 50(9):809–17. doi: 10.1016/j.oraloncology.2014.06.007
101. Choi SJ, Jung SW, Huh S, Chung YS, Cho H, Kang H. Alteration of DNA Methylation in Gastric Cancer With Chemotherapy. *J Microbiol Biotechnol* (2017) 27(8):1367–78. doi: 10.4014/jmb.1704.04035
102. Rodriguez AC, Blanchard Z, Maurer KA, Gertz J. Estrogen Signaling in Endometrial Cancer: A Key Oncogenic Pathway With Several Open Questions. *Horm Cancer* (2019) 10(2-3):51–63. doi: 10.1007/s12672-019-0358-9
103. Liu C, Hu W, Li LL, Wang YX, Zhou Q, Zhang F, et al. Roles of miR-200 Family Members in Lung Cancer: More Than Tumor Suppressors. *Future Oncol* (2018) 14(27):2875–86. doi: 10.2217/fon-2018-0155
104. Mekala JR, Naushad SM, Ponnusamy L, Arivazhagan G, Sakthiprasad V, Pal-Bhadra M. Epigenetic Regulation of miR-200 as the Potential Strategy for the Therapy Against Triple-Negative Breast Cancer. *Gene* (2018) 641:248–58. doi: 10.1016/j.gene.2017.10.018
105. O'Brien SJ, Carter JV, Burton JF, Oxford BG, Schmidt MN, Hallion JC, et al. The Role of the miR-200 Family in Epithelial-Mesenchymal Transition in Colorectal Cancer: A Systematic Review. *Int J Cancer* (2018) 142(12):2501–11. doi: 10.1002/ijc.31282
106. D'Ippolito E, Plantamura I, Bongiovanni L, Casalini P, Baroni S, Piovan C, et al. miR-9 and miR-200 Regulate PDGFRbeta-Mediated Endothelial Differentiation of Tumor Cells in Triple-Negative Breast Cancer. *Cancer Res* (2016) 76(18):5562–72. doi: 10.1158/0008-5472.CAN-16-0140
107. Yang X, Hu Q, Hu LX, Lin XR, Liu JQ, Lin X, et al. miR-200b Regulates Epithelial-Mesenchymal Transition of Chemo-Resistant Breast Cancer Cells by Targeting FN1. *Discovery Med* (2017) 24(131):75–85.
108. Ren S, Liu J, Feng Y, Li Z, He L, Li L, et al. Knockdown of Circdennd4c Inhibits Glycolysis, Migration and Invasion by Up-Regulating miR-200b/C in Breast Cancer Under Hypoxia. *J Exp Clin Cancer Res* (2019) 38(1):388. doi: 10.1186/s13046-019-1398-2
109. Izdebska M, Zielinska W, Grzanka D, Gagat M. The Role of Actin Dynamics and Actin-Binding Proteins Expression in Epithelial-To-Mesenchymal Transition and Its Association With Cancer Progression and Evaluation of Possible Therapeutic Targets. *BioMed Res Int* (2018) 2018:4578373. doi: 10.1155/2018/4578373
110. Sugiyama K, Kajiyama H, Shibata K, Yuan H, Kikkawa F, Senga T. Expression of the Mir200 Family of microRNAs in Mesothelial Cells Suppresses the Dissemination of Ovarian Cancer Cells. *Mol Cancer Ther* (2014) 13(8):2081–91. doi: 10.1158/1535-7163.MCT-14-0135
111. Li S, Geng J, Xu X, Huang X, Leng D, Jiang D, et al. miR-130b-3p Modulates Epithelial-Mesenchymal Crosstalk in Lung Fibrosis by Targeting IGF-1. *PloS One* (2016) 11(3):e0150418. doi: 10.1371/journal.pone.0150418
112. Shui Y, Yu X, Duan R, Bao Q, Wu J, Yuan H, et al. miR-130b-3p Inhibits Cell Invasion and Migration by Targeting the Notch Ligand Delta-Like 1 in Breast Carcinoma. *Gene* (2017) 609:80–7. doi: 10.1016/j.gene.2017.01.036
113. Li M, Zheng R, Yuan FL. MiR-410 Affects the Proliferation and Apoptosis of Lung Cancer A549 Cells Through Regulation of SOCS3/JAK-STAT Signaling Pathway. *Eur Rev Med Pharmacol Sci* (2018) 22(18):5987–93. doi: 10.26355/eurrev_201809_15933
114. Yu X, Zhang Y, Wu B, Kurie JM, Pertsemlidis A. The miR-195 Axis Regulates Chemoresistance Through TUBB and Lung Cancer Progression Through BIRC5. *Mol Ther Oncolytics* (2019) 14:288–98. doi: 10.1016/j.omto.2019.07.004
115. Gao X, Lu M, Xu W, Liu C, Wu J. miR-195 Inhibits Esophageal Cancer Cell Proliferation and Promotes Apoptosis by Downregulating YAP1. *Int J Clin Exp Pathol* (2019) 12(1):275–81.
116. Li B, Wang S, Wang S. MiR-195 Suppresses Colon Cancer Proliferation and Metastasis by Targeting WNT3A. *Mol Genet Genomics* (2018) 293(5):1245–53. doi: 10.1007/s00438-018-1457-y
117. Li WC, Wu YQ, Gao B, Wang CY, Zhang JJ. MiRNA-574-3p Inhibits Cell Progression by Directly Targeting CCND2 in Colorectal Cancer. *Biosci Rep* (2019) 39(12). doi: 10.1042/BSR20190976
118. Wang M, Zhang R, Zhang S, Xu R, Yang Q. MicroRNA-574-3p Regulates Epithelial Mesenchymal Transition and Cisplatin Resistance via Targeting ZEB1 in Human Gastric Carcinoma Cells. *Gene* (2019) 700:110–9. doi: 10.1016/j.gene.2019.03.043
119. Zhang X, Li Y, Qi P, Ma Z. Biology of MiR-17-92 Cluster and Its Progress in Lung Cancer. *Int J Med Sci* (2018) 15(13):1443–8. doi: 10.7150/ijms.27341
120. Jin J, Kim SN, Liu X, Zhang H, Zhang C, Seo JS, et al. miR-17-92 Cluster Regulates Adult Hippocampal Neurogenesis, Anxiety, and Depression. *Cell Rep* (2016) 16(6):1653–63. doi: 10.1016/j.celrep.2016.06.101
121. Mandelbaum AD, Kredo-Russo S, Aronowitz D, Myers N, Yanowski E, Klochendler A, et al. miR-17-92 and miR-106b-25 Clusters Regulate Beta Cell Mitotic Checkpoint and Insulin Secretion in Mice. *Diabetologia* (2019) 62(9):1653–66. doi: 10.1007/s00125-019-4916-z
122. Liu X, Gan L, Zhang J. miR-543 Inhibites Cervical Cancer Growth and Metastasis by Targeting TRPM7. *Chem Biol Interact* (2019) 302:83–92. doi: 10.1016/j.cbi.2019.01.036
123. Zhao H, Diao C, Wang X, Xie Y, Liu Y, Gao X, et al. MiR-543 Promotes Migration, Invasion and Epithelial-Mesenchymal Transition of Esophageal Cancer Cells by Targeting Phospholipase A2 Group IVA. *Cell Physiol Biochem* (2018) 48(4):1595–604. doi: 10.1159/000492281
124. Zhai F, Cao C, Zhang L, Zhang J. miR-543 Promotes Colorectal Cancer Proliferation and Metastasis by Targeting KLF4. *Oncotarget* (2017) 8 (35):59246–56. doi: 10.18632/oncotarget.19495
125. Quemener C, Gabison EE, Naimi B, Lescaille G, Bougatef F, Podgorniak MP, et al. Extracellular Matrix Metalloproteinase Inducer Up-Regulates the Urokinase-Type Plasminogen Activator System Promoting Tumor Cell Invasion. *Cancer Res* (2007) 67(1):9–15. doi: 10.1158/0008-5472.CAN-06-2448
126. Mezyk-Kopec R, Wyroba B, Stalinska K, Prochnicki T, Wiatrowska K, Kilarski WW, et al. ADAM17 Promotes Motility, Invasion, and Sprouting of Lymphatic Endothelial Cells. *PloS One* (2015) 10(7):e0132661. doi: 10.1371/journal.pone.0132661
127. Furler RL, Nixon DF, Brantner CA, Popratiloff A, Uittenbogaart CH. TGF-Beta Sustains Tumor Progression Through Biochemical and Mechanical Signal Transduction. *Cancers (Basel)* (2018) 10(6). doi: 10.3390/cancers10060199

128. Smirnova T, Bonapace L, MacDonald G, Kondo S, Wyckoff J, Ebersbach H, et al. Serpin E2 Promotes Breast Cancer Metastasis by Remodeling the Tumor Matrix and Polarizing Tumor Associated Macrophages. *Oncotarget* (2016) 7(50):82289–304. doi: 10.18632/oncotarget.12927
129. Jia ZH, Jia Y, Guo FJ, Chen J, Zhang XW, Cui MH. Phosphorylation of STAT3 at Tyr705 Regulates MMP-9 Production in Epithelial Ovarian Cancer. *PloS One* (2017) 12(8):e0183622. doi: 10.1371/journal.pone.0183622
130. Peeney D, Jensen SM, Castro NP, Kumar S, Noonan S, Handler C, et al. TIMP-2 Suppresses Tumor Growth and Metastasis in Murine Model of Triple-Negative Breast Cancer. *Carcinogenesis* (2020) 41(3):313–25. doi: 10.1093/carcin/bgz172
131. Park H, Huang X, Lu C, Cairo MS, Zhou X. MicroRNA-146a and microRNA-146b Regulate Human Dendritic Cell Apoptosis and Cytokine Production by Targeting TRAF6 and IRAK1 Proteins. *J Biol Chem* (2015) 290(5):2831–41. doi: 10.1074/jbc.M114.591420
132. Yu Y, Kanwar SS, Patel BB, Oh PS, Nautiyal J, Sarkar FH, et al. MicroRNA-21 Induces Stemness by Downregulating Transforming Growth Factor Beta Receptor 2 (TGFbetaR2) in Colon Cancer Cells. *Carcinogenesis* (2012) 33 (1):68–76. doi: 10.1093/carcin/bgr246
133. Pan BL, Tong ZW, Li SD, Wu L, Liao JL, Yang YX, et al. Decreased microRNA-182-5p Helps Alendronate Promote Osteoblast Proliferation and Differentiation in Osteoporosis via the Rap1/MAPK Pathway. *Biosci Rep* (2018) 38(6). doi: 10.1042/BSR20180696
134. Tian Y, Liu Y, Wang T, Zhou N, Kong J, Chen L, et al. A microRNA-Hippo Pathway That Promotes Cardiomyocyte Proliferation and Cardiac Regeneration in Mice. *Sci Transl Med* (2015) 7(279):279ra38. doi: 10.1126/scitranslmed.3010841
135. Rao DS, O'Connell RM, Chaudhuri AA, Garcia-Flores Y, Geiger TL, Baltimore D. MicroRNA-34a Perturbs B Lymphocyte Development by Repressing the Forkhead Box Transcription Factor Foxp1. *Immunity* (2010) 33(1):48–59. doi: 10.1016/j.immuni.2010.06.013
136. Mildner A, Chapnik E, Varol D, Aychek T, Lampl N, Rivkin N, et al. MicroRNA-142 Controls Thymocyte Proliferation. *Eur J Immunol* (2017) 47 (7):1142–52. doi: 10.1002/eji.201746987
137. Ghosh T, Soni K, Scaria V, Halimani M, Bhattacharjee C, Pillai B. MicroRNA-Mediated Up-Regulation of an Alternatively Polyadenylated Variant of the Mouse Cytoplasmic {Beta}-Actin Gene. *Nucleic Acids Res* (2008) 36(19):6318–32. doi: 10.1093/nar/gkn624
138. Han M, Dong LH, Zheng B, Shi JH, Wen JK, Cheng Y. Smooth Muscle 22 Alpha Maintains the Differentiated Phenotype of Vascular Smooth Muscle Cells by Inducing Filamentous Actin Bundling. *Life Sci* (2009) 84(13-14):394–401. doi: 10.1016/j.lfs.2008.11.017
139. Shah MY, Ferrajoli A, Sood AK, Lopez-Berestein G, Calin GA. microRNA Therapeutics in Cancer - An Emerging Concept. *EBioMedicine* (2016) 12:34–42. doi: 10.1016/j.ebiom.2016.09.017
140. Bonneau E, Neveu B, Kostantin E, Tsongalis GJ, De Guire V. How Close are miRNAs From Clinical Practice? A Perspective on the Diagnostic and Therapeutic Market. *EJIFCC* (2019) 30(2):114–27.
141. Valoczi A, Hornyik C, Varga N, Burgyan J, Kauppinen S, Havelda Z. Sensitive and Specific Detection of microRNAs by Northern Blot Analysis Using LNA-Modified Oligonucleotide Probes. *Nucleic Acids Res* (2004) 32 (22):e175. doi: 10.1093/nar/gnh171
142. Kloosterman WP, Wienholds E, de Bruijn E, Kauppinen S, Plasterk RH. In Situ Detection of miRNAs in Animal Embryos Using LNA-Modified Oligonucleotide Probes. *Nat Methods* (2006) 3(1):27–9. doi: 10.1038/nmeth843
143. Neely LA, Patel S, Garver J, Gallo M, Hackett M, McLaughlin S, et al. A Single-Molecule Method for the Quantitation of microRNA Gene Expression. *Nat Methods* (2006) 3(1):41–6. doi: 10.1038/nmeth825
144. Hagiwara K, Kosaka N, Yoshioka Y, Takahashi RU, Takeshita F, Ochiya T. Stilbene Derivatives Promote Ago2-Dependent Tumour-Suppressive microRNA Activity. *Sci Rep* (2012) 2:314. doi: 10.1038/srep00314
145. Ankenbruck N, Kumbhare R, Naro Y, Thomas M, Gardner L, Emanuelson C, et al. Small Molecule Inhibition of microRNA-21 Expression Reduces Cell Viability and Microtumor Formation. *Bioorg Med Chem* (2019) 27 (16):3735–43. doi: 10.1016/j.bmc.2019.05.044
146. Takahashi RU, Prieto-Vila M, Kohama I, Ochiya T. Development of miRNA-Based Therapeutic Approaches for Cancer Patients. *Cancer Sci* (2019) 110(4):1140–7. doi: 10.1111/cas.13965
147. Nguyen DD, Chang S. Development of Novel Therapeutic Agents by Inhibition of Oncogenic MicroRNAs. *Int J Mol Sci* (2017) 19(1). doi: 10.3390/ijms19010065
148. Zhang P, Wang L, Rodriguez-Aguayo C, Yuan Y, Debeb BG, Chen D, et al. miR-205 Acts as a Tumour Radiosensitizer by Targeting ZEB1 and Ubc13. *Nat Commun* (2014) 5:5671. doi: 10.1038/ncomms6671
149. Cortez MA, Ivan C, Valdecanas D, Wang X, Peltier HJ, Ye Y, et al. PDL1 Regulation by P53 via miR-34. *J Natl Cancer Inst* (2016) 108(1). doi: 10.1093/jnci/djv303
150. Winer A, Adams S, Mignatti P. Matrix Metalloproteinase Inhibitors in Cancer Therapy: Turning Past Failures Into Future Successes. *Mol Cancer Ther* (2018) 17(6):1147–55. doi: 10.1158/1535-7163.MCT-17-0646
151. Chakraborty C, Sharma AR, Sharma G, Lee SS. Therapeutic Advances of miRNAs: A Preclinical and Clinical Update. *J Adv Res* (2021) 28:127–38. doi: 10.1016/j.jare.2020.08.012
152. Chen Y, Gao DY, Huang L. In Vivo Delivery of miRNAs for Cancer Therapy: Challenges and Strategies. *Adv Drug Deliv Rev* (2015) 81:128–41. doi: 10.1016/j.addr.2014.05.009
153. Munoz JL, Bliss SA, Greco SJ, Ramkissoon SH, Ligon KL, Rameshwar P. Delivery of Functional Anti-miR-9 by Mesenchymal Stem Cell-Derived Exosomes to Glioblastoma Multiforme Cells Conferred Chemosensitivity. *Mol Ther Nucleic Acids* (2013) 2:e126. doi: 10.1038/mtna.2013.60


**Conflict of Interest:** The authors declare that the research was conducted in the absence of any commercial or financial relationships that could be construed as a potential conflict of interest.

frontiers in Oncology

MINI REVIEW
published: 11 February 2022
doi: 10.3389/fonc.2022.836630

# The Biological Relevance of NHERF1 Protein in Gynecological Tumors

*Margherita Sonnessa[1†], Sara Sergio[2†], Concetta Saponaro[1*], Michele Maffia[2], Daniele Vergara[2], Francesco Alfredo Zito[1] and Andrea Tinelli[3]*

[1] Functional Biomorphology Laboratory, Pathology Department, IRCCS Istituto Tumori "Giovanni Paolo II", Bari, Italy,
[2] Department of Biological and Environmental Sciences and Technologies (DiSTeBA), University of Salento, Lecce, Italy,
[3] Department of Obstetrics and Gynecology, "Veris delli Ponti" Hospital, Lecce, Italy

Gynecological cancer management remains challenging and a better understanding of molecular mechanisms that lead to carcinogenesis and development of these diseases is needed to improve the therapeutic approaches. The $Na^+/H^+$ exchanger regulatory factor 1 (NHERF1) is a scaffold protein that contains modular protein-interaction domains able to interact with molecules with an impact on carcinogenesis and cancer progression. During recent years, its involvement in gynecological cancers has been explored, suggesting that NHERF1 could be a potential biomarker for the development of new targeted therapies suitable to the management of these tumors. This comprehensive review provides an update on the recent study on NHERF1 activity and its pathological role in cervical and ovarian cancer, as well as on its probable involvement in the therapeutic landscape of these cancer types.

**Keywords: NHERF1, gynecological cancers, cervical cancer, ovarian cancer, Wnt/beta-catenin pathway**

OPEN ACCESS

***Edited by:***
*Elena Ioana Braicu, Charité Universitätsmedizin Berlin, Germany*

***Reviewed by:***
*Gianluca Baldanzi, Università degli Studi del Piemonte Orientale, Italy*

***Correspondence:**
*Concetta Saponaro*
*c.saponaro@oncologico.bari.it*

*[†]These authors have contributed equally to this work and share first authorship*

***Specialty section:***
*This article was submitted to Gynecological Oncology, a section of the journal Frontiers in Oncology*

***Received:*** *15 December 2021*
***Accepted:*** *21 January 2022*
***Published:*** *11 February 2022*

***Citation:***
*Sonnessa M, Sergio S, Saponaro C, Maffia M, Vergara D, Zito FA and Tinelli A (2022) The Biological Relevance of NHERF1 Protein in Gynecological Tumors. Front. Oncol. 12:836630. doi: 10.3389/fonc.2022.836630*

## GYNECOLOGICAL CANCERS: EMERGING MOLECULAR ASPECTS

Gynecological cancers include a diverse group of neoplasms that originate in a woman's reproductive system. This includes tumors that originate from these distinct anatomical sites including vulva, vagina, corpus uteri, fallopian tube and ovary (1). These tumor types represent an important cause of cancer morbidity and mortality worldwide.

Recent findings have defined the molecular profile of gynecological tumors at a systemic level. In this scenario, a work published in 2019 comprehensively defined the mutational, gene and protein expression profile of a cohort (Pan-Gynecologic from the The Cancer Genome Atlas) of over 2000 cases of four gynecological types plus breast (2). Results of this study demonstrated that pan-gyn tumors are unique compared to other tumor types and result from the interplay of different factors including multiple genomic and epigenomic features and somatic copy-number alterations. Among the pan-gyn tumors, studies of expression profiles suggest that at least nine and five clusters with distinct clinicopathologic characteristics can be observed at the mRNA and protein level, respectively.

The results of a subsequent study conducted on a cohort of 209 patients diagnosed with cervical, endometrial and ovarian cancer further defines the molecular differences and similarities between these different cancer types and assessed whether molecular heterogeneity is observed in an early or late stage of tumorigenesis (3). The results of this study led to two important conclusion: i) the identification of a common reprogramming process emerging at the early stages of tumorigenesis

which involves the activation of phosphatidylinositol 3-kinase (PI3K) protein, defects in mismatch repair program and cilium organization, as well as disruption in interferon signaling and immune recognition; ii) a cell-type specific program that is activated at a late-stage tumor development.

Although gynecological tumors emerge from a common precursor (coelomic epithelium, also known as mesothelium), data from these studies demonstrate the presence of molecular pathways relevant to sustain this tumor heterogeneity useful for diagnostic and therapeutic purposes. Central nodes include PI3K, AKT, and Wnt-β-catenin pathways among the others, that are involved in the regulation of biological processes such as cell cycle, motility, metabolism, and differentiation. In pan-gyn tumors, the mutational landscape and expression levels of these kinases is well described but less is known about other regulatory mechanisms. For instance, their biological activity is regulated through the dynamic interactions with scaffold proteins that bind and direct the cellular localization of their interaction partners. One of these scaffold proteins with a well-established role in the regulation of cell signaling is the protein sodium/hydrogen exchanger regulatory factor 1 (NHERF1). In this review article, we describe the functional significance of NHERF1 in gynecological tumors. As it is upregulated in tumor tissues compared to normal samples (**Figure 1**), NHERF1 could represent a potential target for clinical applications.

## STRUCTURAL AND FUNCTIONAL ASPECTS OF NA(+)/H(+) EXCHANGE REGULATORY COFACTOR NHERF1 PROTEIN

The sodium/hydrogen exchanger regulatory factor 1 (NHERF1), known also as the 50-kDa ezrin-binding protein (EBP50) comes into sight in the scientific landscape in the late 1990s as a co-regulator of the exchanger of the sodium–hydrogen antiporter 3 (NHE3) in rabbit kidney epithelia. In detail, NHERF1 is an adaptive protein, encoded by the *SLC9A31R1* gene, physiologically expressed in the sub-plasma membranous region of human tissues including, lung, gastrointestinal tract, liver and gallbladder, kidney and urinary bladder, male and female tissues (data from https://www.proteinatlas.org/ENSG00000109062-SLC9A3R1/tissue).

NHERF1 belongs to the NHERF family of protein–protein interaction modules (PDZ)-scaffold proteins. The PDZ family of proteins is one of the largest in the human proteome including membrane-associated guanylate kinases (MAGUKs), involved in different molecular signal networks (4); nitric oxide synthase 1 (neuronal) (NOS1), engaged in neurotoxicity associated with neurodegenerative diseases (5); segment polarity protein dishevelled homolog DVL1-2-3 (DVL1-2-3), implicated in cell proliferation and molecular transducer for different human diseases (6). Scaffolding proteins play a critical role in coordinating cellular response by the assembly of multiple complexes that make faster and more effective the molecular signals. Thanks to this ability, they can improve the efficiency and selectivity of intracellular signaling and have a pivotal role in oncogenic development.

In specific, NHERF family consists of four members including NHERF1/*SLC9A31R1*, NHERF2/*SLC9A3R2*, NHERF3/*PDZK1*, and NHERF4/*PDZD3*. Each member presents a unique molecular organization and tissue distribution. In detail, the N-terminal domain of NHERF1 is characterized by two post-synaptic density 95/disc-large/zona occludens (PDZ) repeated domains. A hallmark of these domains is the ability to target specific proteins. In fact, most NHERF1 associated proteins bind to the first PDZ domain and only a few proteins, such as NHE3 (7), β-catenin (8) and Yap 65 (9), specifically interact with the second PDZ domain. The C-terminal region is identified as an EZRIN binding domain (EB) that mediates the connection with the family of EZRIN-Radixin-Moesin (ERM) proteins (10). The EB domain ends in a PDZ

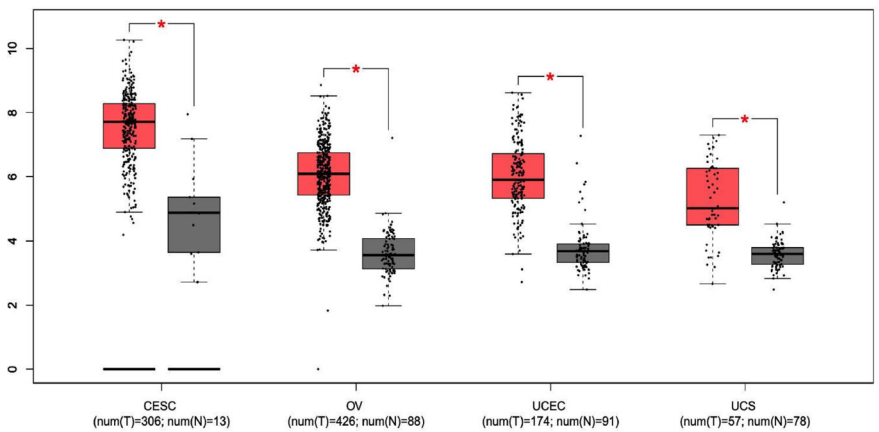


**FIGURE 1** | The expression of NHERF1 protein in different gynecological tissues. Boxplot results of the expression levels of NHERF1 in cervical squamous cell carcinoma and endocervical adenocarcinoma (CESC), ovarian cancer (OV), uterine corpus endometrial carcinoma (UCEC) and uterine carcinosarcoma (UCS) analyzed using GEPIA database. Red box, tumor samples; green box, normal samples. T, tumor; N, normal. P-value was set up at 0.01. (* = $p < 0.01$).

motif similar to the ($S/T_XL$) PDZ motif present in other NHERF1 ligands (11). The binding of EB to the PDZ2 domain of NHERF1 creates an intra-molecular interaction that induces a self-inhibited conformation status. This prevents both PDZ domains from binding their specific ligands. After the binding of ERM proteins to the EB region, the intramolecular head-to-tail conformation is lost, allowing the association among NHERF1 binding partners and PDZ domains (**Figures 2A, B**).

It has been demonstrated the ability of the two PDZ domains to regulate differently the metastatic properties of cancer cells. Indeed, the selective inactivation of one of the two domains in a model of breast cancer supports the activation of a visceral or bone metastatic dissemination route. This highlights the substantial molecular differences in the phenotypic programs regulated by the two PDZ domains (12).

NHERF1 functions as molecular scaffolds to coordinate different signaling processes. However, recent works have demonstrated that NHERF1 is more than a mere scaffold or anchor in the cell. Indeed, in a variety of diseases and tissues, NHERF1 has been shown to contribute to:

- Cell polarity and regulation of actin cytoskeleton dynamics, through the interaction with ERM proteins and β-catenin;

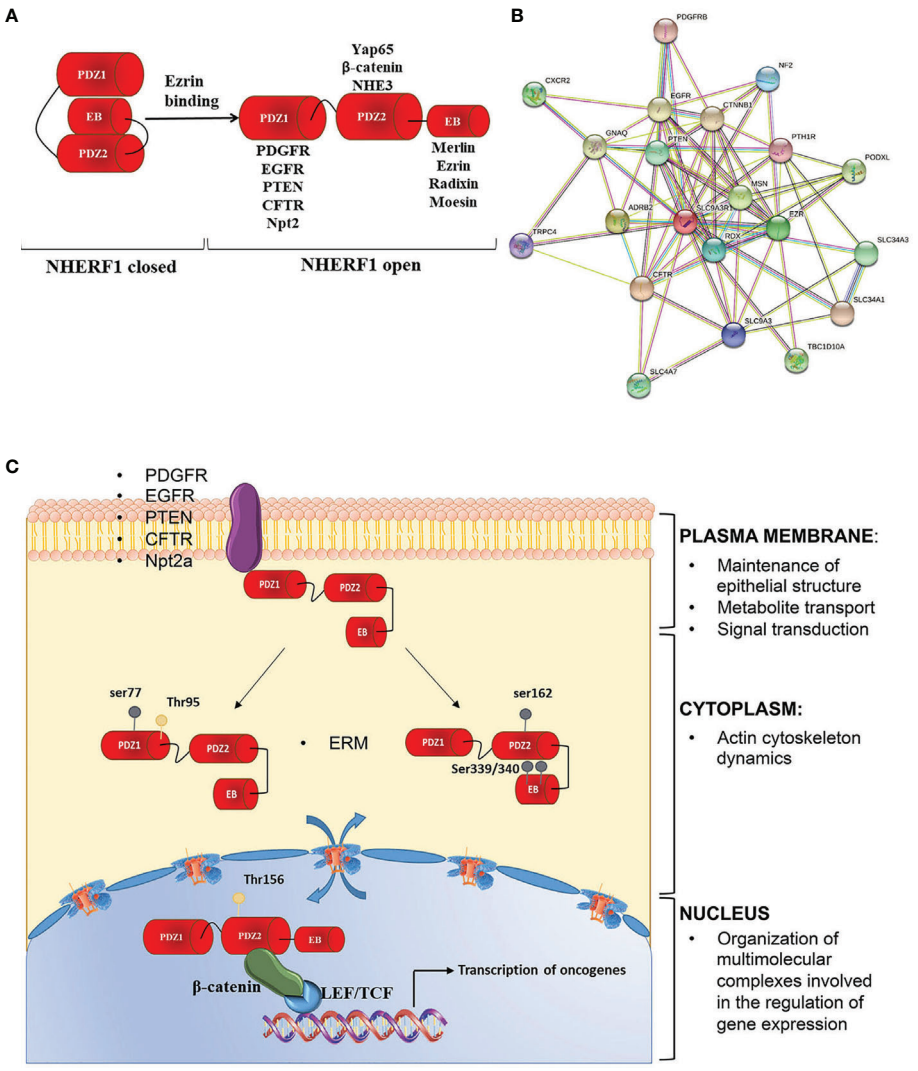


**FIGURE 2** | NHERF1 molecular structure and functions. **(A)** NHERF1/EBP50 presents a closed conformation in which the PDZ2 domain binds to the C-terminal EB region in a "head to tail" interaction masking the PDZ domains. Binding of the ERM proteins to the EB region switches NHERF1 to an open conformation in which the PDZ domains are unmasked and able to bind their interactive partners. **(B)** NHERF1 protein-protein interaction network, according to STRING software. **(C)** NHERF1 functions are influenced by its subcellular localization, phosphorylation and expression. NHERF1 is normally located at the plasma membrane where it has a protective role. Phosphorylation on ser 339/340 on the EB domain or on Thr 156 in PDZ2 domain increases NHERF1 binding affinity to its targets promoting its translocation in the cytoplasm where NHERF1 can have a pro-neoplastic and metastatic role and can alter integrity of actin cytoskeleton. Phosphorylation on Thr 156 causes NHERF1 nuclear localization where it is involved in regulation of oncogenes expression and cancer progression. Possible interactors of NHERF1 are also indicated.

- Metabolite transport at the cell membrane, through the interaction with the type 2a sodium-phosphate cotransporter (NPT2a) and the cystic fibrosis transmembrane conductance regulator (CFTR);
- Signal transduction, through the interaction with the protein phosphatase and tensin homolog (PTEN), the platelet-derived growth factor receptor (PDGFR) and the epidermal growth factor receptor (EGFR);
- Gene transcription, through the interaction with β-catenin.

These different functions can be altered by NHERF1 localization, phosphorylation and expression (**Figure 2C**) (13).

When NHERF1 is localized at the plasma membrane, the protein preserves the epithelial polarity through the formation of tight junctions (14), targets several proteins to the apical or basolateral membrane (15, 16) and cooperates in the formation and assembly of protein complexes at the microvillus (17). Instead, when located within the cell NHERF1 reduces the integrity of the actin cytoskeleton, by increasing α-actinin IV ubiquitination and degradation (18).

The localization and oligomerization, as well as the assembly and disassembly from protein complexes of NHERF1 are regulated through phosphorylation. In detail, phosphorylation on human serine 339/340 (serine 337/338 in rat) favors NHERF1 oligomerization by increasing PDZ2 accessibility and NHERF1 binding affinity to its targets (19), while phosphorylation on other sites influences NHERF1 subcellular localization. Indeed, it has been observed that NHERF1 phosphorylation on human serine 339/340 by protein kinase C (PKC) induces NHERF1 relocalization from cell periphery to the cytosol (20). Phosphorylation at serine 77 the PDZ I domain impairs NHERF1 affinity for plasma membrane proteins thus influencing its subcellular localization (21). Although NHERF1 does not present a nuclear localization signal, it has been found in the nucleus of proliferative cells. However, at present little is known on the traffic between the cytosol and the nucleus. Recently, it has been shown that NHERF1 phosphorylation is involved in its cytoplasm nuclear trafficking (22). In contrast, NHERF1 dephosphorylation by the phosphatase of regenerating liver 3 (PRL-3) causes the nucleus export of NHERF1 to the cytoplasm (23).

NHERF1 can be also regulated at the transcriptional level. NHERF1 gene overexpression is associated with: i) the development of acute inflammatory response (24), ii) a protective role against acute injury (25) and iii) the promotion of metastatic tumor behavior (12). The transcription of NHERF1 is regulated by β-catenin. Indeed, Saponaro and colleagues demonstrated that mRNA and protein levels of NHERF1 expression are negatively regulated by oncogenic β-catenin signalling in colorectal cell lines harboring different Wnt/β-catenin mutations. In particular, nuclear activated β-catenin can regulate NHERF1 directly through the transcriptional factor TCF4 (26).

## NHERF1 AND CERVICAL CANCER

In the last decade, NHERF1 acquired a key role as a prognostic biomarker in cervical cancer (CC) progression (**Figure 3**). The bioinformatics analysis of two GEO datasets and the analysis of validation performed in 31 tissue specimens, demonstrated a down-regulation of NHERF1 expression in cervical cancer samples compared to adjacent normal tissues. Moreover, the down-regulation of NHERF1 was significantly associated with both Wnt signaling and cell proliferation thus suggesting a potential tumor-suppressive role (27). It is likely that NHERF1 inhibits cervical cancer cell proliferation through the downregulation of the actin cross-linking protein α-Actinin-4 (ACTN4). In fact, ACTN4 is functionally implicated in the regulation of β-catenin expression by NHERF1 (27).

One of the mechanisms proposed to explain the down-regulation of NHERF1 in CC is through the interaction of

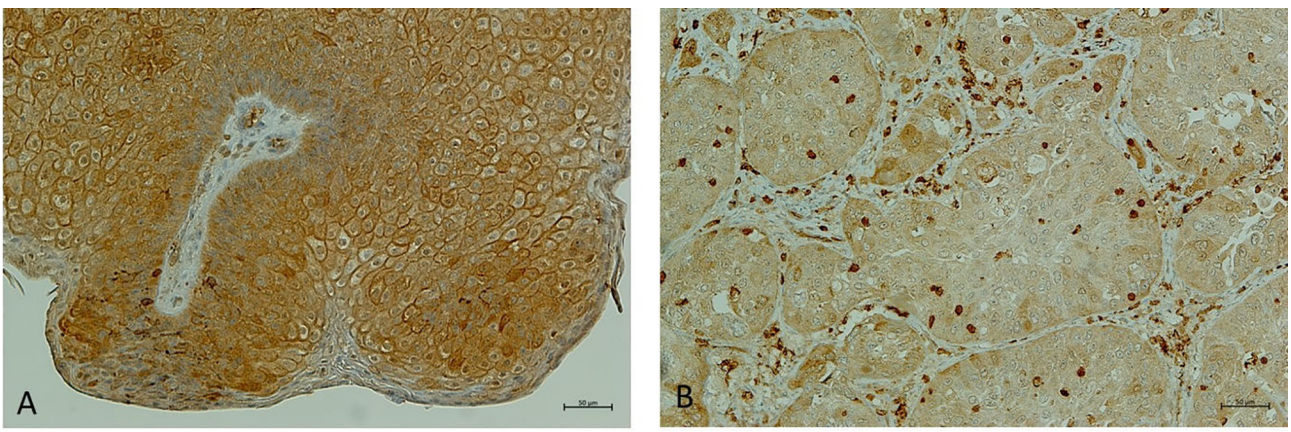


**FIGURE 3** | NHERF1 expression in cervical wart. **(A)** Representative image of immunohistochemical staining of high membranous NHERF1 expression in cervical wart; **(B)** Representative image of loss of membranous NHERF1 expression in Cervical squamous cell carcinoma. Original magnification of images ×200. Images were obtained on an Axion Image 2 upright microscope (Zeiss, Oberkochen, Germany) with an Axiocam 512 color camera.

high-risk human papillomavirus (HPV) E6 protein. At COOH terminus, the high-risk HPV-derived E6 oncoprotein presents a PBM domain (PDZ-binding motif) that can bind PDZ proteins, including NHERF1. Importantly, a main functional consequence of E6-induced NHERF-1 degradation is the activation of the PI3K signaling pathway (28). NHERF-1 degradation by E6 appears to be mediated by the protein ubiquitin cell ligase E6-Associated Protein (E6AP). The high-risk HPV E6 proteins bind E6AP and recruit p53 and some PDZ cellular proteins for ubiquitination and degradation by the proteasome. In particular, papillomavirus E6 proteins bind the LQELL sequence of E6AP and stimulate its ubiquitin ligase activity (28). Recently, Drews and colleagues reported NHERF1 degradation by both high and low-risk E6 proteins in association with E6AP, leading to the activation of the Wnt/β-catenin pathway (29). Overall, this supports the E6 oncoprotein role in the activation of the canonical Wnt/β-catenin pathway through NHERF1 degradation in CC.

The contribution of NHERF1 in the regulation of cell motility and invasion in CC has also emerged and several targets identified. For instance, NHERF1 could regulate actin remodeling through ACTN4. In detail, the interaction between NHERF1 and ACTN4 increased ACTN4 ubiquitination and degradation by the proteasome, impacting actin cytoskeleton organization and tumor cell migration and invasion (18). In addition, *in vitro* studies have demonstrated that NHERF1 knockdown is associated with enhanced metalloproteinase 2 (MMP-2) activity, thus further supporting a role for NHERF1 in cancer invasion (30).

In CC samples, NHERF1 has been associated with drug resistance through the regulation of Wnt signaling. A study conducted on patients following cisplatin treatment and patients without cisplatin-treatment, shows a better outcome in patients cisplatin-treated with high NHERF1 expression levels. Similarly, low levels of NHERF1 expression in HeLa cells showed significant cisplatin resistance. These findings indicate that NHERF1 can regulate sensitivity of cervical cancer cells to cisplatin, suggesting the importance to further investigate the molecular mechanisms responsible for cisplatin resistance (31). Previously, other authors described a role for NHERF1 in the multidrug resistance (MDR) process. They reported a closed relationship of NHERF1 with multidrug resistance protein 4 (MPR4), an ATP-binding cassette (ABC)-transporter, in which NHERF1 supported the internalization of this protein. In fact, the down-regulation of NHERF1 in HeLa cells increased the MRP4 expression at the plasma membrane, supposing an inhibition of MRP4 internalization, with consequent growth of drug efflux by this transporter (32).

*Ex vivo* and *in vitro* studies reported a negative correlation of NHERF1 with cell proliferation and epidermal growth factor receptor (EGFR) signaling in CC. Indeed, NHERF1 enacts its tumor suppressive program through the binding of EGFR and inhibition of EGFR-mediated signaling. In CC models, NHERF1 knockdown abolished the inhibition of EGF-induced ERK activation. This highlights the importance of NHERF1 in the regulation of cell proliferation signaling pathways in CC (33).

## NHERF1 AND OVARIAN CANCER

The biological relevance of NHERF1 in ovarian cancer (OC) pathology has been investigated in several studies. Main findings derive from *ex vivo* and *in vitro* studies that investigated the expression levels of NHERF1 in human samples and defined possible signaling pathways that modulate NHERF1 localization.

*Ex vivo* studies demonstrated an upregulation of NHERF1 in mucinous ovarian carcinomas and ovarian clear cell carcinoma (OCCC). In detail, Tabrizi and colleagues demonstrated an unfavorable prognosis in mucinous ovarian carcinomas with NHERF1 expression (34). In the study of Matsumoto and colleagues, NHERF1 up-regulation has been linked to OCCC recurrence and chemoresistance. The cytoplasmic/nuclear, but not membrane, high expression was significantly observed in recurrent OCCC with respect to primary tumors. Its cytoplasmic overexpression in OCCC cells was associated with a lower susceptibility to cisplatin. Further, the authors demonstrated that NHERF1 was also associated with an increase of poly (ADP-ribose) polymerase 1 (PARP1) expression that is stabilized through the PDZ1 domain of NHERF1. The over-expression of cytoplasmic/nuclear NHERF1 and PARP1 affected patients' prognosis, being associated with a worse overall and progression-free survival (35).

Kreimann and colleagues investigated the sequence of exons 2 and 3 together with flanking intronic sequences of the *SLC9A3R1* gene that encodes the PDZ2 domain of the NHERF1 protein. In detail, the authors observed the presence of two intronic mutations in the donor splicing site of exon 2 in 8/31 epithelial OC samples analyzed. As this domain is implicated in the binding between NHERF1/β-catenin and NHERF1/E-cadherin, these splicing alterations could potentially modify the localization of these partners (36).

The localization of NHERF1 is regulated by lysophosphatidic acid (LPA). *In vitro*, the treatment of ovarian cancer cells with LPA induces a mobilization of NHERF1 from cytosol to plasma membrane and then into migratory pseudopodia. The translocation is dependent on NHERF1/ERM interaction and the mechanism that underlies this binding is through the ERM phosphorylation (37). In fact, LPA-treatment of OVCAR-3 cells induces a rapid phosphorylation of ERM (cpERM) and the subsequent binding of NHERF1 through its C-terminal ERM-binding domain. Accordingly, the phosphorylation-defective ezrin mutant (Ezrin-T567A) blocked LPA-induced migration of OVCAR-3 cells (37). Overall, the LPA/NHERF1/cpERM axis represents an ideal pathway for molecules able to prevent OC migration and metastasis.

## CONCLUSIONS

It has long been clear that NHERF1 exerts an important role in the regulation of signal transduction pathways acting as a scaffold protein. In human tumors, NHERF1 has been found overexpressed in breast cancer, schwannoma, hepatocellular carcinoma and other human tumors. As part of different

multiprotein signaling complexes, NHERF1 plays an important role in the propagation of information within the cells. In the last few years, several works have described a double role for NHERF1 in tumorigenesis, according to its subcellular localization. Indeed, NHERF1 displays anti-tumor properties when it is located underneath the plasma membrane; on the contrary, it acts as an oncogene when localized in the cytoplasm or in the nucleus. As multiple levels of regulation exist, translating these data into the clinic is not without complexity.

As the examples in this review highlight, NHERF1 exerts direct biological influences in gynecological tumors. For instance, the overexpression of NHERF1 seems to be required to drive the early phases of cancer onset in different tumor types (**Figure 1**). Moreover, in CC and OC its membrane down-regulation and cytoplasmic over-expression, respectively, trigger signaling pathways linked to cancer progression and drug resistance, among these, the role in the regulation of β-catenin is well described. Overall, these findings suggest possible diagnostic and prognostic clinical implications. In practice, this can be performed in the clinic by immunohistochemistry.

There is also a specific challenge to therapeutically targeting NHERF1. Preliminary findings obtained *in vitro* support the potential therapeutic value of targeted approaches aiming at modulating NHERF1 activity in combination with antagonists of β-catenin (38). Further studies using gynecological models should be designed to demonstrate a defined clinical effect of NHERF1 anti-cancer agents.

## AUTHOR CONTRIBUTIONS

Concept or design: MS and SS. Acquisition of data: CS and DV. Analysis or interpretation of data: FZ, AT, and CS. Drafting of the article: MS and SS. Critical revision for important intellectual content: AT, DV, MM and FZ. All authors contributed to the article and approved the submitted version.

## REFERENCES


1. Prat J, Mutch DG. Pathology of Cancers of the Female Genital Tract Including Molecular Pathology. *Int J Gynaecol Obstet* (2018) 143:93–108. doi: 10.1002/ijgo.12617
2. Berger AC, Korkut A, Kanchi RS, Hegde AM, Lenoir W, Liu W, et al. A Comprehensive Pan-Cancer Molecular Study of Gynecologic and Breast Cancers. *Cancer Cell* (2018) 33(4):690–705.e9. doi: 10.1016/j.ccell.2018.03.014
3. Guo Y, Liu J, Luo J, You X, Weng H, Wang M, et al. Molecular Profiling Reveals Common and Specific Development Processes in Different Types of Gynecologic Cancers. *Front Oncol* (2020) 10:584793. doi: 10.3389/fonc.2020.584793
4. Kotelevets L, Chastre E. A New Story of the Three Magi: Scaffolding Proteins and lncRNA Suppressors of Cancer. *Cancers* (2021) 13(17):4264. doi: 10.3390/cancers13174264
5. Saini R, Azam Z, Sapra L, Srivastava RK. Neuronal Nitric Oxide Synthase (nNOS) in Neutrophils: An Insight. *Rev Physiol Biochem Pharmacol* (2021) 180:49–83. doi: 10.1007/112_2021_61
6. Kafka A, Bašić-Kinda S, Pećina-Šlaus N. The Cellular Story of Dishevelleds. *Croat Med J* (2014) 55(5):459–67. doi: 10.3325/cmj.2014.55.459
7. Weinman EJ, Boddeti A, Cunningham R, Akom M, Wang F, Wang Y, et al. NHERF-1 Is Required for Renal Adaptation to a Low-Phosphate Diet. *Am J Physiol Renal Physiol* (2003) 285(6):F1225–32. doi: 10.1152/ajprenal.00215.2003
8. Shibata T, Chuma M, Kokubu A, Sakamoto M, Hirohashi S. EBP50, a Beta-Catenin-Associating Protein, Enhances Wnt Signaling and Is Over-Expressed in Hepatocellular Carcinoma. *Hepatology* (2003) 38(1):178–86. doi: 10.1053/jhep.2003.50270
9. Mohler PJ, Kreda SM, Boucher RC, Sudol M, Stutts MJ, Milgram SL. Yes-Associated Protein 65 Localizes P62(C-Yes) to the Apical Compartment of Airway Epithelia by Association With EBP50. *J Cell Biol* (1999) 147(4):879–90. doi: 10.1083/jcb.147.4.879
10. Reczek D, Berryman M, Bretscher A. Identification of EBP50: A PDZ-Containing Phosphoprotein That Associates With Members of the Ezrin-Radixin-Moesin Family. *J Cell Biol* (1997) 139:169–79. doi: 10.1083/jcb.139.1.169
11. Hall RA, Premont RT, Chow CW, Blitzer JT, Pitcher JA, Claing A, et al. The Beta2-Adrenergic Receptor Interacts With the Na+/H+-Exchanger Regulatory Factor to Control Na+/H+ Exchange. *Nature* (1998) 392(6676):626–30. doi: 10.1038/33458
12. Cardone RA, Greco MR, Capulli M, Weinman EJ, Busco G, Bellizzi A, et al. NHERF1 Acts as a Molecular Switch to Program Metastatic Behavior and Organotropism *via* its PDZ Domains. *Mol Biol Cell* (2012) 23(11):2028–40. doi: 10.1091/mbc.E11-11-0911
13. Centonze M, Saponaro C, Mangia A. NHERF1 Between Promises and Hopes: Overview on Cancer and Prospective Openings. *Transl Oncol* (2018) 11:374–90. doi: 10.1016/j.tranon.2018.01.006
14. Bryant DM, Roignot J, Datta A, Overeem AW, Kim M, Yu W, et al. A Molecular Switch for the Orientation of Epithelial Cell Polarization. *Dev Cell* (2014) 31(2):171–87. doi: 10.1016/j.devcel.2014.08.027
15. Jeong J, Kim W, Hens J, Dann P, Schedin P, Friedman PA, et al. NHERF1 Is Required for Localization of PMCA2 and Suppression of Early Involution in the Female Lactating Mammary Gland. *Endocrinology* (2019) 160(8):1797–810. doi: 10.1210/en.2019-00230
16. Wang JQ, Qin F, Zhu L. Expression of Na/H Exchanger Regulatory Factor 1 in Autosomal-Dominant Polycystic Kidney Disease. *J Int Med Res* (2015) 43:629–38. doi: 10.1177/0300060515581182
17. Garbett D, Bretscher A. PDZ Interactions Regulate Rapid Turnover of the Scaffolding Protein EBP50 in Microvilli. *J Cell Biol* (2012) 198(2):195–203. doi: 10.1083/jcb.201204008
18. Sun L, Zheng J, Wang Q, Song R, Liu H, Meng R, et al. NHERF1 Regulates Actin Cytoskeleton Organization Through Modulation of α-Actinin-4 Stability. *FASEB J* (2016) 30(2):578–89. doi: 10.1096/fj.15-275586
19. Li J, Poulikakos PI, Dai Z, Testa JR, Callaway DJE, Bu Z. Protein Kinase C Phosphorylation Disrupts Na+/H+ Exchanger Regulatory Factor 1 Autoinhibition and Promotes Cystic Fibrosis Transmembrane Conductance Regulator Macromolecular Assembly. *J Biol Chem* (2007) 282(37):27086–99. doi: 10.1074/jbc.M702019200
20. Chen JY, Lin YY, Jou TS. Phosphorylation of EBP50 Negatively Regulates β-PIX-Dependent Rac1 Activity in Anoikis. *Cell Death Differ* (2012) 19(6):1027–37. doi: 10.1038/cdd.2012.4
21. Weinman EJ, Biswas R, Steplock D, Douglass TS, Cunningham R, Shenolikar S. Sodium-Hydrogen Exchanger Regulatory Factor 1 (NHERF-1) Transduces Signals That Mediate Dopamine Inhibition of Sodium-Phosphate Co-Transport in Mouse Kidney. *J Biol Chem* (2010) 285(18):13454–60. doi: 10.1074/jbc.M109.094359
22. Lim HC, Jou TS. Ras-Activated RSK1 Phosphorylates EBP50 to Regulate its Nuclear Localization and Promote Cell Proliferation. *Oncotarget* (2016) 7(9):10283–96. doi: 10.18632/oncotarget.7184
23. Fang XY, Song R, Chen W, Yang YY, Gu YH, Shu YQ, et al. PRL-3 Promotes the Malignant Progression of Melanoma *via* Triggering Dephosphorylation and Cytoplasmic Localization of NHERF1. *J Invest Dermatol* (2015) 135(9):2273–82. doi: 10.1038/jid.2015.154
24. Al Ghouleh I, Meijles DN, Mutchler S, Zhang Q, Sahoo S, Gorelova A, et al. Binding of EBP50 to Nox Organizing Subunit P47phox Is Pivotal to Cellular

Reactive Species Generation and Altered Vascular Phenotype. *Proc Natl Acad Sci USA* (2016) 113(36):E5308–17. doi: 10.1073/pnas.1514161113
25. Li M, Mennone A, Soroka CJ, Hagey LR, Ouyang X, Weinman EJ, et al. Na (+)/H(+) Exchanger Regulatory Factor 1 Knockout Mice Have an Attenuated Hepatic Inflammatory Response and Are Protected From Cholestatic Liver Injury. *Hepatology* (2015) 62:1227–36. doi: 10.1002/hep.27956
26. Saponaro C, Sergio S, Coluccia A, De Luca M, La Regina G, Mologni L, et al. β-Catenin Knockdown Promotes NHERF1-Mediated Survival of Colorectal Cancer Cells: Implications for a Double-Targeted Therapy. *Oncogene* (2018) 37(24):3301–16. doi: 10.1038/s41388-018-0170-y
27. Wang Q, Qin Q, Song R, Zhao C, Liu H, Yang Y, et al. NHERF1 Inhibits Beta-Catenin-Mediated Proliferation of Cervical Cancer Cells Through Suppression of Alpha-Actinin-4 Expression. *Cell Death Dis* (2018) 9(6):668. doi: 10.1038/s41419-018-0711-x
28. Accardi R, Rubino R, Scalise M, Gheit T, Shahzad N, Thomas M, et al. E6 and E7 From Human Papillomavirus Type 16 Cooperate to Target the PDZ Protein Na/H Exchange Regulatory Factor 1. *J Virol* (2011) 85(16):8208–16. doi: 10.1128/JVI.00114-11
29. Drews CM, Case S, Vande Pol SB. E6 Proteins From High-Risk HPV, Low-Risk HPV, and Animal Papillomaviruses Activate the Wnt/β-Catenin Pathway Through E6AP-Dependent Degradation of NHERF1. *PloS Pathog* (2019) 15(4):e1007575. doi: 10.1371/journal.ppat.1007575
30. Wang L, Qi Y, Xiong Y, Peng Z, Ma Q, Zhang Y, et al. Ezrin-Radixin-Moesin Binding Phosphoprotein 50 (EBP50) Suppresses the Metastasis of Breast Cancer and HeLa Cells by Inhibiting Matrix Metalloproteinase-2 Activity. *Anticancer Res* (2017) 37(8):4353–60. doi: 10.21873/anticanres.11829
31. Tao T, Yang X, Qin Q, Shi W, Wang Q, Yang Y, et al. NHERF1 Enhances Cisplatin Sensitivity in Human Cervical Cancer Cells. *Int J Mol Sci* (2017) 18 (1):5. doi: 10.3390/ijms18010005
32. Hoque MT, Cole SP. Down-Regulation of Na+/H+ Exchanger Regulatory Factor 1 Increases Expression and Function of Multidrug Resistance Protein 4. *Cancer Res* (2008) 68(12):4802–9. doi: 10.1158/0008-5472.CAN-07-6778
33. Peng Z, Wang Q, Zhang Y, He J, Zheng J. EBP50 Interacts With EGFR and Regulates EGFR Signaling to Affect the Prognosis of Cervical Cancer Patients. *Int J Oncol* (2016) 49(4):1737–45. doi: 10.3892/ijo.2016.3655
34. Tabrizi AD, Kalloger SE, Köbel M, Cipollone J, Roskelley CD, Mehl E, et al. Primary Ovarian Mucinous Carcinoma of Intestinal Type: Significance of Pattern of Invasion and Immunohistochemical Expression Profile in a Series of 31 Cases. *Int J Gynecol Pathol* (2010) 29(2):99–107. doi: 10.1097/PGP.0b013e3181bbbcc1
35. Matsumoto T, Yoki A, Konno R, Oguri Y, Hashimura M, Tochimoto M, et al. Cytoplasmic EBP50 and Elevated PARP1 Are Unfavorable Prognostic Factors in Ovarian Clear Cell Carcinoma. *Carcinogenesis* (2021) 42(9):1162–70. doi: 10.1093/carcin/bgab070
36. Kreimann EL, Ratajska M, Kuzniacka A, Demacopulo B, Stukan M, Limon J. A Novel Splicing Mutation in the SLC9A3R1 Gene in Tumors From Ovarian Cancer Patients. *Oncol Lett* (2015) 10(6):3722–6. doi: 10.3892/ol.2015.3796
37. Oh YS, Heo K, Kim EK, Jang JH, Bae SS, Park JB, et al. Dynamic Relocalization of NHERF1 Mediates Chemotactic Migration of Ovarian Cancer Cells Toward Lysophosphatidic Acid Stimulation. *Exp Mol Med* (2017) 49(7):e351. doi: 10.1038/emm.2017.88
38. Coluccia A, La Regina G, Naccarato V, Nalli M, Orlando V, Biagioni S, et al. Drug Design and Synthesis of First in Class PDZ1 Targeting NHERF1 Inhibitors as Anticancer Agents. *ACS Med Chem Lett* (2019) 10(4):499–503. doi: 10.1021/acsmedchemlett.8b00532

**Conflict of Interest:** The authors declare that the research was conducted in the absence of any commercial or financial relationships that could be construed as a potential conflict of interest.

**Publisher's Note:** All claims expressed in this article are solely those of the authors and do not necessarily represent those of their affiliated organizations, or those of the publisher, the editors and the reviewers. Any product that may be evaluated in this article, or claim that may be made by its manufacturer, is not guaranteed or endorsed by the publisher.

frontiers | Frontiers in Oncology

TYPE Review
PUBLISHED 29 July 2022
DOI 10.3389/fonc.2022.924945



OPEN ACCESS

EDITED BY
Sarah M. Temkin,
National Institutes of Health (NIH),
United States

REVIEWED BY
Saira Fatima,
Aga Khan University, Pakistan
Sophia George,
University of Miami, United States

*CORRESPONDENCE
Sandra Orsulic
sorsulic@mednet.ucla.edu

SPECIALTY SECTION
This article was submitted to Gynecological Oncology, a section of the journal Frontiers in Oncology

RECEIVED 20 April 2022
ACCEPTED 27 June 2022
PUBLISHED 29 July 2022

CITATION
Orsulic S, John J, Walts AE and Gertych A (2022) Computational pathology in ovarian cancer. *Front. Oncol.* 12:924945. doi: 10.3389/fonc.2022.924945



# Computational pathology in ovarian cancer

Sandra Orsulic[1,2,3]*, Joshi John[1,4], Ann E. Walts[5] and Arkadiusz Gertych[5,6,7]

[1]Veterans Affairs Greater Los Angeles Healthcare System, Los Angeles, CA, United States, [2]Department of Obstetrics and Gynecology, David Geffen School of Medicine, University of California Los Angeles, Los Angeles, CA, United States, [3]Jonsson Comprehensive Cancer Center, University of California Los Angeles, Los Angeles, CA, United States, [4]Department of Psychiatry, David Geffen School of Medicine, University of California Los Angeles, Los Angeles, CA, United States, [5]Department of Pathology and Laboratory Medicine, Cedars-Sinai Medical Center, Los Angeles, CA, United States, [6]Department of Surgery, Cedars-Sinai Medical Center, Los Angeles, CA, United States, [7]Faculty of Biomedical Engineering, Silesian University of Technology, Zabrze, Poland

Histopathologic evaluations of tissue sections are key to diagnosing and managing ovarian cancer. Pathologists empirically assess and integrate visual information, such as cellular density, nuclear atypia, mitotic figures, architectural growth patterns, and higher-order patterns, to determine the tumor type and grade, which guides oncologists in selecting appropriate treatment options. Latent data embedded in pathology slides can be extracted using computational imaging. Computers can analyze digital slide images to simultaneously quantify thousands of features, some of which are visible with a manual microscope, such as nuclear size and shape, while others, such as entropy, eccentricity, and fractal dimensions, are quantitatively beyond the grasp of the human mind. Applications of artificial intelligence and machine learning tools to interpret digital image data provide new opportunities to explore and quantify the spatial organization of tissues, cells, and subcellular structures. In comparison to genomic, epigenomic, transcriptomic, and proteomic patterns, morphologic and spatial patterns are expected to be more informative as quantitative biomarkers of complex and dynamic tumor biology. As computational pathology is not limited to visual data, nuanced subvisual alterations that occur in the seemingly "normal" pre-cancer microenvironment could facilitate research in early cancer detection and prevention. Currently, efforts to maximize the utility of computational pathology are focused on integrating image data with other -omics platforms that lack spatial information, thereby providing a new way to relate the molecular, spatial, and microenvironmental characteristics of cancer. Despite a dire need for improvements in ovarian cancer prevention, early detection, and treatment, the ovarian cancer field has lagged behind other cancers in the application of computational pathology. The intent of this review is to encourage ovarian cancer research teams to apply existing and/or develop additional tools in computational pathology for ovarian cancer and actively contribute to advancing this important field.

KEYWORDS

**artificial intelligence, computational pathology, convolutional neural network (CNN), deep learning, artificial neural network, digital pathology, machine learning, ovarian cancer**

## Computational imaging as a tool to study cancer from a novel perspective

Opinions about the role of computational imaging in the future of pathology range from the belief that computers will entirely replace pathologists to the conviction that computers will never achieve the competency of a well-trained pathologist. Similar to advanced chess-playing software, which is now practically unbeatable by humans, it is likely that computers will be faster and more accurate than pathologists in performing specific tasks, but the main purpose of computational pathology is not to outperform pathologists in routine analyses but to provide them with a completely new and complementary set of tools, some of which are highlighted below:

### Large-scale searchable integrative quantitation

Ovarian cancer is the fifth most deadly cancer in women, accounting for more than 200,000 deaths per year worldwide (1). Pathologic diagnosis is primarily confirmed by histopathologic evaluation and interpretation of H&E stained sections of tumor obtained during surgical debulking and/or biopsies obtained during treatment. Years of training with meticulous attention to histopathologic details in numerous examples of normal, altered but benign, and cancerous tissues enable pathologists to extract and empirically integrate an array of visual information from H&E slides into discrete features, such as tumor type, grade, mitotic count, and lymphovascular invasion. Using these features and additional pathological parameters allows the pathologist to categorize each tumor within a universally accepted classification, such as the World Health Organization (WHO) classification of tumors, which ultimately guides clinicians in patient management. Whereas each pathologist is variably limited by a composite of experience, memory, ability to recall visual detail, and case-correlated clinical outcome information locally available, computer algorithms take advantage of a searchable database with quantitative image features linked to clinical outcomes from thousands of patients. By applying computational image analyses, a new patient's tumor can be compared to tumors in the database to find similar tumor phenotypes and help predict the most likely clinical outcome for the new patient.

### Subvisual features

The invention of microscopes enabled the visualization of subcellular details, including nuclear enlargement, atypia, nucleolar prominence, hyperchromatism, and mitotic activity, which are usually important in establishing cancer diagnoses. However, a computer can extract and quantify hundreds, if not thousands, of additional visual and subvisual features (Figure 1), which can be configured into an algorithm to predict specific tumor behavior (i.e. likelihood of sensitivity to immunotherapy) or assess the efficacy of chemotherapy in tumor biopsies obtained at different time points during treatment. Extracting and analyzing information that is beyond human visual perception might also help identify new tissue, cellular, or subcellular structures, features, and/or spatial relationships that are difficult to characterize in H&E slides, such as liquid flow and vacuolarity, and intratumoral areas with increased tension, pH, metabolic activity, and/or genotoxic stress.

### Complex spatial information

In most solid malignancies, including ovarian cancer, cancer cells exist within a complex microenvironment that supports tumor growth. In general, the presence of immune cells is associated with better prognosis while the presence of cancer-associated fibroblasts (CAFs) is associated with worse prognosis. In addition to phenotypic diversity, it is becoming apparent that spatial relationships between cancer cells, immune cells, and CAFs play key roles in tumor aggressiveness and response to therapy. However, our knowledge and understanding about the composition of, and the spatial organization within, the tumor microenvironment is still in its infancy. Higher-order spatial patterns, such as cell-cell interactions, tissue interfaces, collagen alignment, and extent of tumor heterogeneity (Figure 2), are important readouts of the complexities of tumor pathophysiology and response to treatment yet remain largely unexplored. While the quantitation of individual cell types and the algorithms that are currently applied to summarize the extent and intensity of tumor staining in a biomarker panel are sufficient for patient stratification into broad groups, i.e. responders and non-responders, comprehensive spatial and morphometric readouts will be necessary to effectively tailor medical treatment to the individual characteristics of each patient (2, 3).

### Unbiased discovery

Knowing where and what to look for when examining a specimen or a histologic slide is crucial. Information that is not considered clinically relevant is more likely to be only cursorily examined or implicitly overlooked. For example, precursor lesions in the fallopian tube became obvious to pathologists only at the beginning of the 21$^{st}$ century after decades of searching for these lesions in the ovary, which at the time seemed to be the most logical place for ovarian cancer initiation. Computers can record information extracted from hundreds of scanned slide images in a

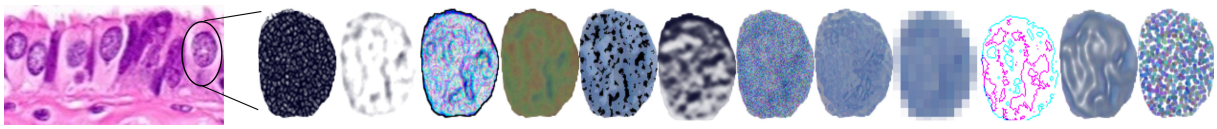

FIGURE 1
Artistic rendering of how a computer may "see" quantifiable nuclear features.

matter of hours. Using unbiased systematic processing of the recorded data, new and/or non-intuitive patterns can emerge (4). For example, although precursor lesions, such as serous tubal intraepithelial carcinoma (STIC) are identifiable in serially sectioned fallopian tubes processed with standard histopathology methods (5), the morphologic events that precede STIC formation are still unknown. Indeed, it is likely that STIC lesions are preceded by subtle morphologic changes that are either not visible to the human eye or are too nuanced to detect without prior knowledge of where and what to look for. A recent analysis of global stromal features in fallopian tubes from postmenopausal women showed that fallopian tubes with STIC lesions exhibit subvisual global changes in the stroma that might precede STIC formation and/or provide a permissible microenvironment for the neoplastic transformation of tubal epithelial cells (6). The ability to detect and understand what constitutes a "permissible" microenvironment for cancerous transformation provides new opportunities for the early detection of cancer and for the identification of rate-limiting events in the early stages of cancer development.

## Artificial intelligence, machine learning, and neural networks

Artificial Intelligence (AI) comprises a set of algorithms that mimic human intelligence, enabling machines to perform complex tasks, such as cognitive perception, decision-making, and communication. Machine learning is a subcategory of AI in which a machine is initially provided with large amounts of training data needed to build models to accurately analyze and interpret new data (7, 8). Machine learning models can automatically learn, improve their performance, and solve problems. Support vector machines, clustering algorithms, k-nearest neighbor classifiers, and logistic regression models (7, 8) are examples of commonly used models. However, because they can learn only a handful of features, they are being replaced by models that use deep learning. Deep learning is a type of machine learning that uses a neural network consisting of three or more functional layers, which include an input layer, multiple hidden layers, and an output layer (9, 10). The hidden layers promote learning and refinement of information "seen" by the input layers to increase the accuracy of predictions of the model's output. The layers are connected to each other, and the strengths of these connections (termed "weights") are learned from the training data.

A convolutional neural network (CNN) is a type of a deep learning model used to build advanced decision-making workflows in digital image analysis, ranging from image processing, classification and segmentation of tissue images to the prediction of patient outcomes. CNN often employs more than three convolutional sets of learnable filters (kernels) to extract features from the images. Kernel filters provide low, high and selective filtering (smoothing and sharpening, respectively). The filters distill various basic features such as edges, shapes, color, intensity and location of objects in the image. By flattening

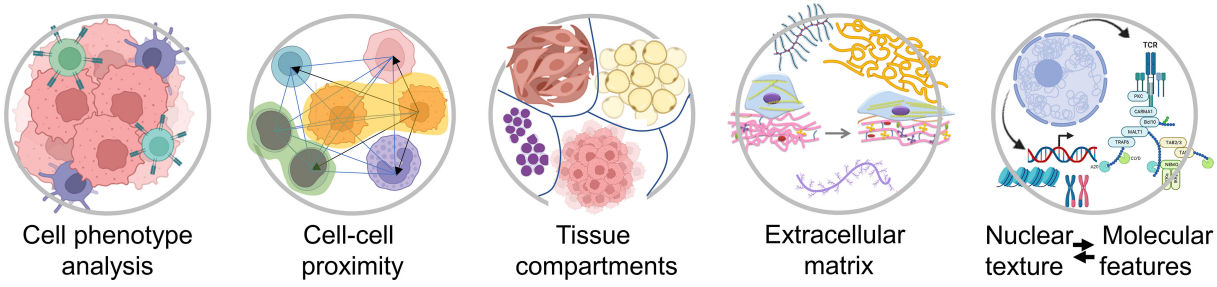


FIGURE 2
Examples of spatial characteristics within the tumor microenvironment that can be quantified using different types of computational image software. Created with BioRender.com.

an image, removing or reducing the dimensions, convolutional kernels conduct pre-processing steps that enable selection and organization of the most informative learned features and recognition of these features in previously unseen images. In deeper layers of the CNN, the features are transformed into feature maps that summarize the presence of detected features in the input image (11). Another model that could prove useful in pathology is the fully convolutional network (FCN), characterized by a hierarchy of convolutional layers that are not fully connected. Unlike CNN, which learns from repetitive features that occur throughout the entire image, FCN learns from every pixel thereby allowing detection of objects or features that might be only sporadically present in an entire image (12), for example cancer stem cells which comprise a minute fraction of the tumor. CNN and FCN models are well suited for tumor/object detection, classification, and segmentation tasks (13–16). A recurrent neural network (RNN) model is characterized by dynamic behavior, meaning that it can memorize inputs over different time points or time intervals and learn from them in a sequential manner. RNN could be useful to analyze serial biopsies from a patient who is under surveillance for disease development, progression, or emergence of therapy resistance (17). Machine learning can be applied in a supervised or unsupervised manner. Supervised machine learning uses labeled data sets to train algorithms that classify data or predict outcomes. As input data are fed into the model, the significance of the individual data is adjusted until the model has been appropriately fitted to infer a function that maps input images to a designated outcome label or an object. In contrast, unsupervised machine learning uses unlabeled images to infer a function and detect patterns in the data, clustering them by any distinguishing characteristic(s). Both supervised and unsupervised learning can be useful to reveal new non-intuitive patterns that correlate with specific clinical outcomes.

## Computational pathology as a window into the molecular composition of cancer

Oncologists in consultation with pathologists increasingly rely on molecular assays to guide patient-tailored cancer therapy. Such assays can be costly and time-consuming in comparison to routine H&E slides, which can be digitized and analyzed on site. If the application of AI to H&E stained slides could provide molecular information, i.e. predict mutation status or expression levels of actionable cancer drivers in a patient's tumor, several of the currently used technologies, such as immunohistochemistry, *in situ* hybridization, and next generation sequencing, might become superfluous. Recent efforts to integrate digitized H&E image data with molecular data indicate that determining molecular information from digitized H&E slides is not only feasible (18–21) but might achieve greater accuracy than other techniques that are subject to human error-prone steps, such as specialized specimen preparation and complex laboratory tasks.

Since tissue and cellular morphologies are known to reflect their physiological and pathological conditions, it would be reasonable to expect that higher-order features extracted from histopathology slides are associated with distinct molecular profiles, such as specific gene and protein expression, metabolism, and sensitivity to specific drugs. For example, a higher-order chromatin structure was shown to be the main determinant of genomic instability and mutation frequency in cancer cells (22–24) as well as a strong prognostic indicator in a pan-cancer study (25). Relying only on tumor histomorphology in H&E slides, recent reports indicate that it was possible to predict microsatellite instability in gastrointestinal cancers (26–28), determine molecular expression of ER, PR, and HER2 in breast cancer (29), and detect mutations in prognostically and therapeutically relevant driver genes in different cancer types, including BRAF in melanoma (30), APC, KRAS, PIK3CA, SMAD4, and TP53 in colorectal cancer (31), EGFR, KRAS, TP53, STK11, FAT1, and SETBP1 in lung cancer (32), TP53, CTNNB, FMN2, and ZFX4 in hepatocellular carcinoma (33), FGFR3 in bladder cancer (34), and IDH1 in glioma (35).

## Biomarker discovery

With an increasing number of available cancer therapies, it is crucial to develop companion diagnostic tests that identify and stratify subpopulations of patients by their likelihood to benefit from specific therapies. For example, in ovarian cancer, immunotherapy can be associated with serious side effects but only shows efficacy in about 10% of ovarian cancer patients (36). Another example is the need to identify patients who could benefit from PARP inhibitors. In the absence of better biomarkers, detection of a gene mutation (i.e. BRCA1 mutation) or elevated protein expression (i.e. PD-1 and PD-L1) of the intended therapeutic target are frequently used as proxies for treatment response. However, most of the current treatment response biomarkers perform poorly. While it is logical to expect that BRCA mutation carriers would be more sensitive to PARP inhibitors, clinical trials have shown that many non-carriers are responsive to PARP inhibitors although the rationale for this response is still unclear (37). Similarly, immunohistochemical detection of tumor-infiltrating lymphocytes and PD-L1 is a poor proxy for sensitivity to immunotherapy in most cancer types, including ovarian cancer (38). In fact, microsatellite instability, a less specific biomarker, seems to be a better predictor of sensitivity to immunotherapy in various solid cancers (39), possibly because microsatellite instability encompasses multiple proteins and pathways that are involved in the immune response. Using the same reasoning, it is likely that morphometric tumor features that reflect complex pathophysiological states will prove to be

more clinically useful biomarkers even if they are initially non-intuitive or currently non-explainable.

Finding a biomarker in an unexpected place is exemplified in the tumor microenvironment. While cancer research has mostly focused on cancer cells, the unbiased application of deep imaging to digitized H&E slides combined with software that identifies areas of the image that influence algorithm-based classification has frequently revealed stromal features as better biomarkers of clinical outcomes than features of cancer cells (40). In ovarian cancer, a high ratio of stromal CAFs to cancer cells is an independent biomarker of poor survival and chemotherapy resistance (41–44). Indeed, stromal features were identified as the most effective biomarkers in colon cancer (45–47), mesothelioma (48), breast cancer (49, 50), lung adenocarcinoma (51) and early-stage non-small cell lung cancer (52). The discovery of stromal features as the most relevant predictors of clinical outcomes is not surprising as multiple molecular studies of expression profiles and proteomic signatures have also shown that an increased stroma/cancer ratio and increased expression of gene signatures associated with stromal remodeling were the strongest predictors of clinical outcomes (53–62). Studies in several cancer types have also shown that the signature of TGFβ-mediated extracellular matrix remodeling is the best predictor of therapy failure (63). The tumor stroma could contribute to poor survival and therapeutic resistance through multiple mechanisms, including promotion of tumor growth, angiogenesis, invasion and metastasis, provision of protective niches for cancer stem cells, creation of an immunosuppressive microenvironment that excludes immune cells from proximity to cancer cells, and/or generation of physical barriers that block access of chemotherapies and immunotherapies to cancer cells (64–68). Thus, it is unlikely that a single molecular pathway will be sufficient as a biomarker of the complex biology that dictates clinical outcomes. A recent computational image analysis of H&E slides of non-small cell lung and gynecologic cancers has shown that the spatial architecture and the interaction of cancer cells and tumor-infiltrating lymphocytes can predict clinical benefit in patients receiving immune checkpoint inhibitors. Importantly, the computational image classifier was associated with clinical outcome independent of clinical factors and PD-L1 expression levels (69). In addition to identifying new biomarkers by highlighting specific structures and regions, computational tissue imaging could assist with the identification of new therapeutic targets. For example, targeting CAFs with various TGFβ inhibitors was effective in improving immunotherapeutic efficacy in several preclinical cancer models (66–68).

## Future implementation of computational pathology in clinical practice

Potential applications of computational pathology in cancer include diagnosis, phenotyping, subtype classification, early detection, prognostication, assessment of sensitivity to chemotherapy and immunotherapy, and identification of suitable targeted therapies (20). For example, open-source software, QuPath (70), was capable of classifying serous borderline ovarian tumors and high-grade serous ovarian cancer with >90% accuracy by examining only a small number of tiles extracted from whole H&E slide images (71). While this approach does not reach the accuracy achieved by pathologists who examine multiple sections from different areas of each tumor and have access to surgical records and other clinical information, this example suggests that improvements in the software recognition pattern and computational capacity to analyze pathology slides could achieve clinical-grade tumor classification (72).

Several examples report the utility of computational imaging to automate cancer diagnoses without compromising accuracy. For example, a CNN trained to classify images as malignant melanoma or benign nevi demonstrated superior performance compared to manual scoring by histopathologists (73, 74). Another study that assessed the ability of deep learning algorithms to accurately detect breast cancer metastases in H&E slides of lymph node sections reported that the algorithms were superior in detecting micrometastases and equivalent to the best performing pathologists when under time constraints in detecting macrometastases (75). Similarly, an AI system has reached a clinically acceptable level of cancer detection accuracy in prostate needle biopsies (76). A study of deep CNN in Gleason scoring of prostatectomy specimens reported that the deep learning-based Gleason classification achieved higher sensitivity and specificity than 9 out of 10 pathologists (77). Computational analyses of H&E images have been applied for the prediction of patient survival and recurrence. Deep learning-based algorithms have also been reported to predict prostate cancer recurrence comparably to a genomic companion diagnostic test (78). Other studies utilizing deep learning-based classification involve determining histologic subtype in ovarian cancer (79), predicting platinum resistance in ovarian cancer (41, 80), predicting survival outcome in patients with mesothelioma (48), predicting metastatic recurrence and death in patients with primary melanoma (81) and colon cancer (46), predicting lung cancer recurrence after surgical resection to identify patients who should receive additional adjuvant therapy (52, 82), and predicting response to ipilimumab immunotherapy in patients with malignant melanoma (83). A computational quantitative characterization of the architecture of tumor-infiltrating lymphocytes and their interplay with cancer cells from H&E slides of three different gynecologic cancer types (ovarian, cervical, and endometrial) and across three different treatment approaches (platinum, radiation and immunotherapy) showed that the geospatial profile was prognostic of disease progression and survival irrespective of the treatment modality (84). This computationally-derived profile even outperformed the stage variable, which is the

current standard for gynecologic oncology (84). Upon closer inspection, features related to the increased density of lymphocytes in the epithelium and invasive tumor front were associated with better survival compared with features related to the increased density of lymphocytes in the stromal compartment (84). Although these patterns can be observed by conventional pathology examination, the value of the computational geospatial profile is in the inherently quantitative output rather than the descriptive output from conventional pathology.

Computational pathology has already become an integral component of cancer research and is increasingly being used in anatomic pathology to automate tasks, reduce subjectivity, and improve accuracy and reproducibility (17, 85, 86). The development of high-resolution whole slide image scanners, which are specialized microscopes fitted with high resolution cameras, high magnification objectives, and software for the identification and automated correction of out-of-focus points, constitutes a major advance in computational pathology. Two of these high-quality scanners, the Leica Aperio AT2 DX System and the Philips IntelliSite Pathology Solution, now have FDA approval for clinical review and expert interpretation of pathology slides in routine diagnoses (87). To facilitate the adoption and implementation of this technology into pathology workflows, the Digital Pathology Association has published several practical guides to whole slide imaging (88–91). Digitization of pathology slides enables simultaneous review of slides by multiple pathologists at different institutions and the creation and growth of centralized cloud-based image repositories and databases that are accessible for remote high-throughput studies and/or the development of multiple freely-available machine learning-based tools that can recognize and quantify positive immunostaining or basic structures, such as epithelial-lined ducts, blood vessels, and mitotic figures in H&E slides. Proof-of-concept studies show that automated analyses of simple morphologic patterns can assist pathologists and researchers, allowing them to focus on more complex tasks (2, 92).

Academic pathology departments are increasingly interested in adopting AI in routine practice to optimize operations, reduce costs, and improve patient care. A survey of physician perspectives on the integration of AI into diagnostic pathology revealed that 75% of pathologists across more than fifty countries are interested in using AI as a diagnostic tool in cancer care (93). With the continuous increase in the aged population and the growing number of available tests for persionalized medicine, pathologists are overburdened by tasks, such as counting mitotic figures or scoring Ki67 staining, that could be easily performed by machines. Hence, automated computational imaging platforms for the detection and quantitation of stained markers in defined cell subpopulations are the first candidates to be integrated into pathology workflows as these analyses could provide accurate, unbiased, reproducible, and standardized results that can be viewed and verified (72, 89, 94–96). In contrast, results of artificial neural network analyses that cannot be verified visually are more likely to be met with mistrust by the pathology community because the pathologist needs to be confident in the result before signing out a report (97). This problem might be solved by the further development of tools that introduce transparency for non-linear machine learning methods, such as gradient-weighted class activation mapping (grad-CAM) that overlays images and heatmaps to better visualize the cell type or region in which the informative features were expressed (98).

Although research results utilizing computational imaging in pathology are promising, significant improvements need to be made to achieve the safety and reliability required for endorsement by medical specialty societies, legal approvals, and implementation of this technology into daily clinical pathological diagnostics (99–101). One of the first steps will involve the standardization of slide scanners, display devices, image formats, platforms for image processing and analysis as well as the standardization of the interfaces with clinical information systems and reimbursement mechanisms. Among the technical challenges that must be overcome are normalization methods for histological data preparation at different institutions. This is a pressing issue given that histologic slides are stained either manually or with auto-stainers using site-specific protocols and then digitized on scanners from various manufacturers. Tissue handling and processing can also introduce artefacts, such as air bubbles, fingerprints, excessive glue, blurry/out of focus tissue image, unstained or overstained tissue, and folded or cauterized tissue and digitization (102). While the human eye might not be sensitive to slight differences in tissue fixation, sectioning, staining, and coverslip mounting, all of these factors indiscriminately impact machine learning, and each can have drastic implications on the final results (102). For these reasons, the computational pathology community strongly promotes rigorous algorithm development and testing schemes. First, innovative methods must be used to address pixel data normalization, color standardization, and recognition of the areas on the slide that are out of focus, blurred or contain folded or damaged tissue (103–109). Second, algorithm generalizability on unseen digitized specimens collected at different institutions or deposited in public repositories, such as The Cancer Genome Atlas (TCGA) (110) and The Cancer Imaging Archive (TCIA) (111), will need to be tested and standardized (7, 112, 113).

Many commercial and freely available viewers and image analysis software packages support different whole slide image formats for Windows, Linux, and MacOS. Commercial slide viewers include ImageScope (Aperio/Leica), CaseViewer (3DHistech), and ObjectiveView. The development of web-based viewing interfaces and custom computational pathology pipelines is supported by OpenSlide and SlideIO software libraries. For users with little to no programming skills, the most popular free software packages for general tissue image analysis include ImageJ (114), Fiji (115), Icy (116), Orbit (117), ilastik (118), Cell Profiler (119), QuPath (70), SlicerScope (120),

and PathML (121). These platforms have been embraced in the research arena because they can be easily adapted to different types of image analyses by introducing new codes or incorporating plugins from other programs. They are also flexible in processing different types of image files. Additionally, a plethora of fit-for-purpose packages with custom-made computational pathology pipelines can be found on GitHub (https://github.com/). Commercial digital pathology solutions, such as PerkinElmer (USA), Tissue Gnostics (Austria), Halo (United States), Visophram (Denmark) and Definiens (Germany), are often preferred by pathology departments because these platforms offer built-in databases of analytical engines and available technical support. Recognizing the importance of standardization in clinical practice, the freely-accessible Pathology Analytic Imaging Standards (PAIS) was created to support the standardization of image analysis algorithms and image features (122, 123). Resources of web-based interfaces and online tools, such as The Cancer Digital Slide Archive (CDSA, http://cancer.digitalslidearchive.net/), for visualization and analysis of pathology image data are also becoming more readily available (124).

## Conclusion

Computational image analysis holds great promise in advancing ovarian cancer research, including a better understanding of the events that provide a permissible microenvironment for early cancerous transformation in the fallopian tube, the role of the stroma in therapeutic resistance, and biomarkers for the selection of patients most likely to benefit from different therapeutic approaches. Although computational pathology in the ovarian cancer research field is still too rudimentary to use in a clinical setting, we anticipate that it will become one of the main tools for cancer research and precision medicine in the next decade, surpassing current methods for the selection of patient-tailored therapy, such as immunostaining, mutation sequencing, and expression profiling. Among the key factors that will propel computational pathology to the forefront of medical research are the accessibility of histopathology slides, the low-cost of image analysis and storage, seamless integration with other computational imaging platforms, and the potential for rapid, accurate, and reliable prediction of patient outcomes.

## Author contributions

All authors contributed to the article writing and revisions and approved the submitted version.

## Funding

SO is supported by the Veterans Administration Merit Award VA-ORD BX004974, the Iris Cantor-UCLA Women's Health Center/UCLA National Center of Excellence in Women's Health Pilot Research Project NCATS UCLA CTSI grant UL1TR00188, the Sandy Rollman Ovarian Cancer Foundation, the Mary Kay Foundation, and the Annenberg Foundation. AG is supported by the Initiative of Excellence - Research University - a grant program at Silesian University of Technology (year 2021, no.07/010/SDU/10-21-01).

## Conflict of interest

The authors declare that the research was conducted in the absence of any commercial or financial relationships that could be construed as a potential conflict of interest.

## Publisher's note



## References

1. Sung H, Ferlay J, Siegel RL, Laversanne M, Soerjomataram I, Jemal A, et al. Global cancer statistics 2020: GLOBOCAN estimates of incidence and mortality worldwide for 36 cancers in 185 countries. *CA: A Cancer J Clin* (2021) 71:209. doi: 10.3322/caac.21660

2. Acs B, Rantalainen M, Hartman J. Artificial intelligence as the next step towards precision pathology. *J Intern Med* (2020) 288:62. doi: 10.1111/joim.13030

3. Dlamini Z, Francies FZ, Hull R, Marima R. Artificial intelligence (AI) and big data in cancer and precision oncology. *Comput Struct Biotechnol J* (2020) 18:2300. doi: 10.1016/j.csbj.2020.08.019

4. Großerueschkamp F, Jütte H, Gerwert K, Tannapfel A. Advances in digital pathology: From artificial intelligence to label-free imaging. *Visc Med* (2021) 37:482. doi: 10.1159/000518494

5. Nik NN, Vang R, Shih Ie M, Kurman RJ. Origin and pathogenesis of pelvic (ovarian, tubal, and primary peritoneal) serous carcinoma. *Annu Rev Pathol* (2014) 9:27. doi: 10.1146/annurev-pathol-020712-163949

6. Wu J, Raz Y, Recouvreux MS, Diniz MA, Lester J, Karlan BY, et al. Focal serous tubal intra-epithelial carcinoma lesions are associated with global changes in the fallopian tube epithelia and stroma. *Front Oncol* (2022) 12:853755. doi: 10.3389/fonc.2022.853755

7. Komura D, Ishikawa S. Machine learning methods for histopathological image analysis. *Comput Struct Biotechnol J* (2018) 16:34. doi: 10.1016/j.csbj.2018.01.001

8. Cui M, Zhang DY. Artificial intelligence and computational pathology. *Lab Invest* (2021) 101:412. doi: 10.1038/s41374-020-00514-0

9. LeCun Y, Bengio Y, Hinton G. Deep learning. *Nature* (2015) 521:436. doi: 10.1038/nature14539

10. Wang S, Yang DM, Rong R, Zhan X, Xiao G. Pathology image analysis using segmentation deep learning algorithms. *Am J Pathol* (2019) 189:1686. doi: 10.1016/j.ajpath.2019.05.007

11. Mobadersany P, Yousefi S, Amgad M, Gutman DA, Barnholtz-Sloan JS, Velázquez Vega JE, et al. Predicting cancer outcomes from histology and genomics using convolutional networks. *Proc Natl Acad Sci USA* (2018) 115:E2970. doi: 10.1073/pnas.1717139115

12. Xing F, Cornish TC, Bennett T, Ghosh D, Yang L. Pixel-to-Pixel learning with weak supervision for single-stage nucleus recognition in Ki67 images. *IEEE Trans BioMed Eng* (2019) 66:3088. doi: 10.1109/TBME.2019.2900378

13. Gertych A, Swiderska-Chadaj Z, Ma Z, Ing N, Markiewicz T, Cierniak S, et al. Convolutional neural networks can accurately distinguish four histologic growth patterns of lung adenocarcinoma in digital slides. *Sci Rep* (2019) 9:1483. doi: 10.1038/s41598-018-37638-9

14. Li W, Li J, Sarma KV, Ho KC, Shen S, Knudsen BS, et al. Path r-CNN for prostate cancer diagnosis and Gleason grading of histological images. *IEEE Trans Med Imaging* (2018) 38:945. doi: 10.1109/TMI.2018.2875868

15. Klimov S, Xue Y, Gertych A, Graham RP, Jiang Y, Bhattarai S, et al. Predicting metastasis risk in pancreatic neuroendocrine tumors using deep learning image analysis. *Front Oncol* (2020) 10:593211. doi: 10.3389/fonc.2020.593211

16. Golden JA. Deep learning algorithms for detection of lymph node metastases from breast cancer: Helping artificial intelligence be seen. *JAMA* (2017) 318:2184. doi: 10.1001/jama.2017.14580

17. Bera K, Schalper KA, Rimm DL, Velcheti V, Madabhushi A. Artificial intelligence in digital pathology - new tools for diagnosis and precision oncology. *Nat Rev Clin Oncol* (2019) 16:703. doi: 10.1038/s41571-019-0252-y

18. Schmauch B, Romagnoni A, Pronier E, Saillard C, Maillé P, Calderaro J, et al. A deep learning model to predict RNA-seq expression of tumours from whole slide images. *Nat Commun* (2020) 11:3877. doi: 10.1038/s41467-020-17678-4

19. Montalto MC, Edwards R. And they said it couldn't be done: Predicting known driver mutations from H&E slides. *J Pathol Inform* (2019) 10:17. doi: 10.4103/jpi.jpi_91_18

20. Kather JN, Heij LR, Grabsch HI, Loeffler C, Echle A, Muti HS, et al. Pan-cancer image-based detection of clinically actionable genetic alterations. *Nat Cancer* (2020) 1:789. doi: 10.1038/s43018-020-0087-6

21. Fu Y, Jung AW, Torne RV, Gonzalez S, Vöhringer H, Shmatko A, et al. Pan-cancer computational histopathology reveals mutations, tumor composition and prognosis. *Nat Cancer* (2020) 1:800. doi: 10.1038/s43018-020-0085-8

22. Schuster-Bockler B, Lehner B. Chromatin organization is a major influence on regional mutation rates in human cancer cells. *Nature* (2012) 488:504. doi: 10.1038/nature11273

23. Dixon JR, Jung I, Selvaraj S, Shen Y, Antosiewicz-Bourget JE, Lee AY, et al. Chromatin architecture reorganization during stem cell differentiation. *Nature* (2015) 518:331. doi: 10.1038/nature14222

24. Gisselsson D, Bjork J, Hoglund M, Mertens F, Dal Cin P, Akerman M, et al. Abnormal nuclear shape in solid tumors reflects mitotic instability. *Am J Pathol* (2001) 158:199. doi: 10.1016/S0002-9440(10)63958-2

25. Kleppe A, Albregtsen F, Vlatkovic L, Pradhan M, Nielsen B, Hveem TS, et al. Chromatin organisation and cancer prognosis: a pan-cancer study. *Lancet Oncol* (2018) 19:356. doi: 10.1016/S1470-2045(17)30899-9

26. Kather JN, Pearson AT, Halama N, Jäger D, Krause J, Loosen SH, et al. Deep learning can predict microsatellite instability directly from histology in gastrointestinal cancer. *Nat Med* (2019) 25:1054. doi: 10.1038/s41591-019-0462-y

27. Schrammen PL, Ghaffari Laleh N, Echle A, Truhn D, Schulz V, Brinker TJ, et al. Weakly supervised annotation-free cancer detection and prediction of genotype in routine histopathology. *J Pathol* (2022) 256:50. doi: 10.1002/path.5800

28. Echle A, Grabsch HI, Quirke P, van den Brandt PA, West NP, Hutchins GGA, et al. Clinical-grade detection of microsatellite instability in colorectal tumors by deep learning. *Gastroenterology* (2020) 159:1406. doi: 10.1053/j.gastro.2020.06.021

29. Shamai G, Binenbaum Y, Slossberg R, Duek I, Gil Z, Kimmel R. Artificial intelligence algorithms to assess hormonal status from tissue microarrays in patients with breast cancer. *JAMA Netw Open* (2019) 2:e197700. doi: 10.1001/jamanetworkopen.2019.7700

30. Kim RH, Nomikou S, Coudray N, Jour G, Dawood Z, Hong R, et al. Deep learning and pathomics analyses reveal cell nuclei as important features for mutation prediction of BRAF-mutated melanomas. *J Invest Dermatol* (2021) 142:1650. doi: 10.1016/j.jid.2021.09.034.

31. Jang HJ, Lee A, Kang J, Song IH, Lee SH. Prediction of clinically actionable genetic alterations from colorectal cancer histopathology images using deep learning. *World J Gastroenterol* (2020) 26:6207. doi: 10.3748/wjg.v26.i40.6207

32. Coudray N, Ocampo PS, Sakellaropoulos T, Narula N, Snuderl M, Fenyö D, et al. Classification and mutation prediction from non-small cell lung cancer histopathology images using deep learning. *Nat Med* (2018) 24:1559. doi: 10.1038/s41591-018-0177-5

33. Chen M, Zhang B, Topatana W, Cao J, Zhu H, Juengpanich S, et al. Classification and mutation prediction based on histopathology H&E images in liver cancer using deep learning. *NPJ Precis Oncol* (2020) 4:14. doi: 10.1038/s41698-020-0120-3

34. Loeffler CML, Ortiz Bruechle N, Jung M, Seillier L, Rose M, Laleh NG, et al. Artificial intelligence-based detection of FGFR3 mutational status directly from routine histology in bladder cancer: A possible preselection for molecular testing? *Eur Urol Focus* (2021). doi: 10.1016/j.euf.2021.04.007

35. Chang P, Grinband J, Weinberg BD, Bardis M, Khy M, Cadena G, et al. Deep-learning convolutional neural networks accurately classify genetic mutations in gliomas. *AJNR Am J Neuroradiol* (2018) 39:1201. doi: 10.3174/ajnr.A5667

36. Kandalaft LE, Odunsi K, Coukos G. Immune therapy opportunities in ovarian cancer. *Am Soc Clin Oncol Educ Book* (2020) 40:1. doi: 10.1200/EDBK_280539

37. Miller RE, Leary A, Scott CL, Serra V, Lord CJ, Bowtell D, et al. ESMO recommendations on predictive biomarker testing for homologous recombination deficiency and PARP inhibitor benefit in ovarian cancer. *Ann Oncol* (2020) 31:1606. doi: 10.1016/j.annonc.2020.08.2102

38. Chan TA, Yarchoan M, Jaffee E, Swanton C, Quezada SA, Stenzinger A, et al. Development of tumor mutation burden as an immunotherapy biomarker: utility for the oncology clinic. *Ann Oncol* (2019) 30:44. doi: 10.1093/annonc/mdy495

39. Chang L, Chang M, Chang HM, Chang F. Microsatellite instability: A predictive biomarker for cancer immunotherapy. *Appl Immunohistochem Mol Morphol* (2018) 26:e15. doi: 10.1097/PAI.0000000000000575

40. Diao JA, Wang JK, Chui WF, Mountain V, Gullapally SC, Srinivasan R, et al. Human-interpretable image features derived from densely mapped cancer pathology slides predict diverse molecular phenotypes. *Nat Commun* (2021) 12:1613. doi: 10.1038/s41467-021-21896-9

41. Yu KH, Hu V, Wang F, Matulonis UA, Mutter GL, Golden JA, et al. Deciphering serous ovarian carcinoma histopathology and platinum response by convolutional neural networks. *BMC Med* (2020) 18:236. doi: 10.1186/s12916-020-01684-w

42. Lan C, Heindl A, Huang X, Xi S, Banerjee S, Liu J, et al. Quantitative histology analysis of the ovarian tumour microenvironment. *Sci Rep* (2015) 5:16317. doi: 10.1038/srep16317

43. Lan C, Li J, Huang X, Heindl A, Wang Y, Yan S, et al. Stromal cell ratio based on automated image analysis as a predictor for platinum-resistant recurrent ovarian cancer. *BMC Cancer* (2019) 19:159. doi: 10.1186/s12885-019-5343-8

44. Verhaak RG, Tamayo P, Yang JY, Hubbard D, Zhang H, Creighton CJ, et al. Prognostically relevant gene signatures of high-grade serous ovarian carcinoma. *J Clin Invest* (2013) 123:517. doi: 10.1172/JCI65833

45. Jiao Y, Li J, Qian C, Fei S. Deep learning-based tumor microenvironment analysis in colon adenocarcinoma histopathological whole-slide images. *Comput Methods Programs BioMed* (2021) 204:106047. doi: 10.1016/j.cmpb.2021.106047

46. Kwak MS, Lee HH, Yang JM, Cha JM, Jeon JW, Yoon JY, et al. Deep convolutional neural network-based lymph node metastasis prediction for colon cancer using histopathological images. *Front Oncol* (2020) 10:619803. doi: 10.3389/fonc.2020.619803

47. Bilal M, Raza SEA, Azam A, Graham S, Ilyas M, Cree IA, et al. Novel deep learning algorithm predicts the status of molecular pathways and key mutations in colorectal cancer from routine histology images. *Lancet Digital Health* (2021) 3:e763. doi: 10.1016/S2589-7500(21)00180-1

48. Courtiol P, Maussion C, Moarii M, Pronier E, Pilcer S, Sefta M, et al. Deep learning-based classification of mesothelioma improves prediction of patient outcome. *Nat Med* (2019) 25:1519. doi: 10.1038/s41591-019-0583-3

49. Mittal S, Yeh K, Leslie LS, Kenkel S, Kajdacsy-Balla A, Bhargava R. Simultaneous cancer and tumor microenvironment subtyping using confocal infrared microscopy for all-digital molecular histopathology. *Proc Natl Acad Sci U.S.A.* (2018) 115:E5651. doi: 10.1073/pnas.1719551115

50. Li H, Bera K, Toro P, Fu P, Zhang Z, Lu C, et al. Collagen fiber orientation disorder from H&E images is prognostic for early stage breast cancer: clinical trial validation. *NPJ Breast Cancer* (2021) 7:104. doi: 10.1038/s41523-021-00310-z

51. Wang S, Rong R, Yang DM, Fujimoto J, Yan S, Cai L, et al. Computational staining of pathology images to study the tumor microenvironment in lung cancer. *Cancer Res* (2020) 80:2056. doi: 10.1158/0008-5472.CAN-19-1629

52. Wang X, Janowczyk A, Zhou Y, Thawani R, Fu P, Schalper K, et al. Prediction of recurrence in early stage non-small cell lung cancer using computer extracted nuclear features from digital H&E images. *Sci Rep* (2017) 7:13543. doi: 10.1038/s41598-017-13773-7

53. Jia D, Liu Z, Deng N, Tan TZ, Huang RY, Taylor-Harding B, et al. A COL11A1-correlated pan-cancer gene signature of activated fibroblasts for the prioritization of therapeutic targets. *Cancer Lett* (2016) 382:203. doi: 10.1016/j.canlet.2016.09.001

54. Cheon DJ, Tong Y, Sim MS, Dering J, Berel D, Cui X, et al. A collagen-remodeling gene signature regulated by TGF-beta signaling is associated with metastasis and poor survival in serous ovarian cancer. *Clin Cancer Res* (2014) 20:711. doi: 10.1158/1078-0432.CCR-13-1256

55. Hu Y, Taylor-Harding B, Raz Y, Haro M, Recouvreux MS, Taylan E, et al. Are epithelial ovarian cancers of the mesenchymal subtype actually intraperitoneal metastases to the ovary? *Front Cell Dev Biol* (2020) 8:647. doi: 10.3389/fcell.2020.00647

56. Huang R, Wu D, Yuan Y, Li X, Holm R, Trope CG, et al. CD117 expression in fibroblasts-like stromal cells indicates unfavorable clinical outcomes in ovarian carcinoma patients. *PLoS One* (2014) 9:e112209. doi: 10.1371/journal.pone.0112209

57. Becht E, de Reynies A, Giraldo NA, Pilati C, Buttard B, Lacroix L, et al. Immune and stromal classification of colorectal cancer is associated with molecular subtypes and relevant for precision immunotherapy. *Clin Cancer Res* (2016) 22:4057. doi: 10.1158/1078-0432.CCR-15-2879

58. Kim H, Watkinson J, Varadan V, Anastassiou D. Multi-cancer computational analysis reveals invasion-associated variant of desmoplastic reaction involving INHBA, THBS2 and COL11A1. *BMC Med Genomics* (2010) 3:51. doi: 10.1186/1755-8794-3-51

59. Karlan BY, Dering J, Walsh C, Orsulic S, Lester J, Anderson LA, et al. POSTN/TGFBI-associated stromal signature predicts poor prognosis in serous epithelial ovarian cancer. *Gynecol Oncol* (2014) 132:334. doi: 10.1016/j.ygyno.2013.12.021

60. Zhang S, Jing Y, Zhang M, Zhang Z, Ma P, Peng H, et al. Stroma-associated master regulators of molecular subtypes predict patient prognosis in ovarian cancer. *Sci Rep* (2015) 5:16066. doi: 10.1038/srep16066

61. Liu Z, Beach JA, Agadjanian H, Jia D, Aspuria PJ, Karlan BY, et al. Suboptimal cytoreduction in ovarian carcinoma is associated with molecular pathways characteristic of increased stromal activation. *Gynecol Oncol* (2015) 139:394. doi: 10.1016/j.ygyno.2015.08.026

62. Ryner L, Guan Y, Firestein R, Xiao Y, Choi Y, Rabe C, et al. Upregulation of periostin and reactive stroma is associated with primary chemoresistance and predicts clinical outcomes in epithelial ovarian cancer. *Clin Cancer Res* (2015) 21:2941. doi: 10.1158/1078-0432.CCR-14-3111

63. Chakravarthy A, Khan L, Bensler NP, Bose P, De Carvalho DD. TGF-β-associated extracellular matrix genes link cancer-associated fibroblasts to immune evasion and immunotherapy failure. *Nat Commun* (2018) 9:4692. doi: 10.1038/s41467-018-06654-8

64. Jain RK. Normalizing tumor microenvironment to treat cancer: bench to bedside to biomarkers. *J Clin Oncol* (2013) 31:2205. doi: 10.1200/JCO.2012.46.3653

65. Su S, Chen J, Yao H, Liu J, Yu S, Lao L, et al. CD10(+)GPR77(+) cancer-associated fibroblasts promote cancer formation and chemoresistance by sustaining cancer stemness. *Cell* (2018) 172:841. doi: 10.1016/j.cell.2018.01.009

66. Mariathasan S, Turley SJ, Nickles D, Castiglioni A, Yuen K, Wang Y, et al. TGFbeta attenuates tumour response to PD-L1 blockade by contributing to exclusion of T cells. *Nature* (2018) 554:544. doi: 10.1038/nature25501

67. Tauriello DVF, Palomo-Ponce S, Stork D, Berenguer-Llergo A, Badia-Ramentol J, Iglesias M, et al. TGFbeta drives immune evasion in genetically reconstituted colon cancer metastasis. *Nature* (2018) 554:538. doi: 10.1038/nature25492

68. Grauel AL, Nguyen B, Ruddy D, Laszewski T, Schwartz S, Chang J, et al. TGFβ-blockade uncovers stromal plasticity in tumors by revealing the existence of a subset of interferon-licensed fibroblasts. *Nat Commun* (2020) 11:6315. doi: 10.1038/s41467-020-19920-5

69. Wang X, Barrera C, Bera K, Viswanathan VS, Azarianpour-Esfahani S, Koyuncu C, et al. Spatial interplay patterns of cancer nuclei and tumor-infiltrating lymphocytes (TILs) predict clinical benefit for immune checkpoint inhibitors. *Sci Adv* (2022) 8:eabn3966. doi: 10.1126/sciadv.abn3966

70. Bankhead P, Loughrey MB, Fernandez JA, Dombrowski Y, McArt DG, Dunne PD, et al. QuPath: Open source software for digital pathology image analysis. sci rep. *Sci Rep* (2017) 7:16878. doi: 10.1038/s41598-017-17204-5

71. Jiang J, Tekin B, Guo R, Liu H, Huang Y, Wang C. Digital pathology-based study of cell- and tissue-level morphologic features in serous borderline ovarian tumor and high-grade serous ovarian cancer. *J Pathol Inform* (2021) 12:24. doi: 10.4103/jpi.jpi_76_20

72. Campanella G, Hanna MG, Geneslaw L, Miraflor A, Werneck Krauss Silva V, Busam KJ, et al. Clinical-grade computational pathology using weakly supervised deep learning on whole slide images. *Nat Med* (2019) 25:1301. doi: 10.1038/s41591-019-0508-1

73. Hekler A, Utikal JS, Enk AH, Solass W, Schmitt M, Klode J, et al. Deep learning outperformed 11 pathologists in the classification of histopathological melanoma images. *Eur J Cancer* (2019) 118:91. doi: 10.1016/j.ejca.2019.06.012

74. Esteva A, Kuprel B, Novoa RA, Ko J, Swetter SM, Blau HM, et al. Dermatologist-level classification of skin cancer with deep neural networks. *Nature* (2017) 542:115. doi: 10.1038/nature21056

75. Ehteshami Bejnordi B, Veta M, Johannes van Diest P, van Ginneken B, Karssemeijer N, Litjens G, et al. Diagnostic assessment of deep learning algorithms for detection of lymph node metastases in women with breast cancer. *JAMA* (2017) 318:2199. doi: 10.1001/jama.2017.14585

76. Pantanowitz L, Quiroga-Garza GM, Bien L, Heled R, Laifenfeld D, Linhart C, et al. An artificial intelligence algorithm for prostate cancer diagnosis in whole slide images of core needle biopsies: a blinded clinical validation and deployment study. *Lancet Digit Health* (2020) 2:e407. doi: 10.1016/S2589-7500(20)30159-X

77. Nagpal K, Foote D, Liu Y, Chen PC, Wulczyn E, Tan F, et al. Development and validation of a deep learning algorithm for improving Gleason scoring of prostate cancer. *NPJ Digit Med* (2019) 2:48. doi: 10.1038/s41746-019-0112-2

78. Leo P, Janowczyk A, Elliott R, Janaki N, Bera K, Shiradkar R, et al. Computer extracted gland features from H&E predicts prostate cancer recurrence comparably to a genomic companion diagnostic test: a large multi-site study. *NPJ Precis Oncol* (2021) 5:35. doi: 10.1038/s41698-021-00174-3

79. Wu M, Yan C, Liu H, Liu Q. Automatic classification of ovarian cancer types from cytological images using deep convolutional neural networks. *Biosci Rep* (2018) 38:BSR20180289. doi: 10.1042/BSR20180289

80. Laury AR, Blom S, Ropponen T, Virtanen A, Carpén OM. Artificial intelligence-based image analysis can predict outcome in high-grade serous carcinoma *via* histology alone. *Sci Rep* (2021) 11:19165. doi: 10.1038/s41598-021-98480-0

81. Kulkarni PM, Robinson EJ, Sarin Pradhan J, Gartrell-Corrado RD, Rohr BR, Trager MH, et al. Deep learning based on standard H&E images of primary melanoma tumors identifies patients at risk for visceral recurrence and death. *Clin Cancer Res* (2020) 26:1126. doi: 10.1158/1078-0432.CCR-19-1495

82. Wu Z, Wang L, Li C, Cai Y, Liang Y, Mo X, et al. DeepLRHE: A deep convolutional neural network framework to evaluate the risk of lung cancer recurrence and metastasis from histopathology images. *Front Genet* (2020) 11:768. doi: 10.3389/fgene.2020.00768

83. Harder N, Schönmeyer R, Nekolla K, Meier A, Brieu N, Vanegas C, et al. Automatic discovery of image-based signatures for ipilimumab response prediction in malignant melanoma. *Sci Rep* (2019) 9:7449. doi: 10.1038/s41598-019-43525-8

84. Azarianpour S, Corredor G, Bera K, Leo P, Fu P, Toro P, et al. Computational image features of immune architecture is associated with clinical benefit and survival in gynecological cancers across treatment modalities. *J Immunother Cancer* (2022) 10:e003833. doi: 10.1136/jitc-2021-003833

85. Niazi MKK, Parwani AV, Gurcan MN. Digital pathology and artificial intelligence. *Lancet Oncol* (2019) 20:e253. doi: 10.1016/S1470-2045(19)30154-8

86. Colling R, Pitman H, Oien K, Rajpoot N, Macklin P, Snead D, et al. Artificial intelligence in digital pathology: a roadmap to routine use in clinical practice. *J Pathol* (2019) 249:143. doi: 10.1002/path.5310

87. Evans AJ, Bauer TW, Bui MM, Cornish TC, Duncan H, Glassy EF, et al. US Food and drug administration approval of whole slide imaging for primary diagnosis: A key milestone is reached and new questions are raised. *Arch Pathol Lab Med* (2018) 142:1383. doi: 10.5858/arpa.2017-0496-CP

88. Zarella MD, Bowman D, Aeffner F, Farahani N, Xthona A, Absar SF, et al. A practical guide to whole slide imaging: A white paper from the digital pathology association. *Arch Pathol Lab Med* (2019) 143:222. doi: 10.5858/arpa.2018-0343-RA

89. Abels E, Pantanowitz L, Aeffner F, Zarella MD, van der Laak J, Bui MM, et al. Computational pathology definitions, best practices, and recommendations for regulatory guidance: a white paper from the digital pathology association. *J Pathol* (2019) 249:286. doi: 10.1002/path.5331

90. Aeffner F, Zarella MD, Buchbinder N, Bui MM, Goodman MR, Hartman DJ, et al. Introduction to digital image analysis in whole-slide imaging: A white paper from the digital pathology association. *J Pathol Inform* (2019) 10:9. doi: 10.4103/jpi.jpi_82_18

91. Lujan G, Quigley JC, Hartman D, Parwani A, Roehmholdt B, Meter BV, et al. Dissecting the business case for adoption and implementation of digital pathology: A white paper from the digital pathology association. *J Pathol Inform* (2021) 12:17. doi: 10.4103/jpi.jpi_67_20

92. Rizzardi AE, Johnson AT, Vogel RI, Pambuccian SE, Henriksen J, Skubitz AP, et al. Quantitative comparison of immunohistochemical staining measured by digital image analysis versus pathologist visual scoring. *Diagn Pathol* (2012) 7:42. doi: 10.1186/1746-1596-7-42

93. Sarwar S, Dent A, Faust K, Richer M, Djuric U, Van Ommeren R, et al. Physician perspectives on integration of artificial intelligence into diagnostic pathology. *NPJ Digit Med* (2019) 2:28. doi: 10.1038/s41746-019-0106-0

94. Bhargava R, Madabhushi A. Emerging themes in image informatics and molecular analysis for digital pathology. *Annu Rev BioMed Eng* (2016) 18:387. doi: 10.1146/annurev-bioeng-112415-114722

95. Ghaznavi F, Evans A, Madabhushi A, Feldman M. Digital imaging in pathology: whole-slide imaging and beyond. *Annu Rev Pathol* (2013) 8:331. doi: 10.1146/annurev-pathol-011811-120902

96. Mukhopadhyay S, Feldman MD, Abels E, Ashfaq R, Beltaifa S, Cacciabeve NG, et al. Whole slide imaging versus microscopy for primary diagnosis in surgical pathology: A multicenter blinded randomized noninferiority study of 1992 cases (Pivotal study). *Am J Surg Pathol* (2018) 42:39. doi: 10.1097/PAS.0000000000000948

97. Durán JM, Jongsma KR. Who is afraid of black box algorithms? on the epistemological and ethical basis of trust in medical AI. *J Med Ethics* (2021) 47:329. doi: 10.1136/medethics-2020-106820

98. Teo YYA, Danilevsky A, Shomron N. Overcoming interpretability in deep learning cancer classification. *Methods Mol Biol* (2021) 2243:297. doi: 10.1007/978-1-0716-1103-6_15

99. Serag A, Ion-Margineanu A, Qureshi H, McMillan R, Saint Martin MJ, Diamond J, et al. Translational AI and deep learning in diagnostic pathology. *Front Med (Lausanne)* (2019) 6:185. doi: 10.3389/fmed.2019.00185

100. Muehlematter UJ, Daniore P, Vokinger KN. Approval of artificial intelligence and machine learning-based medical devices in the USA and Europe (2015-20): a comparative analysis. *Lancet Digit Health* (2021) 3:e195. doi: 10.1016/S2589-7500(20)30292-2

101. Benjamens S, Dhunnoo P, Meskó B. The state of artificial intelligence-based FDA-approved medical devices and algorithms: an online database. *NPJ Digit Med* (2020) 3:118. doi: 10.1038/s41746-020-00324-0

102. Schmitt M, Maron RC, Hekler A, Stenzinger A, Hauschild A, Weichenthal M, et al. Hidden variables in deep learning digital pathology and their potential to cause batch effects: Prediction model study. *J Med Internet Res* (2021) 23:e23436. doi: 10.2196/23436

103. Bautista P, Hashimoto N, Yagi Y. Color standardization in whole slide imaging using a color calibration slide. *J Pathol Inf* (2014) 5:4. doi: 10.4103/2153-3539.126153

104. Khan AM, Rajpoot N, Treanor D, Magee D. A nonlinear mapping approach to stain normalization in digital histopathology images using image-specific color deconvolution. *IEEE Trans Biomed Eng* (2014) 61:1729. doi: 10.1109/TBME.2014.2303294

105. Chappelow J, Tomaszewski JE, Feldman M, Shih N, Madabhushi A. HistoStitcher©: An interactive program for accurate and rapid reconstruction of digitized whole histological sections from tissue fragments. *Computerized Med Imaging Graphics* (2011) 35:557. doi: 10.1016/j.compmedimag.2011.01.010

106. Kothari S, Phan J, Wang M. Eliminating tissue-fold artifacts in histopathological whole-slide images for improved image-based prediction of cancer grade. *J Pathol Inf* (2013) 4:22. doi: 10.4103/2153-3539.117448

107. Janowczyk A, Zuo R, Gilmore H, Feldman M, Madabhushi A. HistoQC: An open-source quality control tool for digital pathology slides. *JCO Clin Cancer Inform* (2019) 3:1. doi: 10.1200/CCI.18.00157

108. Senaras C, Niazi MKK, Lozanski G, Gurcan MN. DeepFocus: Detection of out-of-focus regions in whole slide digital images using deep learning. *PloS One* (2018) 13:e0205387. doi: 10.1371/journal.pone.0205387

109. Moles Lopez X, D'Andrea E, Barbot P, Bridoux AS, Rorive S, Salmon I, et al. An automated blur detection method for histological whole slide imaging. *PLoS One* (2013) 8:e82710. doi: 10.1371/journal.pone.0082710

110. Hutter C, Zenklusen JC. The cancer genome atlas: Creating lasting value beyond its data. *Cell* (2018) 173:283. doi: 10.1016/j.cell.2018.03.042

111. Clark K, Vendt B, Smith K, Freymann J, Kirby J, Koppel P, et al. The cancer imaging archive (TCIA): maintaining and operating a public information repository. *J Digit Imaging* (2013) 26:1045. doi: 10.1007/s10278-013-9622-7

112. Lu MY, Chen RJ, Kong D, Lipkova J, Singh R, Williamson DFK, et al. Federated learning for computational pathology on gigapixel whole slide images. *Med Image Anal* (2022) 76:102298. doi: 10.1016/j.media.2021.102298

113. Sheller MJ, Edwards B, Reina GA, Martin J, Pati S, Kotrotsou A, et al. Federated learning in medicine: facilitating multi-institutional collaborations without sharing patient data. *Sci Rep* (2020) 10:12598. doi: 10.1038/s41598-020-69250-1

114. Schneider CA, Rasband WS, Eliceiri KW. NIH Image to ImageJ: 25 years of image analysis. *Nat Methods* (2012) 9:671. doi: 10.1038/nmeth.2089

115. Schindelin J, Arganda-Carreras I, Frise E, Kaynig V, Longair M, Pietzsch T, et al. Fiji: an open-source platform for biological-image analysis. *Nat Methods* (2012) 9:676. doi: 10.1038/nmeth.2019

116. de Chaumont F, Dallongeville S, Chenouard N, Hervé N, Pop S, Provoost T, et al. Icy: an open bioimage informatics platform for extended reproducible research. *Nat Methods* (2012) 9:690. doi: 10.1038/nmeth.2075

117. Stritt M, Stalder AK, Vezzali E. Orbit image analysis: An open-source whole slide image analysis tool. *PloS Comput Biol* (2020) 16:e1007313. doi: 10.1371/journal.pcbi.1007313

118. Sommer C, Straehle C, Köthe U, Hamprecht FA. Ilastik: Interactive learning and segmentation toolkit. In: *2011 IEEE international symposium on biomed imaging: From nano to macro* New York: IEE. (2011). p. 230.

119. Carpenter AE, Jones TR, Lamprecht MR, Clarke C, Kang IH, Friman O, et al. CellProfiler: image analysis software for identifying and quantifying cell phenotypes. *Genome Biol* (2006) 7:R100. doi: 10.1186/gb-2006-7-10-r100

120. Yu X, Zhao B, Huang H, Tian M, Zhang S, Song H, et al. An open source platform for computational histopathology. *IEEE Access* (2021) 9:73651. doi: 10.1109/ACCESS.2021.3080429

121. Rosenthal J, Carelli R, Omar M, Brundage D, Halbert E, Nyman J, et al. Building tools for machine learning and artificial intelligence in cancer research: Best practices and a case study with the PathML toolkit for computational pathology. *Mol Cancer Res* (2022) 20:202. doi: 10.1158/1541-7786.MCR-21-0665

122. Wang F, Kong J, Cooper L, Pan T, Kurc T, Chen W, et al. A data model and database for high-resolution pathology analytical image informatics. *J Pathol Inf* (2011) 2:32. doi: 10.4103/2153-3539.83192

123. Wang F, Kong J, Gao J, Cooper L, Kurc T, Zhou Z, et al. A high-performance spatial database based approach for pathology imaging algorithm evaluation. *J Pathol Inf* (2013) 4:5. doi: 10.4103/2153-3539.108543

124. Gutman DA, Cobb J, Somanna D, Park Y, Wang F, Kurc T, et al. Cancer digital slide archive: an informatics resource to support integrated in silico analysis of TCGA pathology data. *J Am Med Inf Assoc* (2013) 20:1091. doi: 10.1136/amiajnl-2012-001469

# Advantages of publishing in Frontiers

**OPEN ACCESS**
Articles are free to read for greatest visibility and readership

**FAST PUBLICATION**
Around 90 days from submission to decision

**HIGH QUALITY PEER-REVIEW**
Rigorous, collaborative, and constructive peer-review

**TRANSPARENT PEER-REVIEW**
Editors and reviewers acknowledged by name on published articles

**Frontiers**
Avenue du Tribunal-Fédéral 34
1005 Lausanne | Switzerland

**Visit us:** www.frontiersin.org
**Contact us:** frontiersin.org/about/contact

**REPRODUCIBILITY OF RESEARCH**
Support open data and methods to enhance research reproducibility

**DIGITAL PUBLISHING**
Articles designed for optimal readership across devices

**FOLLOW US**
@frontiersin

**IMPACT METRICS**
Advanced article metrics track visibility across digital media

**EXTENSIVE PROMOTION**
Marketing and promotion of impactful research

**LOOP RESEARCH NETWORK**
Our network increases your article's readership